Summary of the
Bulletin of the
International Seismological Centre

2018

July – December

Volume 55 Issue II

The number of phases (red) and number of amplitudes (blue) collected by the ISC for events each year since 1964. The data in grey covers the current period where data are still being collected before the ISC review takes place and are accurate at the time of publication. See Section 8.3.
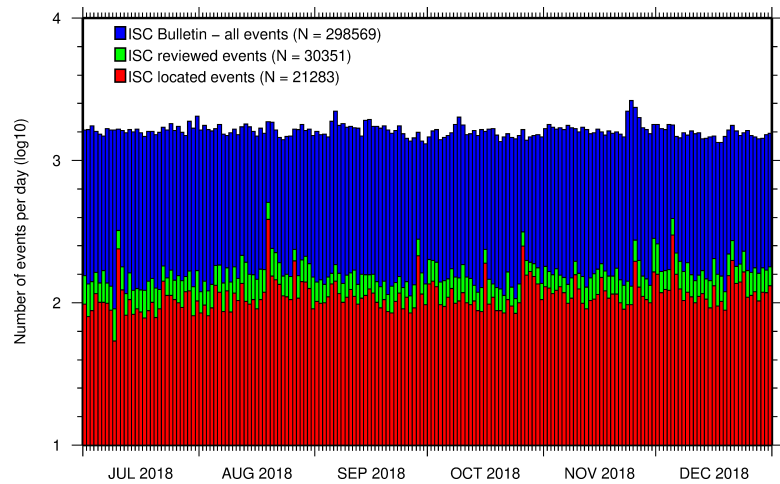
The number of events within the Bulletin for the current summary period. The vertical scale is logarithmic. See Section 9.1.
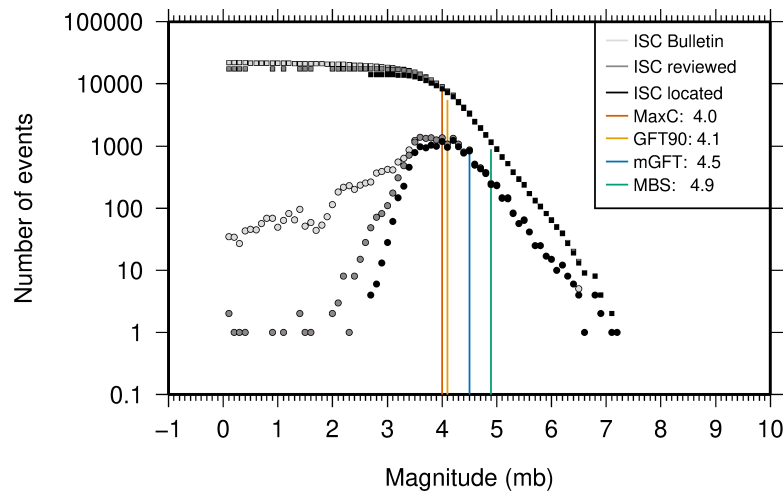
Frequency and cumulative frequency magnitude distribution for all events in the ISC Bulletin, ISC reviewed events and events located by the ISC. The magnitude of completeness (M_C) is shown for the ISC Bulletin. Note: only events with values of m_b are represented in the figure. See Section 9.4.

Summary of the
Bulletin of the
International Seismological Centre

2018

July - December

Volume 55 Issue II

Produced and edited by:
Kathrin Lieser, James Harris and Dmitry Storchak

ISC Data Products

http://www.isc.ac.uk/products/

ISC Bulletin:

> http://www.isc.ac.uk/iscbulletin/search

ISC Bulletin and Catalogue monthly files, to the last reviewed month in FFB or ISF1 format:

> ftp://www.isc.ac.uk/pub/[isf|ffb]/bulletin/*yyyy*/*yyyymm*.gz
>
> ftp://www.isc.ac.uk/pub/[isf|ffb]/catalogue/*yyyy*/*yyyymm*.gz

Datafiles for the ISC data before the rebuild:

> ftp://www.isc.ac.uk/pub/prerebuild/[isf|ffb]/bulletin/*yyyy*/*yyyymm*.gz
>
> ftp://www.isc.ac.uk/pub/prerebuild/[isf|ffb]/catalogue/*yyyy*/*yyyymm*.gz

ISC-EHB Bulletin:

> http://www.isc.ac.uk/isc-ehb/search/

IASPEI Reference Event List (GT bulletin):

> http://www.isc.ac.uk/gtevents/search/

ISC-GEM Global Instrumental Earthquake Catalogue:

> http://http://www.isc.ac.uk/iscgem/download.php

ISC Event Bibliography:

> http://www.isc.ac.uk/event_bibliography/bibsearch.php

International Seismograph Station Registry:

> http://www.isc.ac.uk/registries/search/

Seismological Contacts:

> http://www.isc.ac.uk/projects/seismocontacts/

Contents

1

Preface

Dear Colleague,

This is the second 2018 issue of the Summary of the ISC Bulletin, which remains the most fundamental reason for continued operations at the ISC. This issue covers earthquakes and other seismic events that occurred during the period from July to December 2018. Users can search the ISC Bulletin on the ISC website. The monthly Bulletin files are available from the ISC ftp site. For instructions, please see the www.isc.ac.uk/iscbulletin/.

This publication contains information on the ISC, its staff, Members, Sponsors and Data providers. It offers analysis of the data contributed to the ISC by many seismological agencies worldwide as well as analysis of the data in the ISC Bulletin itself. This somewhat smaller issue misses some of the standard information on routine procedures usually published in the first issue of each year.

We continue publishing invited articles describing the history, current status and operational procedures at those networks that contribute data to the ISC. This time it is the turn for the seismic monitoring network run by the San Calixto Observatory in Bolivia.

We also publish articles on notable earthquakes and other seismic events. This time we included an article on M5.4 Katav-Ivanovsk earthquake – the strongest instrumentally recorded earthquake in Ural Mountains in Russia, followed by a powerful aftershock process.

We hope that you find this publication useful in your work. If your home-institution or company is unable, for one reason or another, to support the long-term international operations of the ISC in full by becoming a Member or a Sponsor, then, please, consider subscribing to this publication by contacting us at admin@isc.ac.uk.

With kind regards to our Data Contributors, Members, Sponsors and users,

Dr Dmitry A. Storchak
Director
International Seismological Centre (ISC)

The ISC is a Charitable Incorporated Organization (CIO)
registered with The Charity Commission for England and Wales.
Registered charity number: 1188971.

2

The International Seismological Centre

2.1 The ISC Mandate

The International Seismological Centre (ISC) was set up in 1964 with the assistance of UNESCO as a successor to the International Seismological Summary (ISS) to carry forward the pioneering work of Prof. John Milne, Sir Harold Jeffreys and other British scientists in collecting, archiving and processing seismic station and network bulletins and preparing and distributing the definitive summary of world seismicity.

Under the umbrella of the International Association of Seismology and Physics of the Earth Interior (IASPEI/IUGG), the ISC has played an important role in setting international standards such as the International Seismic Bulletin Format (ISF), the IASPEI Standard Seismic Phase List (SSPL) and both the old and New IASPEI Manual of the Seismological Observatory Practice (NMSOP-2) (www.iaspei.org/projects/NMSOP.html).

The ISC has contributed to scientific research and prominent scientists such as John Hodgson, Eugine Herrin, Hal Thirlaway, Jack Oliver, Anton Hales, Ola Dahlman, Shigeji Suehiro, Nadia Kondorskaya, Vit Karnik, Stephan Müller, David Denham, Bob Engdahl, Adam Dziewonski, John Woodhouse and Guy Masters all considered it an important duty to serve on the ISC Executive Committee and the Governing Council.

The current mission of the ISC is to maintain:

- the ISC **Bulletin** – the longest continuous definitive summary of World seismicity (collaborating with 130 seismic networks and data centres around the world). (www.isc.ac.uk/iscbulletin/)

- the International Seismographic Station Registry (**IR**, jointly with the World Data Center for Seismology, Denver). (www.isc.ac.uk/registries/)

- the IASPEI Reference Event List (Ground Truth, **GT**, jointly with IASPEI). (www.isc.ac.uk/gtevents/)

These are fundamentally important tasks. Bulletin data produced, archived and distributed by the ISC for almost 50 years are the definitive source of such information and are used by thousands of seismologists worldwide for seismic hazard estimation, for tectonic studies and for regional and global imaging of the Earth's structure. Key information in global tomographic imaging is derived from the analysis of ISC data. The ISC Bulletin served as a major source of data for such well known products as the ak135 global 1-D velocity model and the EHB (*Engdahl et al.*, 1998) and Centennial (*Engdahl and Villaseñor*, 2002) catalogues. It presents an important quality-control benchmark for the Comprehensive Nuclear-Test-Ban Treaty Organization (CTBTO). Hypocentre parameters from the ISC Bulletin are used

by the Data Management Center of the Incorporated Research Institutions for Seismology (IRIS DMC) to serve event-oriented user-requests for waveform data. The ISC-GEM Bulletin is a cornerstone of the ISC-GEM Global Instrumental Reference Earthquake Catalogue for Global Earthquake risk Model (GEM).

The ISC Bulletin contains over 8 million seismic events: earthquakes, chemical and nuclear explosions, mine blasts and mining induced events. Almost 2 million of them are regional and teleseismically recorded events that have been reviewed by the ISC analysts. The ISC Bulletin contains approximately 255 million individual seismic station readings of arrival times, amplitudes, periods, SNR, slowness and azimuth, reported by approximately 19,000 seismic stations currently registered in the IR. Over 9,000 stations have contributed to the ISC Bulletin in recent years. This number includes the numerous sites of the USArray. The IASPEI GT List currently contains 10187 events for which latitude, longitude and depth of origin are known with high confidence (to 5 km or better) and seismic signals were recorded at regional and/or teleseismic distances.

2.2 Brief History of the ISC
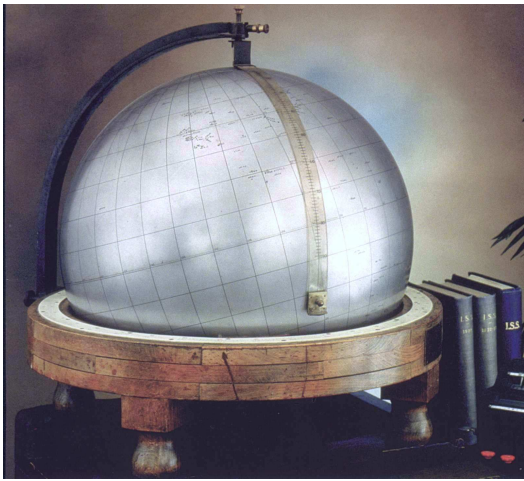
Figure 2.1: *The steel globe bearing positions of early seismic stations was used for locating positions of earthquakes for the International Seismological Summaries.*

Earthquake effects have been noted and documented from the earliest times, but it is only since the development of earthquake recording instruments in the latter half of the 19th century that a proper study of their occurrence has been possible. After the first teleseismic observation of an earthquake in 1889, the need for international exchange of readings was recognised in 1895 by Prof. John Milne and by Ernst von Rebeur Paschwitz together with Georg Gerland, resulting in the publication of the first international seismic bulletins. Milne's "Shide Circulars" were issued under the auspices of the Seismological Committee of the British Association for the Advancement of Science (BAAS), while co-workers of Gerland at the Central Bureau of the International Association of Seismology worked independently in Strasbourg (BCIS).

Following Milne's death in 1913, Seismological Bulletins of the BAAS were continued under Prof. H.H. Turner, later based at Oxford University. Upon formal post-war dissolution of the International Association of Seismology in 1922 the newly founded Seismological Section of the International Union of Geodesy and Geophysics (IUGG) set up the International Seismological Summary (ISS) to continue at Oxford under Turner, to produce the definitive global catalogues from the 1918 data-year onwards, under the auspices of IUGG and with the support of the BAAS.

ISS production, led by several professors at Oxford University, and Sir Harold Jeffreys at Cambridge

University, continued until it was superseded by the ISC Bulletin, after the ISC was formed in Edinburgh in 1964 with Dr P.L. Willmore as its first director.

During the period 1964 to 1970, with the help of UNESCO and other international scientific bodies, the ISC was reconstituted as an international non-governmental body, funded by interested institutions from various countries. Initially there were supporting members from seven countries, now there are almost 60, and member institutions include national academies, research foundations, government departments and research institutes, national observatories and universities. Each member, contributing a minimum unit of subscription or more, appoints a representative to the ISC's Governing Council, which meets every two years to decide the ISC's policy and operational programme. Representatives from the International Association of Seismology and Physics of the Earth's Interior also attend these meetings. The Governing Council appoints the Director and a small Executive Committee to oversee the ISC's operations.

Figure 2.2: ISC building in Thatcham, Berkshire, UK.

In 1975, the ISC moved to Newbury in southern England to make use of better computing facilities there. The ISC subsequently acquired its own computer and in 1986 moved to its own building at Pipers Lane, Thatcham, near Newbury. The internal layout of the new premises was designed for the ISC and includes not only office space but provision for the storage of extensive stocks of ISS and ISC publications and a library of seismological observatory bulletins, journals and books collected over many tens of years.

In 1997 the first set of the ISC Bulletin CD-ROMs was produced (not counting an earlier effort at USGS). The first ISC website appeared in 1998 and the first ISC database was put in day-to-day operations from 2001.

Throughout 2009-2011 a major internal reconstruction of the ISC building was undertaken to allow for more members of staff working in mainstream ISC operations as well as major development projects such as the CTBTO Link, ISC-GEM Catalogue and the ISC Bulletin Rebuild.

2.3 Former Directors of the ISC and its U.K. Predecessors

John Milne
Publisher of the Shide Cicular Reports on Earthquakes
1899-1913

Herbert Hall Turner

Seismological Bulletins of the BAAS

1913-1922
Director of the ISS
1922-1930

Harry Hemley Plaskett
Director of the ISS
1931-1946
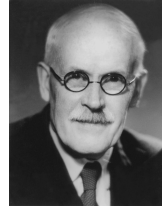
Harold Jeffreys
Director of the ISS
1946-1957

Robert Stoneley
Director of the ISS
1957-1963

P.L. (Pat) Willmore
Director of the ISS
1963-1970
Director of the ISC
1964-1970

Edouard P. Arnold
Director of the ISC
1970-1977

Anthony A. Hughes
Director of the ISC
1977-1997

Raymond J. Willemann
Director of the ISC
1998-2003

Avi Shapira
Director of the ISC
2004-2007

2.4 Member Institutions of the ISC

Article IV(a-b) of the ISC Working Statutes stipulates that any national academy, agency, scientific institution or other non-profit organisation may become a Member of the ISC on payment to the ISC of a sum equal to at least one unit of subscription and the nomination of a voting representative to serve on the ISC's governing body. Membership shall be effective for one year from the date of receipt at the ISC of the annual contribution of the Member and is thereafter renewable for periods of one year.

The ISC is currently supported with funding from its 62 Member Institutions and a four-year Grant Award EAR-1811737 from the US National Science Foundation.

Figures 2.3 and 2.4 show major sectors to which the ISC Member Institutions belong and proportional

financial contributions that each of these sectors make towards the ISC's annual budget.

ISC Members by Sector, %
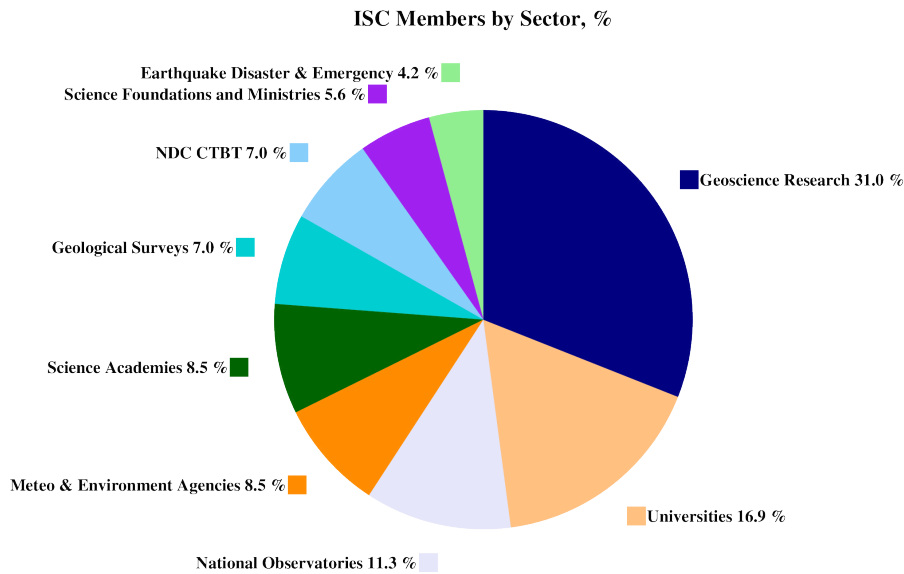
Figure 2.3: *Distribution of the ISC Member Institutions by sector in the time period when the ISC worked on the data covered by this issue of the Summary as a percentage of total number of Members.*

Members's Financial Contribution by Sector, %
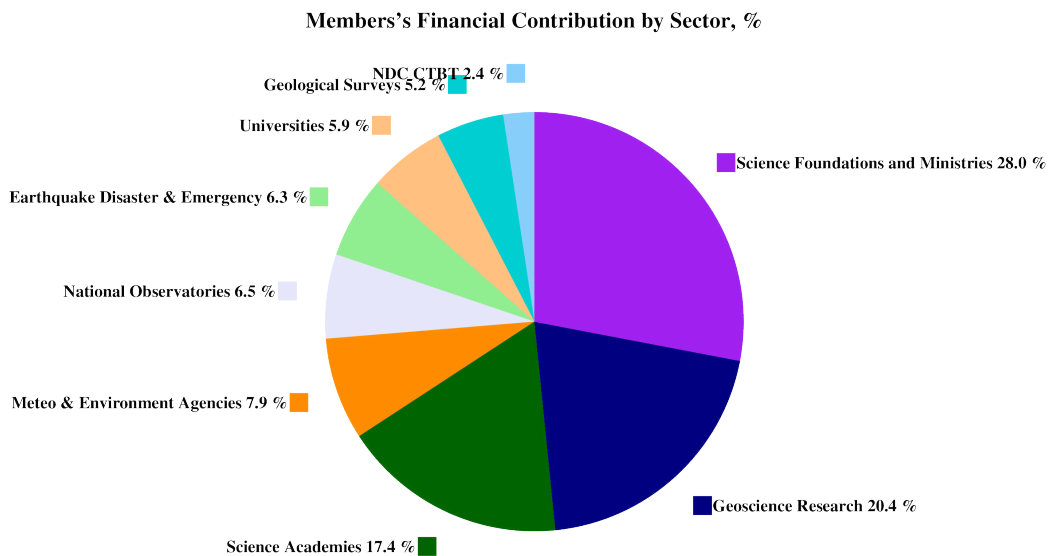
Figure 2.4: *Distribution of Member's financial contributions to the ISC by sector in the time period when the ISC worked on the data covered by this issue of the Summary as a percentage of total annual Member contributions.*

There follows a list of all current Member Institutions with a category (1 through 9) assigned according to the ISC Working Statutes. Each category relates to the number of membership units contributed.

Centre de Recherche en Astronomie, Astrophysique et Géophysique (CRAAG) Algeria www.craag.dz Category: 1

Geoscience Australia Australia www.ga.gov.au Category: 4

Federal Ministry for Education, Science and Research Austria

Category: 2

Centre of Geophysical
Monitoring (CGM) of
the National Academy
of Sciences of Belarus
Belarus
www.cgm.org.by
Category: 1

Belgian Science Policy
Office (BELSPO)
Belgium

Category: 1

Seismological Observatory, Institute of Geosciences, University of
Brasilia
Brazil
www.obsis.unb.br
Category: 1

Observatorio Nacional
Brazil
www.on.br
Category: 1

Universidade de São
Paulo, Centro de Sismologia
Brazil
www.sismo.iag.usp.br
Category: 1

National Institute of
Geophysics, Geodesy
and Geography
(NIGGG), Bulgarian Academy of Sciences
Bulgaria
www.niggg.bas.bg
Category: 1

The Geological Survey
of Canada
Canada
gsc.nrcan.gc.ca
Category: 4

Centro Sismologico
Nacional, Universidad
de Chile
Chile

Category: 1

China Earthquake Administration
China
www.cea.gov.cn
Category: 4

Institute of Earth Sciences, Academia Sinica
Chinese Taipei
www.earth.sinica.edu.tw
Category: 1

Geological Survey Department
Cyprus
www.moa.gov.cy
Category: 1

Institute of Geophysics,
Czech Academy of Sciences
Czech Republic

Category: 1

Geological Survey of
Denmark and Greenland (GEUS)
Denmark
www.geus.dk
Category: 2

National Research Institute for Astronomy and
Geophysics (NRIAG),
Cairo
Egypt
www.nriag.sci.eg
Category: 1

The University of
Helsinki
Finland
www.helsinki.fi
Category: 2

Institute National des
Sciences de l'Univers
France
www.insu.cnrs.fr
Category: 4

Laboratoire de Détection et de Géophysique/CEA
France
www-dase.cea.fr
Category: 2

Institute of Radiological
and Nuclear Safety
(IRSN), joint authority
of the Ministries of Defense, the Environment,
Industry, Research, and
Health
France

Category: 1

Bundesanstalt für Geowissenschaften und
Rohstoffe
Germany
www.bgr.bund.de
Category: 4

GeoForschungsZentrum
Potsdam
Germany
www.gfz-potsdam.de
Category: 2

The Seismological Institute, National Observatory of Athens
Greece
www.noa.gr
Category: 1

Institute of Earth
Physics and Space Science (EPSS), Hungarian Research Network
(ELKH)
Hungary

Category: 1

The Icelandic Meteorological Office
Iceland
www.vedur.is
Category: 1

National Geophysical
Research Institute
(NGRI), Council of
Scientific and Industrial
Research (CSIR)
India

Category: 2
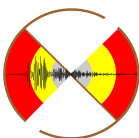
National Centre for
Seismology, Ministry of
Earth Sciences of India
India
www.moes.gov.in
Category: 4

Iraqi Meteorological Organization and Seismology
Iraq
www.imos-tm.com
Category: 1

Dublin Institute for Advanced Studies
Ireland
www.dias.ie
Category: 1

Geological Survey of Israel
Israel

Category: 1

Soreq Nuclear Research Centre (SNRC)
Israel
www.soreq.gov.il
Category: 1

Istituto Nazionale di Geofisica e Vulcanologia
Italy
www.ingv.it
Category: 3

Istituto Nazionale di Oceanografia e di Geofisica Sperimentale
Italy
www.ogs.trieste.it
Category: 1

University of the West Indies at Mona
Jamaica
www.mona.uwi.edu
Category: 1

Japan Agency for Marine-Earth Science and Technology (JAMSTEC)
Japan
www.jamstec.go.jp
Category: 2

National Institute of Polar Research (NIPR)
Japan
www.nipr.ac.jp
Category: 1
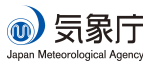
The Japan Meteorological Agency (JMA)
Japan
www.jma.go.jp
Category: 5

Earthquake Research Institute, University of Tokyo
Japan
www.eri.u-tokyo.ac.jp
Category: 3

Centro de Investigación Científica y de Educación Superior de Ensenada (CICESE)
Mexico
resnom.cicese.mx
Category: 1

Institute of Geophysics, National University of Mexico
Mexico
www.igeofcu.unam.mx
Category: 1

The Royal Netherlands Meteorological Institute (KNMI)
Netherlands
www.knmi.nl
Category: 2

GNS Science
New Zealand
www.gns.cri.nz
Category: 3

The University of Bergen
Norway
www.uib.no
Category: 2

Stiftelsen NORSAR
Norway
www.norsar.no
Category: 2

The Centre for Earth Evolution and Dynamics (CEED), the University of Oslo
Norway

Category: 1

Institute of Geophysics, Polish Academy of Sciences
Poland
www.igf.edu.pl
Category: 1

Instituto Português do Mar e da Atmosfera
Portugal
www.ipma.pt
Category: 2

Red Sísmica de Puerto Rico
Puerto Rico
redsismica.uprm.edu
Category: 1

Korean Meterological Administration
Republic of Korea
www.kma.go.kr
Category: 1

National Institute for Earth Physics
Romania
www.infp.ro
Category: 1

Russian Academy of Sciences
Russia
www.ras.ru
Category: 5

Earth Observatory of Singapore (EOS), an autonomous Institute of Nanyang Technological University
Singapore
www.earthobservatory.sg
Category: 1

Environmental Agency of Slovenia
Slovenia
www.arso.gov.si
Category: 1

Council for Geoscience
South Africa
www.geoscience.org.za
Category: 1

Institut Cartogràfic i Geològic de Catalunya (ICGC)
Spain
www.icgc.cat
Category: 1

Institute of Marine Sciences (ICM-CSIC)
Spain

Category: 1

National Defence Research Establishment (FOI)
Sweden
www.foi.se
Category: 1

Uppsala Universitet
Sweden
www.uu.se
Category: 2

The Swiss Academy of Sciences
Switzerland
www.scnat.ch
Category: 2

Disaster and Emergency Management Authority (AFAD)
Turkey
www.deprem.gov.tr
Category: 2

Kandilli Observatory and Earthquake Research Institute
Turkey
www.koeri.boun.edu.tr
Category: 1

The Royal Society
United Kingdom
www.royalsociety.org
Category: 6

British Geological Survey
United Kingdom
www.bgs.ac.uk
Category: 2

AWE Blacknest
United Kingdom
www.blacknest.gov.uk
Category: 1

Texas Seismological Network (TexNet), Bureau of Economic Geology, J.A. and K.G. Jackson School of Geosciences, University of Texas at Austin
U.S.A.
www.beg.utexas.edu
Category: 1

University of Utah Seismograph Stations (UUSS)
U.S.A.

Category: 1

The National Science Foundation of the United States. (Grant No. EAR-1811737)
U.S.A.
www.nsf.gov
Category: 9

Alaska Earthquake Center (AEC), University of Alaska Fairbanks
U.S.A.

Category: 1

National Earthquake Information Center, U.S. Geological Survey
U.S.A.
www.neic.usgs.gov
Category: 1

Incorporated Research Institutions for Seismology
U.S.A.
www.iris.edu
Category: 1

2.5   Sponsoring Organisations

Article IV(c) of the ISC Working Statutes stipulates any commercial organisation with an interest in the objectives and/or output of the ISC may become an Associate Member of the ISC on payment of an Associate membership fee, but without entitlement to representation with a vote on the ISC's governing body.

www.reftek.com

REF TEK designs and manufactures application specific, high-performance, battery-operated, field-portable geophysical data acquisition devices for the global market. With over 35 years of experience, REF TEK provides customers with complete turnkey solutions that include high resolution recorders, broadband sensors, state-of-the-art communications (V-SAT, GPRS, etc), installation, training, and continued customer support. Over 7,000 REF TEK instruments are currently being used globally for multiple applications. From portable earthquake monitoring to telemetry earthquake monitoring, earthquake aftershock recording to structural monitoring and more, REF TEK equipment is suitable for a wide variety of application needs.

http://www.geosig.com/
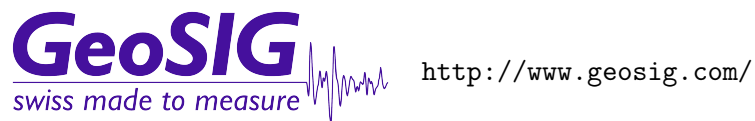
GeoSIG provides earthquake, seismic, structural, dynamic and static monitoring and measuring solutions As an ISO Certified company, GeoSIG is a world leader in design and manufacture of a diverse range of high quality, precision instruments for vibration and earthquake monitoring. GeoSIG instruments are at work today in more than 100 countries around the world with well-known projects such as the NetQuakes installation with USGS and Oresund Bridge in Denmark. GeoSIG offers off-the-shelf solutions as well as highly customised solutions to fulfil the challenging requirements in many vertical markets including the following:

- Earthquake Early Warning and Rapid Response (EEWRR)
- Seismic and Earthquake Monitoring and Measuring
- Industrial Facility Seismic Monitoring and Shutdown
- Structural Analysis and Ambient Vibration Testing
- Induced Vibration Monitoring
- Research and Scientific Applications

http://www.tai-de.com/en/

Zhuhai Taide Enterprise Co., Ltd. (Taide), a China based seismograph manufacturer, was set up in 1992. It is located in the city of Zhuhai, Guangdong Province, south-east China. The main products of Taide include data loggers, digitizers, all-band seismometers and accelerometers, intensity meters, magnetometers, strain meters, and software for earthquake related analysis. Over 80 professional engineers are employed at Taide, responsible for R&D, assembling and updating the hardware and software, and a team of 10 are engaged in stringent quality control and marketing.

In 2016, in collaboration with the Institute of Geophysics (China Earthquake Administration), Taide set up an Engineering Research Center for Earthquake Monitoring Techniques, aiming to improve the quality of earthquake observations. Taide-made instruments have been widely adapted by earthquake observation and monitoring networks, early warning systems, marine geophysical observation projects and deep borehole projects in China, as well as by seismograph networks in Indonesia, Nepal, Cuba, Pakistan and Kenya.

http://www.guralp.com/

Güralp has been developing revolutionary force-feedback broadband seismic instrumentation for more than thirty years. Our sensors record seismic signals of all kinds, from teleseismic events occurring on the other side of the planet, to microseisms induced by unconventional hydrocarbon extraction. Our sophisticated digitisers record these signals with the highest resolution and accurate timing.

We supply individual instruments or complete seismic systems. Our services include field support such as installation and maintenance, to complete network and data management.

We design our instruments to meet increasingly complex requirements for deployment in the most challenging circumstances. As a result, you will find Güralp instruments gathering seismic data in the harshest of environments, from the Antarctic ice sheet; to boreholes 100s of metres deep; to the world's most active volcanoes and deepest ocean trenches.

http://src.com.au/

The Seismology Research Centre is an Australian earthquake observatory that began developing their own seismic recorders and data processing software in the late 1970s when digital recorders were uncommon. The Gecko is the SRC's 7th generation of seismic recorder, now available with a variety of integrated sensors to meet every monitoring requirement, including:

- Strong Motion Accelerographs

- 2Hz and 4.5Hz Blast Vibration Monitors

- Short Period 1Hz Seismographs

- Broadband 200s-1500Hz Optical Seismographs

Visit src.com.au/downloads/waves to grab a free copy of the SRC's MiniSEED waveform viewing and analysis software application, Waves.

MS&**AD**

MS&AD InterRisk Research & Consulting

`http://www.irric.co.jp/en/corporate/`

MS&AD InterRisk Research & Consulting, Inc. is responsible for the core of risk-related service businesses in the MS&AD group. We provide services which meet various expectations of the clients, including consulting, research and investigation, seminars and publications for risk management in addition to the think-tank functions.

2.6 Data Contributing Agencies

In addition to its Members and Sponsors, the ISC owes its existence and successful long-term operations to its 151 seismic bulletin data contributors. These include government agencies responsible for national seismic networks, geoscience research institutions, geological surveys, meteorological agencies, universities, national data centres for monitoring the CTBT and individual observatories. There would be no ISC Bulletin available without the regular stream of data that are unselfishly and generously contributed to the ISC on a free basis.

East African Network

EAF

The Institute of Seismology, Academy of Sciences of Albania
Albania
TIR

Centre de Recherche en Astronomie, Astrophysique et Géophysique
Algeria
CRAAG

Instituto Nacional de Meteorologia e Geofisica - INAMET
Angola
INAM

Instituto Nacional de Prevención Sísmica
Argentina
SJA

Universidad Nacional de La Plata
Argentina
LPA

National Survey of Seismic Protection
Armenia
NSSP

Geoscience Australia
Australia
AUST

Curtin University
Australia
CUPWA

Zentralanstalt für Meteorologie und Geodynamik (ZAMG)
Austria
VIE

International Data Centre, CTBTO
Austria
IDC

Republican Seismic Survey Center of Azerbaijan National Academy of Sciences
Azerbaijan
AZER

Royal Observatory of Belgium
Belgium
UCC

Observatorio San Calixto
Bolivia
SCB

Republic Hydrometeorological Service, Seismological Observatory, Banja Luka
Bosnia and Herzegovina
RHSSO

Botswana Geoscience Institute
Botswana
BGSI

Observatory Seismological of the University of Brasilia
Brazil
OSUNB

Instituto Astronomico e Geofísico
Brazil
VAO

National Institute of Geophysics, Geology and Geography
Bulgaria
SOF

Seismological Observatory of Mount Cameroon
Cameroon
SOMC

Canadian Hazards Information Service, Natural Resources Canada
Canada
OTT

Centro Sismológico Nacional, Universidad de Chile
Chile
GUC

China Earthquake Networks Center
China
BJI

Institute of Earth Sciences, Academia Sinica
Chinese Taipei
ASIES

Central Weather Bureau (CWB)
Chinese Taipei
TAP

Red Sismológica Nacional de Colombia
Colombia
RSNC

Sección de Sismología, Vulcanología y Exploración Geofísica
Costa Rica
UCR

Seismological Survey of the Republic of Croatia
Croatia
ZAG

Servicio Sismológico Nacional Cubano
Cuba
SSNC

Cyprus Geological Survey Department
Cyprus
NIC

The Institute of Physics of the Earth (IPEC)
Czech Republic
IPEC

Institute of Geophysics, Czech Academy of Sciences
Czech Republic
PRU

Institute of Geophysics, Czech Academy of Sciences
Czech Republic
WBNET

Korea Earthquake Administration
Democratic People's Republic of Korea
KEA

Geological Survey of Denmark and Greenland
Denmark
DNK

Universidad Autonoma de Santo Domingo
Dominican Republic
SDD

Observatorio Sismologico Politecnico Loyola
Dominican Republic
OSPL

Servicio Nacional de Sismología y Vulcanología
Ecuador
IGQ

National Research Institute of Astronomy and Geophysics
Egypt
HLW

Servicio Nacional de Estudios Territoriales
El Salvador
SNET

Seismological Observatory Skopje
North Macedonia
SKO

Institute of Seismology, University of Helsinki
Finland
HEL

Laboratoire de Détection et de Géophysique/CEA
France
LDG

Institut de Physique du Globe de Paris
France
IPGP

EOST / RéNaSS
France
STR
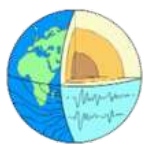
Laboratoire de Géophysique/CEA
French Polynesia
PPT

Institute of Earth Sciences/ National Seismic Monitoring Center
Georgia
TIF

Seismological Observatory Berggießhübel, TU Bergakademie Freiberg
Germany
BRG
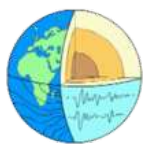
Geophysikalisches Observatorium Collm
Germany
CLL

Bundesanstalt für Geowissenschaften und Rohstoffe
Germany
BGR

Alfred Wegener Institute for Polar and Marine Research
Germany
AWI

Department of Geophysics, Aristotle University of Thessaloniki
Greece
THE

University of Patras, Department of Geology
Greece
UPSL

National Observatory of Athens
Greece
ATH

INSIVUMEH
Guatemala
GCG

Hong Kong Observatory
Hong Kong
HKC

Geodetic and Geophysical Reasearch Institute, Hungarian Academy of Sciences
Hungary
KRSZO

Icelandic Meteorological Office
Iceland
REY
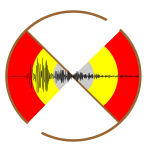
National Centre for Seismology of the Ministry of Earth Sciences of India
India
NDI

National Geophysical Research Institute
India
HYB

Badan Meteorologi, Klimatologi dan Geofisika
Indonesia
DJA

Tehran University
Iran
TEH

International Institute of Earthquake Engineering and Seismology (IIEES)
Iran
THR

Iraqi Meteorological and Seismology Organisation
Iraq
ISN

Dublin Institute for Advanced Studies
Ireland
DIAS

The Geophysical Institute of Israel
Israel
GII

Dipartimento per lo Studio del Territorio e delle sue Risorse (RSNI)
Italy
GEN

Istituto Nazionale di Oceanografia e di Geofisica Sperimentale (OGS)
Italy
TRI

MedNet Regional Centroid - Moment Tensors
Italy
MED_RCMT

Laboratory of Research on Experimental and Computational Seimology
Italy
RISSC

Istituto Nazionale di Geofisica e Vulcanologia
Italy
ROM

Station Géophysique de Lamto
Ivory Coast
LIC

Jamaica Seismic Network
Jamaica
JSN
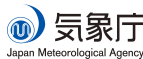
Japan Meteorological Agency
Japan
JMA

National Institute of Polar Research
Japan
SYO

National Research Institute for Earth Science and Disaster Resilience
Japan
NIED

Jordan Seismological Observatory
Jordan
JSO

National Nuclear Center
Kazakhstan
NNC

Seismological Experimental Methodological Expedition
Kazakhstan
SOME

Institute of Seismology, Academy of Sciences of Kyrgyz Republic
Kyrgyzstan
KRNET

Kyrgyz Seismic Network
Kyrgyzstan
KNET

Latvian Seismic Network
Latvia
LVSN

National Council for Scientific Research
Lebanon
GRAL

Geological Survey of Lithuania
Lithuania
LIT

Macao Meteorological and Geophysical Bureau
Macao, China
MCO

Geological Survey Department Malawi
Malawi
GSDM

Instituto de Geofísica de la UNAM
Mexico
MEX

Centro de Investigación Científica y de Educación Superior de Ensenada
Mexico
ECX

Institute of Geophysics and Geology
Moldova
MOLD

Seismological Institute of Montenegro
Montenegro
PDG

Centre National de Recherche
Morocco
CNRM

The Geological Survey of Namibia
Namibia
NAM

National Seismological Centre, Nepal
Nepal
DMN

IRD Centre de Nouméa
New Caledonia
NOU

Institute of Geological and Nuclear Sciences
New Zealand
WEL

Central American Tsunami Advisory Center
Nicaragua
CATAC

University of Bergen
Norway
BER

Stiftelsen NORSAR
Norway
NAO

Sultan Qaboos University
Oman
OMAN

Universidad de Panama
Panama
UPA

Philippine Institute of Volcanology and Seismology
Philippines
MAN

Manila Observatory
Philippines
QCP

Private Observatory of Pawel Jacek Wiejacz, D.Sc.
Poland
PJWWP

Institute of Geophysics, Polish Academy of Sciences
Poland
WAR

Instituto Dom Luiz, University of Lisbon
Portugal
IGIL

Instituto Português do Mar e da Atmosfera, I.P.
Portugal
INMG

Sistema de Vigilância Sismológica dos Açores
Portugal
SVSA

Centre of Geophysical Monitoring of the National Academy of Sciences of Belarus
Republic of Belarus
BELR
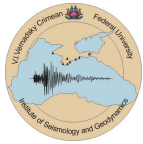
Inst. of Seismology and Geodynamics, V.I. Vernadsky Crimean Federal University
Republic of Crimea
CFUSG

Korea Meteorological Administration
Republic of Korea
KMA

National Institute for Earth Physics
Romania
BUC

Yakutiya Regional Seismological Center, GS SB RAS
Russia
YARS

North Eastern Regional Seismological Centre, GS RAS
Russia
NERS

Federal Center for Integrated Arctic Research
Russia
FCIAR

Baykal Regional Seismological Centre, GS SB RAS
Russia
BYKL

Altai-Sayan Seismological Centre, GS SB RAS
Russia
ASRS
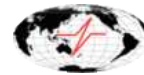
Geophysical Survey of Russian Academy of Sciences
Russia
MOS

Mining Institute of the Ural Branch of the Russian Academy of Sciences
Russia
MIRAS

Kamchatka branch of the Geophysical Survey of the Russian Academy of Sciences
Russia
KRSC
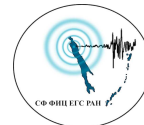
Sakhalin Experimental and Methodological Seismological Expedition, GS RAS
Russia
SKHL

Kola Regional Seismic Centre, GS RAS
Russia
KOLA

Saudi Geological Survey
Saudi Arabia
SGS

Seismological Survey of Serbia
Serbia
BEO

Geophysical Institute, Slovak Academy of Sciences
Slovakia
BRA

Slovenian Environment Agency
Slovenia
LJU

Council for Geoscience
South Africa
PRE

Real Instituto y Observatorio de la Armada
Spain
SFS

Instituto Geográfico Nacional
Spain
MDD

Institut Cartogràfic i Geològic de Catalunya
Spain
MRB

University of Uppsala
Sweden
UPP

Swiss Seismological Service (SED)
Switzerland
ZUR

Thai Meteorological Department
Thailand
BKK

The Seismic Research Centre
Trinidad and Tobago
TRN

Institut National de la Météorologie
Tunisia
TUN

Disaster and Emergency Management Presidency
Turkey
AFAD

Kandilli Observatory and Research Institute
Turkey
ISK

Pacific Northwest Seismic Network
U.S.A.
PNSN

IRIS Data Management Center
U.S.A.
IRIS

Red Sísmica de Puerto Rico
U.S.A.
RSPR

National Earthquake Information Center
U.S.A.
NEIC
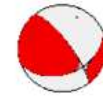
The Global CMT Project
U.S.A.
GCMT

Subbotin Institute of Geophysics, National Academy of Sciences
Ukraine
SIGU

Main Centre for Special Monitoring
Ukraine
MCSM

Dubai Seismic Network
United Arab Emirates
DSN

British Geological Survey
United Kingdom
BGS

International Seismological Centre
United Kingdom
ISC

Institute of Seismology, Academy of Sciences, Republic of Uzbekistan
Uzbekistan
ISU

Fundación Venezolana de Investigaciones Sismológicas
Venezuela
FUNV

Institute of Geophysics, Viet Nam Academy of Science and Technology
Viet Nam
PLV

Geological Survey Department of Zambia
Zambia
LSZ

Goetz Observatory
Zimbabwe
BUL

2.7   ISC Staff

Listed below are the staff (and their country of origin) who were employed at the ISC during the time period when the ISC worked on the data covered by this issue of the Summary.

- Dmitry Storchak

- Director

- Russia / United Kingdom

- Lynn Elms

- Administration Officer

- United Kingdom

- James Harris

- Senior System and Database Administrator

- United Kingdom

- Oliver Rea
- System Administrator
- United Kingdom

- John Eve
- Data Collection Officer
- United Kingdom

- Gary Job
- Data Collection Officer
- United Kingdom

- Domenico Di Giacomo
- Senior Seismologist
- Italy/UK

- Konstantinos Lentas

- Seismologist / Senior Developer

- Greece

- Tom Garth

- Seismologist / Senior Developer

- United Kingdom

- Ryan Gallacher

- Seismologist / Developer

- United Kingdom

- Rosemary Hulin

- Analyst

- United Kingdom

- Blessing Shumba
- Seismologist / Senior Analyst
- Zimbabwe

- Rebecca Verney
- Analyst
- United Kingdom

- Elizabeth Ayres
- Analyst / Historical Data Officer
- United Kingdom

- Kathrin Lieser
- Analyst Administrator / Summary Editor / Seismologist
- Germany

- Charikleia Gkarlaouni
- Seismologist / Analyst
- Greece

- Peter Franek
- Seismologist / Analyst
- Slovakia

- Burak Sakarya
- Seismologist / Analyst
- Turkey

- Daniela Olaru
- Historical and
  Bibliographical Data Officer
- Romania/UK

3

Availability of the ISC Bulletin

The ISC Bulletin is available from the following sources:

- Web searches

  The entire ISC Bulletin is available directly from the ISC website via tailored searches.
  (www.isc.ac.uk/iscbulletin/search)
  (isc-mirror.iris.washington.edu/iscbulletin/search)

    - Bulletin search - provides the most verbose output of the ISC Bulletin in ISF or QuakeML.

    - Event catalogue - only outputs the prime hypocentre for each event, producing a simple list of events, locations and magnitudes.

    - Arrivals - search for arrivals in the ISC Bulletin. Users can search for specific phases for selected stations and events.

- CD-ROMs/DVD-ROMs

  CDs/DVDs can be ordered from the ISC for any published volume (one per year), or for all back issues of the Bulletin (not including the latest volume). The data discs contain the Bulletin as a PDF, in IASPEI Seismic Format (ISF), and in Fixed Format Bulletin (FFB) format. An event catalogue is also included, together with the International Registry of seismic station codes.

- FTP site

  The ISC Bulletin is also available to download from the ISC ftp site, which contains the Bulletin in PDF, ISF and FFB formats. (ftp://www.isc.ac.uk)
  (ftp://isc-mirror.iris.washington.edu)

Mirror service

A mirror of the ISC database, website and ftp site is available at IRIS DMC (isc-mirror.iris.washington.edu), which benefits from their high-speed internet connection, providing an alternative method of accessing the ISC Bulletin.

4

Citing the International Seismological Centre

Data from the ISC should always be cited. This includes use by academic or commercial organisations, as well as individuals. A citation should show how the data were retrieved and may be in one of these suggested forms:

4.1 The ISC Bulletin

International Seismological Centre (2021), On-line Bulletin, `https://doi.org/10.31905/D808B830`

The procedures used for producing the ISC Bulletin have been described in a number of scientific articles. Depending on the use of the Bulletin, users are encouraged to follow the citation suggestions below:

a) For current ISC location procedure:

Bondár, I. and D.A. Storchak (2011). Improved location procedures at the International Seismological Centre, *Geophys. J. Int.*, *186*, 1220-1244, `https://doi.org/10.1111/j.1365-246X.2011.05107.x`

b) For Rebuilt ISC Bulletin (currently: 1964-1990):

Storchak, D.A., Harris, J., Brown, L., Lieser, K., Shumba, B., Verney, R., Di Giacomo, D., Korger, E. I. M. (2017). Rebuild of the Bulletin of the International Seismological Centre (ISC), part 1: 1964–1979. *Geosci. Lett.* (2017) 4: 32. `https://doi.org/10.1186/s40562-017-0098-z`

c) For principles of the ISC data collection process:

R J Willemann, D A Storchak (2001). Data Collection at the International Seismological Centre, *Seis. Res. Lett.*, *72*, 440-453, `https://doi.org/10.1785/gssrl.72.4.440`

d) For interpretation of magnitudes:

Di Giacomo, D., and D.A. Storchak (2016). A scheme to set preferred magnitudes in the ISC Bulletin, *J. Seism.*, *20(2)*, 555-567, `https://doi.org/10.1007/s10950-015-9543-7`

e) For use of source mechanisms:

Lentas, K., Di Giacomo, D., Harris, J., and Storchak, D. A. (2020). The ISC Bulletin as a comprehensive source of earthquake source mechanisms, *Earth Syst. Sci. Data*, *11*, 565-578,`https://doi.org/10.5194/essd-11-565-2020`

Lentas, K. (2018). Towards routine determination of focal mechanisms obtained from first motion P-wave arrivals, *Geophys. J. Int.*, *212(3)*, 1665–1686.`https://doi.org/10.1093/gji/ggx503`

f) For use of the original (pre-Rebuild) ISC Bulletin as a historical perspective:

Adams, R.D., Hughes, A.A., and McGregor, D.M. (1982). Analysis procedures at the International Seismological Centre. *Phys. Earth Planet. Inter. 30:* 85-93,`https://doi.org/10.1016/0031-9201(82)90093-0`

4.2   The Summary of the Bulletin of the ISC

International Seismological Centre (2021), Summary of the Bulletin of the International Seismological Centre, July - December 2018, *55(II)*,`https://doi.org/10.31905/FPHTHHU7`

4.3   The historical printed ISC Bulletin (1964-2009)

International Seismological Centre, Bull. Internatl. Seismol. Cent., 46(9-12), Thatcham, United Kingdom, 2009.

4.4   The IASPEI Reference Event List

International Seismological Centre (2021), IASPEI Reference Event (GT) List, `https://doi.org/10.31905/32NSJF7V`

Bondár, I. and K.L. McLaughlin (2009). A New Ground Truth Data Set For Seismic Studies, *Seismol. Res. Lett.*, *80*, 465-472, `https://doi.org/10.1785/gssrl.80.3.465`

Bondár, E. Engdahl, X. Yang, H. Ghalib, A. Hofstetter, V. Kirichenko, R. Wagner, I. Gupta, G. Ekström, E. Bergman, H. Israelsson, and K. McLaughlin (2004). Collection of a reference event set for regional and teleseismic location calibration, *Bull. Seismol. Soc. Am.*, *94*, 1528-1545, `https://doi.org/10.1785/012003128`

Bondár, E. Bergman, E. Engdahl, B. Kohl, Y.-L. Kung, and K. McLaughlin (2008). A hybrid multiple event location technique to obtain ground truth event locations, *Geophys. J. Int.*, *175*, `https://doi.org/10.1111/j.1365-246X.2011.05011.x`

4.5   The ISC-GEM Catalogue

International Seismological Centre (2021), ISC-GEM Earthquake Catalogue, `https://doi.org/10.31905/d808b825`, 2021.

Depending on the use of the Catalogue, to quote the appropriate scientific articles, as suggested below.

a) For a general use of the catalogue, please quote the following three papers (Storchak et al., 2013; 2015; Di Giacomo et al., 2018):

Storchak, D.A., D. Di Giacomo, I. Bondár, E.R. Engdahl, J. Harris, W.H.K. Lee, A. Villaseñor and P. Bormann (2013). Public Release of the ISC-GEM Global Instrumental Earthquake Catalogue (1900-2009). *Seism. Res. Lett.*, *84*, 5, 810-815, `https://doi.org/10.1785/0220130034`

Storchak, D.A., D. Di Giacomo, E.R. Engdahl, J. Harris, I. Bondár, W.H.K. Lee, P. Bormann and A. Villaseñor (2015). The ISC-GEM Global Instrumental Earthquake Catalogue (1900-2009): Introduction, *Phys. Earth Planet. Int.*, *239*, 48-63, `https://doi.org/10.1016/j.pepi.2014.06.009`

Di Giacomo, D., E.R. Engdahl and D.A. Storchak (2018). The ISC-GEM Earthquake Catalogue (1904–2014): status after the Extension Project, *Earth Syst. Sci. Data*, *10*, 1877-1899, `https://doi.org/10.5194/essd-10-1877-2018`

b) For use of location parameters, please quote (Bondár et al., 2015):

Bondár, I., E.R. Engdahl, A. Villaseñor, J. Harris and D.A. Storchak, 2015. ISC-GEM: Global Instrumental Earthquake Catalogue (1900-2009): II. Location and seismicity patterns, *Phys. Earth Planet. Int.*, *239*, 2-13, `https://doi.org/10.1016/j.pepi.2014.06.002`

c) For use of magnitude parameters, please quote (Di Giacomo et al., 2015a; 2018):

Di Giacomo, D., I. Bondár, D.A. Storchak, E.R. Engdahl, P. Bormann and J. Harris (2015a). ISC-GEM: Global Instrumental Earthquake Catalogue (1900-2009): III. Re-computed MS and mb, proxy MW, final magnitude composition and completeness assessment, *Phys. Earth Planet. Int.*, *239*, 33-47, `https://doi.org/10.1016/j.pepi.2014.06.005`

Di Giacomo, D., E.R. Engdahl and D.A. Storchak (2018). The ISC-GEM Earthquake Catalogue (1904–2014): status after the Extension Project, *Earth Syst. Sci. Data*, *10*, 1877-1899, `https://doi.org/10.5194/essd-10-1877-2018`

d) For use of station data from historical bulletins, please quote (Di Giacomo et al., 2015b; 2018):

Di Giacomo, D., J. Harris, A. Villaseñor, D.A. Storchak, E.R. Engdahl, W.H.K. Lee and the Data Entry Team (2015b). ISC-GEM: Global Instrumental Earthquake Catalogue (1900-2009), I. Data collection from early instrumental seismological bulletins, *Phys. Earth Planet. Int.*, *239*, 14-24, `https://doi.org/10.1016/j.pepi.2014.06.005`

Di Giacomo, D., E.R. Engdahl and D.A. Storchak (2018). The ISC-GEM Earthquake Catalogue (1904–2014): status after the Extension Project, *Earth Syst. Sci. Data*, *10*, 1877-1899, `https://doi.org/10.5194/essd-10-1877-2018`

e) For use of direct values of M0 from the literature, please quote (Lee and Engdahl, 2015):

Lee, W.H.K. and E.R. Engdahl (2015). Bibliographical search for reliable seismic moments of large earthquakes during 1900-1979 to compute MW in the ISC-GEM Global Instrumental Reference Earthquake Catalogue (1900-2009), *Phys. Earth Planet. Int.*, *239*, 25-32, `https://doi.org/10.1016/j.pepi.2014.06.004`

4.6 The ISC-EHB Dataset

International Seismological Centre (2021), ISC-EHB Dataset, `https://doi.org/10.31905/PY08W6S3`

Engdahl, E.R., R. van der Hilst, and R. Buland (1998). Global teleseismic earthquake relocation with improved travel times and procedures for depth determination, *Bull. Seism. Soc. Am.*, *88*, 3, 722-743.

`http://www.bssaonline.org/content/88/3/722.abstract`

Weston, J., Engdahl, E.R., Harris, J., Di Giacomo, D. and Storchack, D.A. (2018). ISC-EHB: Reconstruction of a robust earthquake dataset, *Geophys. J. Int.*, *214*, 1, 474-484, `https://doi.org/10.1093/gji/ggy155`

4.7   The ISC Event Bibliography

International Seismological Centre (2021), On-line Event Bibliography, `https://doi.org/10.31905/EJ3B5LV6`

Also, please reference the following SRL article that describes the details of this service:

Di Giacomo, D., Storchak, D.A., Safronova, N., Ozgo, P., Harris, J., Verney, R. and Bondár, I., 2014. A New ISC Service: The Bibliography of Seismic Events, *Seismol. Res. Lett.*, *85*, 2, 354-360, `https://doi.org/10.1785/0220130143`

4.8   International Registry of Seismograph Stations

International Seismological Centre (2021), International Seismograph Station Registry (IR), `https://doi.org/10.31905/EL3FQQ40`

4.9   Seismological Dataset Repository

International Seismological Centre (2021), Seismological Dataset Repository, `https://doi.org/10.31905/6TJZECEY`

4.10   Data transcribed from ISC CD-ROMs/DVD-ROMs

International Seismological Centre, Bulletin Disks 1-29 [CD-ROM], Internatl. Seismol. Cent., Thatcham, United Kingdom, 2021.

The ISC is named as a valid data centre for citations within American Geophysical Union (AGU) publications. As such, please follow the AGU guidelines when referencing ISC data in one of their journals. The ISC may be cited as both the institutional author of the Bulletin and the source from which the data were retrieved.

5

Operational Procedures of Contributing Agencies

5.1 Observatorio San Calixto – National Seismic, Infrasound and Strong Motion Network of Bolivia (Plurinational State of)

Mayra Nieto[1], Bastien Joly[2], Gonzalo A. Fernández M [1], Felipe Condori [1], Jonas Baldivieso [1], Teddy Griffiths [1], Walter Arce [1] and Zulma Machaca [1]

(1) Observatorio San Calixto, La Paz, Bolivia (Plurinational State of)
(2) Commissariat à l'Energie Atomique / Département Analyse, Surveillance, Environnement, France

Team of Observatorio San Calixto in La Paz, Bolivia

The history of seismic studies at the Plurinational State of Bolivia begins around the first decade of the past century and is strongly related to the foundation of Observatorio San Calixto (OSC) which is the only institution committed to seismology in Bolivia since 1st May 1913. The Bolivian Jesuit Company took the responsibility to install and operate a seismic station at La Paz, Bolivia, after the suggestion was made by the Second Seismology General Assembly held in 1911.

Thanks to the commitment of the Jesuit Principals that ran our institution (Pierre M. Descotes SJ from 1913 to 1964, Ramon Cabré SJ from 1964 to 1993 and Lawrence Drake SJ from 1993 to 2000) long term agreements were made on behalf of seismology in our country. The first one is with the Air Force Technical Application Center (AFTAC) and United States Geological Survey (USGS) for contributing real time data to the World Wide Standard Seismological Network and to the Comprehensive Test Ban Treaty Organization (CTBTO). The second agreement is with formerly "Laboratoire de Geophysique" (LDG) that later became "Commissariat à l'Energie Atomique / Département Analyse, Surveillance, Environnement" (CEA/DASE) in France. Both agreements allowed us to improve the study of seismology in our country.

Nowadays, our seismic network is called "Red Sismologica Observatorio San Calixto" (RS-OSC) and is

composed of our own stations as well as stations installed by collaborative partners such as CEA/DASE from France for stations BBOB, BBOD, BBOE, BBOJ (short period sensors), SIV (long period station) and an infrasound array (IS08). AFTAC from the U.S contributes one high gain borehole broadband seismic sensor, another high gain borehole short period (LPAZ and LPAZ1) and four short period sensors (SOEP, SOEH, SOEV, REDDE). Data from all of these stations is shared with the seismological community. The University of Sao Paulo (USP) from Brazil provides three broadband sensors (BBSD, BBRT, BBPS). Finally, our own seismic stations are four broadband stations (SOEJ, SOEO, SOEA, SOET) and three strong motion stations (AOEA, AOES, AOVT). Figure 5.6 shows our seismic network configuration with all stations contributing to the seismic and infrasound monitoring over the country.

In this document we would like to highlight the history of our seismic networks and the importance of each one that contributes to the geophysics, seismology and earthquake engineering sciences in our country.

5.1.1   Local Seismicity

The seismic activity in Bolivia is strongly related to the subduction process between the Nazca (oceanic) and South American (continental) plates, where the former subducts underneath the latter along the Peru – Chile trench in ENE-WSW direction with a rate of 78 mm/year (*DeMets et al.,* 1994), (see detailed explanations at e.g., *Ward et al.*, 2013; *Eichelberger et al.*, 2015; *Ryan et al.*, 2016; *Anderson et al.*, 2017).

Bolivia's seismicity is composed of inter-plate and shallow seismicity. Inter-plate seismicity is related to intermediate and deep earthquakes which are linked to the subduction process and can reach depths of 650 km. Below the central part of our country, seismicity caused by the subduction process occurs at depths from 100 to 350 km, and then continues at depths from 500 to 700 km.

The other seismic source, shallow seismicity, is related to crustal deformation and is located at the Bolivian Orocline that is composed of the Eastern and Sub Andes belt Cordillera. The crust from West to East shows a thickness variation from 60 to 45 km and a very complex variation from North to South (*Wigger et al.*, 1994). Moreover, more distant seismic sources (from Chile, Peru and Argentina) are also felt and represent a hazard for us. Figure 5.1 represents all seismological sources from our country.

5.1.2   History of Seismic, Strong Motion and Infrasound Network

First Generation

Seismic Station LPZ (1913-1964):

Installed in 1913, LPZ was the first seismic station of the Plurinational State of Bolivia, located at the San Calixto school crypt at the city of La Paz. The first mechanical equipment had two horizontal bifilar pendulums, the same as for the Mainka seismograph, and were built by Pierre M. Descotes SJ (first principal) and Tortosa and Lizarralde from the Jesuit Company (Fig. 5.2). The masses weighed 1500 kg (vertical component), 2000 kg (N-S component) and 3500 kg (E-W component). The station worked until 1964.
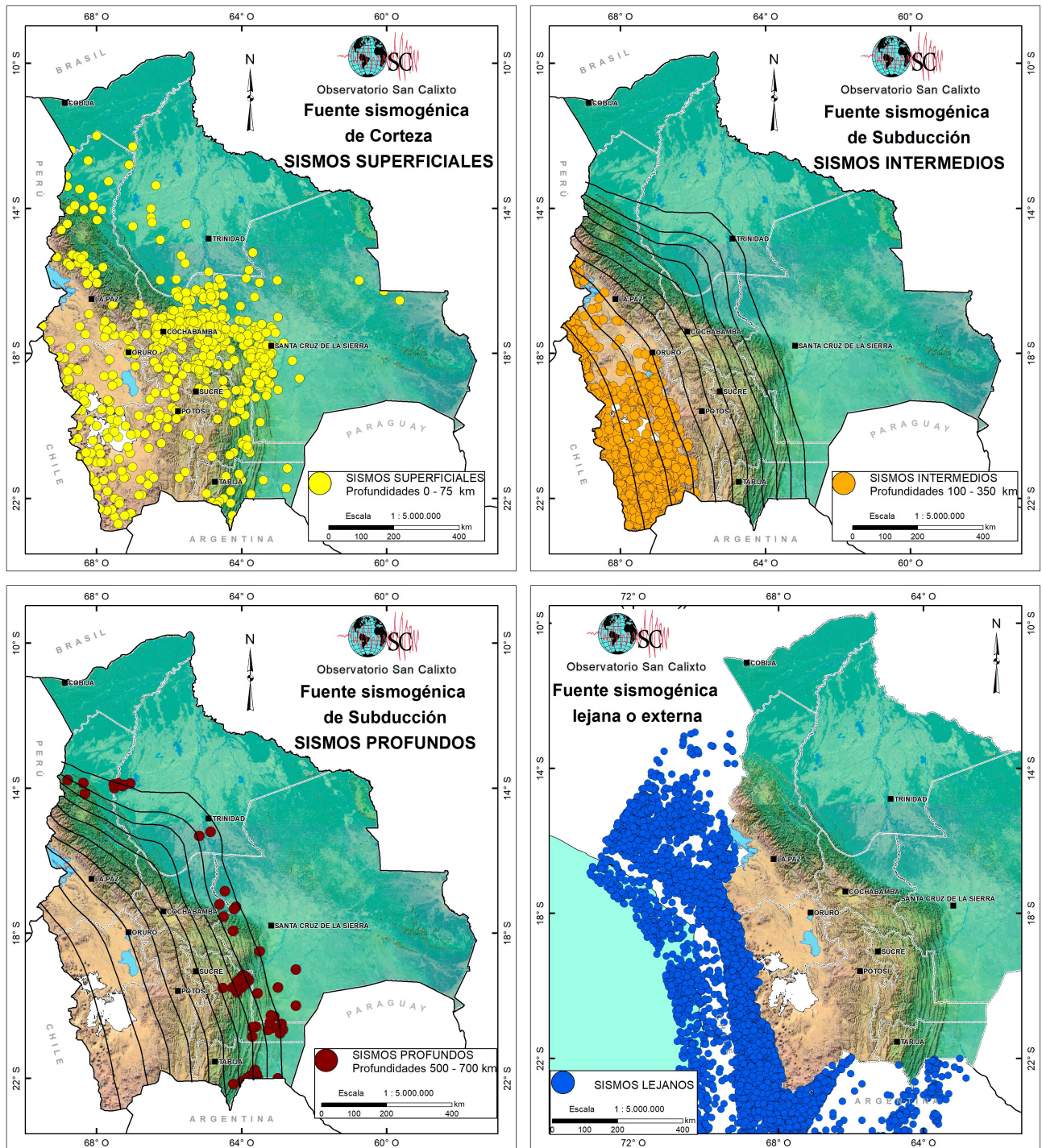
Figure 5.1: *Seismicity of Bolivia from 1650 to 2018 (Mw ≥ 4).* Top left: *Yellow circles are shallow seismicity (depths from 0 to 75 km),* top right: *orange circles are intermediate depth seismicity (depths from 100 to 350 km),* bottom left: *red circles are deep seismicity (depths from 500 to 700 km),* bottom right: *blue circles are distant seismic sources felt in our country.*
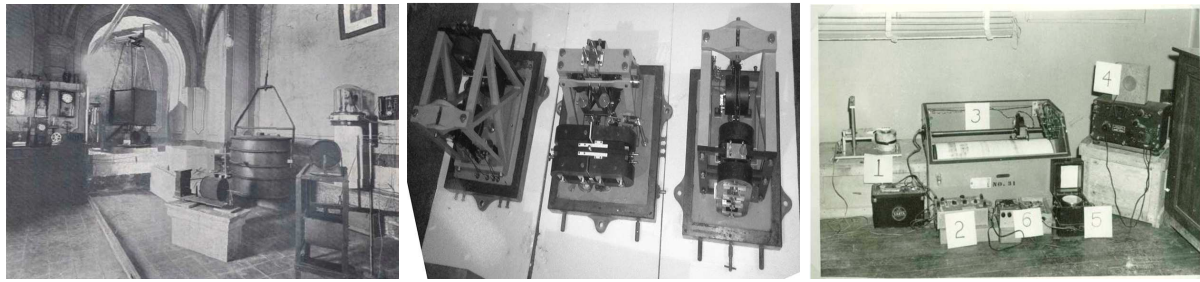
(a) Modified Maika seismometer   (b) Galitzin-Wilip sensors   (c) Spregnether seismic sensor

Figure 5.2: *Different sensors at LPZ seismic station. (*Minaya et al.*, 2013).*

The first Principal was devoted to reading the seismograms to create the seismic bulletins, which were shared with other Jesuit observatories in Spain and France, for that reason he was recognized by the international community. In 1930 a new seismic sensor "Galitzin and Wilip" was installed in the same place and a new helicorder drum was also set up to record the seismograms on film paper. Years later, Gutenberg and Richter assessed that LPZ was one of the best stations in the world and complimented the operators for their great work: "A further improvement followed the installation at La Paz (Bolivia) with reports beginning May 1, 1913. La Paz at once became, and still remains, the most important single seismological station of the world. This is a consequence of its isolated location, the sensitive instruments, and the great care with which records were interpreted and reports issued under the direction of Father Descotes." (*Gutenberg and Richter*, 1949). In 1958 the United States Coast and Geodetic Survey donated a short period vertical component sensor (Spregnether) that was installed in the same place (Fig. 5.2). In 1963 due to the increasing background noise of La Paz LPZ needed to be placed outside the city (*Cabre*, 1974; *Ayala*, 1997).

Estación Sísmica Sucre (1926 - 1948):

In 1926, the same seismic equipment as at LPZ was installed at the "Sagrado Corazón" school (Chuquisaca – Sucre) with the station code SUC. Unfortunately, the earthquake of 27th March 1948 with a magnitude of 6.1 destroyed the sensors when the roof collapsed and there was no solution to fix the mechanical parts of the seismograph (*Cabre and Vega*, 1995).

Second Generation

Seismic Station LPB (1962 - 1997):

In 1962, a new seismic station was installed with the code LPB, located at Seguencoma neighbourhood in La Paz city. This station was part of the World-Wide Standard Station Network (WWSSN) and was supported by the U.S. Coast and Geodetic Survey (*Cabre*, 1965). It was composed of a Benioff short period three component sensor and Spregnether long period three component sensors (Fig. 5.3). A helicorder was used to register the seismograms. LPB shared bulletin data with the international seismological community until 1997, when the station was closed due to the increased background noise of the city (*Ayala*, 2001).

Figure 5.3: Left: *LPB installation at Seguencoma, La Paz - Department,* Right: *Benioff short period seismometer at Seguencoma. (*Minaya et al.*, 2013).*

Andina Seismic Network (1960-1976):

In 1960 within the framework of the International Geophysical year (1957 – 1958) the Earth Magnetism Carnegie Institution of Washington suggested to donate six semi portable seismic sensors to Bolivia. They were installed over the country until 1976. The aim was to gain a better knowledge of the seismicity in our country (*Cabre*, 1974; *Ayala*, 2001).

Geophysical Network of Peñas (1963-1975):

In 1965 the Observatorio San Calixto was in charge of operating and maintaining seven seismic stations (Geotech) financed by the Advanced Research Projects Agency (ARPA) from the U.S. They were installed in the town of Peñas (La Paz – Department). In 1966 an infrasound array was also installed that composed of four elements. In 1970 a set of three elements was added. The seismic network and the infrasound array registered the data on helicorder drums and film paper until 1975 (*Cabre, 1974; Ayala, 2001).*

Third Generation

Tupiza Seismic Station (1985 - 1987):

In 1985 cooperation between the Free University of Berlin and Yacimientos Petroliferos Fiscales Bolivianos allowed us to install a seismic station at Tupiza town (Potosi Department). The code was TZP and it worked until 1987 (*Ayala*, 2001).

Cochabamba Seismic Network (1998 - 1998):

In 1998 a set of three seismic stations was donated by the Japan International Cooperation Agency (JICA) to be installed at Cochabamba Department. The codes assigned to the stations were: BBBO (Bombeo), BAPC (Apacheta) and BIKK (C. Kollo). The waveforms were sent by VHF radio link to

Juan XXIII school located at the center of the city. Unfortunately, vandalism prevented the seismic network operating fully.

Seismic and Infrasound Network CEA/DASE (1975 – Recent):

In 1975, thanks to an agreement with the "Laboratoire de Geophysique" (LDG) in France and the Paris University a long term collaboration began. Years later, the "Commissariat à l'Energie Atomique / Département Analyse, Surveillance, Environnement" (CEA/DASE) assumed the responsibility to continue this project in coordination with our institution.

The same year, three seismic stations (short period, one component, high gain) were installed in Zongo valley (La Paz – Department) with the station codes: BBOA (Zongo), BBOB (Banderani) and BBOC (Huaylipaya). Data was sent in near real time by UHF radio links to our data center located at La Paz city. Years later, from 1982 to 1993, this network was expanded and four more stations were installed: BBOD (Gloria), BBOE (Chanca), BBOF (Collana) and BBOG (Alto Peñas). Moreover, a three-component high gain short period sensor was installed at San Ignacio de Velazco (SIV) at Santa Cruz Department.

In 1999, the CEA/DASE installed an infrasound array of four elements in Peñas town. This array is certified by CTBTO. The station code is IS08 and data is sent in near real time to our data center (La Paz City), the International Data Center (IDC) and the French national data center (CEA/DASE). Data from this station contributed a lot to atmospheric modelling (*Ayala*, 2001; *LePichon et al.*, 2005, 2006).

Fourth Generation

BID Seismic Network (2010-2014):

The "Banco Interamericano del Desarrollo (BID)" financed the installation of 18 seismic stations over the country in cooperation with the national telecom company (ENTEL). The data arrived at our data center through 3G mobile communication (*Minaya et al.*, 2012).

Figure 5.4: Left: *BBOI short period station,* Middle: *BBOK short period station,* Left: *BBOM short period station.*

Figure 5.5: Left: *ZOBO seismic station (Huayna Potosí mountain Tunnel),* Right: *LPAZ seismic station (Milluni). (*Minaya et al.*, 2013).*

Short Period Seismic Network CEA/DASE:

In order to expand the seismic network and to strengthen the agreement with CEA/DASE a new set of seismic stations were installed from 2006 to 2007: BBOI (Colquencha), BBOM (Mururata), BBOK (Pakuani) and BBOJ (Jacaque) (Fig. 5.4). However, due to some incidents (natural and man-made) only BBOJ remained part of the Short Period Seismic network.

Fifth Generation

High Gain Seismic Station LPAZ (1972 – Recent):

In 1972 the National Oceanic and Atmospheric Administration from the U.S supported the installation of a high gain long period seismic sensor (HGLP) around Zongo town (La Paz Department). A 70 m tunnel was built to get a good signal to noise ratio and high-quality waveforms. The tunnel was located at the foot of "Huayna Potosi Mountain". In 1976, this seismic station was upgraded to be part of the Advanced Seismological Research Observatory and the code changed to ZOBO. (*Cabré*, 1988).

In 1993, ZOBO was closed but a major upgrade was done and the station was reopened as LPAZ. A new place was found around Miluuni town (La Paz – Department) where two boreholes were drilled to install a three-component broadband sensor and a vertical component short period sensor (Figure 5.5). The station became part of the Global Telemetered Seismograph Network (GTSN) and data was exchanged with the U.S. National Data Center and AFTAC.

In 1999, this seismic station was certified by CTBTO under the code: PS06, (Primary Station 06). Since then, the data is passed to IDC and becomes open data through the Incorporated Research Institutions for Seismology (IRIS). The data is transmitted by a VSAT C – band in near real time to our data center (*Cabre*, 1974; *Ayala*, 2001).

Long Period Seismic Station – SIV:

In 1998 a lot of effort was made to install a seismic station in coordination with CEA/DASE in the Sub Andes region (Santa Cruz - Department). Initially it was composed of three short period sensors and installed in San Ignacio de Velazco. A central facility was also installed at the Santa Clara Monastery. The data were saved on floppy disk and then sent to our main data center. In 1998 a big upgrade was made at the station and three high gain long period sensors were installed. The data was transmitted from the station to the central facility in Santa Clara Monastery by UHF radio link and from there was sent to our data center and the French national data center through a VSAT C-band. The assigned station code was SIV. In 2008, this station was certified by CTBTO with the code AS08 (Auxiliary Station 08).

Figure 5.6: *Seismological Network Observatorio San Calixto (RS-OSC). Blue triangles are stations of the local seismic network, magenta circles are stations of the local accelerometer network and yellow diamonda are stations of the infrasound permanent network.*

Observatorio San Calixto Seismic Network (RS-OSC):

In order to improve the seismic location within our country and enhance the research in seismology we decided to install four broadband Guralp-6TD and three strong motion Guralp-5C sensors. With a Raspberry Pi board that functions as 3G data bridge data is sent in real time to our data center. The codes for the broadband sensors are SOEJ, SOET, SOEO and SOEA and are distributed over the country. The strong motion stations are AOVT, AOES and AOEA. This small seismic network is called "Red Sismologica Observatorio San Calixto" (RS-OSC) and is shown in Figure 5.6 (*Schamberger et al.,* 2016).

Table 5.1 summarises the seismic stations installed in Bolivia over time.

Table 5.1: *Current (Seismic station installed in Bolivia along the time supported by different projects (some temporary and others permanent). OSC = Observatorio San Calixto, IGB = Instituto Boliviano de Geofisica, WWSSN/USGS = World Wide Standardized Seismograph Network/ United States Geological Survey, ARPA = Advanced Research Projects Agency, CEA/DASE = Commissariat à l'Energie Atomique / Département Analyse, Surveillance, Environnement, RS-OSC = Red Sismica Observatorio San Calixto, JICA = Japan International Cooperation Agency, BID = Banco Interamericano de Desarrollo, AFTAC/USGS = Air Force Technical Application Center / United States Geological Survey, USP = Universidade de Sao Paulo*

	Name	Code	Operating Dates	Lat / deg	Lon / deg	Elev. / m	Geomorph. Region	Main Characteristics	Belongs to
1	Ciudad de La Paz	LPZ	1913-1964	-16.495	-68.133	3651	Eastern Cordillera	1913: San Calixto Seismograph 1500 kg (LP:Z)	OSC
2	Ciudad de La Paz	LPZ	1913-1964	-16.495	-68.133	3651	Eastern Cordillera	1913: Mainka Modified 2000 kg (LP:N)	OSC
3	Ciudad de La Paz	LPZ	1913-1964	-16.495	-68.133	3651	Eastern Cordillera	1913: Mainka Modified 3500 kg (LP:E)	OSC
4	Ciudad de La Paz	LPZ	1930-1958	-16.495	-68.133	3651	Eastern Cordillera	1930: Galitzin-Wilip Seismic Sensor (LP:ZNE)	OSC
5	Ciudad de La Paz	LPZ	1958-1964	-16.495	-68.133	3651	Eastern Cordillera	1958: Sprengnether Seismic Sensor (SP:Z)	OSC
6	Ciudad de Sucre	SUC	1926-1948	-19.047	-65.264	2796	Eastern Cordillera	1926: San Calixto Seismic Sensor 1500 kg (SP:Z)	OSC
7	Ciudad de Sucre	SUC	1926-1948	-19.047	-65.264	2796	Eastern Cordillera	1926: Mainka Modified 3000 kg (LP: NE)	OSC
8	Cochabamba	CCH	1960-1962	-17.458	-66.121	2634	Eastern Cordillera	1960: Wilson-Lamison Seismic Sensor (SP:Z)	IGB
9	Cochabamba	CCH	1963-1975	-17.458	-66.121	2634	Eastern Cordillera	1963. Wilson-Lamison Seismic Sensor (SP:Z)	IGB
10	Coroico	CRO	1961-1962	-16.183	-67.720	1422	Eastern Cordillera	1961: Wilson-Lamison Seismic Sensor (SP:Z)	IGB
11	Mallasilta	MLL	1961-1961	-16.554	-68.111	3407	Eastern Cordillera	1961: Wilson-Lamison Seismic Sensor (SP:Z)	IGB
12	Peñas	PNS	1961-1965	-16.232	-68.513	4057	Altiplano	1961: Wilson-Lamison Seismic Sensor (SP:Z)	IGB

	Name	Code	Operating Dates	Lat / deg	Lon / deg	Elev. / m	Geomorph. Region	Main characteristics	Belongs to
13	Sicasica	SCS	1961-1967	-17.285	-67.815	3897	Altiplano	1961: Wilson-Lamison Seismic Sensor (SP:Z)	IGB
14	Desaguadero	DSG	1961-1965	-16.559	-69.025	3839	Altiplano	1961: Wilson-Lamison Seismic Sensor (SP:Z)	IGB
15	Tarija	TEU	1964-1968	-21.513	-64.776	2004	Eastern Cordillera	1964: Wilson-Lamison Seismic Sensor (SP:Z)	IGB
16	Samaipata	SMB	1964-1966	-18.181	-63.875	1643	Subandean zone	1964: Wilson-Lamison Seismic Sensor (SP:Z)	IGB
17	Riberalta	RTA	1965-1967	-11.007	-66.078	136	Chaco Beniana plain	1965: Wilson-Lamison Seismic Sensor (SP:Z)	IGB
18	Chacaltaya	CHA	1966-1967	-16.346	-68.125	5261	Eastern Cordillera	1966: Wilson-Lamison Seismic Sensor (SP:Z)	IGB
19	Harca	HAA	1970-1971	-16.083	-68.042	1757	Eastern Cordillera	1970: Wilson-Lamison Seismic Sensor (SP:Z)	IGB
20	Zongo	ZLPB	1970-1971	-16.269	-68.119	4439	Eastern Cordillera	1970: Wilson-Lamison Seismic Sensor (SP:Z)	IGB
21	Charaña	CHÑ	1976-1976	-17.555	-69.442	4097	Western Cordillera	1976: Wilson-Lamison Seismic Sensor (SP:Z)	IGB
22	Huachacalla	HUG	1976-1976	-18.770	-68.283	3814	Altiplano	1976: Wilson-Lamison Seismic Sensor (SP:Z)	IGB
23	Seguencoma	LPB	1962-1997	-16.533	-68.098	3294	Eastern Cordillera	Sprengnether Seismic sensor (LP:ZNE)	WWSSN/ USGS
24	Peñas	Z-1	1963-1975	-16.249	-68.494	4254	Altiplano	1963 - 1975: Johnson-Matheson SP:Z (Peñas Seismic Network)	ARPA
25	Peñas	Z-2	1963-1975	-16.249	-68.491	4159	Altiplano	1963 - 1975: Johnson-Matheson SP:Z (Peñas Seismic Network)	ARPA
26	Peñas	Z-3	1963-1975	-16.258	-68.480	3987	Altiplano	1963 - 1975: Johnson-Matheson SP:Z (Peñas Seismic Network)	ARPA
27	Peñas	Z-4	1963-1975	-16.268	-68.475	3978	Altiplano	1963 - 1975: Johnson-Matheson SP:Z (Peñas Seismic Network)	ARPA
28	Peñas	Z-5	1963-1975	-16.264	-68.491	4088	Altiplano	1963 - 1975: Johnson-Matheson SP:Z (Peñas Seismic Network)	ARPA
29	Peñas	Z-6	1963-1975	-16.266	-68.497	3964	Altiplano	1963 - 1975: Johnson-Matheson SP:Z (Peñas Seismic Network)	ARPA
30	Peñas	Z-7	1963-1975	-16.274	-68.508	3942	Altiplano	1963 - 1975: Johnson-Matheson SP:Z (Peñas Seismic Network)	ARPA
31	Zongo	BBOA	1975-1999	-16.269	-68.124	4361	Eastern Cordillera	1975 -2000: Seismic Sensor ZM 500 (SP:Z)	CEA/ DASE

	Name	Code	Operating Dates	Lat / deg	Lon / deg	Elev. / m	Geomorph. Region	Main characteristics	Belongs to
32	Banderani	BBOB	1975 -	-16.144	-68.133	3733	Eastern Cordillera	Since 1976: Seismic Sensor ZM 500 (SP:Z)	CEA/ DASE
33	Huaylipaya	BBOC	1975-1993	-16.051	-68.004	1635	Eastern Cordillera	1977 -2000: Seismic Sensor ZM 500 (SP:Z)	CEA/ DASE
34	Chanca	CNCB	1982-1990	-16.813	-67.982	4305	Eastern Cordillera	1982-1990: Teledyne/Geotech S-13 SP:Z	CEA/ DASE
35	Chanca	BBOE	1988 -	-16.813	-67.982	4305	Eastern Cordillera	1975 -Keep working: Seismic Sensor ZM 500 (SP:Z)	CEA/ DASE
36	Gloria	BBOD	1986 -	-16.637	-68.598	4190	Altiplano	1975 – Keep working: Seismic Sensor ZM 500 (SP:Z)	CEA/ DASE
37	Collana	BBOF	1993-2000	-16.954	-68.338	4285	Altiplano	1975 – 2000: Seismic Sensor ZM 500 (SP:Z)	CEA/ DASE
38	Alto Peñas	BBOG	1999-2000	-16.266	-68.472	3966	Altiplano	1975 - 2000: Seismic Sensor ZM 500 (SP:Z)	CEA/ DASE
39	San Ignacio	SIV	1988-1998	-16.413	-60.984	590	Brazilian shield	1988 – 1998: Seismic Sensor ZM 500 (SP:ZNE)	CEA/ DASE
40	San Ignacio	SIV	1991-. . .	-15.991	-61.072	555	Brazilian shield	1991 – Keep working (certified CTBTO) :ZM 500 (SP:ZNE) and LP 500 (LP:ZNE)	CEA/ DASE
41	Tupiza	TPZ	1985-1987	-21.465	-65.711	2982	Eastern Cordillera	1985-1987: Seismic Sensor Portacofder (SP:Z)	RS-OSC
42	Cochabamba	CCH	1985-1998	-17.384	-66.134	2838	Eastern Cordillera	1985 – 1998: Seismic Sensor Spreagaether MEQ-200 (SP:Z)	JICA
43	Bombeo	BBBO	1998-1999	-17.658	-66.438	3210	Eastern Cordillera	1998 - 1999: Seismic Sensor Lennartz (SP:ZNE)	JICA
44	Apacheta	BAPC	1998-1999	-17.359	-66.025	3598	Eastern Cordillera	1998 – 1999: Seismic Sensor Lennartz (SP:ZNE)	JICA
45	Cr, Ichu, KkoIlu	BIKK	1998-1999	-17.251	-66.326	4577	Eastern Cordillera	1998 – 1999: Seismic Sensor Lennartz (SP:ZNE)	JICA
46	Col Juan XXIII	CJX	1998-1999	-17.375	-66.193	2569	Eastern Cordillera	1998 – 1999: Seismic Sensor Lennartz (SP:ZNE)	JICA
47	Zongo	ZLP	1972-1976	-16.270	-68.118	4511	Eastern Cordillera	1972 – 1976: Seismic Sensor HGLP:LP:ZNE	AFTAC/ USGS
48	Zongo	ZOBO	1976-1993	-16.269	-68.124	4361	Eastern Cordillera	1976 – 1993: Seismic Sensor type ASRO:ZNE	AFTAC/ USGS
49	Zongo	LPAZ	1973 -	-16.288	-68.131	4772	Eastern Cordillera	1976 -1993: Seismic Sensor type ASRO:ZNE	AFTAC/ USGS
50	Montecillos	BB01	2011-2012	-18.070	-65.260	2297	Eastern Cordillera	2011 – 2012: GURALP – 6TD (ZNE)	BID - OSC

	Name	Code	Operating Dates	Lat / deg	Lon / deg	Elev. / m	Geomorph. Region	Main characteristics	Belongs to
51	La Guardia	BB02	2011-2012	-17.900	-63.320	524	Subandean zone	2011 – 2012: GURALP – 6TD (ZNE)	BID - OSC
52	San Juaquin	BB03	2011-2012	-17.030	-64.880	229	Chaco Beni-ana plain	2011 – 2012: GURALP – 6TD (ZNE)	BID - OSC
53	Tambo Quemado	BB04	2012-2012	-18.280	-69.010	4379	Western Cordillera	2011 – 2012: GURALP – 6TD (ZNE)	BID - OSC
54	Carapari	BB05	2012-2012	-21.830	-63.740	831	Subandean zone	2011 – 2012: GURALP – 6TD (ZNE)	BID - OSC
55	Yocalla	BB06	2012-2012	-19.390	-65.910	3420	Eastern Cordillera	2011 – 2012: GURALP – 6TD (ZNE)	BID - OSC
56	Casarave	BB07	2012-2012	-14.861	-64.493	164	Chaco Beni-ana plain	2011 – 2012: GURALP – 6TD (ZNE)	BID - OSC
57	Balcon	SIX 01	2011-2012	-20.730	-65.190	2816	Eastern Cordillera	2011 – 2012: SIXAOLA (SP:ZNE)	BID - OSC
58	Patallajta	SIX02	2011-2012	-19.110	-65.070	2807	Eastern Cordillera	2011 – 2012: SIXAOLA (SP:ZNE)	BID - OSC
59	Mojotorillo	SIX03	2011-2012	-19.320	-64.380	2667	Eastern Cordillera	2011 – 2012: SIXAOLA (SP:ZNE)	BID - OSC
60	Villa Nueva	SIX04	2011-2012	-20.060	-65.340	3313	Eastern Cordillera	2011 – 2012: SIXAOLA (SP:ZNE)	BID - OSC
61	Cuyupaya	SIX05	2011-2012	-17.010	-65.940	1806	Eastern Cordillera	2011 – 2012: SIXAOLA (SP:ZNE)	BID - OSC
62	Camiri	SIX06	2012-2012	-20.020	-63.530	795	Subandean zone	2011 – 2012: SIXAOLA (SP:ZNE)	BID - OSC
63	San Felipe	SIX07	2012-2012	-17.970	-67.130	3900	Altiplano	2011 – 2012: SIXAOLA (SP:ZNE)	BID - OSC
64	Vallegrande	SIX08	2011-2012	-18.500	-64.110	2112	Eastern Cordillera	2011 – 2012: SIXAOLA (SP:ZNE)	BID - OSC
65	Huarina	SIX09	2012-2012	-16.189	-68.609	3833	Altiplano	2011 – 2012: SIXAOLA (SP:ZNE)	BID - OSC
66	Tuti	SIX10	2011-2012	-17.460	-65.860	4018	Eastern Cordillera	2011 – 2012: SIXAOLA (SP:ZNE)	BID - OSC
67	Colquencha	BBOI	2006-2008	-16.956	-68.338	4308	Altiplano	2006 – 2008: Seismic Sensor ZM 500 (SP:Z)	CEA/ DASE
68	Jacaque	BBOJ	2007 -	-16.980	-68.190	4016	Altiplano	Since 2007: Seismic Sensor ZM 500 (SP:Z)	CEA/ DASE
69	Pacuani	BBOK	2007-2008	-16.579	-67.874	4584	Eastern Cordillera	2007 – 2008: Seismic Sensor ZM 500 (SP:Z)	CEA/ DASE
70	Mururata	BBOM	2008-2010	-16.499	-67.854	4792	Eastern Cordillera	2007 – 2010: Seismic Sensor ZM 500 (SP:Z)	CEA/ DASE
71	Ciudad de Tarija	AOVT	2016 -	-21.330	-64.410	2056	Eastern Cordillera	Since 2016: Guralp 5TD.	RS-OSC
72	Roboré	BBRB	2016-2018	-18.278	-59.809	348	Chaco Beni-ana plain	2016 – 2018: Nanometrics Trillium 360GSN (ZNE)	USP

	Name	Code	Operating Dates	Lat / deg	Lon / deg	Elev. / m	Geomorph. Region	Main characteristics	Belongs to
73	Cerro San Diablo	BBSD	2016 -	-17.188	-60.611	374	Brazilian shield	Since 2016: Nanometrics Trillium 360GSN (ZNE)	USP
74	Santa Ana	BBLB	2016-2018	-18.665	-58.800	193	Brazilian shield	2016 − 2018: Nanometrics Trillium 360GSN (ZNE)	USP
75	Jacaque	SOEJ	2016 -	-16.975	-68.192	4076	Altiplano	Since 2016: GURALP − 6TD (ZNE)	RS-OSC
76	Toro Toro	SOET	2016 -	-18.115	-65.811	2846	Eastern Cordillera	Since 2016: GURALP − 6TD (ZNE)	RS-OSC
77	Opoqueri	SOEO	2017 -	-18.563	-67.887	3836	Altiplano	Since 2017: GURALP − 6TD (ZNE)	RS-OSC
78	Incahuasi	SOTI	2017 -	-19.831	-63.662	1130	Subandean zone	Since 2017: GURALP − 6TD (ZNE)	RS-OSC
79	Aiquile	SOEA	2017 -	-18.180	-65.233	2552	Eastern Cordillera	Since 2017: GURALP − 6TD (ZNE)	RS-OSC
80	Aiquile	AOEA	2017 -	-18.180	-65.233	2552	Eastern Cordillera	Since 2017: GURALP − 5TD (ZNE)	RS-OSC
81	Puerto Suarez	BBPS	2018 -	-19.069	-57.843	214	Brazilian shield	Since 2018: Nanometrics Trillium 360GSN (ZNE)	USP
82	Rincón del Tigre	BBRT	2018 -	-18.200	-58.211	196	Brazilian shield	Since 2018: Nanometrics Trillium 360GSN (ZNE)	USP
83	Sucre	AOES	2019 -	-19.140	-65.344	3198	Eastern Cordillera	Since 2019: GURALP − 5TD (ZNE)	RS-OSC

5.1.3 Temporary Seismic Stations with Contribution from OSC

BANJO / SEDA (1994-1995):

A collaboration of the Carnegie Institution of Washington, the Lawrence Livermore National Laboratory, the University of Arizona, the ORSTROM Institute, the University of Chile, the University of Mayor de San Andres and our institution installed 23 broadband seismic stations in Bolivia and Chile to enhance the knowledge of the tectonics of the Central Andes, especially the Altiplano. The project "Broadband Andean Joint Experiment" (BANJO) installed 16 broadband seismometers between 19°S and 20°S, from Chile to the Chaco basin in Bolivia. The project "Seismic Exploration of the Deep Altiplano" (SEDA) installed 7 broadband stations from North to South within the Altiplano region, which registered the then largest deep focus (636 km) Mw 8.3 earthquake of 9th June 1994 (*Silver*, 1994; *Polet et al.*, 1996).

ANCORP Seismic Network (1996–1997):

Between 1996 and 1997 the German Research Centre for Geosciences (GFZ) installed 39 seismic stations at the Altiplano region with the aim of increasing knowledge of the seismicity at the back arc region (*Haberland et al.*, 1996).

Puna Altiplano Volcanic Complex Project (1996-1997):

From 1996 to 1997 the Natural Environment Research Council, UK (NERC) installed 33 seismic sensors at Uturuncu Volcano in collaboration with us to enhance the knowledge about volcanos in the Altiplano region (*Zandt*, 1996).

REFUCA Project (2002 - 2004):

From 2002 to 2004, 60 seismic stations (45 short period and 15 broadband) were installed around 21°S from 70°W to 64°W. The aim of this project was to monitor all seismicity of the Central Andes (*Asch et al.*, 2002).

Volcano Project (2009-2013):

The University of Cornell in collaboration with our institution installed 41 seismic stations distributed at the Uturuncu volcano and volcanos at the border between Chile and Bolivia. The project started in 2009 and finished in 2013 (*Pritchard*, 2009).

Central Andes Uplift and Geodynamic High Topography "CAUGHT" (2010-2012):

Between 2010 and 2012 the University of Arizona and our institution installed a set of 50 temporary broadband seismic stations to enhance the results obtained by the BANJO/SEDA project with a high-resolution tomography of the Altiplano and part of the Eastern Cordillera. The data is openly available through IRIS (*Beck*, 2010; *Ward et al.*, 2013, 2016; *Ryan et al.*, 2016; *Scire et al.*, 2016; *Scire et al.*, 2017; *Garzione et al.*, 2017.)

GPS and Seismic Network PLUTONS Project:

From 2010 to 2013 a set of broadband seismic stations and GPS stations were installed at the Andes volcanos with the main attention focused on Uturuncu (Bolivia) and Lazufre (Argentina). This project involved national (Observatorio San Calixto, Universidad Mayor de San Andes, Universidad Tomas Frias and Servicio Geologico Minero) and international agencies (Universidad de Chile, Cornell University). An extension of this project was done in 2018 but the participation of institutions was reduced to New Mexico University and Cornell University and our institution (*Pritchard et al.*, 2018).

Figure 5.7: *Temporary seismic network installed along our country in 108 years of operations.*

Cuencas Pantanal - Chaco - Paraná (PCPB) Project:

The university of Sao Paulo installed 50 broadband seismic stations in collaboration with different entities from different countries at South America. In our case, 3 broadband seismic stations were installed at the Sub Andes with the main objective to obtain a high resolution of the crust. The project will run until 2022 (*Assumpção et al.*, 2016).

An overview of the temporary seismic networks is displayed in Figure 5.7.

5.1.4 Acquisition and Data Processing

During the first 20 years of our institution the data were recorded on smoked and film paper. Pierre M. Descotes SJ – the first principal - manually picked the seismic phases and wrote the first bulletins, which are safely stored at our library. Over the years and with the help of donations and collaboration with international agencies we improved data acquisition and processing and nowadays use Seiscomp3 (`https://www.seiscomp.de/seiscomp3/`), Seisan (*Havskov and Ottemoller*, 1999; *Havskov, Voss and Ottemoller*, 2020) and Earthworm (`http://www.earthwormcentral.org/`).

Around 1990, the CEA/DASE and AFTAC collaboration migrated the helicorders drums to digital data bases and digital display with graphical user interfaces, the data protocols used were FONYX (CEA/DASE protocol), SAC, CD10 and CD11.

In 2010 a big jump forward was made due to the availability of the Internet and free open access source codes dedicated to seismology. Data integration from open seismic networks was applied at our institution when we initially started to work with Earthworm and open data from Seedlink servers such as IPOC (Integrated Plate Observations Chile), INPRES (Instituto de Prevención Sísmica - Argentina) and USP (Universidade de Sao Paulo – Brazil). Later, we switched to SEISAN for data analysis (*Havskov and Ottemoller*, 1999; *Havskov, Voss and Ottemoller*, 2020). In 2011 CTBTO made alternative software available to state signatories for hypocenter location and waveform analysis. (GEOTOOL). We use it especially for teleseismic earthquakes.

In 2016 CTBTO provided us with a Seiscomp3 (modified) server for state signatories which was integrated to our daily routine as the main software of acquisition. We keep using SEISAN for data analysis, the velocity model is based on the research of *Ryan et al.* (2016). The same year with collaboration with CEA/DASE the software Progressive Multi Correlation Channel (PMCC) was installed to analyse infrasound data from the IS08 station.

Earthquakes Magnitudes Reported Over Time

Over time we calculated different types of magnitudes depending on what procedures were available at certain times.

We began determining body wave magnitudes (mb) when data analysis was still done manually on paper seismograms. m_b is calculated with the following equation for regional and teleseismic events:

$$m_b = \log(A/T) + Q(\Delta, h), \tag{5.1}$$

where A is the amplitude in mm, T period in s and Q a correction term dependant on epicentral distance Δ and focal depth h (*Gutenberg and Richter*, 1956).

OPALES System (CEA/DASE):

The local Magnitude (M_L) is defined by:

$$M_L = \log(A) + 0.84 \log(R) + 0.00102 - 1.85, \tag{5.2}$$

where A is the amplitude of the maximum peak measured in nanometres and R is the hypocentral distance in km.

GEOTOOL (CTBTO):

For local Magnitude (M_L) on a Wood-Anderson filtered seismogram the equation is:

$$M_L = \log(A) - \log(A_0\, R), \tag{5.3}$$

where A is the amplitude in mm, R is the hypocentral distance in km. A_0 is defined by the following Equation 5.4 where C_1 to C_3 are constants.

$$-\log(A_0) = C_1 \log(R/100) + C_2(R - 100) + C_3, \tag{5.4}$$

The equation with constants for Southern California is:

$$-\log(A_0) = 1.11 \log(R/100) + 0.00189\,(R - 100) + 3, \tag{5.5}$$

SEISAN:

For local earthquakes we use the M_L magnitude expressed by:

$$M_L = \log(A) + 1.11 \log(D) + 0.00189 - 2.09, \tag{5.6}$$

where A is the amplitude in mm measured on a Wood-Anderson filtered seismogram and D is the distance in km.

For magnitudes larger than M_L 6.0 we apply the following empirical relations to convert to M_W, for shallow (5.7) and intermediate earthquakes (5.8):

$$M_W = 0.8021\, M_L + 0.8883, \tag{5.7}$$
$$M_W = 1.0325\, M_L + 0.0106. \tag{5.8}$$

SeisComp3 (CTBTO modified):

M_{LV} is automatically calculated with the following equation based on *Richter* (1935):

$$M_{LV} = \log(A) - \log(A_0(\delta)), \tag{5.9}$$

where A is the amplitude on a Wood-Anderson filtered seismogram and A_0 is a distance (δ) dependent calibration function.
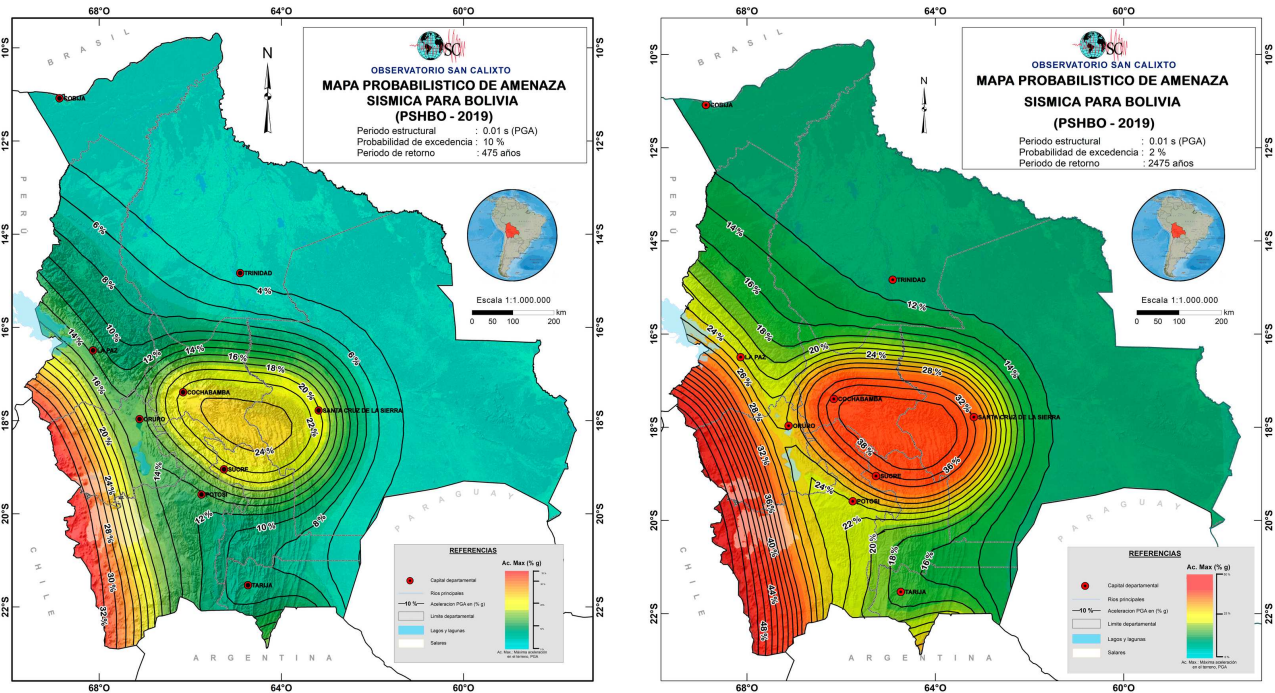
Figure 5.8: *Probabilistic Seismic Hazard Map for Bolivia, an application of our seismic bulletins reported over time.* Left: *475 years return period,* right: *2475 years return period.*

5.1.5 A Product of the Seismic Bulletins: a Probabilistic Hazard Map for Bolivia (Plurinational State of)

Based on our bulletins we decided to provide our country with a probabilistic hazard map for 475 and 2475 years return period. This map is the basis for a new national building code "GBDS-2020". It is not a finalised norm yet and is still being developed.

Figure 5.8 (left) shows the seismic hazard map of Bolivia: PGA for shallow earthquakes (depth < 70 km) located at the central part of Bolivia can reach 26% *g* while for the intermediate earthquakes (depths from 100 to 350 km), mostly located at the Western part of our country, PGA can reach 32% *g*. For deep earthquakes (depth from 500 to 700 km) there are no ground motion prediction equations and no PGA was computed. Figure 5.8 (right) shows higher values of PGA due to the higher return period of 2475 years. In general this map is applied for high buildings, dams, hospitals and / or structures that need more resistance to earthquakes.

5.1.6 Data Availability

Our local and regional seismic bulletins are shared with the International Seismological Centre (ISC) under the agency code SCB, formerly LPZ. Moreover, regional agreements made within CERESIS (Centro Regional de Sismologia para America del Sur) allow member states (South American countries) to have our bulletins for regional research. Good examples of homogenising shared regional data were the following projects:

- SISAN* (Sismicidad Andina) from 1976 to 1982

- SISRA* (Programa de Mitagacion de los Terremotos en la Region Andida) from 1980 to 1986

- CERESIS-91* (Centro Regional de Sismicidad para America del Sur) from 1987 to 1995

- SARA – GEM (South America Risk Assessment* Global Earthquake Modelling) from 2013 to 2016

* report available under the document "Peligro Sismico en Latinoamerica y el Caribe" hosted by the Instituto Panamericano de Geografía e Historia (IPGH) (`https://idl-bnc-idrc.dspacedirect.org/bitstream/handle/10625/36057/107805_v4.pdf?sequence=1`).

Our bulletins for local seismicity are shared via the web page `http://www.osc.org.bo`. Since February 2021 we are starting to share near real time data through IRIS, where a set of three short period three components sensors under the code BV (`https://doi.org/10.7914/SN/BV`) will be available for the research community.

References

Ayala Sánchez, R. (1997), Sismotectonique des andes de bolivie et role de l'orocline bolivien, PhD thesis, École et Observatoire de Physique du Globe, Strasbourg, France.

Ayala Sánchez, R. (2001), La Historia del Observatorio San Calixto de La Paz y su Contribucion al Desarrollo de la Ciencia y la Sismologia en Bolivia, *Revista Geofísica, 101*.

Anderson, R.B., S.P. Long, B.K. Horton, A.Z. Calle and V. Ramirez (2017), Shortening and structural architecture of the Andean fold-thrust belt of southern Bolivia (21°S): implications for kinematic development and crustal thickening of the central Andes, *Geosphere, 13*(2), 538–558, `https://doi.org/10.1130/GES01433.1`.

Assumpção, M., F. Dias, I. Zevallos, and J. Naliboff (2016), Intraplate stress field in South America from earthquake focal mechanisms, *J. South. Am. Earth. Sci., 71*, 278–295, `https://doi.org/10.1016/j.jsames.2016.07.005`.

Asch, G., B. Heit and X. Yuan (2002), The ReFuCA project: Receiver Functions Central Andes, Deutsches Geo Forschungs Zentrum (GFZ), Other/Seismic Network, `https://doi.org/10.14470/MN7557778612`.

Beck, S., G.Z. (2010), Central Andean Uplift and the Geodynamics of the High Topography, International Federation of Digital Seismograph Networks, `https://doi.org/10.7914/SN/ZG_2010`.

Cabre, R (1965), Historia Sismica de Boliva, *Bol. del Insti. Boliviano del Petroleo*, La Paz.

Cabre, R. (1974), Conocimientos sobre el Riesgo Sismico en Bolivia, *Rev. de Geofisica*.

Cabré, S.J. (1988), 75 Años a la vanguardia de la sismología, Observatorio San Calixto (internal publication).

Cabré, R. and A. Vega (1995), Sismo boliviano del 9 de junio de 1994, *Revista Técnica de YPFB (Yacimientos Petrolíferos Fiscales Bolivia), 16*(1-2), 5-8.

DeMets, C., R. Gordon, D. Argus and S. Stein (1994), Effect of recent revision to the geomagnetic

reversal time scale on estimates of current plate motion, *Geophys. Res. Lett.*,*21*(20), 2191–2194, `https://doi.org/10.1029/94GL02118`.

Eichelberger, N., N. McQuarrie, J. Ryan, B. Karimi, S. Beck and G. Zandt (2015), Evolution of crustal thickening in the central Andes, Bolivia, *Earth. Planet. Sci. Lett.*, *426*, 191–203, `https://doi.org/10.1016/j.epsl.2015.06.035`.

Garzione, C.N., N. McQuarrie, N. D. Perez, T.A. Ehlers, S. L. Beck, N. Kar, N. Eichelberger, A. D. Chapman, K. M. Ward, M. N. Ducea, R. O. Lease, C. J. Poulsen, L. S. Wagner, J. E. Saylor, G. Zandt and B.K. Horton (2017), Tectonic Evolution of the Central Andean Plateau and Implications for the Growth of Plateaus, *Ann. Rev. Earth. Planet. Sci.*, *45*(1), `https://doi.org/10.1146/annurev-earth-063016-020612`.

Gutenberg, B and C. F. Richter (1949), Seismicity of the Earth and associated Phenomena, Princeton Univ. Press, Princeton, New Jersey, 273 pp.

Gutenberg, B., and C. F. Richter (1956), Magnitude and Energy of earthquakes, *Ann. Geof.*, *9*, 1–5.

Haberland, C., A. Rietbrock, G. Asch and G. Chong (1996), The ANCORP Seismic Network, GFZ Data Services, Other/Seismic Network, `https://doi.org/10.14470/MR6441682066`.

Havskov, J. and L. Ottemoller (1999), SeisAn Earthquake analysis software, *Seis. Res. Lett.*, *70*(5), 532–534, `https://doi.org/10.1785/gssrl.70.5.532`.

Havskov, J., P.H. Voss and L. Ottemoller (2020), Seismological Observatory Software: 30 Yr of SEISAN. *Seismol. Res. Lett.*, *91*(3), 1846–1852, `https://doi.org/10.1785/0220190313`.

Le Pichon, A., E. Blanc, D.P. Drob, S. Lambotte, J. Dessa, M. Lardy, P. Bani and S. Vergniolle (2005), Infrasound monitoring of volcanoes to probe high-altitude winds, *J. Geophys. Res. Solid Earth*, *110*, `https://doi.org/10.1029/2004JD005587`.

Le Pichon, A., P. Mialle, J. Guilbert and J. Vergoz (2006), Multistation infrasonic observations of the Chilean earthquake of 2005 June 13, *Geophys. J. Int.*, *167*(2), 838–844, `https://doi.org/10.1111/j.1365-246X.2006.03190.x`.

Minaya, E., J. Illanes and G. Fernández (2013), Memoria 100 años OSC, Observatorio San Calixto (internal publication).

Pritchard, M. (2009), The life cycle of Andean volcanoes: Combining space-based and field studies, International Federation of Digital Seismograph Networks. `https://doi.org/10.7914/SN/YS_2009`.

Pritchard, M., S. de Silva, G. Michelfelder, G. Zandt,S. Mcnutt, J. Gottsmann, M.E. West, J. Blundy, D.H. Christensen, N.J. Finnegan, E. Minaya, R.S.J. Sparks, M. Sunagua, M. Unsworth, C. Alvizuri, M. Comeau, R. del Potro, D. Diaz, M. Diez and K.M. Ward (2018), Synthesis: PLUTONS: Investigating the relationship between pluton growth and volcanism in the Central Andes, *Geosphere*, *14*, `https://doi.org/10.1130/GES01578.1`.

Polet J. , P. Silver, G. Zandt, S. Ruppert, R. Kind, G. Bock, G. Asch, S. Beck and T. Wallace (1996), Shear wave anisotropy beneath the central Andes from the BANJO, SEDA and PISCO experiments, *Géodynamique andine : résumés étendus = Andean geodynamics : extended abstracts*, Paris :

ORSTOM, 97-98 (Colloques et Séminaires), ISAG 96 : Symposium International sur la Géodynamique Andine, 3., Saint-Malo (FRA), 1996/09/17-19. ISBN 2-7099-1332-1.

Richter, C.F. (1935), An instrumental earthquake magnitude scale, *Bull. Seismol. Soc. Am.*, *25*(1), 1–32.

Ryan, J., S.L. Beck, G. Zandt, L. Wagner, E. Minaya and H. Tavera (2016), Central Andean crustal structure from receiver function analysis, *Tectonophysics*, *682*, 120–133, `https://doi.org/10.1016/j.tecto.2016.04.048`.

Schamberger, P., G.A. Fernandez, F. Condori and M. Nieto (2016), Reporte Interno del OSC sobre el diseño de uns sistema de transmision de datos por red celular 3G (internal publication).

Scire, A., G. Zandt, S.L. Beck, M.D. Long, L.S. Wagner, E. Minaya and H. Tavera (2016), Imaging the transition from flat to normal subduction: Variations in the structure of the Nazca slab and upper mantle under southern Peru and northwestern Bolivia, *Geophys. J. Int.*, *204*(1), 457-479, `https://doi.org/10.1093/gji/ggv452`.

Scire, A., G. Zandt, S. Beck, M. Long and L.S. Wagner (2017), The deforming Nazca slab in the mantle transition zone and lower mantle: Constraints from teleseismic tomography on the deeply subducted slab between 6°S and 32°S, *Geosphere*, *13*(3), 665–680, `https://doi.org/10.1130/GES01436.1`.

Silver, P., S. B. (1994), Broadband Study of the Altiplano and Central Andes, International Federation of Digital Seismograph Networks, `https://doi.org/10.7914/SN/XE_1994`.

Ward, K.M., R. Porter, G. Zandt, S.L. Beck, L.S. Wagner, E. Minaya and H. Tavera (2013), Ambient noise tomography across the Central Andes, *Geophys. J. Int.*, *194*(3), 1559-1573, `https://doi.org/10.1093/gji/ggt166`.

Ward, K., G. Zandt, S. Beck, L. Wagner and H. Tavera (2016), Lithospheric Structure Beneath the Northern Central Andean Plateau from the Joint Inversion of Ambient Noise and Earthquake Generated Surface Waves, *J. Geophys. Res. Solid Earth*, *121*, `https://doi.org/10.1002/2016JB013237`.

Wigger, P.J., M. Schmitz, M. Araneda, G. Asch, S. Baldzuhn, P. Giese, W.-D. Heinsohn, E. Martínez, E. Ricaldi, P. Röwer and J. Viramonte (1994), Variation in the Crustal Structure of the Southern Central Andes Deduced from Seismic Refraction Investigations, *Tectonics of the Southern Central Andes*, Springer, Berlin, Heidelberg, `https://doi.org/10.1007/978-3-642-77353-2_2`.

Zandt, G. (1996), Altiplano-Puna Volcanic Complex Seismic Experiment, International Federation of Digital Seismograph Networks, `https://doi.org/10.7914/SN/XH_1996`.

6

Summary of Seismicity, July – December 2018

The two largest events in the second half of 2018 both occurred in the Fiji region within three weeks and 300 km of each other. The first event was the strongest with a magnitude of M_W 8.2 (2018/08/19 00:19:39.25 UTC, 18.1136°S 178.0435°W, 578.5 km, 2491 stations (ISC)) while the second one had a magnitude of M_W 7.9 (2018/09/06 15:49:18.79 UTC, 18.5210°S, 179.3278°E, 667.0 km, 2816 stations (ISC)). They are the two largest events ever recorded in this area with the M_W 8.2 event also being the second largest deep focus event globally after the M_W 8.3 Sea of Okhotsk event in 2013. With the second Fiji event being located in a previously relatively aseismic region and occurring very close in space and time to the first event it is very likely that the M_W 7.9 event was triggered by the M_W 8.2 event (*Jia et al.*, 2020; *Fan et al.*, 2019). Both events showed distinct rupture processes: the first event was stronger, showed a faster rupture propagation and produced lots of aftershocks while the second event triggered only a few aftershocks and its rupture propagated more slowly. However, both events lasted about 35 seconds (*Fan et al.*, 2019). Studies of this Fiji doublet support the hypothesis that local slab temperature likely controls rupture of deep earthquakes (*Liu et al.*, 2021; *Jia et al.*, 2020).

The event that was referenced most in the ISC Event Bibliography (*Di Giacomo et al.*, 2020; *International Seismological Centre*, 2021) with currently 75 articles was the M_W 7.6 Palu event in Indonesia (2018/09/28 10:02:43.80 UTC, 0.2775°S, 119.9145°E,15.9 km, 2412 stations (ISC)). This strike slip event produced massive liquefaction in the Palu bay region in Central Sulawesi and triggered unusually large tsunamis with very short arrival times (e.g., *Carvajal et al.*, 2019; *Heidarzadeh et al.*, 2019) causing more than 2000 fatalities (e.g., *Carvajal et al.*, 2019; *Bao et al.*, 2019). Tsunami modelling suggests that large submarine landslides contributed and enhanced tsunami generation (*Heidarzadeh et al.*, 2019; *Carvajal et al.*, 2019; *Natawidjaja et al.*, 2021). In addition to the unusual tsunami heights, the rupture speed of the Palu event is also causing some discussion among the scientific community as it is considered to be a supershear event where the rupture speed is higher than the shear wave speed but for this kind of event it shows an untypical low speed as these types of events are usually considered to steadily propagate above a certain velocity (Eshelby's speed) (e.g *Oral et al.*, 2020; *Natawidjaja et al.*, 2021; *Bao et al.*, 2019).

The number of events in this Bulletin Summary categorised by type are given in Table 6.1.

The period between July and December 2018 produced 12 earthquakes with $M_W \geq 7$; these are listed in Table 6.2.

Figure 6.1 shows the number of moderate and large earthquakes in the second half of 2018. The distribution of the number of earthquakes should follow the Gutenberg-Richter law.

Figures 6.2 to 6.6 show the geographical distribution of moderate and large earthquakes in various magnitude ranges.

Table 6.1: *Summary of events by type between July and December 2018.*

felt earthquake	51
felt induced event	1
known earthquake	242351
known chemical explosion	6137
known induced event	3194
known mine explosion	2979
known rockburst	364
known experimental explosion	289
known ice-quake	2
suspected earthquake	31820
suspected chemical explosion	4266
suspected induced event	20
suspected mine explosion	6890
suspected rockburst	164
suspected experimental explosion	59
total	298587
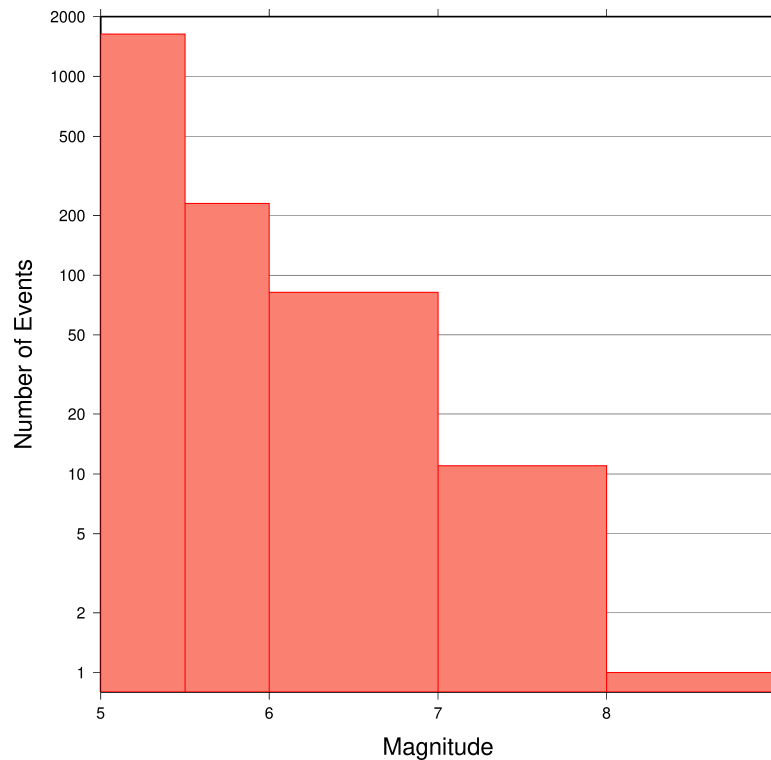
Figure 6.1: *Number of moderate and large earthquakes between July and December 2018. The non-uniform magnitude bias here correspond with the magnitude intervals used in Figures 6.2 to 6.6.*

MW 5 – 5.5, 1635 Events
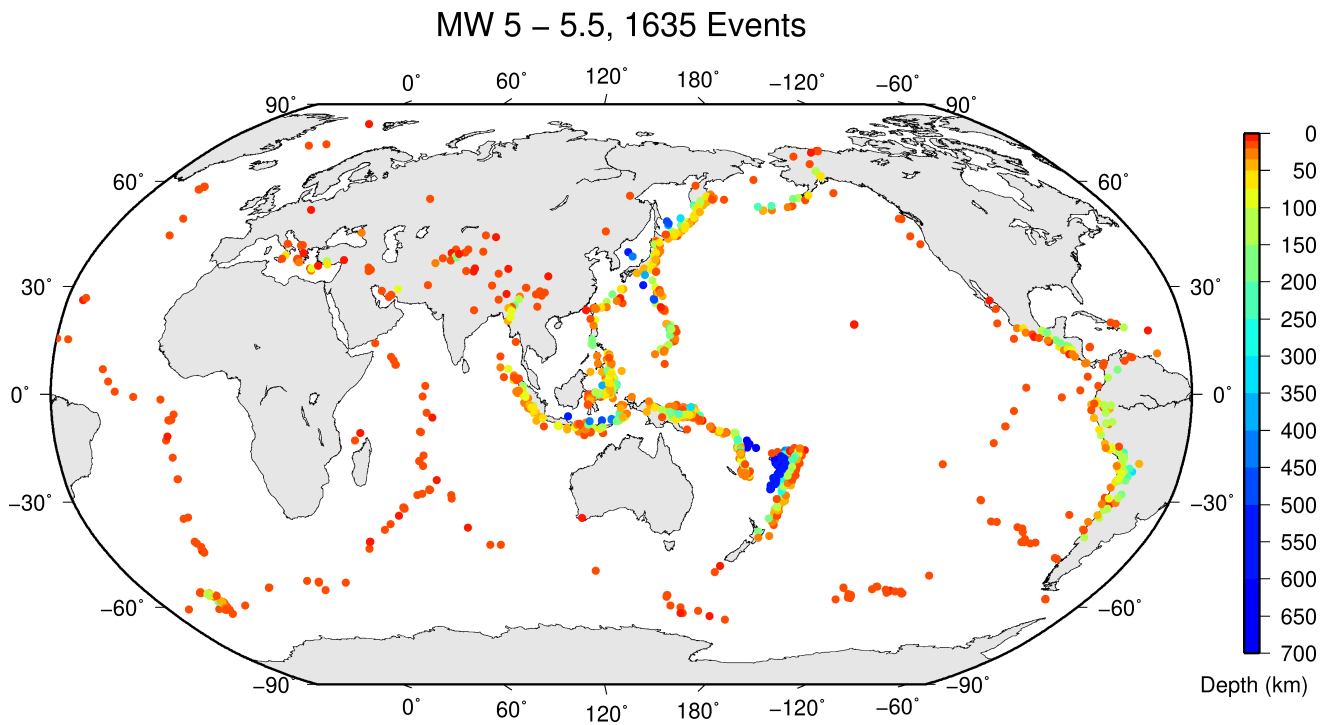
Figure 6.2: *Geographic distribution of magnitude 5-5.5 earthquakes between July and December 2018.*

MW 5.5 – 6, 230 Events
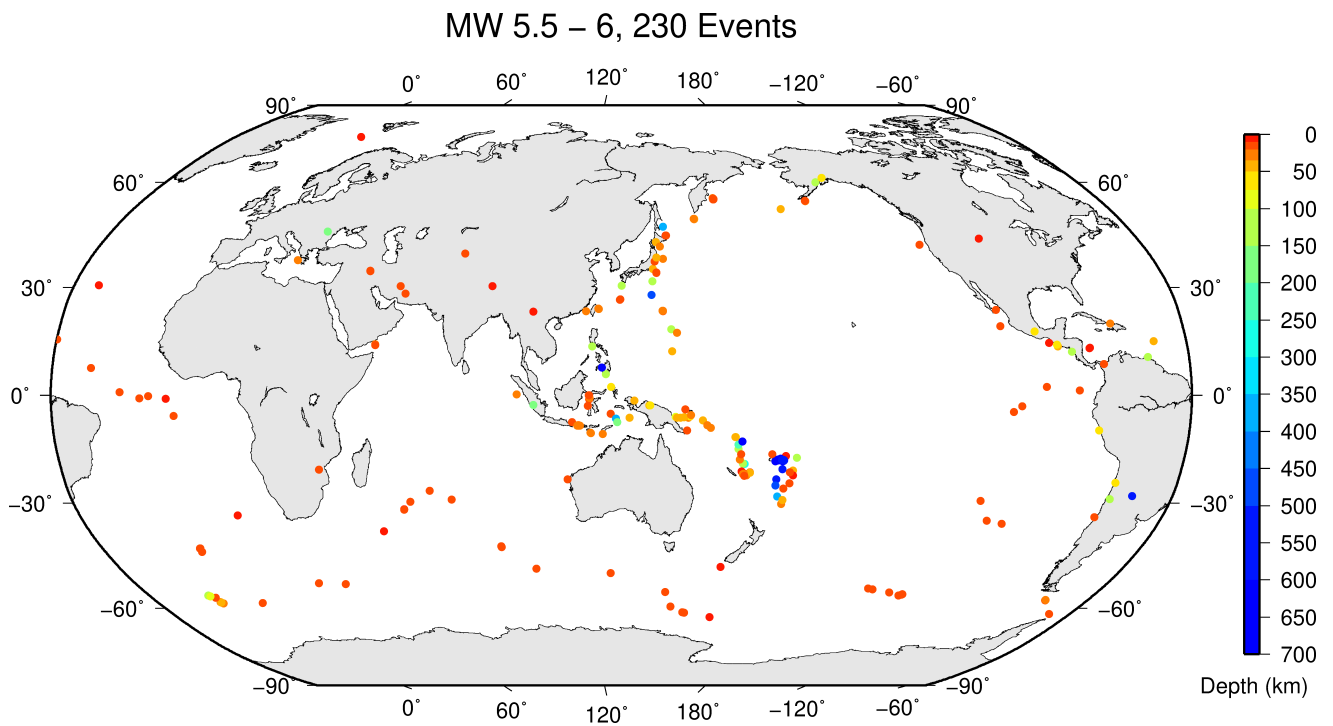
Figure 6.3: *Geographic distribution of magnitude 5.5-6 earthquakes between July and December 2018.*

MW 6 – 7, 82 Events
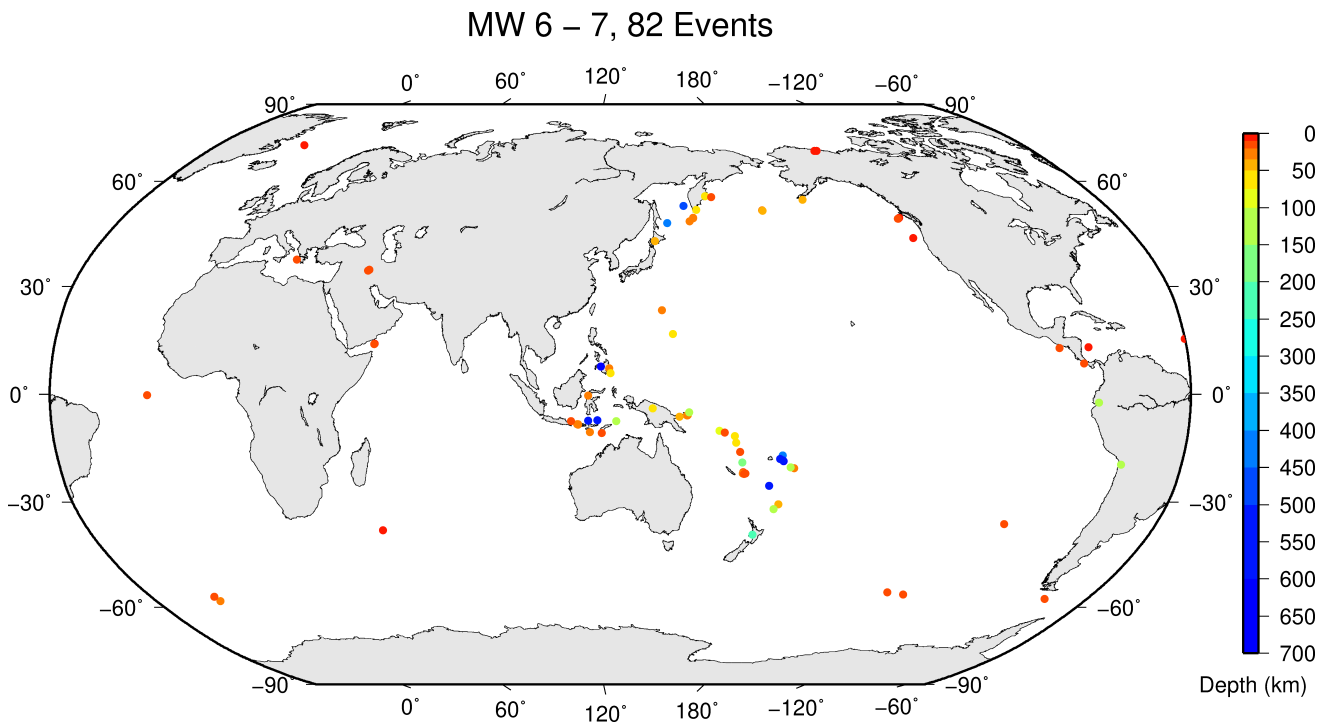
Figure 6.4: *Geographic distribution of magnitude 6-7 earthquakes between July and December 2018.*

MW 7 – 8, 11 Events
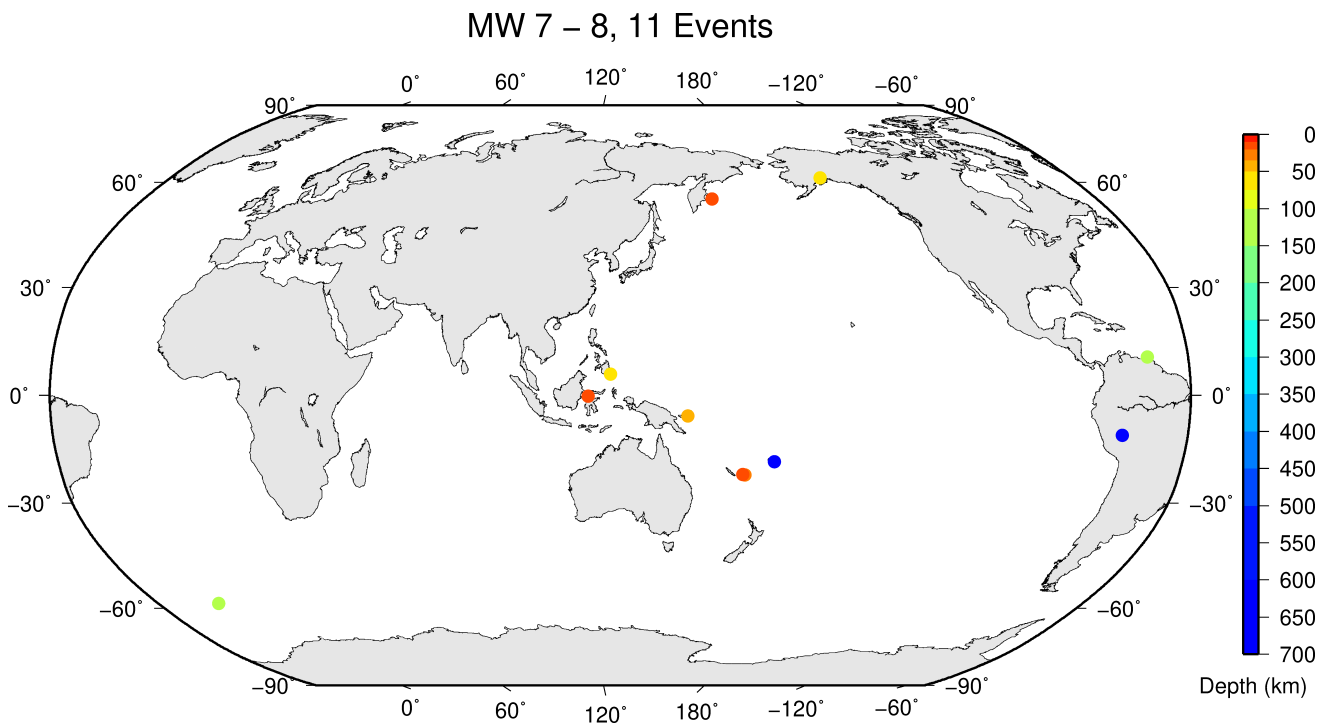
Figure 6.5: *Geographic distribution of magnitude 7-8 earthquakes between July and December 2018.*

Table 6.2: *Summary of the earthquakes of magnitude Mw ≥ 7 between July and December 2018.*

Date	lat	lon	depth	Mw	Flinn-Engdahl Region
2018-08-19 00:19:39	-18.11	-178.04	578	8.2	Fiji Islands region
2018-09-06 15:49:18	-18.52	179.33	666	7.9	Fiji Islands
2018-09-28 10:02:43	-0.28	119.91	15	7.6	Minahassa Peninsula, Sulawesi
2018-12-05 04:18:08	-22.02	169.48	11	7.5	Southeast of Loyalty Islands
2018-08-21 21:31:42	10.71	-62.90	120	7.3	Near coast of Venezuela
2018-12-20 17:01:55	55.00	164.68	17	7.3	Komandorsky Islands region
2018-08-24 09:04:06	-11.07	-70.86	625	7.1	Peru-Brazil border region
2018-08-29 03:51:56	-22.10	170.21	24	7.1	Southeast of Loyalty Islands
2018-12-11 02:26:31	-58.54	-26.53	149	7.1	South Sandwich Islands region
2018-11-30 17:29:27	61.31	-150.03	50	7.0	Southern Alaska
2018-10-10 20:48:20	-5.72	151.33	39	7.0	New Britain region
2018-12-29 03:39:09	5.88	126.87	64	7.0	Mindanao
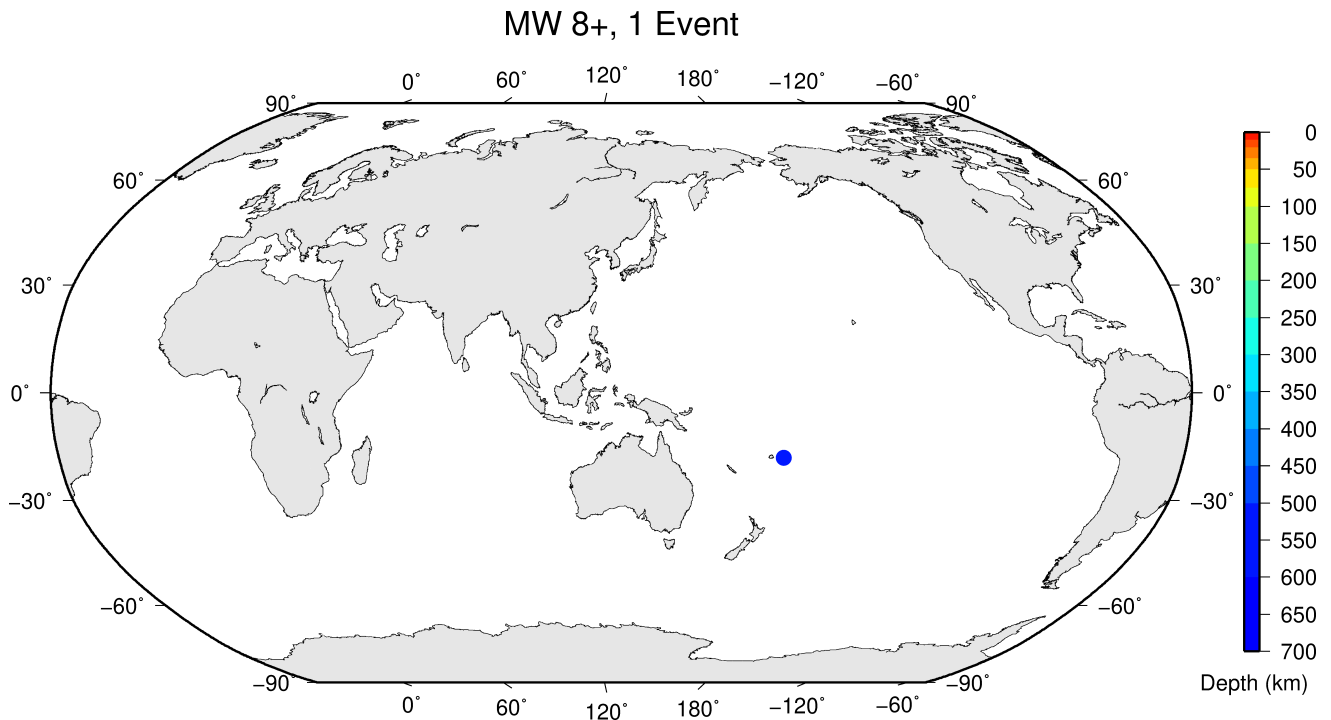
Figure 6.6: *Geographic distribution of magnitude 8+ earthquakes between July and December 2018.*

References

Bao, H., J.P. Ampuero, L. Meng, E.J. Fielding, C. Liang, C.W.D. Milliner, T. Feng and H. Huang (2019), Early and persistent supershear rupture of the 2018 magnitude 7.5 Palu earthquake, *Nat. Geosci.*, *12*, 200–205, `https://doi.org/10.1038/s41561-018-0297-z`.

Carvajal, M., C. Araya-Cornejo, I. Sepúlveda, D. Melnick and J.S. Haase (2019), Nearly instantaneous tsunamis following the Mw 7.5 2018 Palu earthquake, *Geophys. Res. Lett.*, *46*, 5117–5126, `https://doi.org/10.1029/2019GL082578`.

Di Giacomo, D., D.A. Storchak, N. Safronova, P. Ozgo, J. Harris, R. Verney and I. Bondár (2014), A New ISC Service: The Bibliography of Seismic Events, *Seismol. Res. Lett.*, *85*(2), 354–360,

`https://doi.org/10.1785/0220130143`.

Fan, W., S.S. Wei, D. Tian, J.J. McGuire and D.A. Wiens (2019), Complex and diverse rupture processes of the 2018 Mw 8.2 and Mw 7.9 Tonga-Fiji deep earthquakes, *Geophys. Res. Lett.*, *46*, 2434–2448, `https://doi.org/10.1029/2018GL080997`.

Heidarzadeh, M., A. Muhari and A.B. Wijanarto (2019), Insights on the Source of the 28 September 2018 Sulawesi Tsunami, Indonesia Based on Spectral Analyses and Numerical Simulations, *Pure Appl. Geophys.*, *176*, 25–43, `https://doi.org/10.1007/s00024-018-2065-9`.

International Seismological Centre (2021), On-line Event Bibliography, `https://doi.org/10.31905/EJ3B5LV6`.

Jia, Z., Z. Shen, Z. Zhan, C. Li, Z. Peng and M. Gurnis (2020), The 2018 Fiji Mw 8.2 and 7.9 deep earthquakes: One doublet in two slabs, *Earth Planet. Sci. Lett.*, *531*, 115997, `https://doi.org/10.1016/j.epsl.2019.115997`.

Liu, H., M. Gurnis, W. Leng, Z. Jia and Z. Zhan (2021), Tonga slab morphology and stress variations controlled by a relic slab: Implications for deep earthquakes in the Tonga-Fiji region, *Geophys. Res. Lett.*, *48*, e2020GL091331, `https://doi.org/10.1029/2020GL091331`.

Natawidjaja, D.H., M.R. Daryono, G. Prasetya, Udrekh, P. L-F Liu, N.D. Hananto, W. Kongko, W. Triyoso, A.R. Puji, I. Meilano, E. Gunawan, P. Supendi, A. Pamumpuni, M. Irsyam, L. Faizal, S. Hidayati, B. Sapiie, M.A. Kusuma, S. Tawil (2021), The 2018 Mw7.5 Palu 'supershear' earthquake ruptures geological fault's multisegment separated by large bends: results from integrating field measurements, LiDAR, swath bathymetry and seismic-reflection data, *Geophys. J. Int.*, *224*(2), 985–1002, `https://doi.org/10.1093/gji/ggaa498`.

Oral, E., H. Weng and J.P. Ampuero (2020), Does a damaged-fault zone mitigate the near-field impact of supershear earthquakes? - Application to the 2018 Mw7.5 Palu, Indonesia, earthquake, *Geophys. Res. Lett.*, *47*, e2019GL085649, `https://doi.org/10.1029/2019GL085649`.

7

Notable Events

7.1 The mb=5.4 Katav-Ivanovsk Earthquake (Urals) on 04 September 2018

Ruslan A. Dyagilev[1], Filipp G. Verkholantsev[2], Yuliya V. Varlashova[3], Denis Yu. Shulakov[3]

[1] Geophysical Survey of Russian Academy of Sciences (GS RAS), Obninsk, Russia

[2] Geophysical Survey of Russian Academy of Sciences (GS RAS), Perm, Russia

[3] Mining Institute of Ural Branch of Russian Academy of Sciences (MI UB RAS), Perm, Russia

Ruslan A. Dyagilev   Filipp G. Verkholantsev   Yuliya V. Varlashova   Denis Yu. Shulakov

The article summarises the instrumental and macroseismic data of the Katav-Ivanovsk earthquake, which occurred on September 4, 2018, in the Chelyabinsk region, Russia. The earthquake was the strongest instrumentally recorded earthquake in the Urals (mb=5.4) and at the same time, it had the most seismic intensity compared to other earthquakes in Russia in 2018 (I0=6 points). For the first time in the Urals the aftershock process was recorded, the active stage of which lasted more than 1 year. Like the mainshock, some aftershocks had a significant macroseismic effect.

7.1.1 Introduction

The earthquake in the area of Katav-Ivanovsk, Chelyabinsk region, which occurred on September 4, 2018, was an unexpected and unusual natural phenomenon for the South Urals. In 2018, this earthquake in Russia became the event with the greatest macroseismic effect. Seismicity in this area is not properly studied, the nature of seismic events that previously occurred here is controversial, since the available instrumental data are unrepresentative. Data on the focal mechanisms in this area are almost completely lacking. Studies carried out in the source area after the Katav-Ivanovsk earthquake made it possible to obtain a large amount of information in a relatively short period of time and to remove many questions about the nature of the seismicity of the area. Macroseismic data on the main shock and its three strongest aftershocks are collected. The significant magnitude of the earthquake made it possible to use
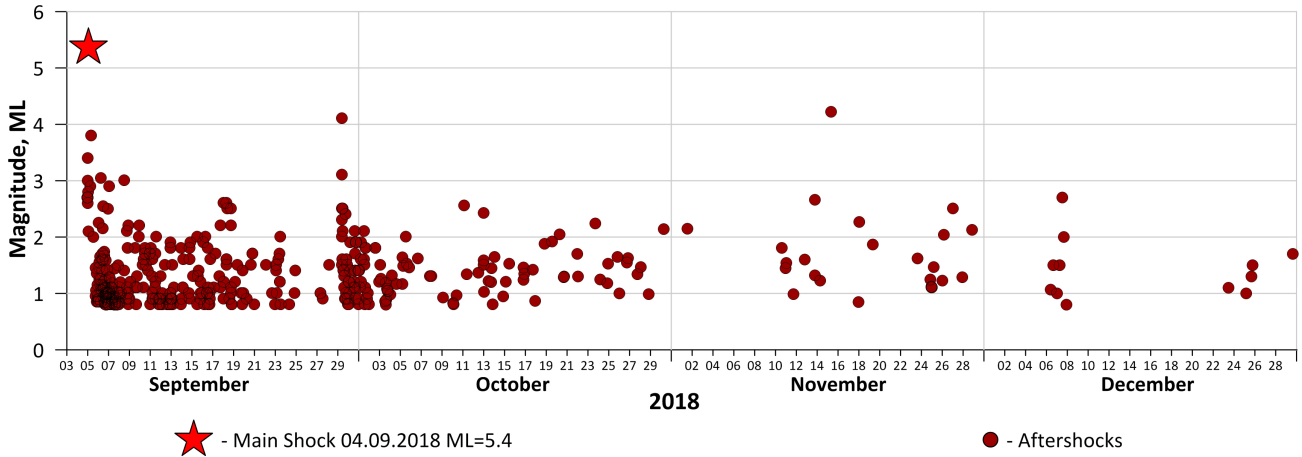
Figure 7.1: *Temporal distribution of aftershocks of the Katav-Ivanovsk earthquake*

data from dozens of teleseismic stations to determine the depth and the mechanism of the earthquake source.

The Katav-Ivanovsk earthquake of 2018 is one of the three strongest (M≥5.0) earthquakes known in the Urals. The first two occurred quite a long time ago (1798 – Perm-Kungur, 1914 – Bilimbai), the primary information about them consists mainly of macroseismic descriptions. These, with a small amount of instrumental data (only concerns the Bilimbai earthquake), became the basis for determining the events main parameters (*Godzikovskaya*, 2016; *Malovichko et al.*, 2020). To study the conditions for the occurrence of the Katav-Ivanovsk earthquake, the amount of instrumental data obtained in 2018 was significantly larger and supplemented by the same information received from the local network of temporary stations deployed in the epicentral zone a day after the main shock. The local network made it possible to obtain a fairly complete picture of the focal area, due to the fact that for the first time in the Urals a powerful aftershock process was recorded.

7.1.2   Instrumental Data

In total, more than 1200 seismic events were recorded and processed in the epicentral zone. Their temporal dynamics are shown in Figure 7.1, and a map of those earthquakes recorded by at least three stations is shown in Figure 7.2. It can also be seen in the map that the local network changed its spatial configuration, however, events with magnitudes of M0.8 and above were registered at all times (see Fig. 7.3).

The calculation of the coordinates of the epicenter, based on the data from teleseismic stations and the regional network (57 stations in total), indicates the position of the source in the area of the Karaulovka village (Fig. 7.2). However, the cloud of aftershocks obtained from the data of the temporary network indicates that this epicenter was determined with a large error (about 10 km). The subsequent recalculation using the relative location procedure of *Spence* (1980), where the aftershock of November 15, 2018 which could be more accurately located (location error of less than 0.5 km) because of the additional stations from the temporary network was used as the master event, showed that the main event occurred near the western outskirts of Katav-Ivanovsk. The same procedure was performed for two other strong aftershocks that occurred on the first day, while the temporary network was not yet functioning. The
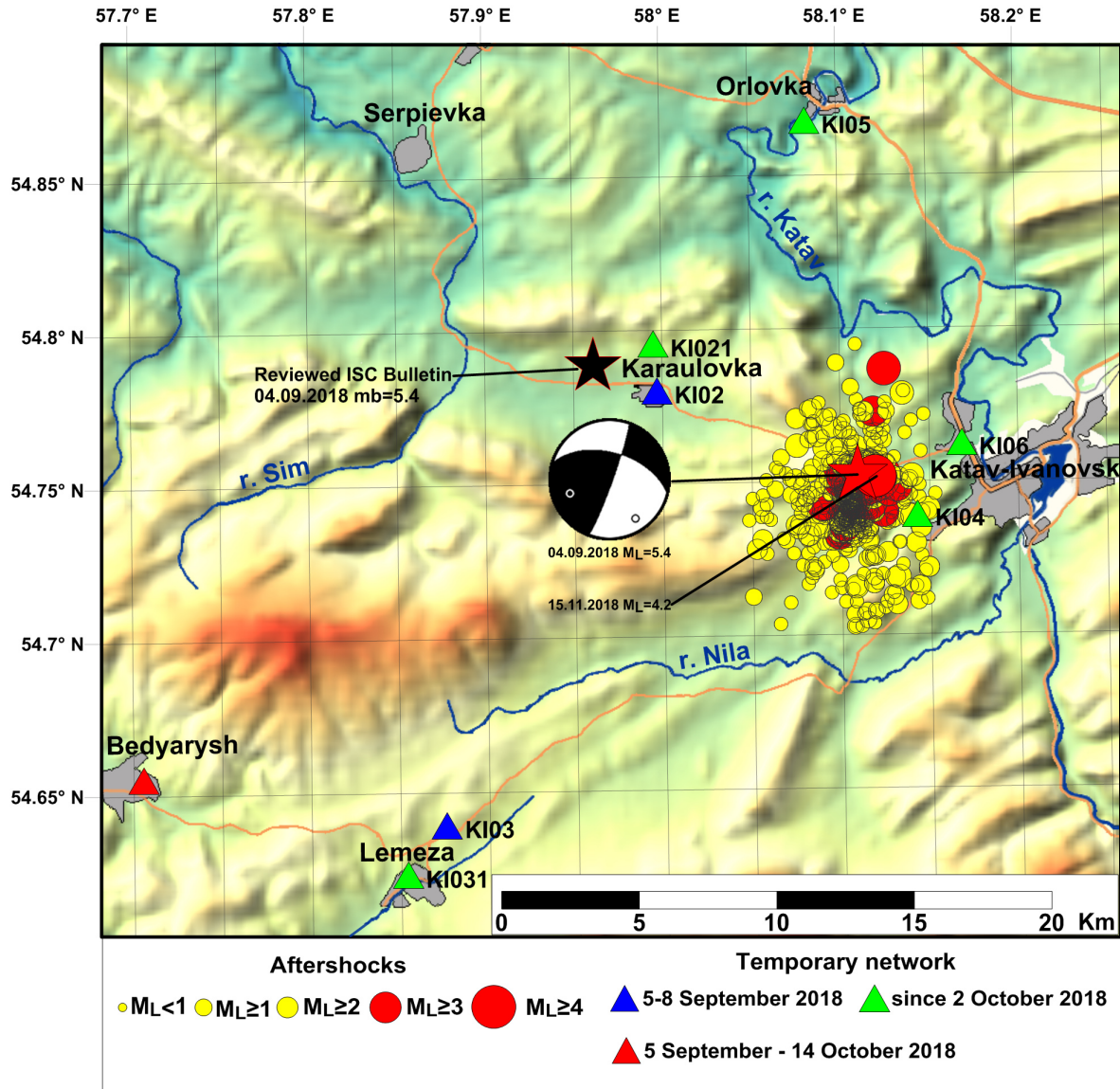
Figure 7.2: *Map of aftershocks of the Katav-Ivanovsk earthquake. Orange lines = roads.*

Date	Orig. time	Hypocentre							Magnitude
		Lat/deg	**Lon/deg**	**a/km**	**b/km**	**Az/deg**	**h/km**	**δ/km**	
04/09/2018	22:58:19	54.752	58.110	2.25	1.35	137	5.9	1.0	mb=5.4, ML=5.4, MS=4.8
05/09/2018	07:27:15	54.757	58.106	2.95	0.82	101	3.2f	–	mb=4.7, ML=3.8
29/09/2018	09:06:46	54.757	58.099	2.00	0.65	110	3.2f	–	mb=4.4, ML=4.1
15/11/2018	07:48:24	54.752	58.119	0.44	0.44	-	3.15	0.30	mb=4.4, ML=4.2

Table 7.1: *Parameter of the Katav-Ivanovsk earthquake and its three strongest aftershocks according to instrumental data. f - fixed depth; a, b – axes of error ellipse; Az – azimuth of longest axis.*

refined parameters of the hypocenters for all three relocated events and the master event are presented in Table 7.1.

The focal mechanism was calculated based on the polarity of the first arrivals of P-waves at 42 stations, of which compression motion (positive polarity) was recorded at 20 stations, and tension (negative polarity) at 22 stations. The stations are located between 1.5 and 94.6° epicentral distance and in the azimuthal range of AZ=12–355°. Data on the focal mechanism are given in Table 7.2. The nodal plane NP1 corresponds to the right-hand strike slip with elements of uplift, the plane NP2 corresponds to
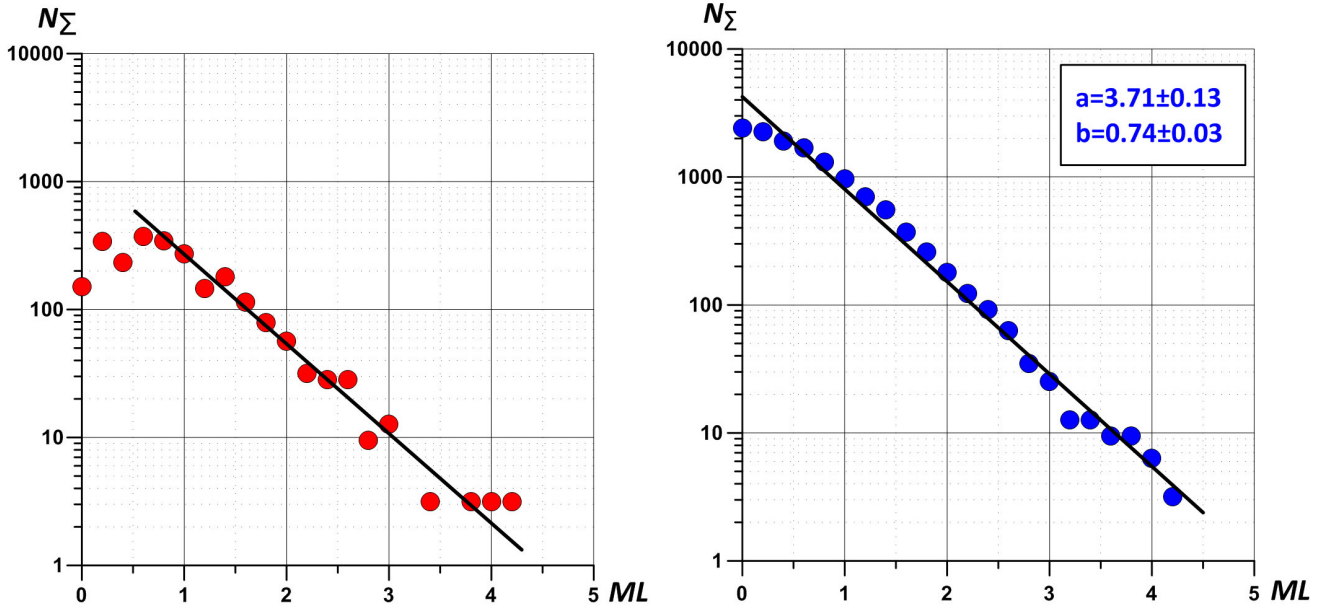
Figure 7.3: *Frequency (left) and cumulative frequency (right) magnitude distribution for the aftershock sequence of the Katav-Ivanovsk earthquake.*

Principal stress axes					
T		**P**		**N**	
Plunge/deg	**Azimuth/deg**	**Plunge/deg**	**Azimuth/deg**	**Plunge/deg**	**Azimuth/deg**
29	249	21	147	27	53
Nodal planes					
NP1			**NP2**		
Strike/deg	**Dip/deg**	**Rake/deg**	**Strike/deg**	**Dip/deg**	**Rake/deg**
285	54	173	19	85	37

Table 7.2: *Focal mechanism solution of the Katav-Ivanovsk earthquake.*

the left-hand reverse strike slip. Taking into account the orientation of the cloud of aftershocks, the NP2 plane is seen as the most probable variant of movement. The same decision is in good agreement with the tectonic condition of the area. The stress direction in the source actually coincides with the stresses obtained by alternative methods in the area (*Tevelev et al.*, 2019), and the rupture along the NP2 plane coincides in strike and slip pattern with the ruptures of the Bakal-Satka fault zone in the nearby Chelyabinsk Region.

7.1.3 Macroseismic Data

The earthquake in Katav-Ivanovsk had a significant macroseismic effect. Most of the macroseismic information was collected during the first week after the event as a result of a survey of the population in the settlements closest to the epicenter. Also, data collection was carried out through a survey of the population via the Internet. Due to the vastness of the survey geography (the radius of the earthquake sensibility zone was 200–300 km), the questionnaires in social media networks were partially filled out by specialists when replies were shared in posts rather than put into the questionnaires. In particular, the latter method made it possible to collect representative data on shaking in the nearest regional centres: Chelyabinsk, Ufa, Yekaterinburg and Perm. Systematization of macroseismic data was carried

Figure 7.4: *Damages to the hospital in Katav-Ivanovsk.*

out according to the new seismic intensity scale – SIS-2017 (*GOST R 57546-2017*, 2017), which is fully compatible with MSK-64, but allows for more objective assessments of seismic intensity in settlements based on people's feelings, reactions of household items and damage to buildings.

The strongest shaking (up to 6 points), according to the collected data, was observed in an area with a radius of 30 km from the epicenter, which included three cities – Katav-Ivanovsk, Ust'-Katav and Yuryuzan and several small settlements. Since the event took place at night, people woke up, experienced a strong fright and sometimes ran out of their houses. In houses, light household items reacted strongly – they swayed, shifted and fell while heavy objects reacted less frequently and more weakly. The largest amount of damage to buildings was noted in the city of Katav-Ivanovsk and the village Orlovka. The building of the city hospital in Katav-Ivanovsk suffered the worst damage, where there were cracks in the partitions, cracks in the load-bearing walls and large pieces of plaster falling off (Fig. 7.4). After the incident, the activities of the institution were suspended. In total, 454 cases of damage to private houses were officially registered in the city. Most of the damage was done to the interior decoration of the premises, although sometimes cracks in the foundation were noted, and in some cases collapsed stoves and chimneys.

Also, strong shaking caused a landslide on the eastern slope of Peschanaya Mountain, located directly

Figure 7.5: *Landslide on the eastern slope of Peschanaya Mountain triggered by the main shock.*

above the main shock (Fig. 7.5). The landslide was noticed in the forest by local residents on September 25, 2018, when the viscous water saturated soil, along with the trees growing on it, began to slowly slide down a slope with a dip angle of 5°. In the most intense phase of movement, the mud flowed with a width of 10 to 30 m and moved at a speed of about 1 m/s. As a result, a large volume of soil moved down the slope for about 0.5 km leaving a 3-5 m deep ditch behind along its path. The entire volume of the removed soil (about 5000 m^3) stopped on the slope below, forming piles up to 3 m high. The presence of such a landslide, according to the SIS-2017 classification, confirms the intensity of shaking at the epicenter up to 6 points.

After collecting the macroseismic data, they were geographically grouped and processed. These results served as the basis for constructing a map of the macroseismic field, which is shown in Figure 7.6.

Isoseismal lines on the map were constructed using the approach described in *Kul'chitskii* (2014), allowing for the azimuthal heterogeneity of the distribution of the macroseismic effect under conditions of low spatial coverage of the initial data, which is especially important in sparsely populated areas of the Urals. The macroseismic epicenter (maximum of macroseismic field) is located in the Orlovka village and has the coordinates: 54.877°N, 58.110°E, which is 14 km north of the instrumental epicenter. The macroseismic field is oriented to the Northwest, which is in good agreement with the results of macroseismic surveys of other strong earthquakes in the Urals (*Dyagilev et al.*, 2018).

It should be noted that in 2004 and 2006 five smaller earthquakes of magnitudes 2.3≤M≤3.0 were recorded in the same area. One of them had a macroseismic effect with an intensity of up to 4 points. Doublet earthquakes were observed twice, which were separated from each other in time by several minutes. Due to the low density of the stationary seismic network in this area, it was difficult to conclude anything about the nature of these events, because for the South Urals, due to the active development of deposits, induced seismicity is also typical. For the induced seismicity, aftershocks over a short period in time were also noted at the nearby mining facilities. Now, after detailed observations of the epicentral zone, it has become quite obvious that technogenic sources in the vicinity of Katav-Ivanovsk do not occur, and the events of 2004-2006 are weak tectonic earthquakes with aftershocks, of which only the strongest ones were observed instrumentally.
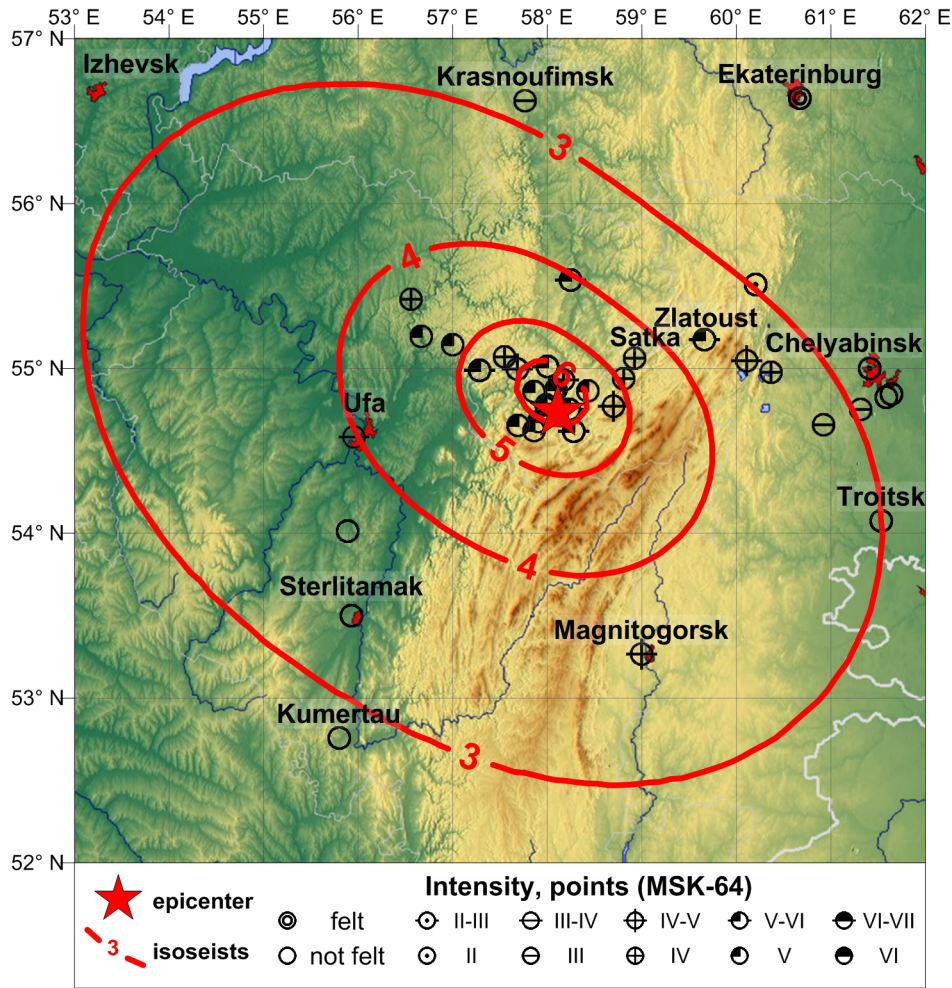
Figure 7.6: *Map of the macroseismic field of the Katav-Ivanovsk earthquake.*

7.1.4 Conclusion

The Katav-Ivanovsk earthquake became the strongest instrumentally recorded earthquake in the Urals (mb=5.4) and at the same time the most perceptible on the territory of Russia in 2018 (I_0=6 according to SIS-2017). The uniqueness of this event was given by the fact that after it, for the first time in the Urals, a powerful aftershock process was recorded, the active stage of which lasted for more than one year. Analysis of the historical seismicity showed that this area has been seismically active for a long time. The available data indicate the predisposition of many tectonic events of the Southern Urals to be accompanied by aftershocks and the Katav-Ivanovsk earthquake itself became the most productive of them.

The application of traditional approaches to the processing of primary data yielded approximate parameters of the main shock and two strong aftershocks, which spatially poorly matched the seismicity recorded after the installation of the network of temporary stations around the epicenter. The relative location procedure made it possible to clarify the location of problem hypocenters and to considerably reduce the location error. Calculations of the parameters of the focal mechanism together with the orientation of the aftershock field indicate slip along a left-hand reverse fault with a sub meridional strike.

The macroseismic effect of the main shock is analysed in terms of the SIS-2017 scale. As a result of this analysis, a map of the macroseismic field was built taking into account the azimuthal heterogeneity of the distribution of the macroseismic effect. The resulting field indicates predominant propagation of ground shaking in the Northwest direction.

7.1.5 Acknowledgements

7.1.6 References

Dyagilev, R., N. Guseva and F. Verkholantsev (2018), Macroseismic Field Anisotropy of the ML 4.7 Earthquake of 18 October 2015 in Central Urals, Russia, *Summary of the Bulletin of the International Seismological Centre*, *52*(II), 50–59, `https://doi.org/10.31905/KP7ZNV1Z`.

GOST R 57546-2017 (2017), Earthquakes Seismic Intensity Scale, National Standard of Russian Federation, Moscow, Russia, 28 p. (In Russian)

Godzikovskaya, A.A. (2016), Catalogue of seismic events of the Ural region since ancient time till 2002 (Accompanying primary data), *IPE RAS Publ.*, Moscow, Russia 258 p. (In Russian)

Kul'chitskii, V.E. (2014), Estimation of anisotropic macroseismic field decay parameters, *Geophysical Journal*, *36*(2), 138–149. (In Russian)

Malovichko, A.A., A.N. Morozov, N.V Vaganova, V.E. Asming, R.A. Dyagilev and Z.A. Evtiugina (2020), The August 17, 1914 Bilimbaev earthquake: relocation based on instrumental data, *Russian Journal of Seismology*, *2*(1), 40–47, `https://doi.org/10.35540/2686-7907.2020.1.04`. (In Russian)

Spence, W. (1980), Relative epicenter determination using P-wave arrival-time differences, *Bull. Seism. Soc. Am.*, *70*(1), 171–183, `https://doi.org/10.1785/BSSA0700010171`.

Tevelev, Al.V., Ark.V. Tevelev, A.O. Khotylev, I.A. Prudnikov, E.A. Volodina and V.M. Moseichuk (2019), Earthquakes of 2018 in Katav-Ivanovsk (Southern Urals): kinematics of initiating failures. *Problems of tectonics of continents and oceans. Proceedings of LI seminar on tectonics*, 286-290, Moscow, Russia: GEOS Publ. (In Russian)

8

Statistics of Collected Data

8.1 Introduction

The ISC Bulletin is based on the parametric data reports received from seismological agencies around the world. With rare exceptions, these reports include the results of waveform review done by analysts at network data centres and observatories. These reports include combinations of various bulletin elements such as event hypocentre estimates, moment tensors, magnitudes, event type and felt and damaging data as well as observations of the various seismic waves recorded at seismic stations.

Data reports are received in different formats that are often agency specific. Once an authorship is recognised, the data are automatically parsed into the ISC database and the original reports filed away to be accessed when necessary. Any reports not recognised or processed automatically are manually checked, corrected and re-processed. This chapter describes the data that are received at the ISC before the production of the reviewed Bulletin.

Notably, the ISC integrates all newly received data reports into the automatic ISC Bulletin (available on-line) soon after these reports are made available to ISC, provided it is done before the submission deadline that currently stands at 12 months following an event occurrence.

With data constantly being reported to the ISC, even after the ISC has published its review, the total data shown as collected, in this chapter, is limited to two years after the time of the associated reading or event, i.e. any hypocentre data collected two years after the event are not reflected in the figures below.

8.2 Summary of Agency Reports to the ISC

A total of 151 agencies have reported data for July 2018 to December 2018. The parsing of these reports into the ISC database is summarised in Table 8.1.

Table 8.1: *Summary of the parsing of reports received by the ISC from a total of 151 agencies, containing data for this summary period.*

	Number of reports
Total collected	5985
Automatically parsed	4909
Manually parsed	1075

Data collected by the ISC consists of multiple data types. These are typically one of:

- Bulletin, hypocentres with associated phase arrival observations.

- Catalogue, hypocentres only.

- Unassociated phase arrival observations.

In Table 8.2, the number of different data types reported to the ISC by each agency is listed. The number of each data type reported by each agency is also listed. Agencies reporting indirectly have their data type additionally listed for the agency that reported it. The agencies reporting indirectly may also have 'hypocentres with associated phases' but with no associated phases listed - this is because the association is being made by the agency reporting directly to the ISC. Summary maps of the agencies and the types of data reported are shown in Figure 8.1 and Figure 8.2.

Table 8.2: *Agencies reporting to the ISC for this summary period. Entries in bold are for new or renewed reporting by agencies since the previous six-month period.*

Agency	Country	Directly or indirectly reporting (D/I)	Hypocentres with associated phases	Hypocentres without associated phases	Associated phases	Unassociated phases	Amplitudes
TIR	Albania	D	680	2	11477	121	3136
CRAAG	Algeria	D	275	0	2039	108	0
INAM	**Angola**	**D**	**49**	**0**	**155**	**0**	**0**
LPA	Argentina	D	0	0	0	158	0
SJA	Argentina	D	2997	2	88785	118	19593
NSSP	Armenia	D	47	0	594	0	0
AUST	Australia	D	1557	11	64335	0	55665
CUPWA	Australia	D	70	0	890	0	0
IDC	Austria	D	19334	1	629845	0	582613
VIE	Austria	D	5169	112	55078	0	54841
AZER	Azerbaijan	D	1379	0	27910	0	0
UCC	Belgium	D	1632	243	10010	45	2937
LPZ	Bolivia	I ECX	22	0	0	0	0
SCB	Bolivia	D	517	0	5646	0	948
RHSSO	Bosnia and Herzegovina	D	908	0	19172	8763	0
BGSI	Botswana	D	266	0	3157	10	717
OSUNB	Brazil	D	101	0	1474	0	0
VAO	Brazil	D	1008	80	27258	0	0
SOF	Bulgaria	D	194	0	2458	3165	0
SOMC	Cameroon	D	0	0	0	10	0
OTT	Canada	D	1416	11	42413	0	5029
PGC	Canada	I OTT	724	0	26353	0	0
GUC	Chile	D	3553	244	96027	6302	27045
BJI	China	D	1543	1	135154	37177	93793
ASIES	Chinese Taipei	D	0	149	0	0	0
TAP	Chinese Taipei	D	19101	0	821971	0	0
RSNC	Colombia	D	12170	219	221942	0	18727
UCR	Costa Rica	D	437	1	12972	11	0
ZAG	Croatia	D	0	0	0	37417	0
SSNC	Cuba	D	896	0	19020	0	7693
NIC	Cyprus	D	385	0	10905	0	4556
IPEC	Czech Republic	D	590	4	4139	24491	1860
PRU	Czech Republic	D	4928	15	39997	557	9818
WBNET	Czech Republic	D	308	0	5839	0	5839
KEA	Democratic People's Republic of Korea	D	132	0	1276	0	633
DNK	Denmark	D	2202	1157	26291	24510	7707
ARO	**Djibouti**	**I EAF**	**0**	**0**	**0**	**22**	**0**
OSPL	Dominican Republic	D	1140	9	15283	0	5231
SDD	Dominican Republic	D	1349	0	30798	0	14685
IGQ	Ecuador	D	124	0	4938	0	0
HLW	Egypt	D	46	0	624	0	0
SNET	El Salvador	D	1219	2	23322	1	2615
EST	Estonia	I HEL	228	28	0	0	0
AAE	Ethiopia	I EAF	95	0	722	786	0

Table 8.2: *(continued)*

Agency	Country	Directly or indirectly reporting (D/I)	Hypocentres with associated phases	Hypocentres without associated phases	Associated phases	Unassociated phases	Amplitudes
SKO	North Macedonia	D	471	0	6654	2724	1015
FIA0	Finland	I HEL	4	1	0	0	0
HEL	Finland	D	8184	758	195229	0	35110
CSEM	France	I AWI	3549	462	0	0	0
IPGP	France	D	0	148	0	0	0
LDG	France	D	2578	79	39771	4	16895
STR	France	D	4384	0	91272	50	0
PPT	French Polynesia	D	1377	11	13337	66	13369
TIF	Georgia	D	0	61	0	1093	0
AWI	Germany	D	7763	3	37763	1576	19075
BGR	Germany	D	760	271	19864	0	7182
BNS	Germany	I BGR	4	40	0	0	0
BRG	Germany	D	0	0	0	13218	5176
BUG	Germany	I BGR	18	30	0	0	0
CLL	Germany	D	2	0	34	10786	3981
GDNRW	Germany	I BGR	2	25	0	0	0
GFZ	Germany	I PRE	105	2	0	0	0
HLUG	Germany	I BGR	0	5	0	0	0
LEDBW	Germany	I BGR	17	1	0	0	0
ATH	Greece	D	9194	29	302766	0	113066
THE	Greece	D	4034	0	92649	5594	30533
UPSL	Greece	D	0	11	0	0	0
GCG	Guatemala	D	392	0	2468	0	0
HKC	Hong Kong	D	0	0	0	39	0
KRSZO	Hungary	D	469	238	8169	0	1056
REY	Iceland	D	33	0	1437	0	0
HYB	India	D	539	0	1524	0	257
NDI	India	D	517	419	19543	263	7131
DJA	Indonesia	D	8775	94	105100	0	73457
TEH	Iran	D	8164	1	69615	0	0
THR	Iran	D	61	0	1268	430	347
ISN	Iraq	D	924	0	7806	6	2475
DIAS	Ireland	D	0	0	0	444	0
GII	Israel	D	3033	2	56525	0	6389
GEN	Italy	D	693	0	12793	0	0
MED_RCMT	Italy	D	0	268	0	0	0
RISSC	Italy	D	6	0	113	0	0
ROM	Italy	D	9911	604	818150	272501	554174
TRI	Italy	D	0	0	0	11234	0
LIC	Ivory Coast	D	132	0	396	0	395
JSN	Jamaica	D	174	1	618	16	0
JMA	Japan	D	107049	3726	754380	0	17968
NIED	Japan	D	0	696	0	0	0
SYO	Japan	D	0	0	0	858	0
JSO	Jordan	D	573	0	7784	0	0
NNC	Kazakhstan	D	8491	0	91999	0	87371
SOME	Kazakhstan	D	4860	88	73976	0	65243
NAI	**Kenya**	**I EAF**	**0**	**0**	**0**	**305**	**0**
KNET	Kyrgyzstan	D	973	0	8057	0	2414
KRNET	Kyrgyzstan	D	1758	0	37482	0	0
LVSN	Latvia	D	190	0	2748	0	1590
GRAL	Lebanon	D	312	0	2887	464	0
LIT	Lithuania	D	754	751	6333	1876	3
MCO	Macao, China	D	0	0	0	29	0
GSDM	Malawi	D	0	0	0	564	0
ECX	Mexico	D	917	0	24568	0	4840
MEX	Mexico	D	12617	73	231407	93	0
MOLD	Moldova	D	14	0	105	1030	562
PDG	Montenegro	D	573	0	11902	0	6095
CNRM	Morocco	D	1536	0	15870	0	0
NAM	Namibia	D	1454	0	32610	2	10648
DMN	Nepal	D	9	0	167	0	54
DBN	Netherlands	I BGR	0	1	0	0	0
NOU	New Caledonia	D	5415	1	100591	0	4148
WEL	New Zealand	D	7013	369	235492	15404	214940
CATAC	Nicaragua	D	1715	0	84852	0	31799

Table 8.2: *(continued)*

Agency	Country	Directly or indirectly reporting (D/I)	Hypocentres with associated phases	Hypocentres without associated phases	Associated phases	Unassociated phases	Amplitudes
BER	Norway	D	2034	1512	44731	4431	12173
NAO	Norway	D	2702	900	5640	0	2516
OMAN	Oman	D	622	0	35453	0	0
UPA	Panama	D	1665	7	24383	449	1027
ARE	**Peru**	**I NEIC**	**0**	**2**	**0**	**0**	**0**
MAN	Philippines	D	0	24	0	7065	1748
QCP	Philippines	D	0	0	0	113	0
PJWWP	**Poland**	**D**	**18**	**0**	**45**	**0**	**0**
WAR	Poland	D	0	0	0	8396	326
IGIL	Portugal	D	750	0	3524	0	1159
INMG	Portugal	D	1594	0	69327	3468	14545
SVSA	Portugal	D	766	0	14403	2835	5998
BELR	Republic of Belarus	D	0	0	0	27527	9513
CFUSG	Republic of Crimea	D	37	1	802	309	649
KMA	Republic of Korea	D	16	0	595	0	0
BUC	Romania	D	662	46	15997	62918	2375
ASRS	Russia	D	101	35	3120	0	1151
BYKL	Russia	D	61	1	7314	0	2548
DRS	Russia	I MOS	151	120	0	0	0
FCIAR	Russia	D	126	0	1114	826	471
IDG	Russia	I MOS	0	29	0	0	0
KOLA	Russia	D	592	101	5517	0	0
KRSC	Russia	D	1258	0	37029	0	0
MIRAS	Russia	D	160	16	2108	0	1750
MOS	Russia	D	3021	487	367853	0	127150
NERS	Russia	D	54	5	1435	0	632
NORS	Russia	I MOS	22	134	0	0	0
SKHL	Russia	D	1057	1097	23187	0	11302
VKMS	Russia	I MOS	0	17	0	0	0
YARS	Russia	D	360	21	3661	0	2590
SGS	Saudi Arabia	D	2875	0	48519	0	0
BEO	Serbia	D	1523	9	27890	0	0
BRA	Slovakia	D	0	0	0	24747	0
LJU	Slovenia	D	1429	8	18522	3688	6761
PRE	South Africa	D	1291	1	32684	33	11254
MDD	Spain	D	2820	0	64154	0	17717
MRB	Spain	D	548	0	14499	312	5866
SFS	Spain	D	1101	0	19574	0	0
UPP	Sweden	D	2200	1068	22930	0	0
ZUR	Switzerland	D	686	0	9896	0	6480
BKK	**Thailand**	**D**	**75**	**2**	**590**	**0**	**0**
TRN	Trinidad and Tobago	D	1235	9	15766	34788	0
TUN	Tunisia	D	90	0	344	0	0
AFAD	Turkey	D	11556	2	261460	0	93072
ISK	Turkey	D	10789	0	150809	4978	80779
AEIC	U.S.A.	I NEIC	3273	1419	125293	0	0
ANF	U.S.A.	I IRIS	278	719	0	0	0
BUT	U.S.A.	I NEIC	0	50	459	0	0
GCMT	U.S.A.	D	0	2618	0	0	0
HVO	U.S.A.	I NEIC	1233	7	29051	0	0
IRIS	U.S.A.	D	2548	719	375188	0	0
LDO	U.S.A.	I NEIC	6	5	71	0	0
NCEDC	U.S.A.	I NEIC	70	13	7273	0	0
NEIC	U.S.A.	D	20866	11791	2097505	0	1103965
PAS	U.S.A.	I NEIC	74	4	10286	0	0
PNSN	U.S.A.	D	0	101	0	0	0
REN	U.S.A.	I NEIC	37	12	1790	0	0
RSPR	U.S.A.	D	1880	827	32527	0	0
SEA	U.S.A.	I NEIC	33	1	1869	0	0
SLM	U.S.A.	I NEIC	46	0	981	0	0
TUL	U.S.A.	I NEIC	110	0	0	0	0
UUSS	U.S.A.	I NEIC	35	17	1146	0	0
ENT	**Uganda**	**I EAF**	**0**	**0**	**0**	**6**	**0**
MCSM	Ukraine	D	1296	303	26850	0	16254

Table 8.2: (continued)

Agency	Country	Directly or indirectly reporting (D/I)	Hypocentres with associated phases	Hypocentres without associated phases	Associated phases	Unassociated phases	Amplitudes
SIGU	Ukraine	D	25	25	588	0	294
DSN	United Arab Emirates	D	607	0	8287	0	0
BGS	United Kingdom	D	325	78	10669	0	3826
EAF	Unknown	D	527	0	4885	1602	135
ISU	Uzbekistan	D	414	0	3236	0	0
FUNV	Venezuela	D	293	0	4168	0	0
PLV	Viet Nam	D	18	3	268	0	148
LSZ	Zambia	D	60	0	185	164	0
BUL	Zimbabwe	D	866	0	8357	92	0
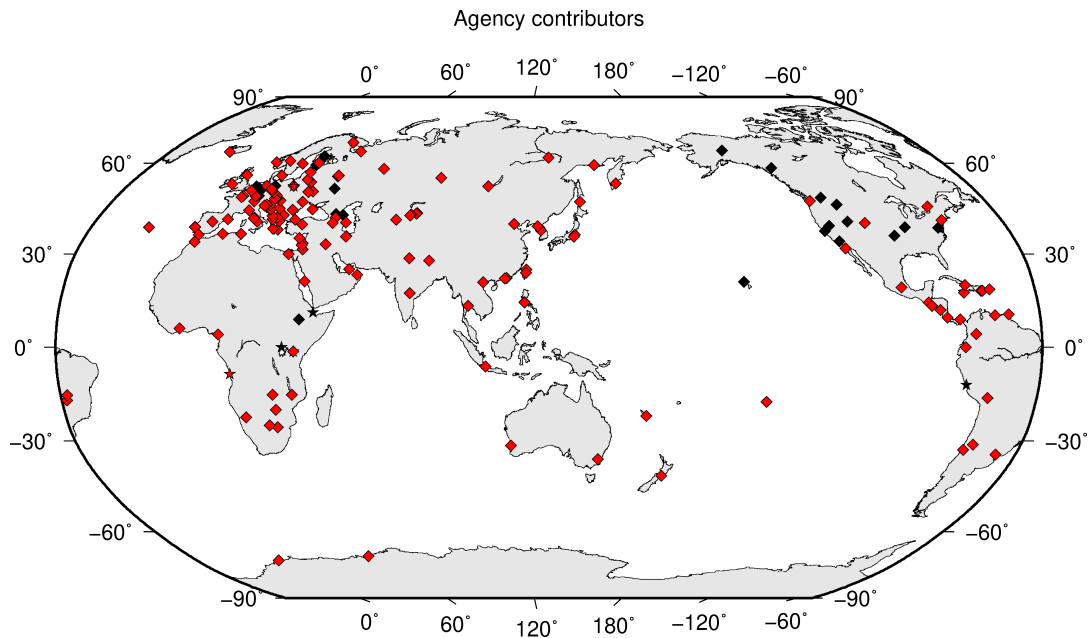
Figure 8.1: *Map of agencies that have contributed data to the ISC for this summary period. Agencies that have reported directly to the ISC are shown in red. Those that have reported indirectly (via another agency) are shown in black. Any new or renewed agencies, since the last six-month period, are shown by a star. Each agency is listed in Table 8.2.*

Types of reports to the ISC for data from 2018/07/01 to 2018/12/31
○ Hypocentres associated to phase data: 151 agencies
● Phases associated to hypocentres: 139 agencies
● Hypocentres without directly associated phase data: 97 agencies
□ Unassociated phases – phase data not directly associated with a hypocentre: 67 agencies
◆ Moment tensor solutions: 10 agencies
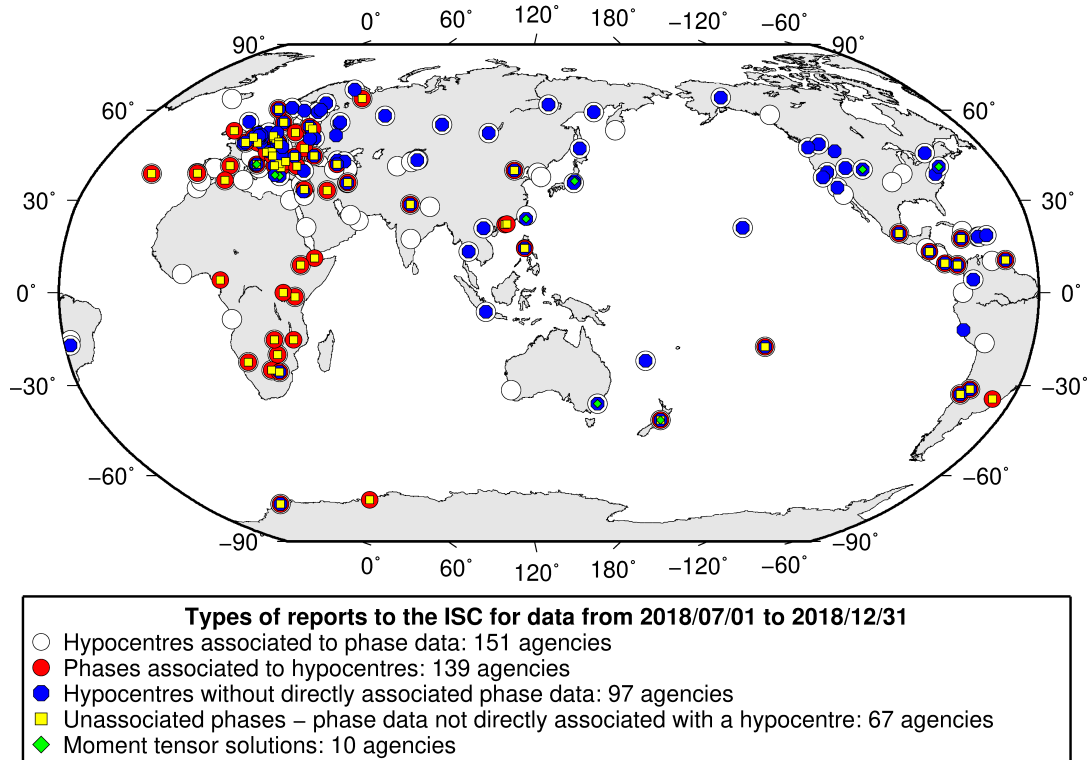
Figure 8.2: *Map of the different data types reported by agencies to the ISC. A full list of the data types reported by each agency is shown in Table 8.2.*

8.3   Arrival Observations

The collection of phase arrival observations at the ISC has increased dramatically with time. The increase in reported phase arrival observations is shown in Figure 8.3.

The reports with phase data are summarised in Table 8.3. This table is split into three sections, providing information on the reports themselves, the phase data, and the stations reporting the phase data. A map of the stations contributing these phase data is shown in Figure 8.4.

The ISC encourages the reporting of phase arrival times together with amplitude and period measurements whenever feasible. Figure 8.5 shows the percentage of events for which phase arrival times from each station are accompanied with amplitude and period measurements.

Figure 8.6 indicates the number of amplitude and period measurement for each station.

Together with the increase in the number of phases (Figure 8.3), there has been an increase in the number of stations reported to the ISC. The increase in the number of stations is shown in Figure 8.7. This increase can also be seen on the maps for stations reported each decade in Figure 8.8.
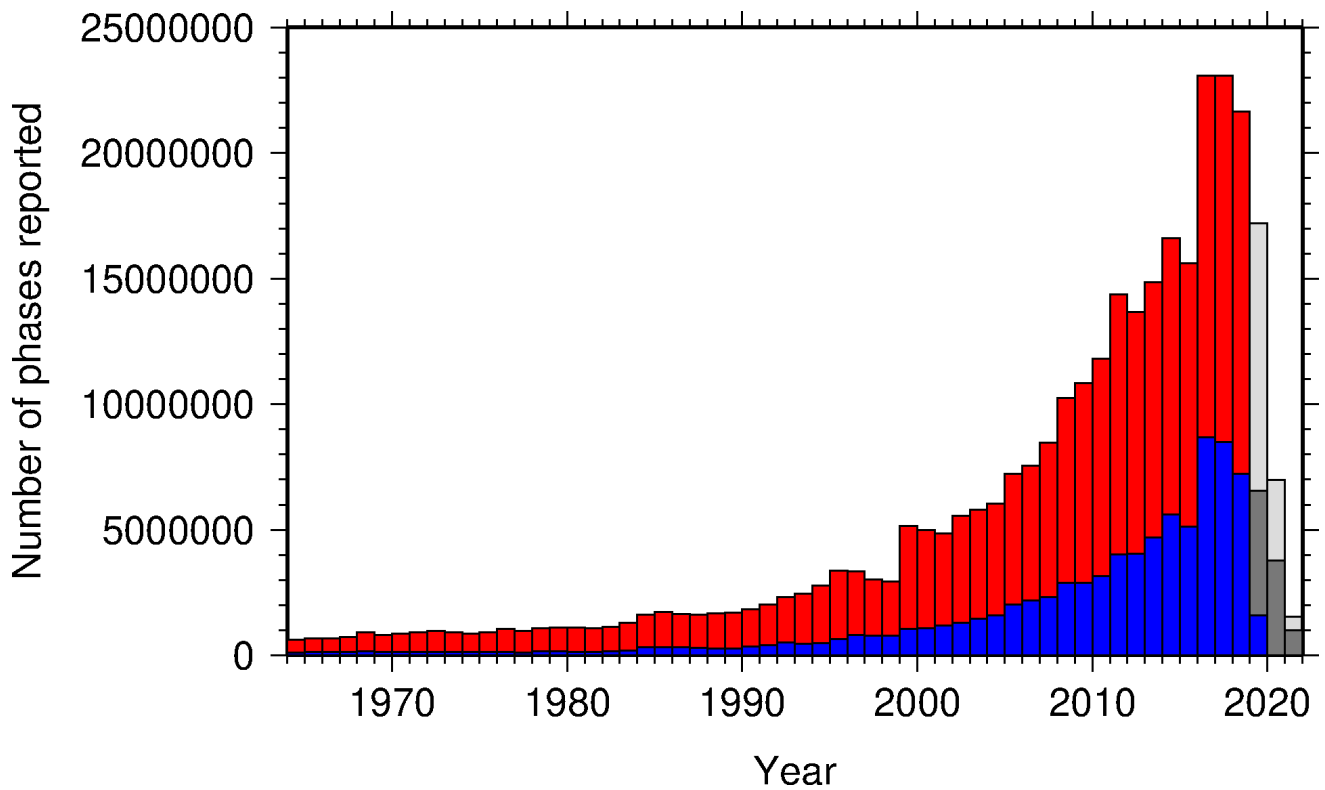
Figure 8.3: *Histogram showing the number of phases (red) and number of amplitudes (blue) collected by the ISC for events each year since 1964. The data in grey covers the current period where data are still being collected before the ISC review takes place and is accurate at the time of publication.*

Table 8.3: *Summary of reports containing phase arrival observations.*

Reports with phase arrivals	5696
Reports with phase arrivals including amplitudes	3253
Reports with only phase arrivals (no hypocentres reported)	195
Total phase arrivals received	10495528
Total phase arrival-times received	9652601
Number of duplicate phase arrival-times	733246 (7.6%)
Number of amplitudes received	3754090
Stations reporting phase arrivals	9616
Stations reporting phase arrivals with amplitude data	5485
Max number of stations per report	2159

Amplitude data were collected by the ISC from **5445** stations sent by
92 agencies for readings from **2018/07/01** to **2018/12/31**
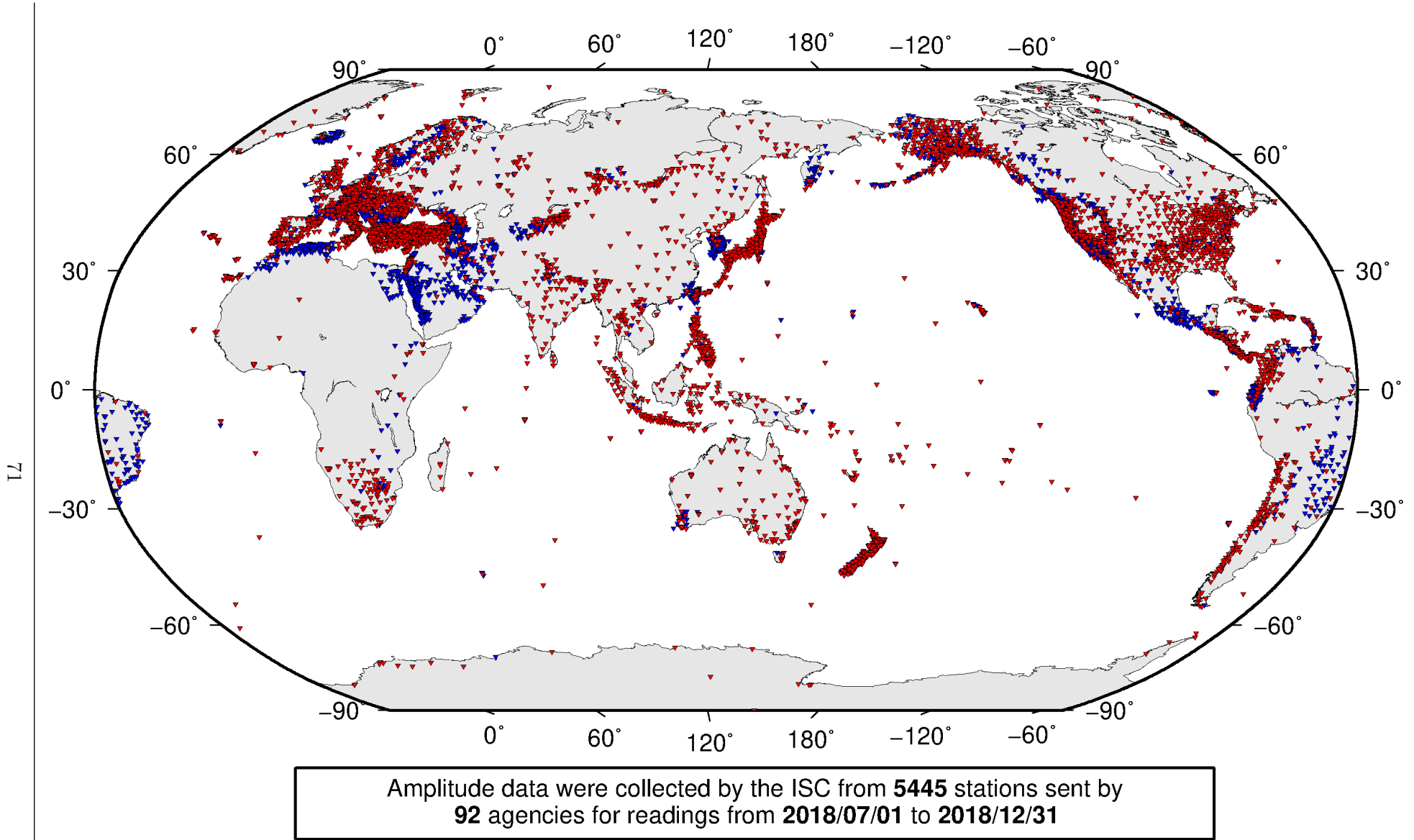
Figure 8.4: *Stations contributing phase data to the ISC for readings from July 2018 to the end of December 2018. Stations in blue provided phase arrival times only; stations in red provided both phase arrival times and amplitude data.*

Amplitude data were collected by the ISC from **5448** stations sent by **92** agencies for readings from **2018/07/01** to **2018/12/31**
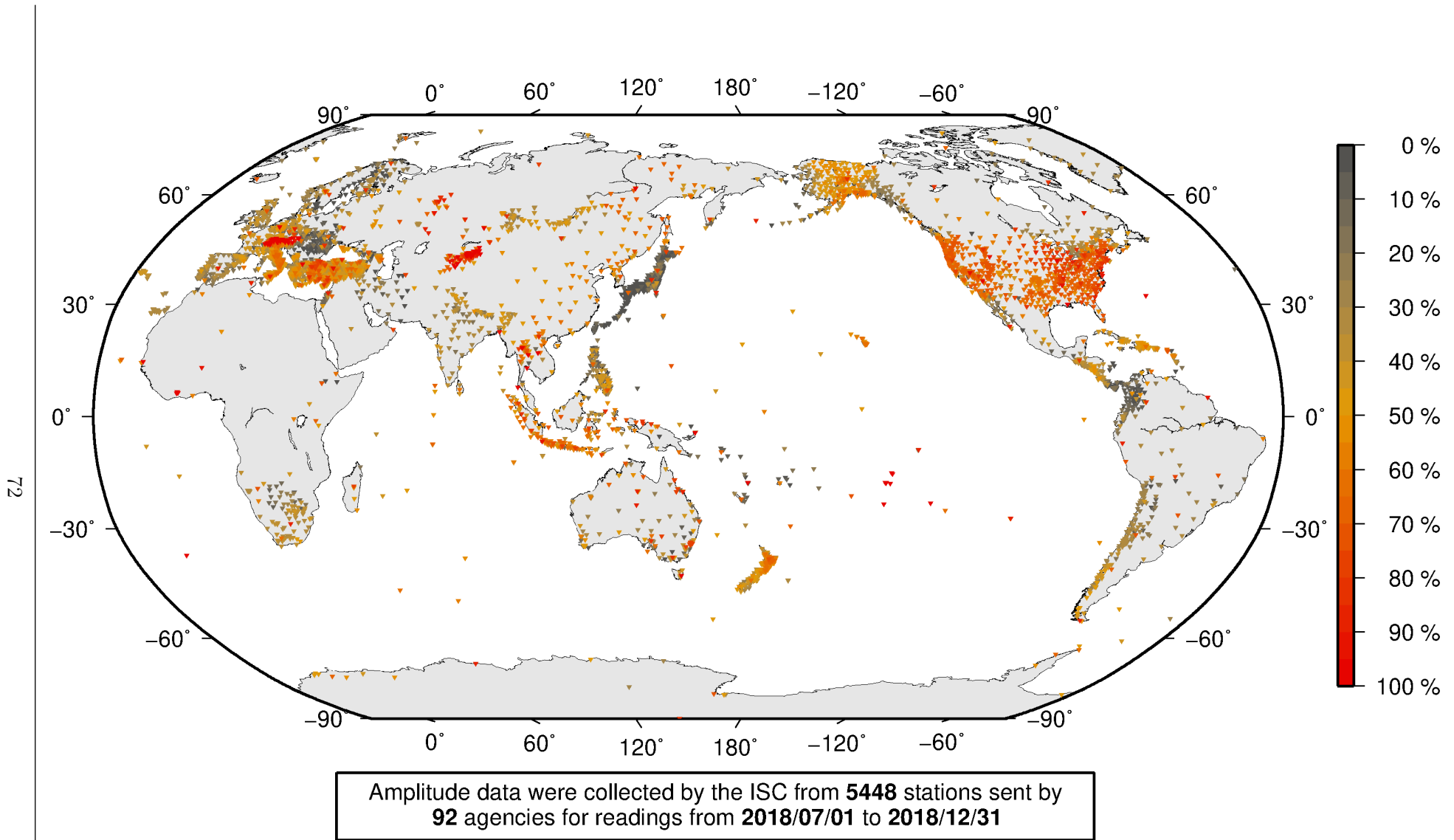
Figure 8.5: *Percentage of events for which phase arrival times from each station are accompanied with amplitude and period measurements.*
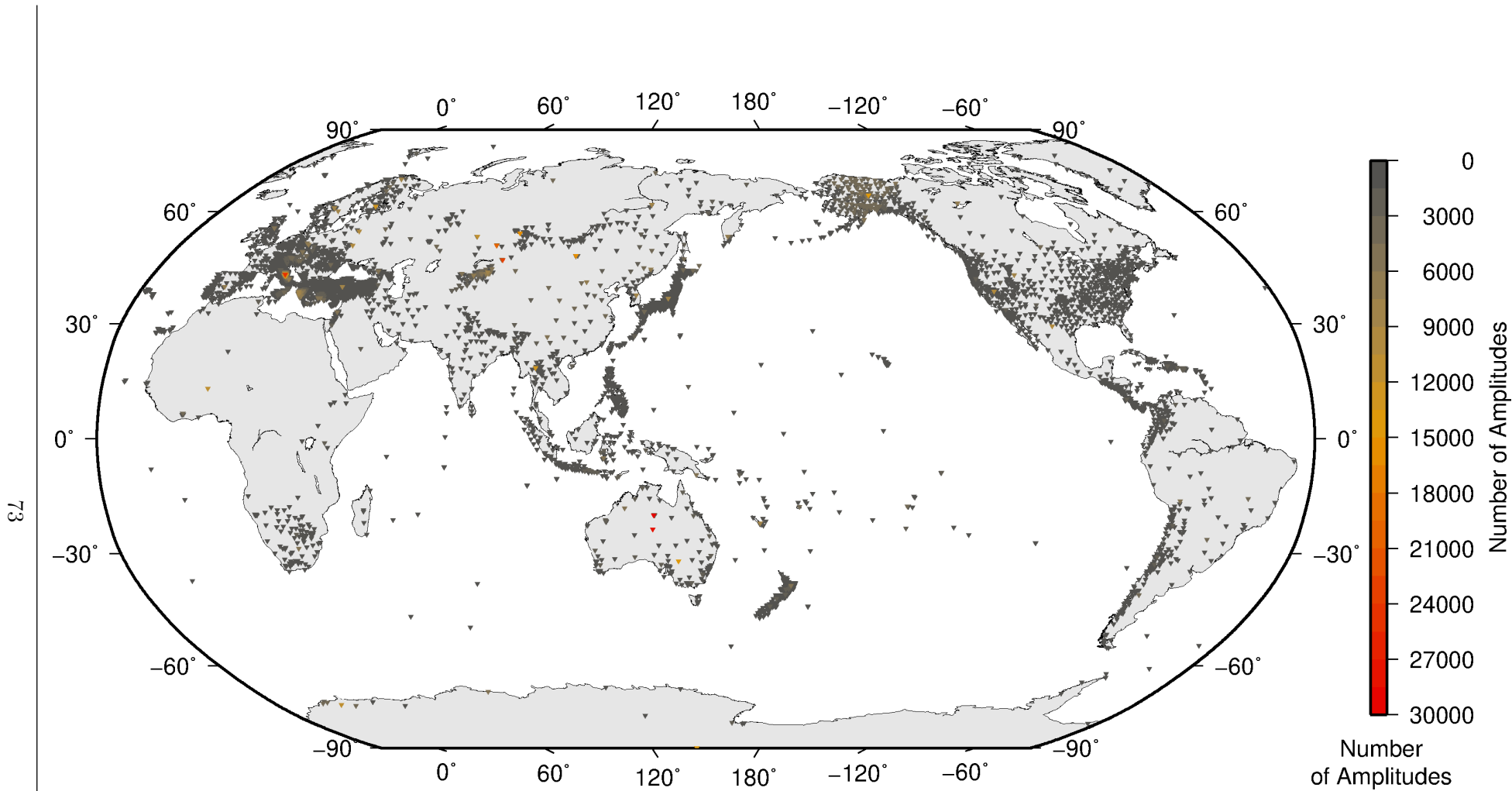
Amplitude data were collected by the ISC from **5448** stations sent by
92 agencies for readings from **2018/07/01** to **2018/12/31**

Figure 8.6: *Number of amplitude and period measurements for each station.*
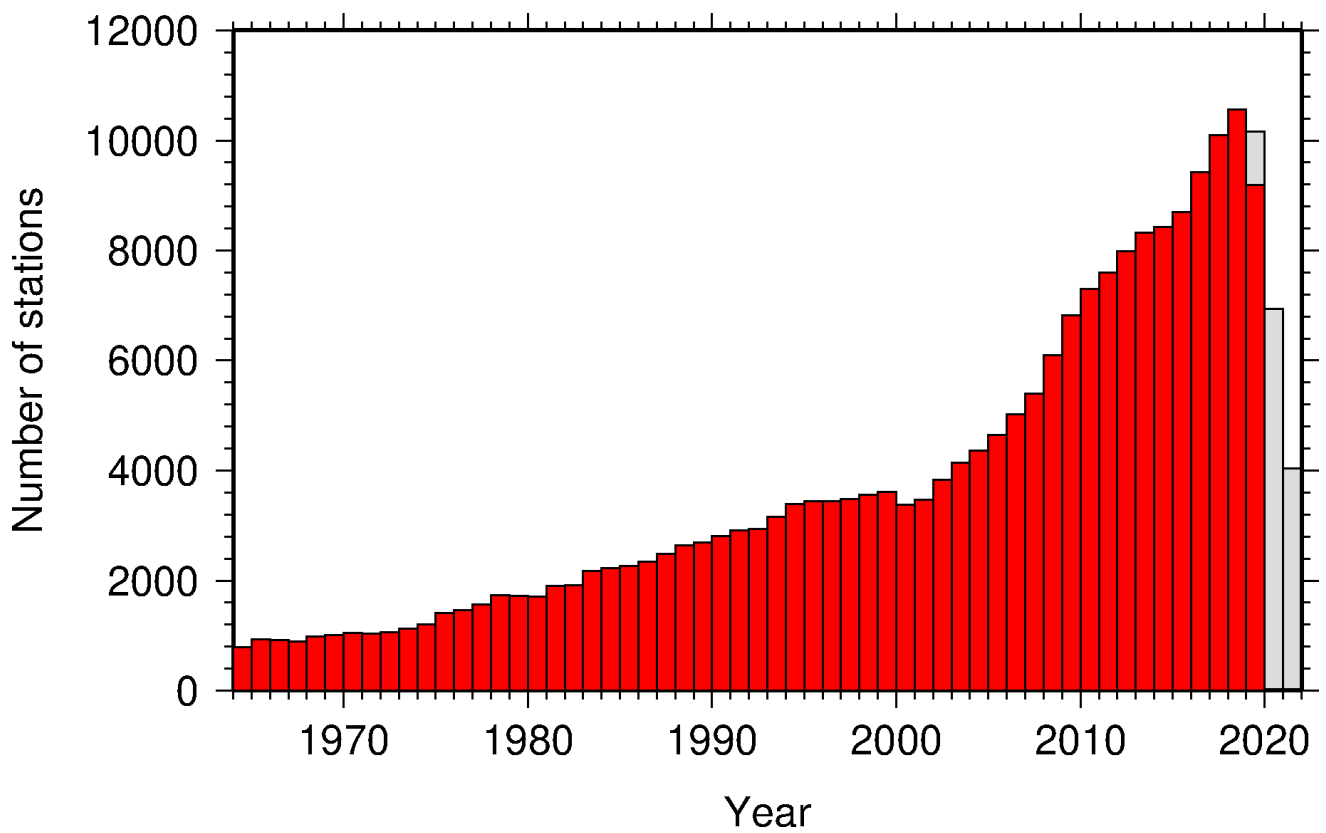
Figure 8.7: *Histogram showing the number of stations reporting to the ISC each year since 1964. The data in grey covers the current period where station information is still being collected before the ISC review of events takes place and is accurate at the time of publication.*
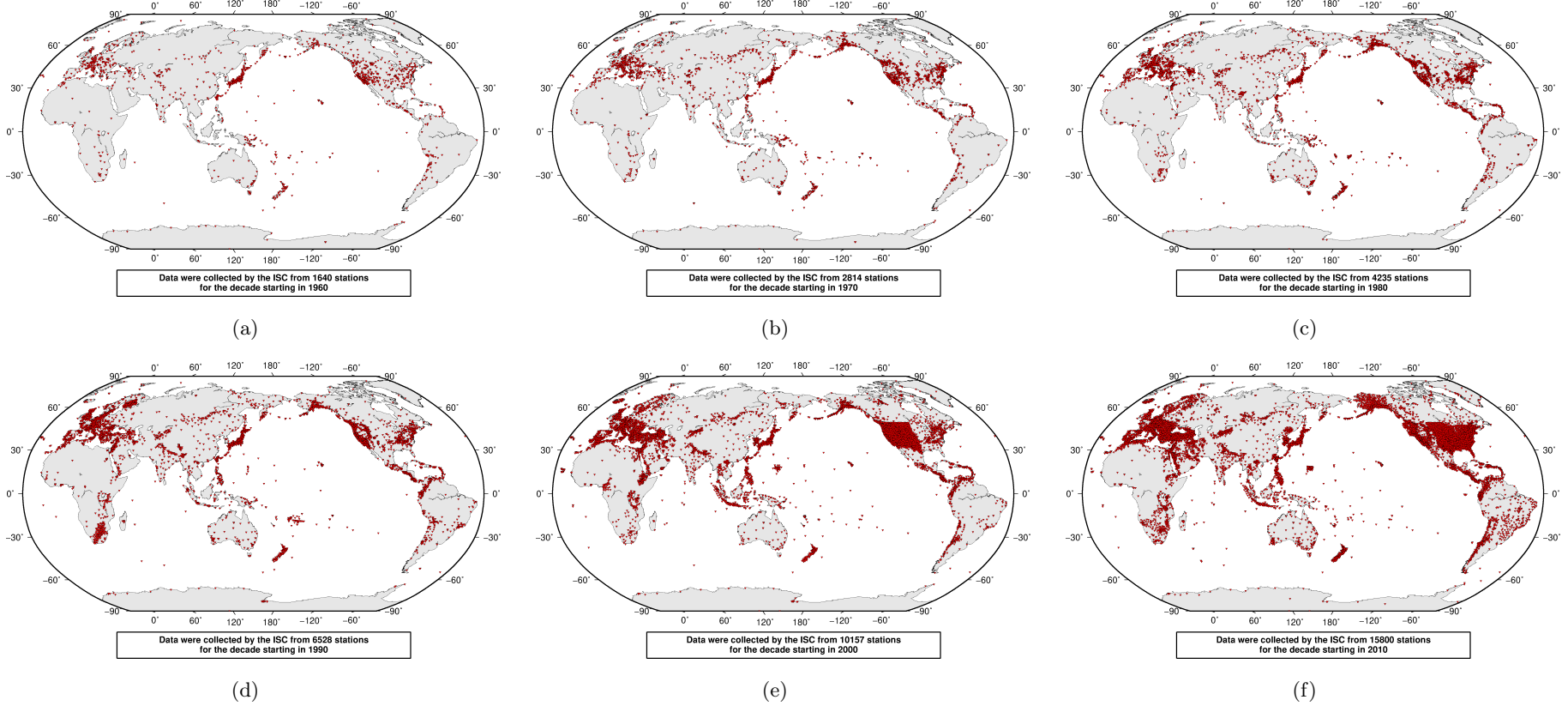
Figure 8.8: *Maps showing the stations reported to the ISC for each decade since 1960. Note that the last map covers a shorter time period.*

8.4   Hypocentres Collected

The ISC Bulletin groups multiple estimates of hypocentres into individual events, with an appropriate prime hypocentre solution selected. The collection of these hypocentre estimates are described in this section.

The reports containing hypocentres are summarised in Table 8.4. The number of hypocentres collected by the ISC has also increased significantly since 1964, as shown in Figure 8.9. A map of all hypocentres reported to the ISC for this summary period is shown in Figure 8.10. Where a network magnitude was reported with the hypocentre, this is also shown on the map, with preference given to reported values, first of M_W followed by M_S, m_b and M_L respectively (where more than one network magnitude was reported).

Table 8.4: *Summary of the reports containing hypocentres.*

Reports with hypocentres	5790
Reports of hypocentres only (no phase readings)	289
Total hypocentres received	421826
Number of duplicate hypocentres	13410 (3.2%)
Agencies determining hypocentres	167
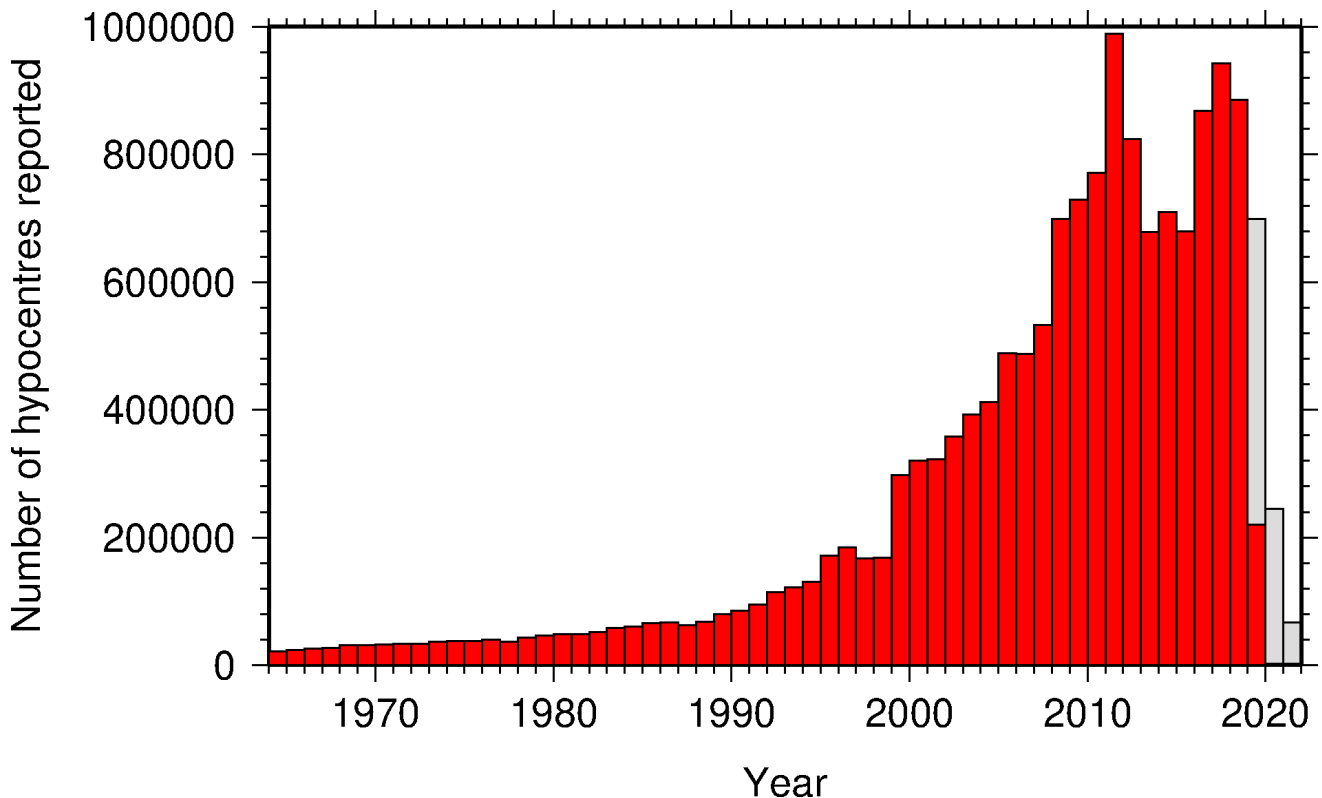
Figure 8.9: *Histogram showing the number of hypocentres collected by the ISC for events each year since 1964. For each event, multiple hypocentres may be reported.*

All the hypocentres that are reported to the ISC are automatically grouped into events, which form the basis of the ISC Bulletin. For this summary period 443886 hypocentres (including ISC) were grouped into 305196 events, the largest of these having 58 hypocentres in one event. The total number of events
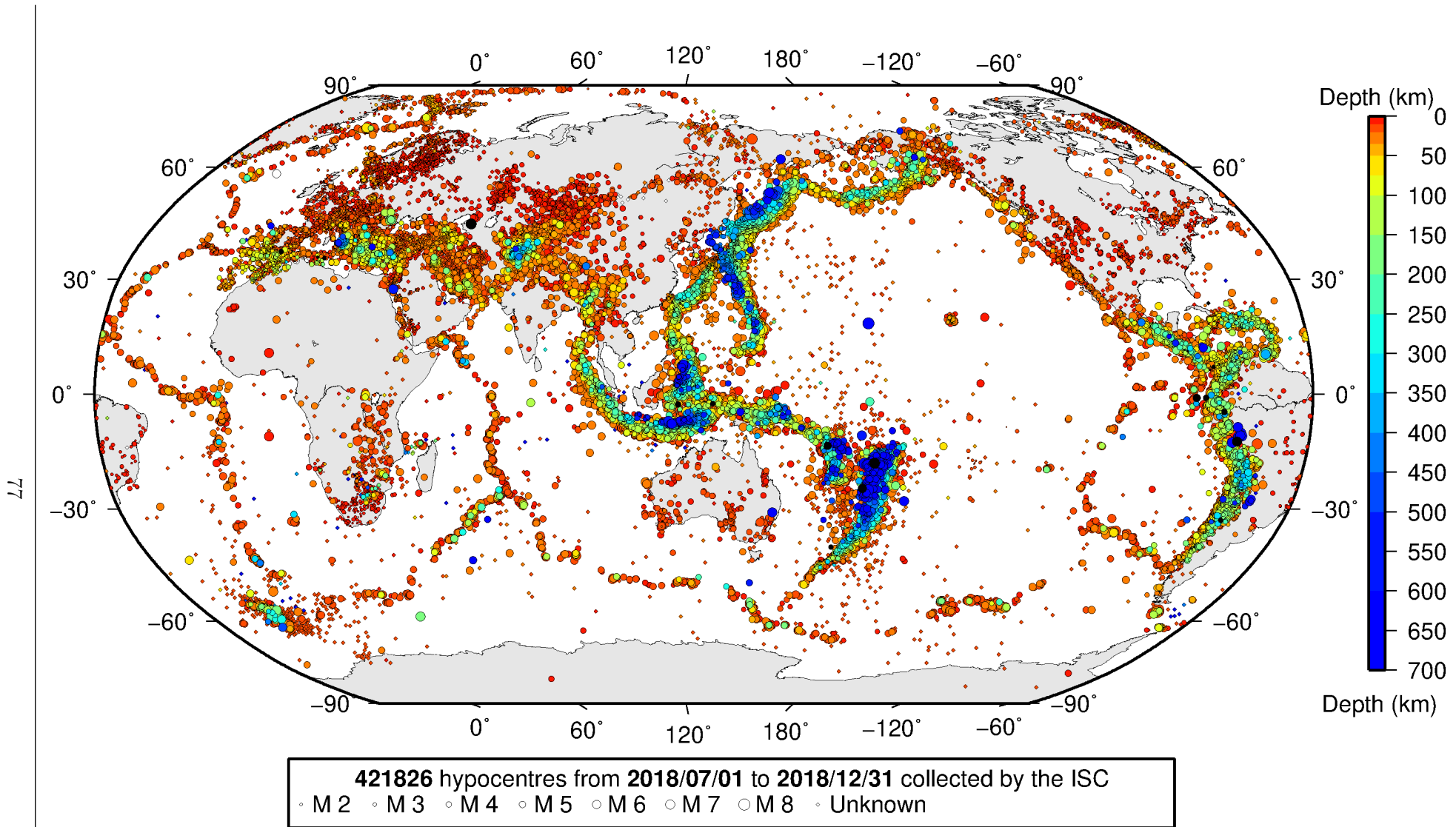
Figure 8.10: *Map of all hypocentres collected by the ISC. The scatter shows the large variation of the multiple hypocentres that are reported for each event. The magnitude corresponds with the reported network magnitude. If more than one network magnitude type was reported, preference was given to values of M_W, M_S, m_b and M_L respectively. Compare with Figure 9.2*

shown here is the result of an automatic grouping algorithm, and will differ from the total events in the published ISC Bulletin, where both the number of events and the number of hypocentre estimates will have changed due to further analysis. The process of grouping is detailed in Section 11.1.3 of the January to June 2018 Bulletin Summary. Figure 9.2 on page 90 shows a map of all prime hypocentres.

8.5 Collection of Network Magnitude Data

Data contributing agencies normally report earthquake hypocentre solutions along with magnitude estimates. For each seismic event, each agency may report one or more magnitudes of the same or different types. This stems from variability in observational practices at regional, national and global level in computing magnitudes based on a multitude of wave types. Differences in the amplitude measurement algorithm, seismogram component(s) used, frequency range, station distance range as well as the instrument type contribute to the diversity of magnitude types. Table 8.5 provides an overview of the complexity of reported network magnitudes reported for seismic events during the summary period.

Table 8.5: *Statistics of magnitude reports to the ISC; M – average magnitude of estimates reported for each event.*

	M<3.0	3.0≤M<5.0	M≥5.0
Number of seismic events	237029	47562	643
Average number of magnitude estimates per event	1.3	3.0	20.5
Average number of magnitudes (by the same agency) per event	1.2	1.8	2.8
Average number of magnitude types per event	1.2	2.3	9.6
Number of magnitude types	25	37	35

Table 8.6 gives the basic description, main features and scientific paper references for the most commonly reported magnitude types.

Table 8.6: *Description of the most common magnitude types reported to the ISC.*

Magnitude type	Description	References	Comments
M	Unspecified		Often used in real or near-real time magnitude estimations
mB	Medium-period and Broad-band body-wave magnitude	*Gutenberg (1945a); Gutenberg (1945b); IASPEI (2005); IASPEI (2013); Bormann et al. (2009); Bormann and Dewey (2012)*	
mb	Short-period body-wave magnitude	*IASPEI (2005); IASPEI (2013); Bormann et al. (2009); Bormann and Dewey (2012)*	Classical mb based on stations between 21°-100° distance

Table 8.6: *continued*

Magnitude type	Description	References	Comments
mb1	Short-period body-wave magnitude	*IDC* (1999) and references therein	Reported only by the IDC; also includes stations at distances less than 21°
mb1mx	Maximum likelihood short-period body-wave magnitude	*Ringdal* (1976); *IDC* (1999) and references therein	Reported only by the IDC
mbtmp	short-period body-wave magnitude with depth fixed at the surface	*IDC* (1999) and references therein	Reported only by the IDC
mbLg	Lg-wave magnitude	*Nuttli* (1973); *IASPEI* (2005); *IASPEI* (2013); *Bormann and Dewey* (2012)	Also reported as MN
Mc	Coda magnitude		
MD (Md)	Duration magnitude	*Bisztricsany* (1958); *Lee et al.* (1972)	
ME (Me)	Energy magnitude	*Choy and Boatwright* (1995)	Reported only by NEIC
MJMA	JMA magnitude	*Tsuboi* (1954)	Reported only by JMA
ML (Ml)	Local (Richter) magnitude	*Richter* (1935); *Hutton and Boore* (1987); *IASPEI* (2005); *IASPEI* (2013)	
MLSn	Local magnitude calculated for Sn phases	*Balfour et al.* (2008)	Reported by PGC only for earthquakes west of the Cascadia subduction zone
MLv	Local (Richter) magnitude computed from the vertical component		Reported only by DJA and BKK
MN (Mn)	Lg-wave magnitude	*Nuttli* (1973); *IASPEI* (2005)	Also reported as mbLg
MS (Ms)	Surface-wave magnitude	*Gutenberg* (1945c); *Vaněk et al.* (1962); *IASPEI* (2005)	Classical surface-wave magnitude computed from station between 20°-160° distance
Ms1	Surface-wave magnitude	*IDC* (1999) and references therein	Reported only by the IDC; also includes stations at distances less than 20°
ms1mx	Maximum likelihood surface-wave magnitude	*Ringdal* (1976); *IDC* (1999) and references therein	Reported only by the IDC

Table 8.6: *continued*

Magnitude type	Description	References	Comments
Ms7	Surface-wave magnitude	*Bormann et al.* (2007)	Reported only by BJI and computed from records of a Chinese-made long-period seismograph in the distance range 3°-177°
MW (Mw)	Moment magnitude	*Kanamori* (1977); *Dziewonski et al.* (1981)	Computed according to the *IASPEI* (2005) and *IASPEI* (2013) standard formula
Mw(mB)	Proxy Mw based on mB	*Bormann and Saul* (2008)	Reported only by DJA and BKK
Mwp	Moment magnitude from P-waves	*Tsuboi et al.* (1995)	Reported only by DJA and BKK and used in rapid response
mbh	Unknown		
mbv	Unknown		
MG	Unspecified type		Contact contributor
Mm	Unknown		
msh	Unknown		
MSV	Unknown		

Table 8.7 lists all magnitude types reported, the corresponding number of events in the ISC Bulletin and the agency codes along with the number of earthquakes.

Table 8.7: *Summary of magnitude types in the ISC Bulletin for this summary period. The number of events with values for each magnitude type is listed. The agencies reporting these magnitude types are listed, together with the total number of values reported.*

Magnitude type	Events	Agencies reporting magnitude type (number of values)
M	6748	WEL (6041), KRSZO (316), IGQ (95), KOLA (91), BKK (66), ASRS (35), IDG (29), PRU (24), VKMS (17), MIRAS (16), YARS (15), MOS (10), NERS (5), SKHL (4), ROM (1), BYKL (1)
MB	120	CATAC (107), MOLD (14)
mB	2208	BJI (1229), DJA (706), RSNC (402), WEL (137), MCSM (86), GII (35), BKK (11), NOU (7), SFS (2), OTT (1), KEA (1)
mb	25063	IDC (17711), NEIC (8239), NNC (4121), MOS (1907), KRNET (1757), VIE (1689), DJA (1513), BJI (1272), RSNC (789), NOU (580), NAO (453), VAO (423), BGR (290), MCSM (208), OMAN (165), CATAC (138), MDD (97), AUST (68), IASPEI (66), CFUSG (36), DSN (33), NDI (29), MAN (22), SIGU (19), BKK (14), MOLD (13), SFS (13), PPT (12), PGC (11), OSUNB (6), DNK (5), BGS (4), SSNC (4), PDG (4), PRE (3), YARS (3), ROM (3), CRAAG (2), INMG (1), IGIL (1), THR (1), AZER (1), INAM (1), OTT (1)

Table 8.7: *Continued.*

Magnitude type	Events	Agencies reporting magnitude type (number of values)
mb(Pn)	367	BER (367)
mB_BB	26	BGR (26)
mb_Lg	3198	MDD (2700), NEIC (496), OTT (4), TEH (1)
mBc	22	RSNC (22)
mbR	62	VAO (62)
mbtmp	19105	IDC (19105)
MC	3	AFAD (3)
Mc	43	KRSC (43)
MD	10290	RSPR (2089), LDG (1839), SDD (1330), TRN (1235), GII (861), SSNC (821), ECX (749), JMA (387), GCG (386), TIR (342), GRAL (311), UPA (301), ROM (195), SOF (186), PDG (131), JSN (89), PNSN (89), TUN (79), MEX (71), SLM (45), BUG (45), HLW (38), LSZ (26), SNET (13), DNK (10), NCEDC (6), HVO (5), UUSS (3), THR (3), MCSM (1), OTT (1)
Mjma	120	BKK (64), AUST (54), RSNC (2)
ML	138567	TAP (19101), RSNC (11874), AFAD (11210), ISK (10789), IDC (10671), ROM (9985), ATH (9125), HEL (8313), TEH (8163), NEIC (7572), WEL (5582), AEIC (4680), THE (4033), GUC (3716), SJA (2949), SGS (2868), UPP (2865), VIE (2589), LDG (1899), SFS (1706), CATAC (1695), INMG (1616), BEO (1510), DNK (1410), AZER (1383), SDD (1330), LJU (1292), NAM (1285), KRSC (1256), PRE (1198), BER (1190), HVO (1186), SNET (1166), OSPL (1147), CNRM (1141), ISN (921), RHSSO (908), AUST (859), ECX (829), SSNC (827), TIR (666), BUC (647), GEN (606), IPEC (590), MRB (548), PGC (534), SCB (516), KOLA (505), PDG (491), IGIL (441), UPA (410), ANF (400), SKO (395), NIC (385), WBNET (308), NAO (265), CRAAG (193), DSN (192), OMAN (188), LVSN (184), NDI (183), KNET (179), BGS (178), NOU (170), BJI (164), ASIES (149), MIRAS (145), UCC (131), BGR (123), BGSI (118), TUL (110), PAS (68), KRSZO (63), BKK (63), PPT (61), THR (54), BUT (50), UUSS (49), BUG (48), HLW (46), BNS (44), REN (40), OTT (40), KEA (34), SEA (34), NCEDC (33), CUPWA (24), MAN (22), PLV (21), LDO (11), DMN (8), RISSC (6), RSPR (4), FIA0 (4), DJA (2), VAO (2), MCSM (2), HYB (2), TRN (1), ARE (1), INAM (1), EAF (1), CSEM (1), CLL (1), YARS (1)
MLh	664	ZUR (561), ASRS (100), RSNC (3)
MLSn	295	PGC (295)
MLv	21207	DJA (7770), WEL (6071), STR (4384), NOU (1799), SFS (871), RSNC (296), MCSM (230), BKK (66), AUST (55), KRSZO (41), PPT (12), OSUNB (4), OTT (2), ASRS (1)
MN	546	OTT (546)
MPV	5	NERS (5)
mpv	4473	NNC (4473)
MPVA	212	MOS (188), NORS (156)

Table 8.7: *Continued.*

Magnitude type	Events	Agencies reporting magnitude type (number of values)
mR	90	OSUNB (90)
MS	8147	IDC (7973), BJI (1003), MOS (520), BGR (175), OMAN (55), NSSP (47), SOME (40), VIE (30), IASPEI (29), MAN (22), GUC (5), DSN (3), DNK (3), BGS (1), YARS (1), BER (1), SSNC (1)
Ms(BB)	13	RSNC (13)
Ms7	999	BJI (999)
Ms_20	224	NEIC (224)
Ms_VX	3	NEIC (3)
MV	105568	JMA (105568)
MW	7842	SJA (2305), GCMT (1307), SDD (1252), NIED (696), UPA (571), UCR (377), PGC (327), AFAD (321), FUNV (273), SSNC (240), SCB (213), ASIES (149), IPGP (145), NDI (143), JMA (142), MED_RCMT (134), DJA (66), WEL (39), ATH (29), RSNC (21), ROM (18), BER (11), UPSL (11), GUC (8), INMG (6), CRAAG (2), AZER (2), AUST (2), IEC (2), GFZ (1), NEIC (1)
Mw(mB)	140	WEL (127), BKK (11), SFS (2)
Mwb	206	NEIC (206)
Mwc	3	NEIC (3)
MwMwp	3	BKK (2), AUST (1)
Mwp	304	DJA (150), RSNC (147), OMAN (11), ROM (3), BKK (2), AUST (1)
Mwpd	1	ROM (1)
Mwr	421	NEIC (338), GUC (58), NCEDC (18), SLM (16), OTT (11), PAS (11), REN (5), BUC (2), VIE (1)
Mws	962	GII (962)
Mww	630	NEIC (630), GUC (2)

The most commonly reported magnitude types are short-period body-wave, surface-wave, local (or Richter), moment, duration and JMA magnitude type. For a given earthquake, the number and type of reported magnitudes greatly vary depending on its size and location. The large earthquake of October 25, 2010 gives an example of the multitude of reported magnitude types for large earthquakes (Listing 8.1). Different magnitude estimates come from global monitoring agencies such as the IDC, NEIC and GCMT, a local agency (GUC) and other agencies, such as MOS and BJI, providing estimates based on the analysis of their networks. The same agency may report different magnitude types as well as several estimates of the same magnitude type, such as NEIC estimates of Mw obtained from W-phase, centroid and body-wave inversions.

Listing 8.1: *Example of reported magnitudes for a large event*

```
Event   15264887 Southern Sumatera
  Date       Time        Err   RMS Latitude Longitude Smaj  Smin  Az Depth   Err Ndef Nsta Gap  mdist  Mdist Qual   Author      OrigID
2010/10/25 14:42:22.18   0.27 1.813  -3.5248  100.1042 4.045 3.327 54  20.0  1.37 2102 2149  23   0.76 176.43 m i de ISC        01346132
  (#PRIME)


Magnitude  Err Nsta Author       OrigID
mb      6.1      61 BJI          15548963
mB      6.9      68 BJI          15548963
Ms      7.7      85 BJI          15548963
Ms7     7.5      86 BJI          15548963
```

```
mb      5.3 0.1    48 IDC       16686694
mb1     5.3 0.1    51 IDC       16686694
mb1mx   5.3 0.0    52 IDC       16686694
mbtmp   5.3 0.1    51 IDC       16686694
ML      5.1 0.2     2 IDC       16686694
MS      7.1 0.0    31 IDC       16686694
Ms1     7.1 0.0    31 IDC       16686694
ms1mx   6.9 0.1    44 IDC       16686694
mb      6.1       243 ISCJB     01677901
MS      7.3       228 ISCJB     01677901
M       7.1       117 DJA       01268475
mb      6.1 0.2   115 DJA       01268475
mB      7.1 0.1   117 DJA       01268475
MLv     7.0 0.2    26 DJA       01268475
        7.1 0.4   117 DJA       01268475
Mwp     6.9 0.2   102 DJA       01268475
mb      6.4        49 MOS       16742129
MS      7.2        70 MOS       16742129
mb      6.5       110 NEIC      01288303
ME      7.3           NEIC      01288303
MS      7.3       143 NEIC      01288303
MW      7.7           NEIC      01288303
MW      7.8       130 GCMT      00125427
mb      5.9           KLM       00255772
ML      6.7           KLM       00255772
MS      7.6           KLM       00255772
mb      6.4        20 BGR       16815854
Ms      7.2         2 BGR       16815854
mb      6.3 0.3   250 ISC       01346132
MS      7.3 0.1   237 ISC       01346132
```

An example of a relatively small earthquake that occurred in northern Italy for which we received magnitude reports of mostly local and duration type from six agencies in Italy, France and Austria is given in Listing 8.2.

Listing 8.2: Example of reported magnitudes for a small event

```
Event 15089710 Northern Italy
   Date       Time       Err    RMS Latitude Longitude  Smaj  Smin  Az Depth   Err Ndef Nsta Gap  mdist  Mdist Qual  Author       OrigID
2010/08/08 15:20:46.22  0.94  0.778  45.4846    8.3212 2.900 2.539 110  28.6  9.22  172  110  82   0.41   5.35 m i ke ISC         01249414
  (#PRIME)

Magnitude  Err Nsta Author       OrigID
ML    2.4        10 ZUR       15925566
Md    2.6 0.2    19 ROM       16861451
Ml    2.2 0.2     9 ROM       16861451
ML    2.5           GEN       00554757
ML    2.6 0.3    28 CSEM      00554756
Md    2.3 0.0     3 LDG       14797570
Ml    2.6 0.3    32 LDG       14797570
```

Figure 8.11 shows a distribution of the number of agencies reporting magnitude estimates to the ISC according to the magnitude value. The peak of the distribution corresponds to small earthquakes where many local agencies report local and/or duration magnitudes. The number of contributing agencies rapidly decreases for earthquakes of approximately magnitude 5.5 and above, where magnitudes are mostly given by global monitoring agencies.
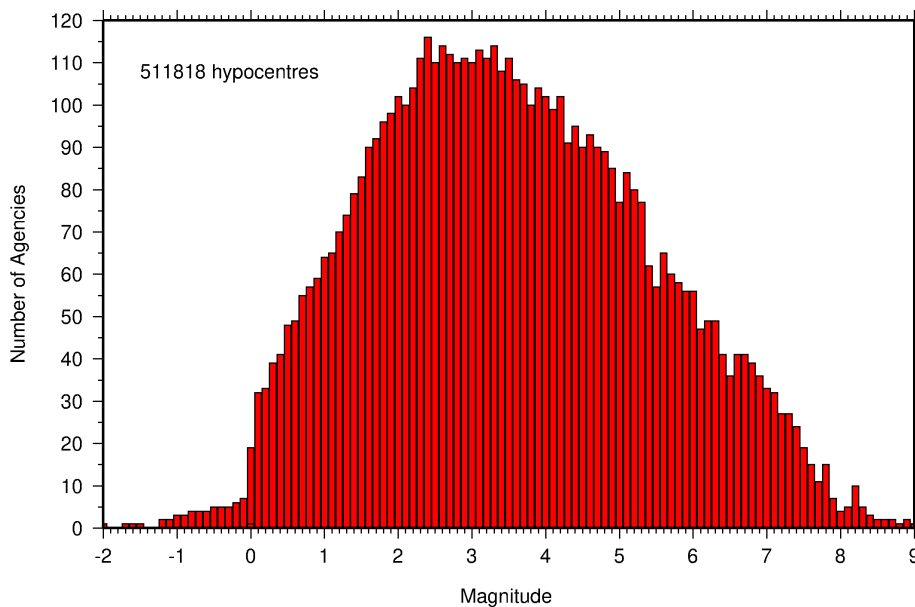
Figure 8.11: Histogram showing the number of agencies that reported network magnitude values. All magnitude types are included.

8.6 Moment Tensor Solutions

The ISC Bulletin publishes moment tensor solutions, which are reported to the ISC by other agencies. The collection of moment tensor solutions is summarised in Table 8.8. A histogram showing all moment tensor solutions collected throughout the ISC history is shown in Figure 8.12. Several moment tensor solutions from different authors and different moment tensor solutions calculated by different methods from the same agency may be present for the same event.

Table 8.8: *Summary of reports containing moment tensor solutions.*

Reports with Moment Tensors	162
Total moment tensors received	19276
Agencies reporting moment tensors	10

The number of moment tensors for this summary period, reported by each agency, is shown in Table 8.9. The moment tensor solutions are plotted in Figure 8.13.
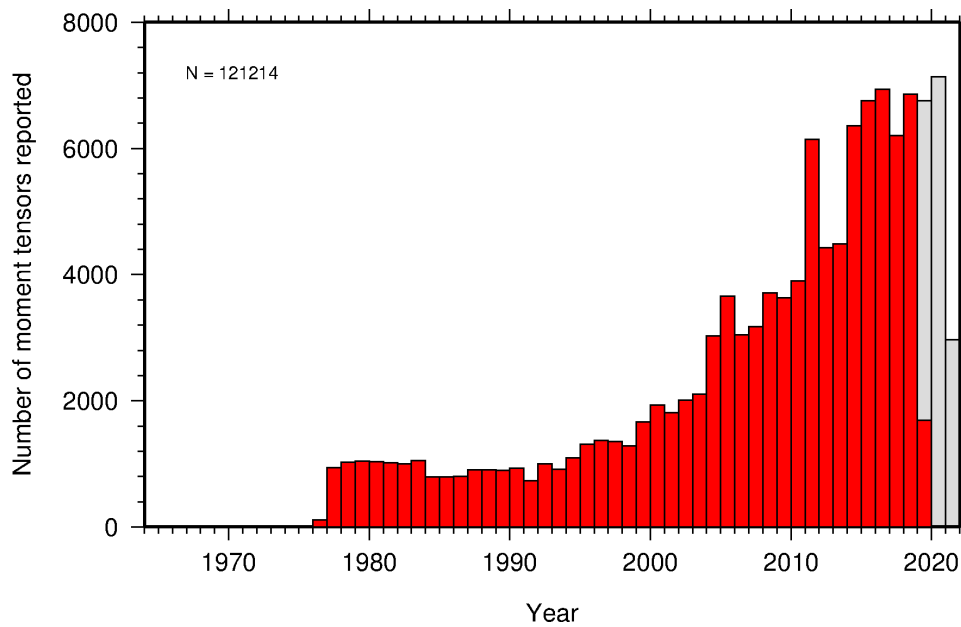
Figure 8.12: *Histogram showing the number of moment tensors reported to the ISC since 1964. The regions in grey represent data that are still being actively collected.*
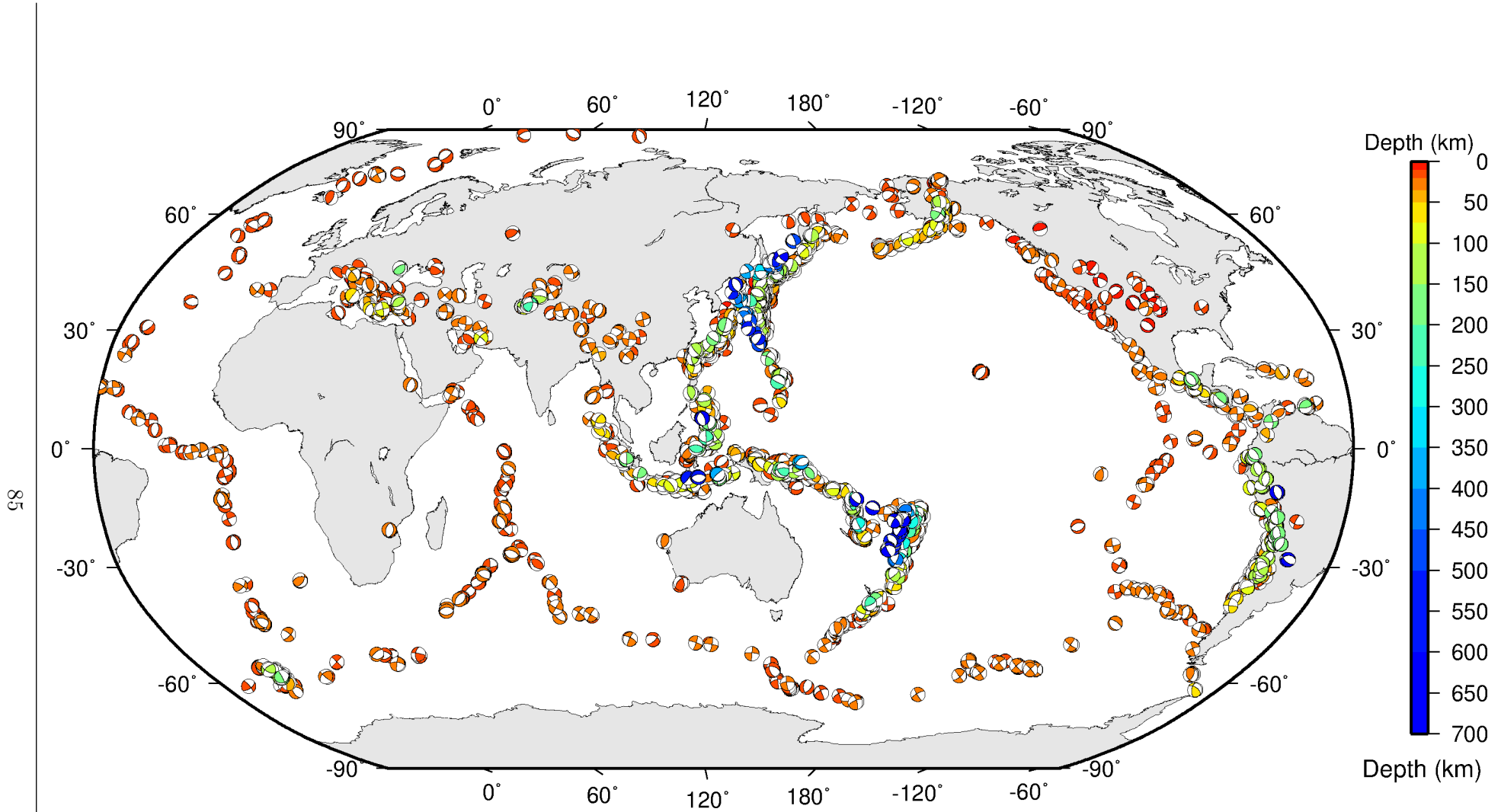
ISC Bulletin: **3581** focal mechanism solutions for **2430** events from **2018/07/01** to **2018/12/31**

Figure 8.13: *Map of all moment tensor solutions in the ISC Bulletin for this summary period.*

Table 8.9: *Summary of moment tensor solutions in the ISC Bulletin reported by each agency.*

Agency	Number of moment tensor solutions	Agency	Number of moment tensor solutions
GCMT	1309	ATH	29
NEIC	1195	ROM	17
ISC	1126	ECX	15
NIED	696	UPSL	11
IPGP	290	PRE	6
ASIES	149	IEC	4
MED_RCMT	134	UPA	3
PNSN	89	AUST	2
UCR	40	SNET	1
WEL	39	SDD	1
MOS	30		

8.7   Timing of Data Collection

Here we present the timing of reports to the ISC. Please note, this does not include provisional alerts, which are replaced at a later stage. Instead, it reflects the final data sent to the ISC. The absolute timing of all hypocentre reports, regardless of magnitude, is shown in Figure 8.14. In Figure 8.15 the reports are grouped into one of six categories - from within three days of an event origin time, to over one year. The histogram shows the distribution with magnitude (for hypocentres where a network magnitude was reported) for each category, whilst the map shows the geographic distribution of the reported hypocentres.
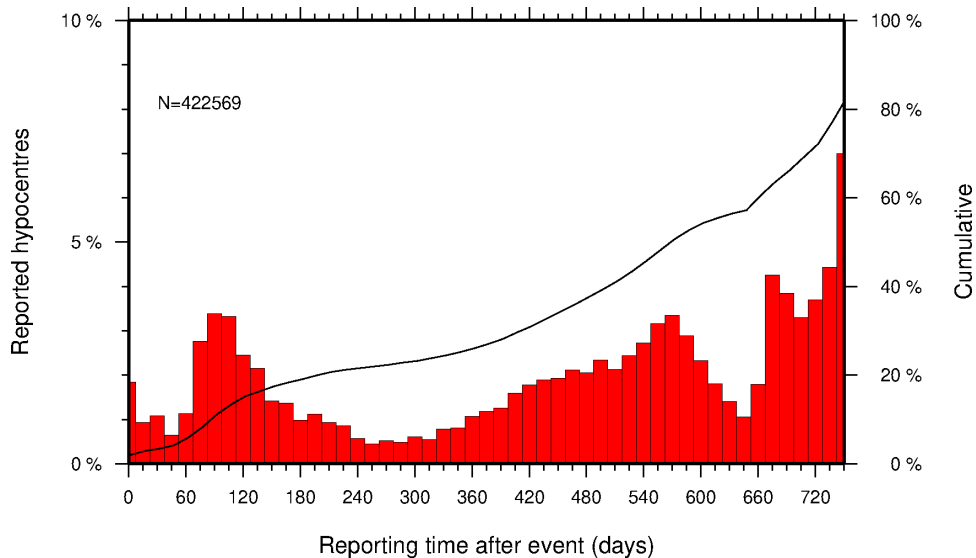
Figure 8.14: *Histogram showing the timing of final reports of the hypocentres (total of N) to the ISC. The cumulative frequency is shown by the solid line.*
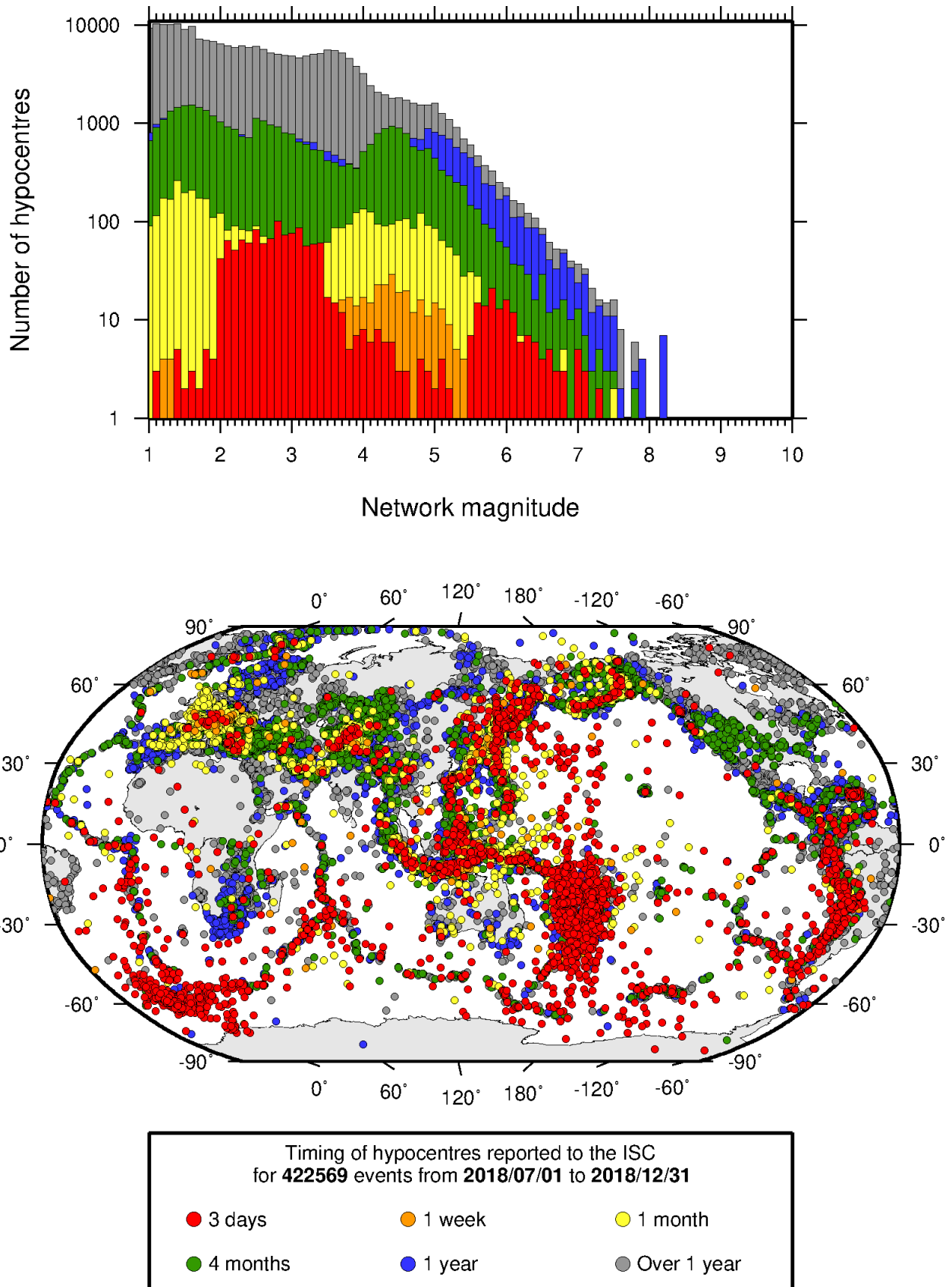
Figure 8.15: *Timing of hypocentres reported to the ISC. The colours show the time after the origin time that the corresponding hypocentre was reported. The histogram shows the distribution with magnitude. If more than one network magnitude was reported, preference was given to a value of M_W followed by M_S, m_b and M_L respectively; all reported hypocentres are included on the map. Note: early reported hypocentres are plotted over later reported hypocentres, on both the map and histogram.*

9

Overview of the ISC Bulletin

This chapter provides an overview of the seismic event data in the ISC Bulletin. We indicate the differences between all ISC events and those ISC events that are reviewed or located. We describe the wealth of phase arrivals and phase amplitudes and periods observed at seismic stations worldwide, reported in the ISC Bulletin and often used in the ISC location and magnitude determination. Finally, we make some comparisons of the ISC magnitudes with those reported by other agencies, and discuss magnitude completeness of the ISC Bulletin.

9.1   Events

The ISC Bulletin had 298569 reported events in the summary period between July and December 2018. Some 91% (274465) of the events were identified as earthquakes, the rest (24104) were of anthropogenic origin (including mining and other chemical explosions, rockbursts and induced events) or of unknown origin. In this summary period 10% of the events were reviewed and 7% of the events were located by the ISC. For events that are not located by the ISC, the prime hypocentre is identified according to the rules described in Section 11.1.3 of the January to June 2018 Bulletin Summary.

Of the 10759589 reported phase observations, 37% are associated to ISC-reviewed events, and 35% are associated to events selected for ISC location. Note that all large events are reviewed and located by the ISC. Since large events are globally recorded and thus reported by stations worldwide, they will provide the bulk of observations. This explains why only about one-fifth of the events in any given month is reviewed although the number of phases associated to reviewed events has increased nearly exponentially in the past decades.

Figure 9.1 shows the daily number of events throughout the summary period. Figure 9.2 shows the locations of the events in the ISC Bulletin; the locations of ISC-reviewed and ISC-located events are shown in Figures 9.3 and 9.4, respectively.

Figure 9.5 shows the hypocentral depth distributions of events in the ISC Bulletin for the summary period. The vast majority of events occur in the Earth's crust. Note that the peaks at 0, 10, 35 km, and at every 50 km intervals deeper than 100 km are artifacts of analyst practices of fixing the depth to a nominal value when the depth cannot be reliably resolved.

Figure 9.6 shows the depth distribution of free-depth solutions in the ISC Bulletin. The depth of a hypocentre reported to the ISC is assumed to be determined as a free parameter, unless it is explicitly labelled as a fixed-depth solution. On the other hand, as described in Section 11.1.4 of the January to June 2018 Bulletin Summary, the ISC locator attempts to get a free-depth solution if, and only if, there is resolution for the depth in the data, i.e. if there is a local network and/or sufficient depth-sensitive phases are reported.
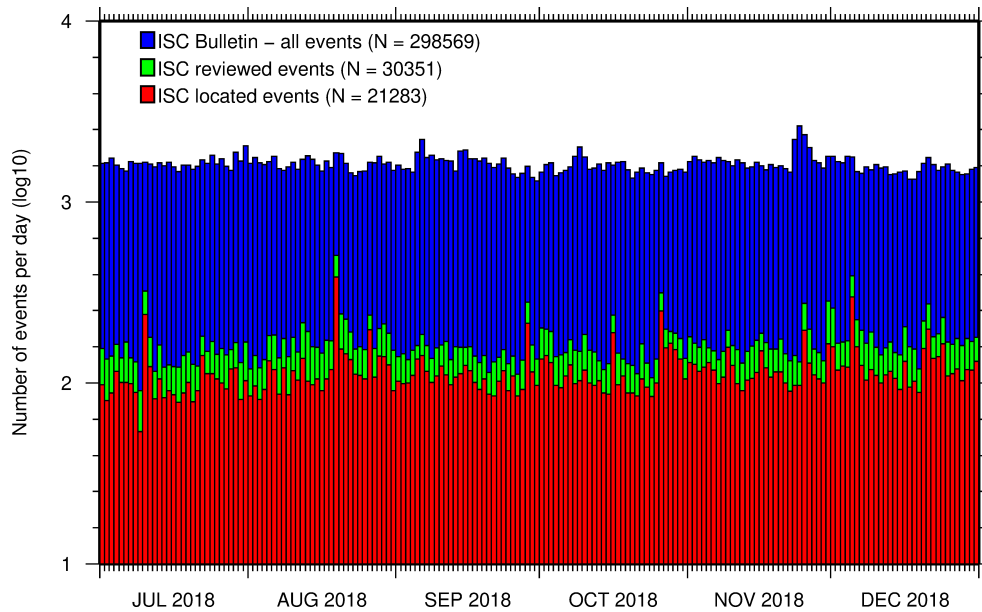
Figure 9.1: *Histogram showing the number of events in the ISC Bulletin for the current summary period. The vertical scale is logarithmic.*

Figure 9.7 shows the depth distribution of fixed-depth solutions in the ISC Bulletin. Except for a fraction of events whose depth is fixed to a shallow depth, this set comprises mostly ISC-located events. If there is no resolution for depth in the data, the ISC locator fixes the depth to a value obtained from the ISC default depth grid file, or if no default depth exists for that location, to a nominal default depth assigned to each Flinn-Engdahl region (see details in Section 11.1.4 of the January to June 2018 Bulletin Summary). During the ISC review editors are inclined to accept the depth obtained from the default depth grid, but they typically change the depth of those solutions that have a nominal (10 or 35 km) depth. When doing so, they usually fix the depth to a round number, preferably divisible by 50.

For events selected for ISC location, the number of stations typically increases as arrival data reported by several agencies are grouped together and associated to the prime hypocentre. Consequently, the network geometry, characterised by the secondary azimuthal gap (the largest azimuthal gap a single station closes), is typically improved. Figure 9.8 illustrates that the secondary azimuthal gap is indeed generally smaller for ISC-located events than that for all events in the ISC Bulletin. Figure 9.9 shows the distribution of the number of associated stations. For large events the number of associated stations is usually larger for ISC-located events than for any of the reported event bulletins. On the other hand, events with just a few reporting stations are rarely selected for ISC location. The same is true for the number of defining stations (stations with at least one defining phase that were used in the location). Figure 9.10 indicates that because the reported observations from multiple agencies are associated to the prime, large ISC-located events typically have a larger number of defining stations than any of the reported event bulletins.

The formal uncertainty estimates are also typically smaller for ISC-located events. Figure 9.11 shows the distribution of the area of the 90% confidence error ellipse for ISC-located events during the summary period. The distribution suffers from a long tail indicating a few poorly constrained event locations. Nevertheless, half of the events are characterised by an error ellipse with an area less than 190 km^2, 90% of the events have an error ellipse area less than 1456 km^2, and 95% of the events have an error ellipse

ISC Bulletin – all events
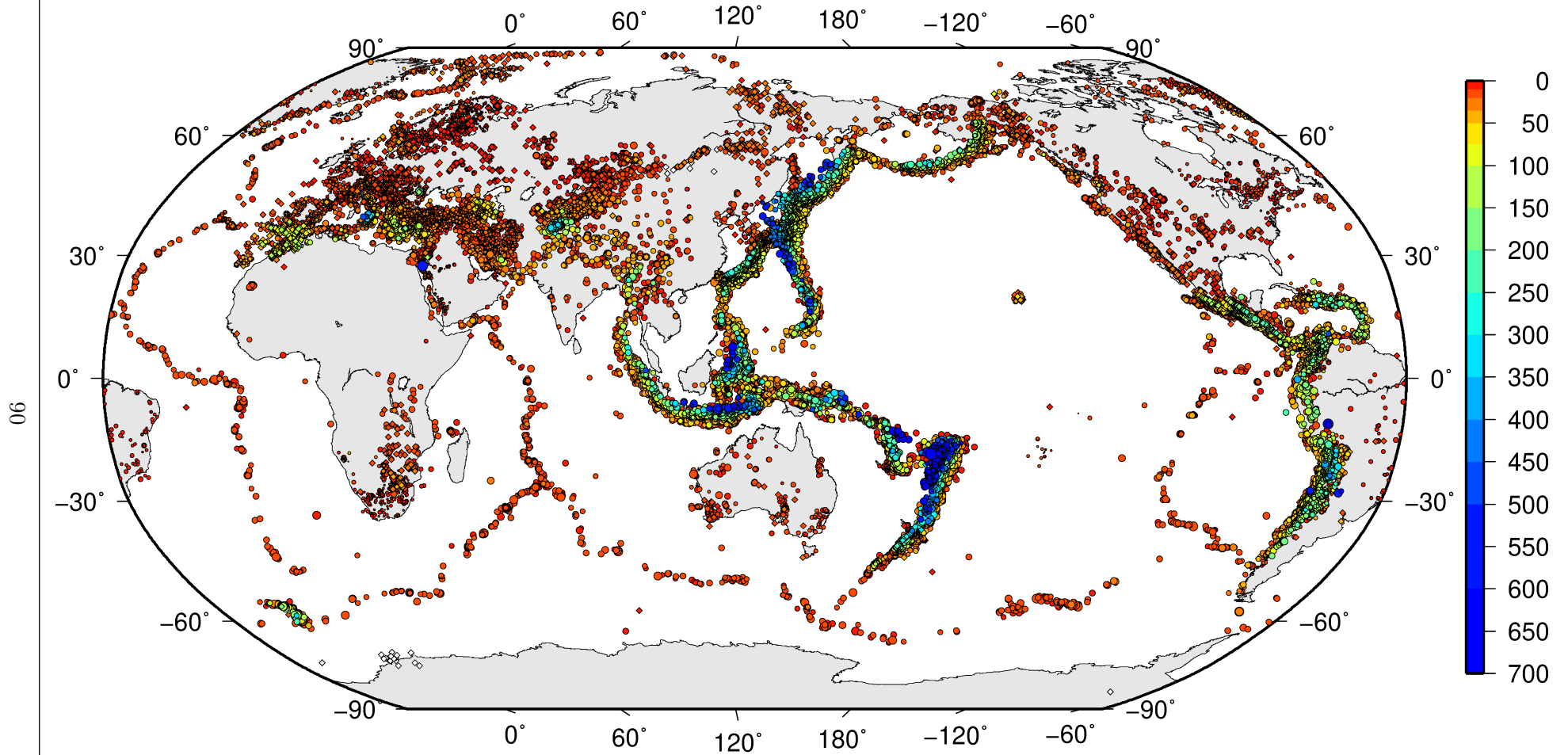
ISC Bulletin: **298569** reported events from **2018/07/01** to **2018/12/31**

∘ M 2   ∘ M 3   ∘ M 4   ∘ M 5   ∘ M 6   ∘ M 7   ∘ M 8   ⋄ Unknown

Figure 9.2: *Map of all events in the ISC Bulletin. Prime hypocentre locations are shown. Compare with Figure 8.10.*

ISC Bulletin – reviewed events
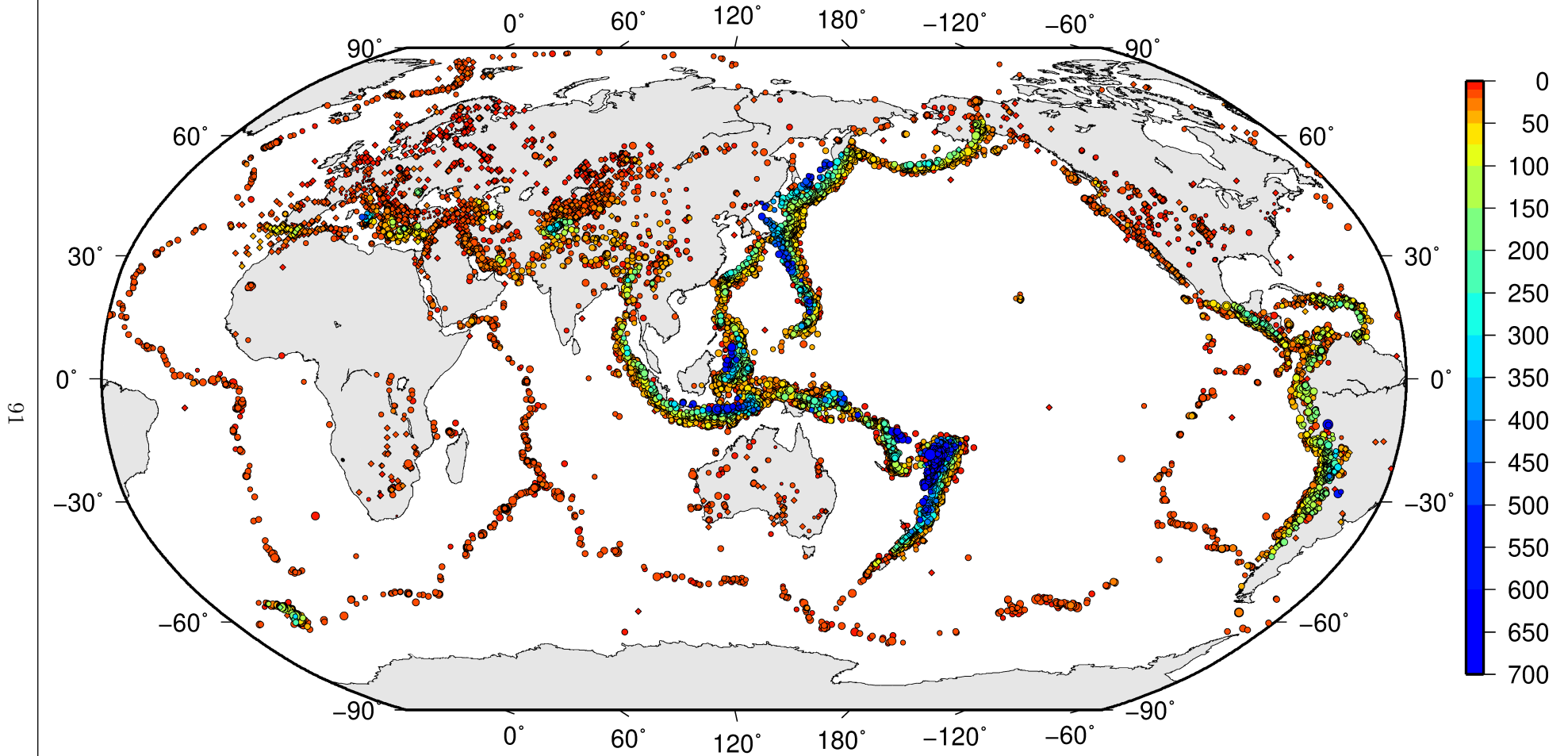
ISC Bulletin: **30351** reviewed events from **2018/07/01** to **2018/12/31**

∘ M 2   ∘ M 3   ∘ M 4   ∘ M 5   ∘ M 6   ○ M 7   ○ M 8   ⋄ Unknown

Figure 9.3: *Map of all events reviewed by the ISC for this time period. Prime hypocentre locations are shown.*

ISC Bulletin – ISC located events
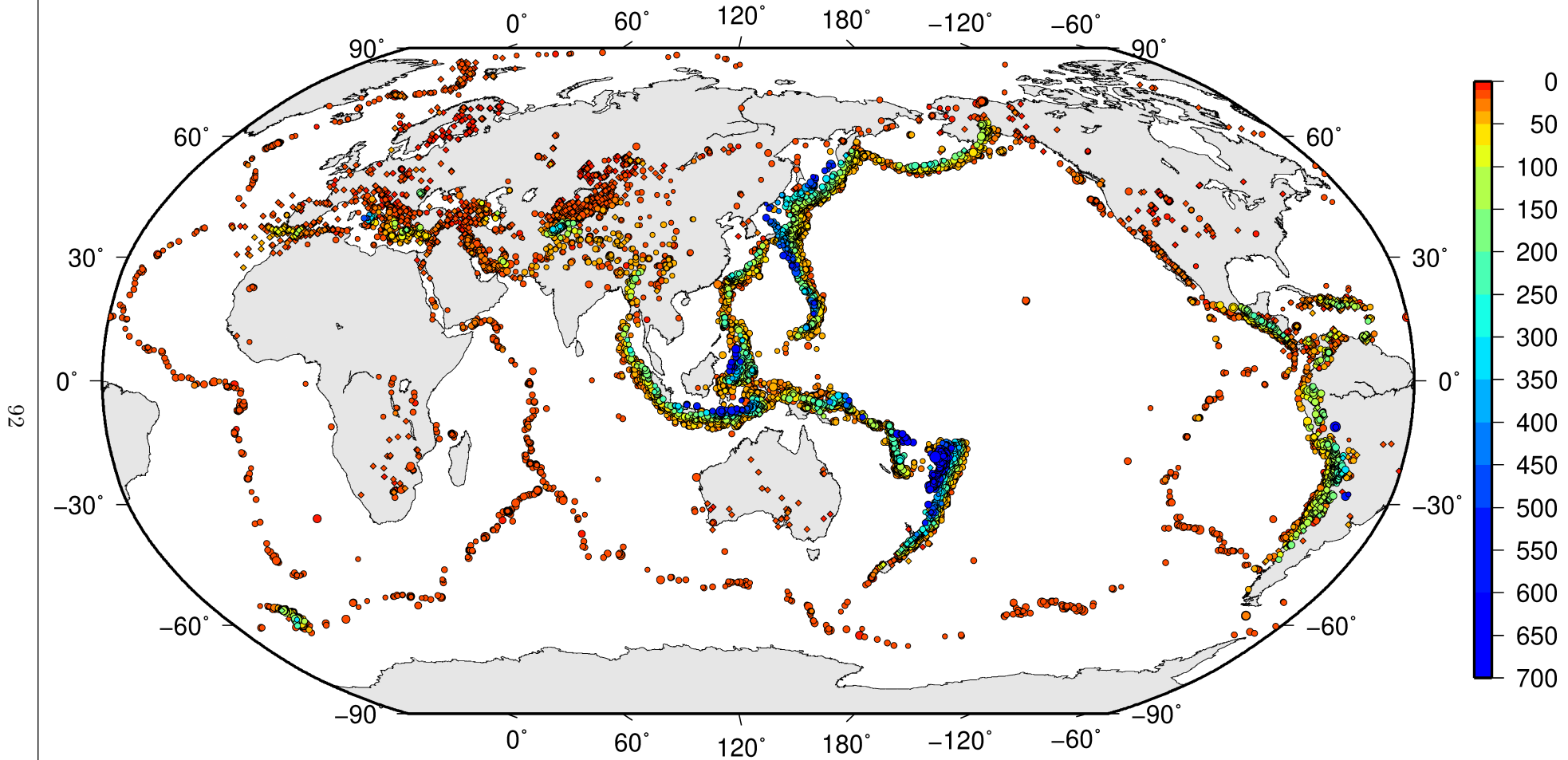
ISC Bulletin: **21283** ISC located events from **2018/07/01** to **2018/12/31**

∘ M 2   ∘ M 3   ∘ M 4   ∘ M 5   ○ M 6   ○ M 7   ○ M 8   ◇ Unknown

Figure 9.4: *Map of all events located by the ISC for this time period. ISC determined hypocentre locations are shown.*
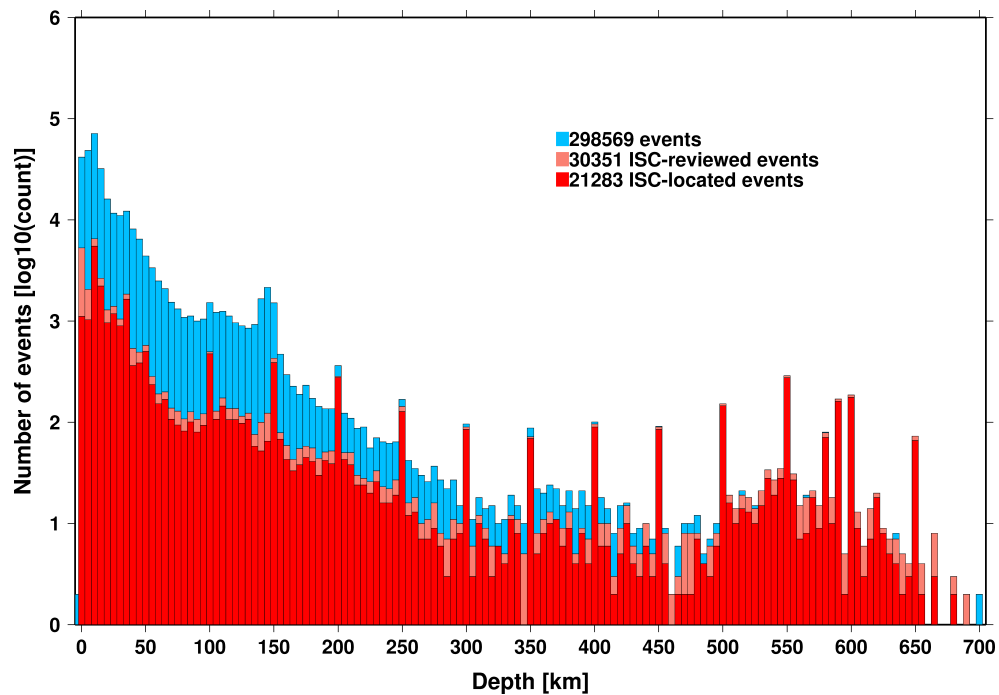
Figure 9.5: *Distribution of event depths in the ISC Bulletin (blue) and for the ISC-reviewed (pink) and the ISC-located (red) events during the summary period. All ISC-located events are reviewed, but not all reviewed events are located by the ISC. The vertical scale is logarithmic.*
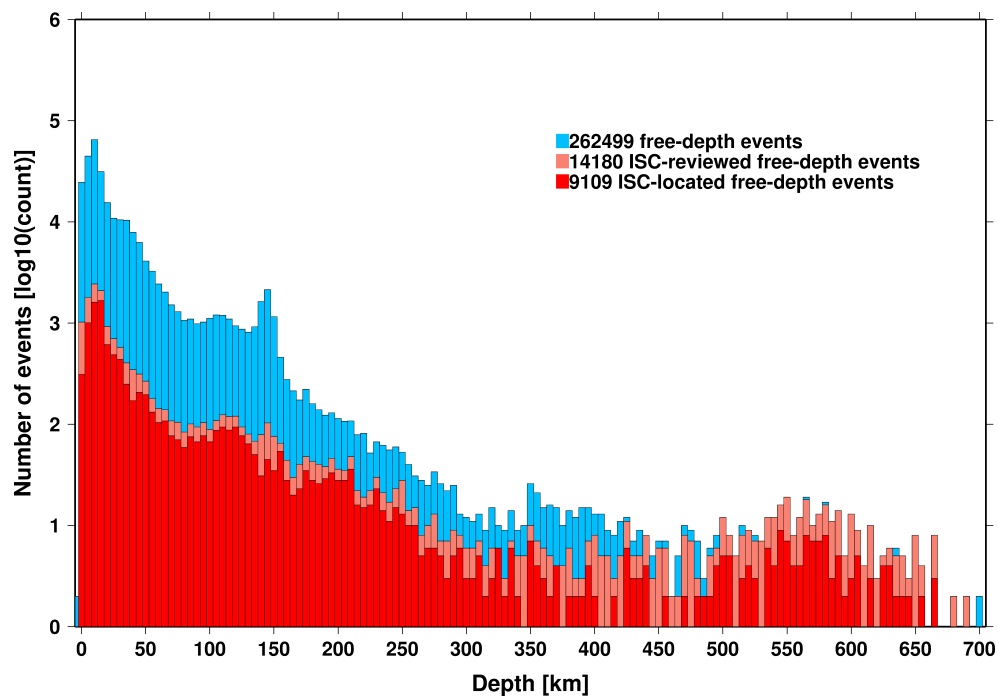
Figure 9.6: *Hypocentral depth distribution of events where the prime hypocentres are reported/located with a free-depth solution in the ISC Bulletin. The vertical scale is logarithmic.*
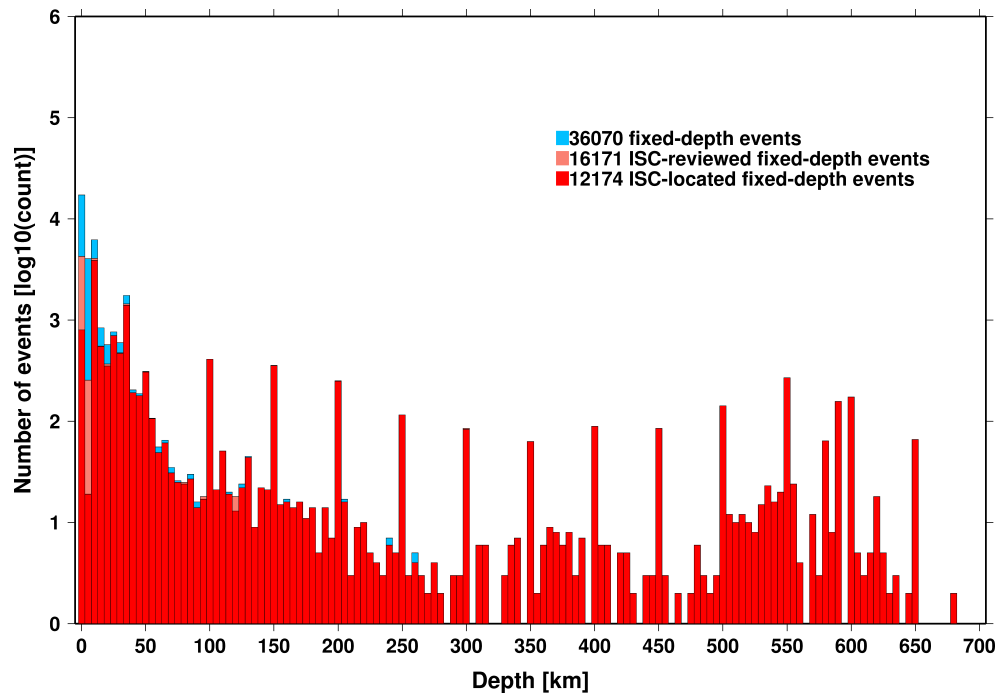
Figure 9.7: *Hypocentral depth distribution of events where the prime hypocentres are reported/located with a fixed-depth solution in the ISC Bulletin. The vertical scale is logarithmic.*
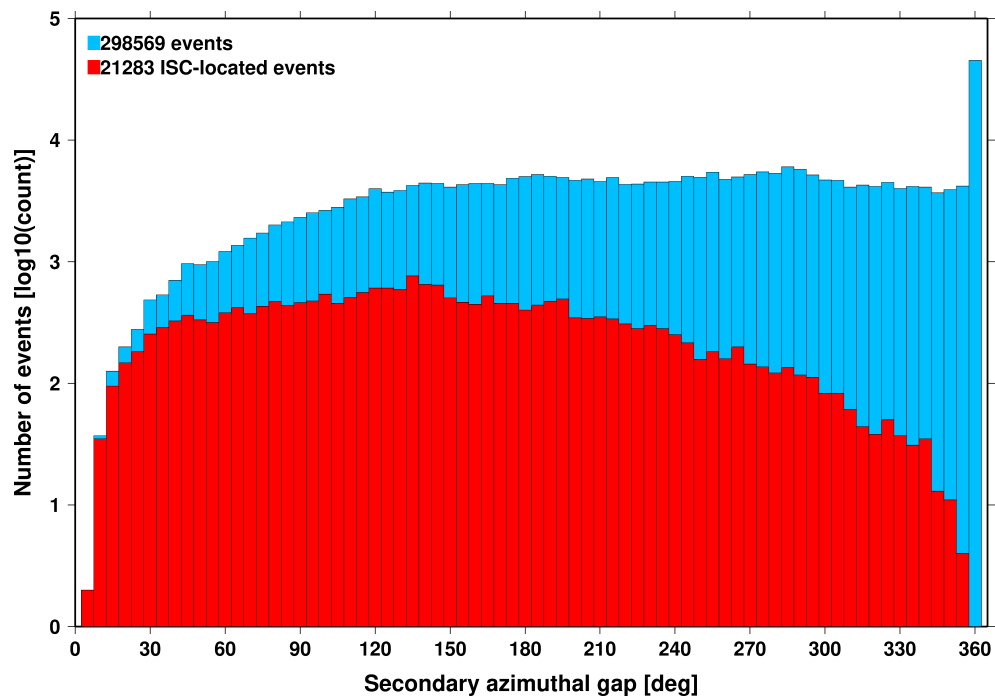
Figure 9.8: *Distribution of secondary azimuthal gap for events in the ISC Bulletin (blue) and those selected for ISC location (red). The vertical scale is logarithmic.*
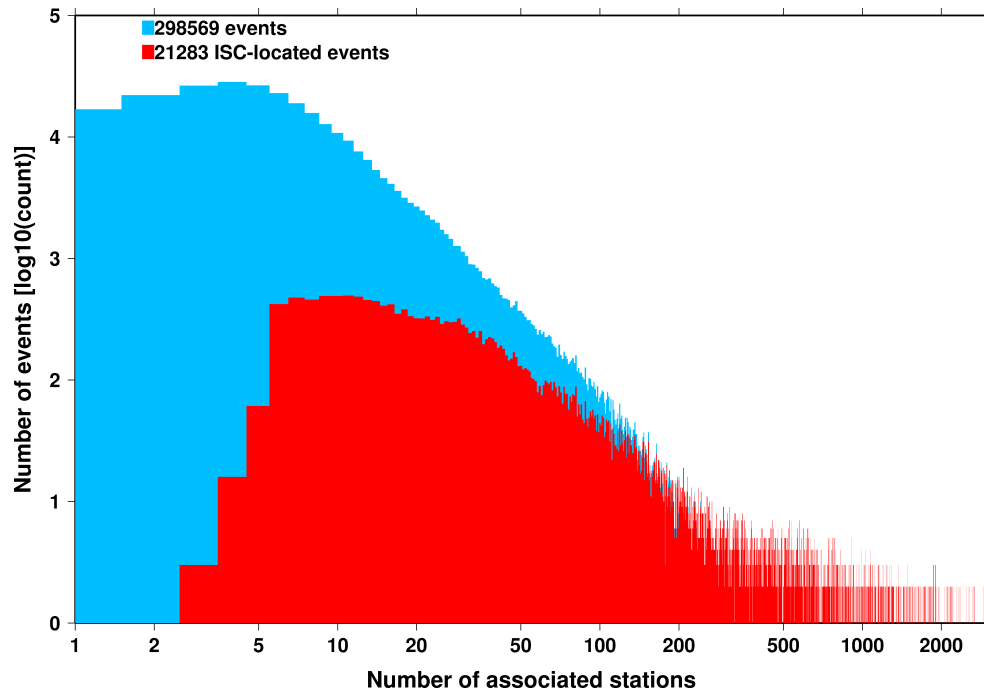
Figure 9.9: *Distribution of the number of associated stations for events in the ISC Bulletin (blue) and those selected for ISC location (red). The vertical scale is logarithmic.*
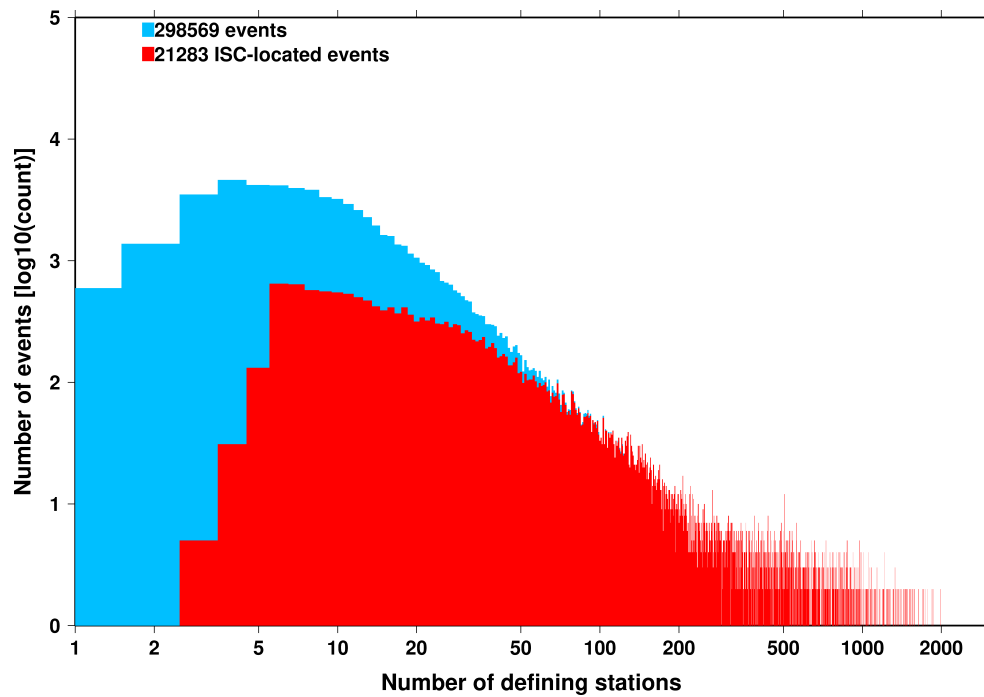
Figure 9.10: *Distribution of the number of defining stations for events in the ISC Bulletin (blue) and those selected for ISC location (red). The vertical scale is logarithmic.*

area less than 2653 km^2.
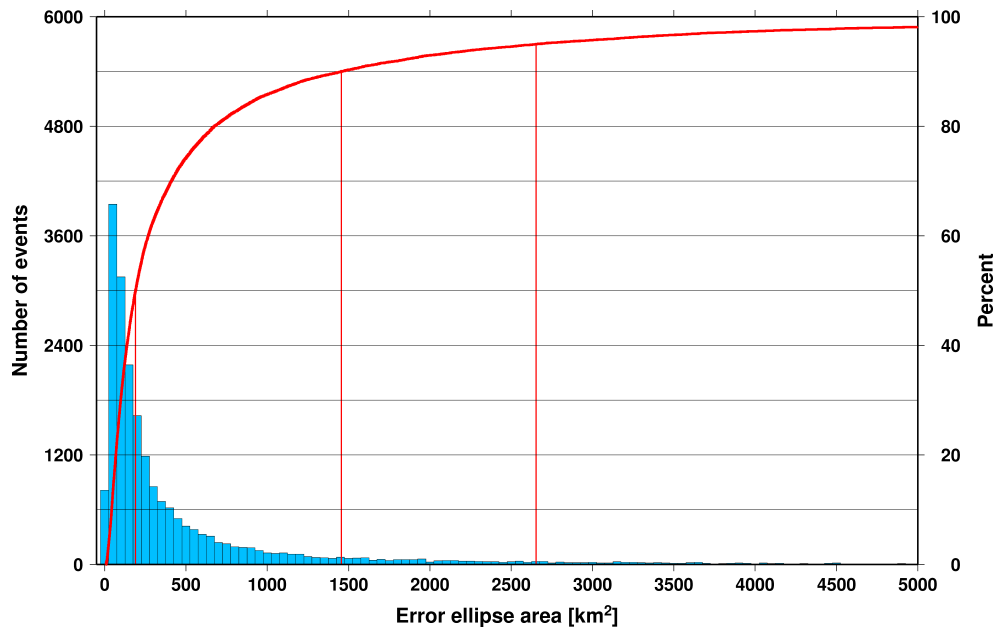
Figure 9.11: *Distribution of the area of the 90% confidence error ellipse of the ISC-located events. Vertical red lines indicate the 50th, 90th and 95th percentile values.*

Figure 9.12 shows one of the major characteristic features of the ISC location algorithm (Bondár and Storchak, 2011). Because the ISC locator accounts for correlated travel-time prediction errors due to unmodelled velocity heterogeneities along similar ray paths, the area of the 90% confidence error ellipse does not decrease indefinitely with increasing number of stations, but levels off once the information carried by the network geometry is exhausted, thus providing more realistic uncertainty estimates.
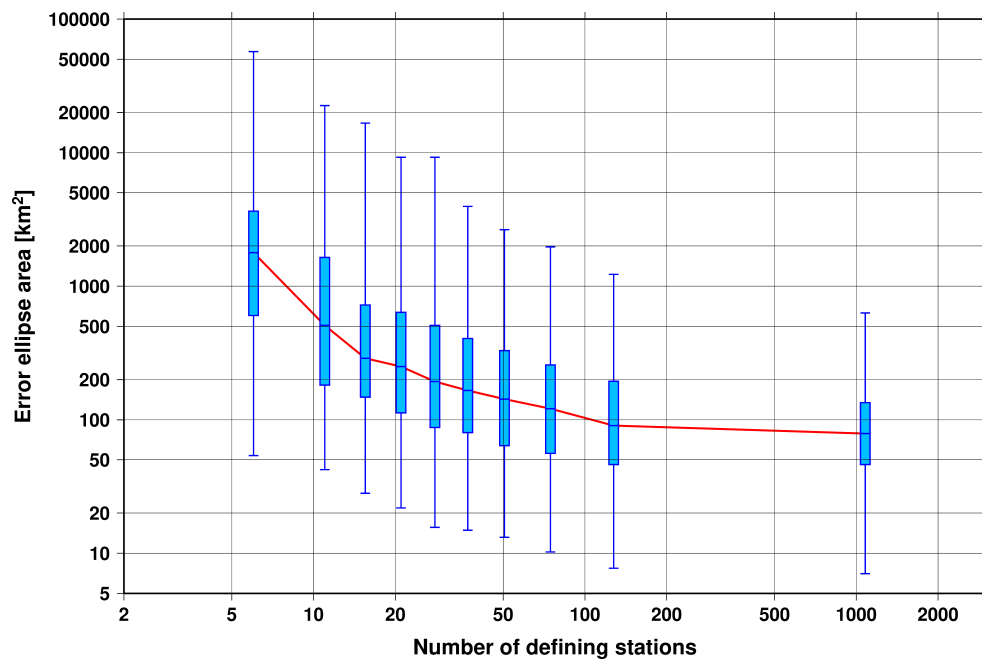
Figure 9.12: *Box-and-whisker plot of the area of the 90% confidence error ellipse of the ISC-located events as a function of the number of defining stations. Each box represents one-tenth-worth of the total number of data. The red line indicates the median 90% confidence error ellipse area.*

9.2 Seismic Phases and Travel-Time Residuals

The number of phases that are associated to events over the summary period in the ISC Bulletin is shown in Figure 9.13. Phase types and their total number in the ISC Bulletin is shown in the Appendix, Table 11.2. A summary of phase types is indicated in Figure 9.14.
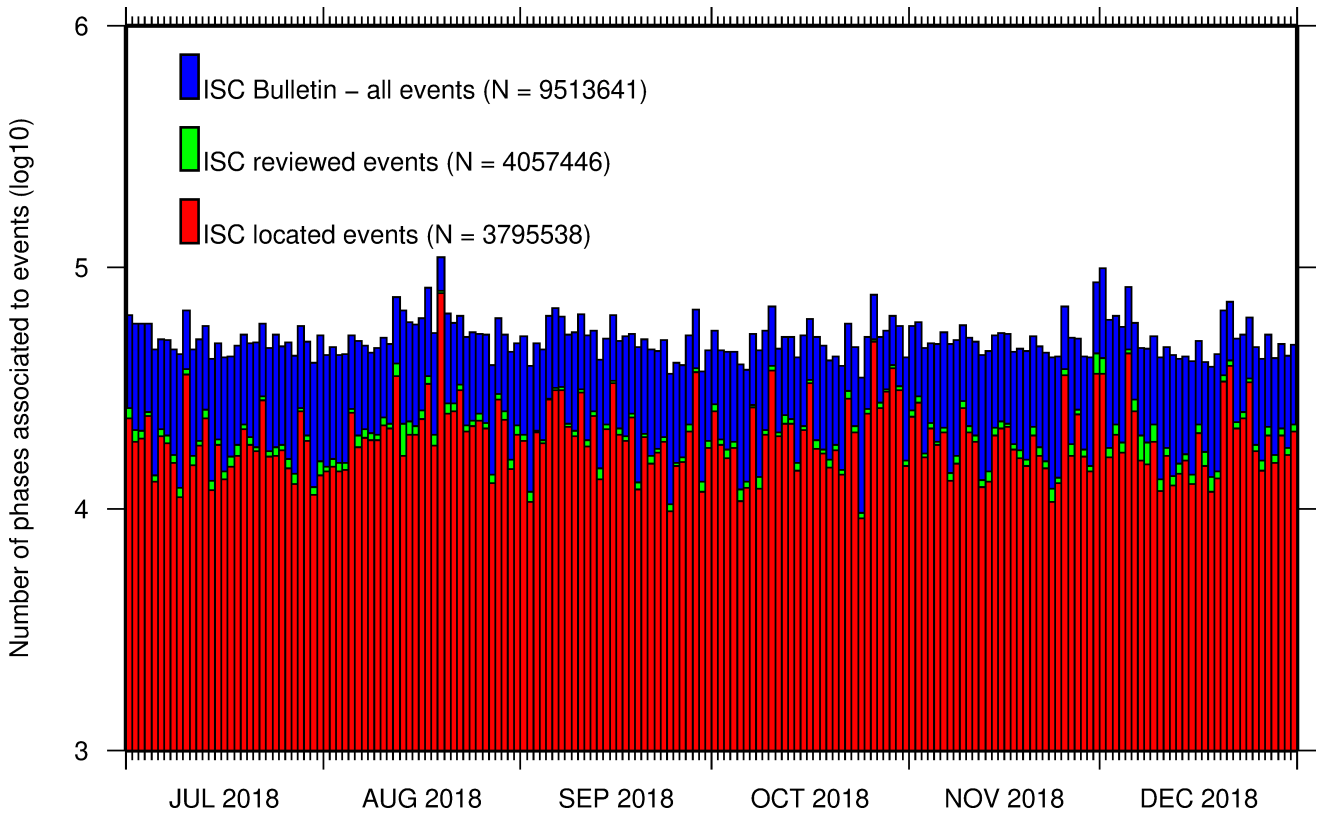
Figure 9.13: *Histogram showing the number of phases (N) that the ISC has associated to events within the ISC Bulletin for the current summary period.*

In computing ISC locations, the current (for events since 2009) ISC location algorithm (*Bondár and Storchak*, 2011) uses all *ak135* phases where possible. Within the Bulletin, the phases that contribute to an ISC location are labelled as *time defining*. In this section, we summarise these time defining phases.

In Figure 9.15, the number of defining phases is shown in a histogram over the summary period. Each defining phase is listed in Table 9.1, which also provides a summary of the number of defining phases per event. A pie chart showing the proportion of defining phases is shown in Figure 9.16. Figure 9.17 shows travel times of seismic waves. The distribution of residuals for these defining phases is shown for the top five phases in Figures 9.18 through 9.22.

Table 9.1: *Numbers of 'time defining' phases (N) within the ISC Bulletin for 21283 ISC located events.*

Phase	Number of 'defining' phases	Number of events	Max per event	Median per event
P	1121902	15162	2724	16
Pn	655951	18896	897	15
Sn	183711	15801	253	6
Pb	91557	8748	118	6
Pg	70349	7062	103	6
PKPdf	66620	5106	683	2
Sb	58034	8107	160	4
S	55424	3876	645	3

Table 9.1: *(continued)*

Phase	Number of 'defining' phases	Number of events	Max per event	Median per event
Sg	51448	6417	129	5
PKiKP	38357	3602	400	2
PKPbc	37805	4301	264	2
PKPab	22988	3280	250	2
PcP	14315	4048	63	2
Pdif	11220	1099	325	2
PP	10526	1268	166	2
pP	10351	1529	190	3
SS	5555	1193	64	2
ScP	4346	1147	65	2
SKSac	4328	548	100	2
sP	4254	1265	48	2
PKKPbc	2718	449	104	3
pwP	1960	670	33	2
SnSn	1257	677	10	1
PnPn	1231	664	10	1
ScS	1192	346	53	2
SKPbc	1057	364	30	2
pPKPdf	1007	377	57	1
sS	829	423	14	1
P'P'df	822	200	35	2
PKKPdf	679	235	43	1
SKiKP	646	339	16	1
pPKPab	633	181	35	1
PKKPab	611	242	53	1
pPKPbc	492	194	23	1
PS	433	196	48	1
SKPab	232	152	9	1
sPKPdf	230	161	6	1
PcS	223	152	7	1
SKPdf	196	97	9	1
SKKSac	184	100	20	1
SKSdf	170	83	16	1
SP	153	45	24	1
SKKPbc	135	35	27	2
PnS	123	103	4	1
pPKiKP	113	36	11	2
PKSdf	113	59	7	1
sPKPbc	105	79	5	1
sPKPab	104	51	14	1
pS	96	77	3	1
pPdif	94	34	10	1
Sdif	89	56	5	1
P'P'bc	68	36	18	1
SKKPab	35	16	12	1
SKKPdf	33	14	9	2
P'P'ab	23	14	7	1
SKKSdf	17	16	2	1
sPdif	13	12	2	1
SPn	9	9	1	1
PbPb	8	7	2	1
SbSb	7	6	2	1
PKSbc	4	4	1	1
sSKSac	3	3	1	1
sPKiKP	3	3	1	1
S'S'ac	3	3	1	1
sSKSdf	1	1	1	1
sPn	1	1	1	1
sSdif	1	1	1	1
pSKSac	1	1	1	1
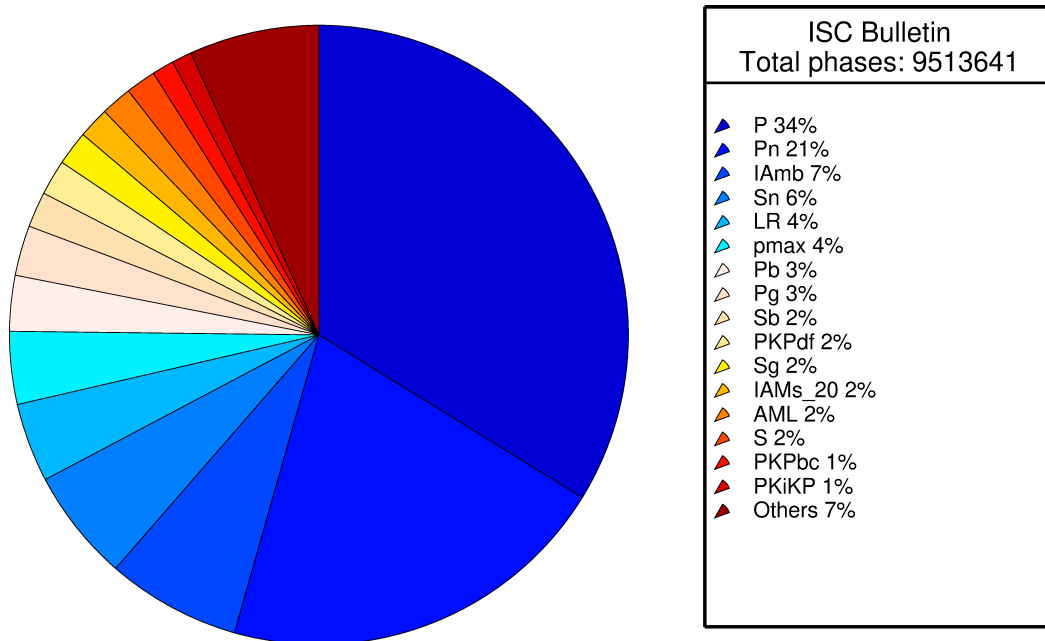
Figure 9.14: *Pie chart showing the fraction of various phase types in the ISC Bulletin for this summary period.*
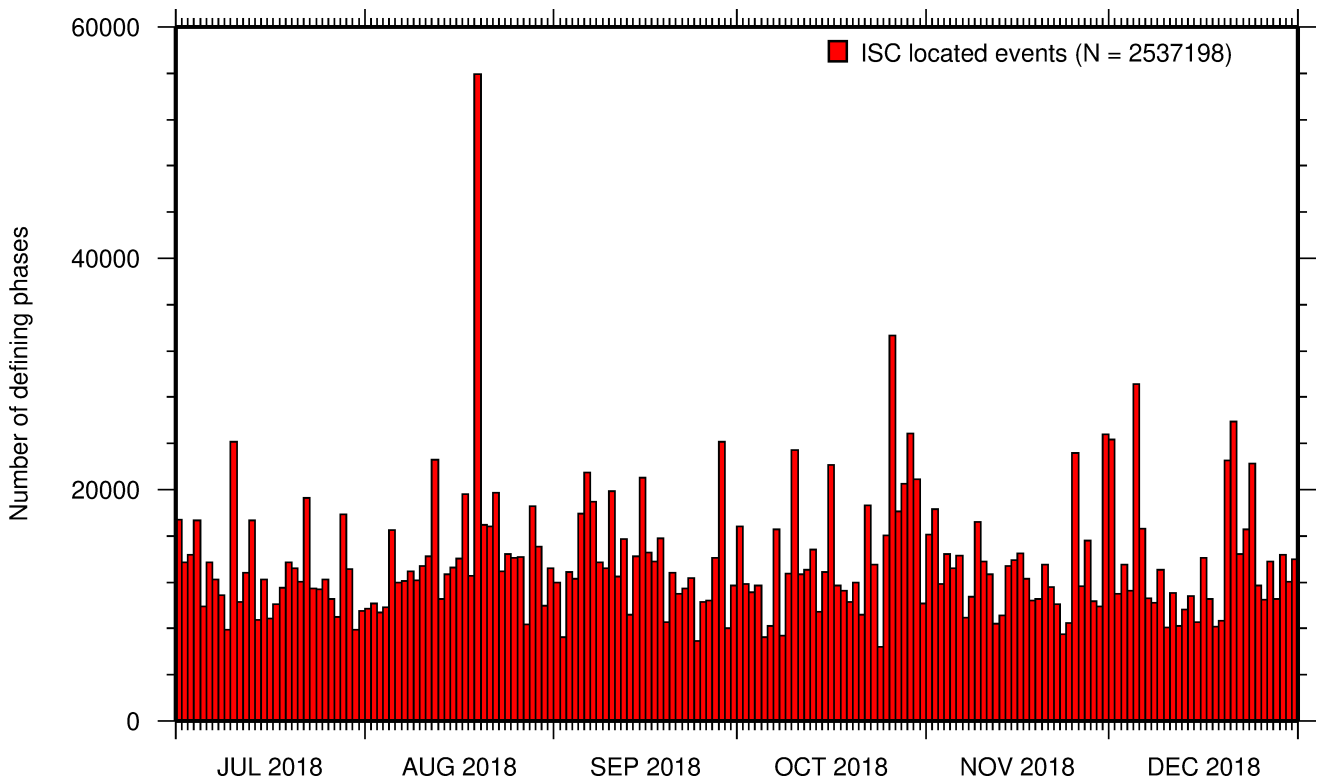
Figure 9.15: *Histogram showing the number of defining phases in the ISC Bulletin, for events located by the ISC.*
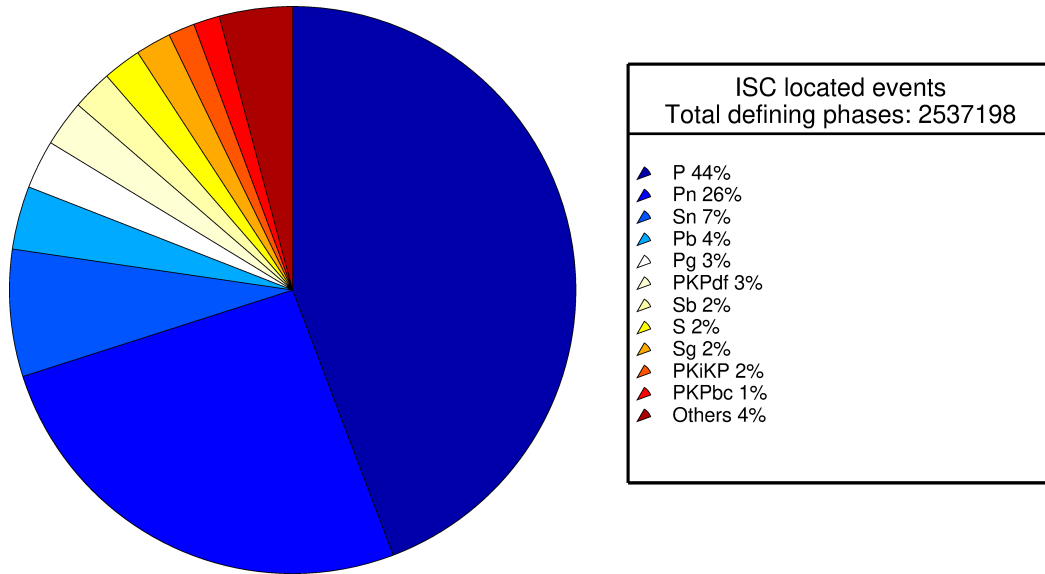
Figure 9.16: *Pie chart showing the defining phases in the ISC Bulletin, for events located by the ISC. A complete list of defining phases is shown in Table 9.1.*
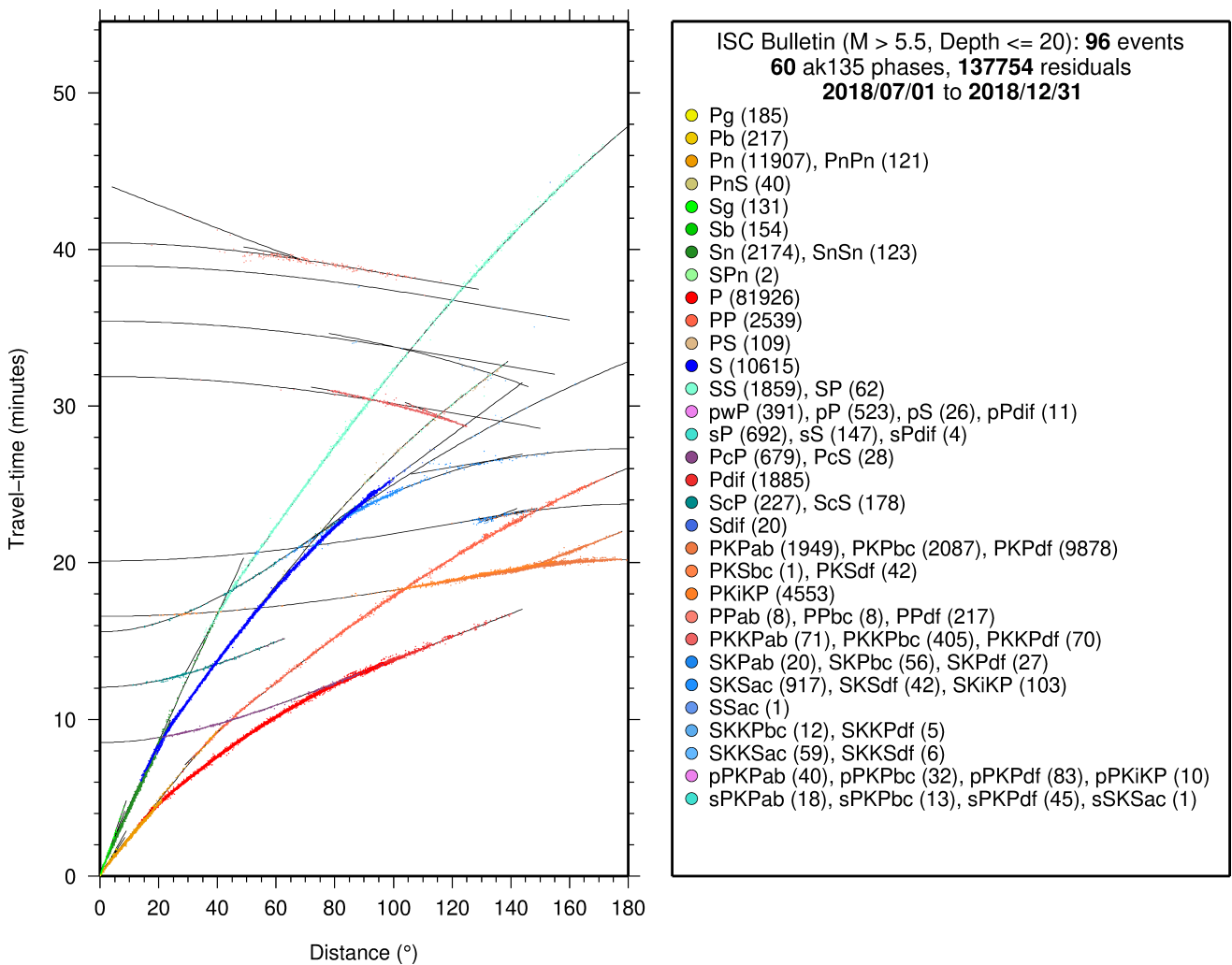
Figure 9.17: *Distribution of travel-time observations in the ISC Bulletin for events with M > 5.5 and depth less than 20 km. The travel-time observations are shown relative to a 0 km source and compared with the theoretical ak135 travel-time curves (solid lines). The legend lists the number of each phase plotted.*
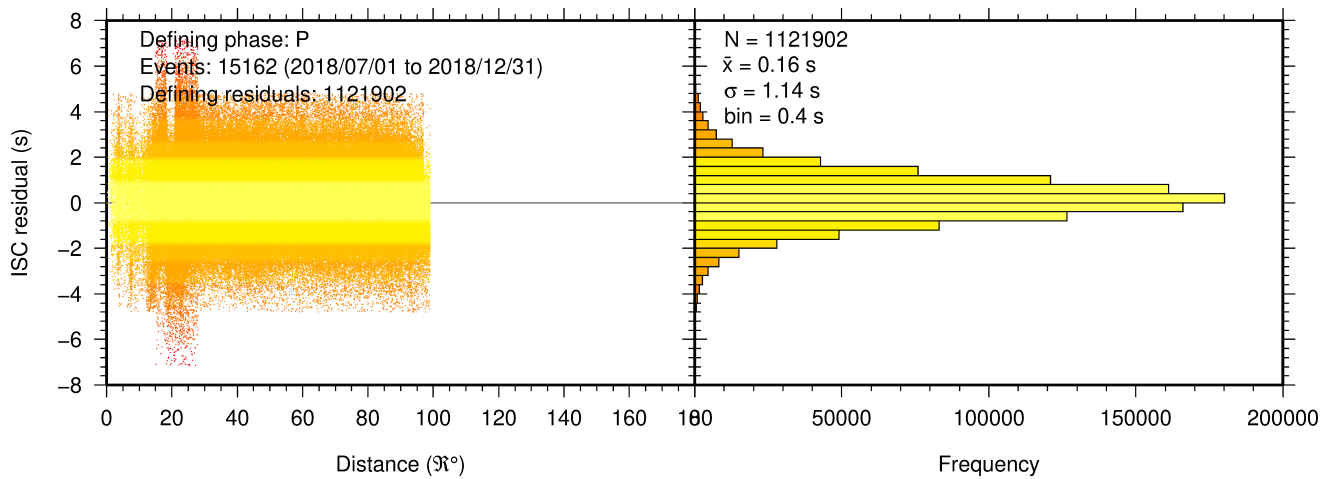
Figure 9.18: *Distribution of travel-time residuals for the defining P phases used in the computation of ISC located events in the Bulletin.*
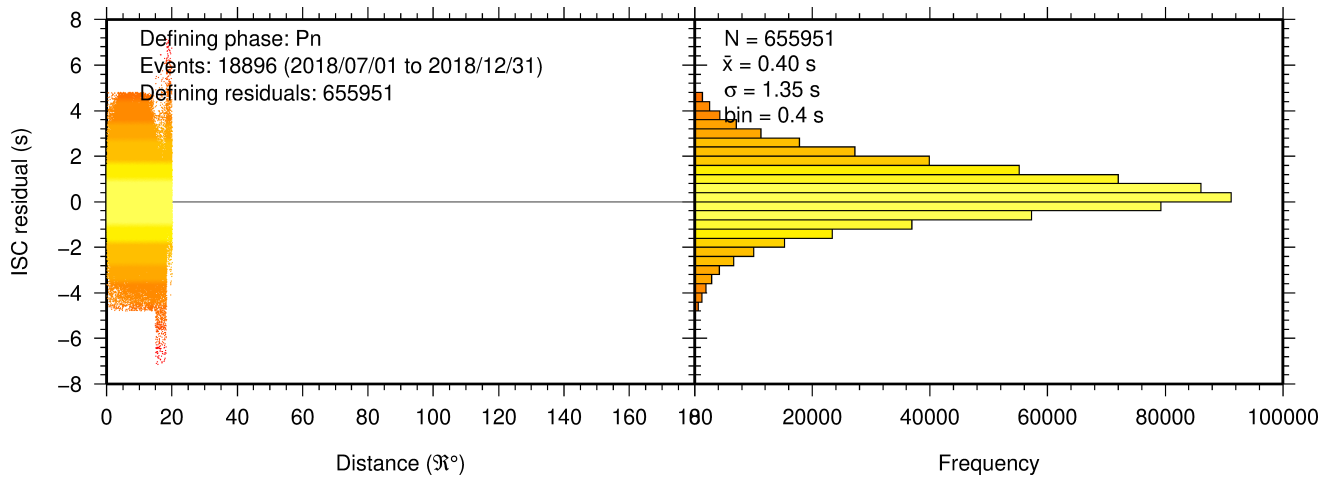
Figure 9.19: *Distribution of travel-time residuals for the defining Pn phases used in the computation of ISC located events in the Bulletin.*
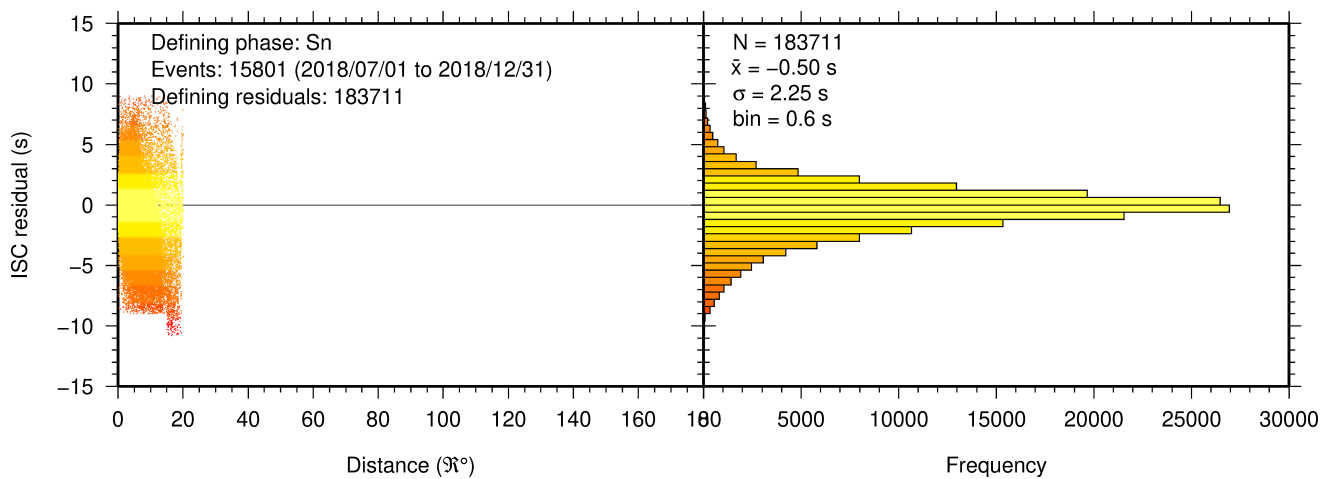
Figure 9.20: *Distribution of travel-time residuals for the defining Sn phases used in the computation of ISC located events in the Bulletin.*
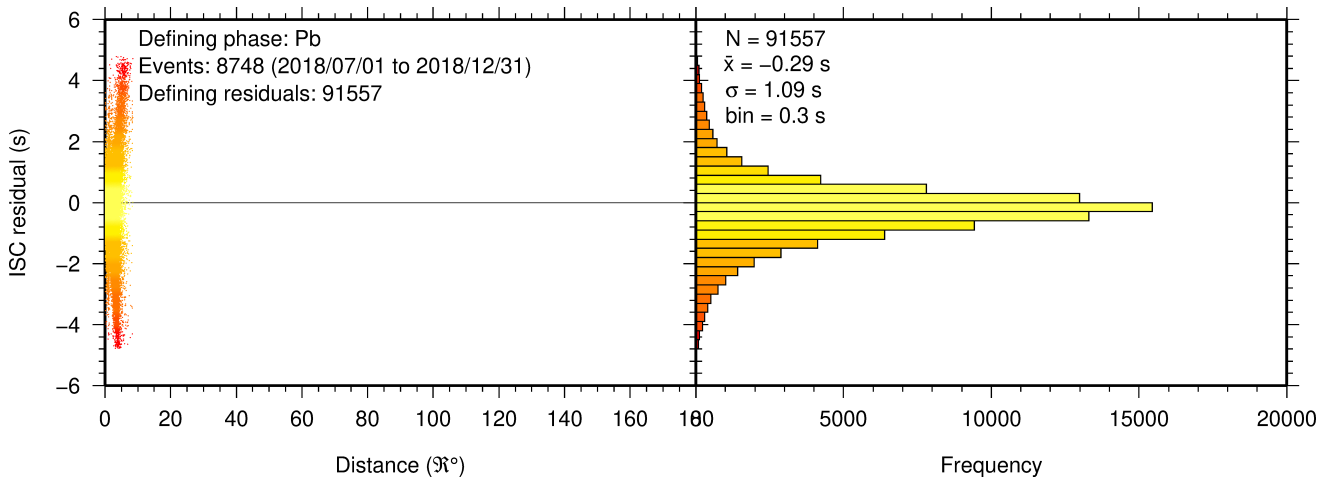
Figure 9.21: *Distribution of travel-time residuals for the defining Pb phases used in the computation of ISC located events in the Bulletin.*
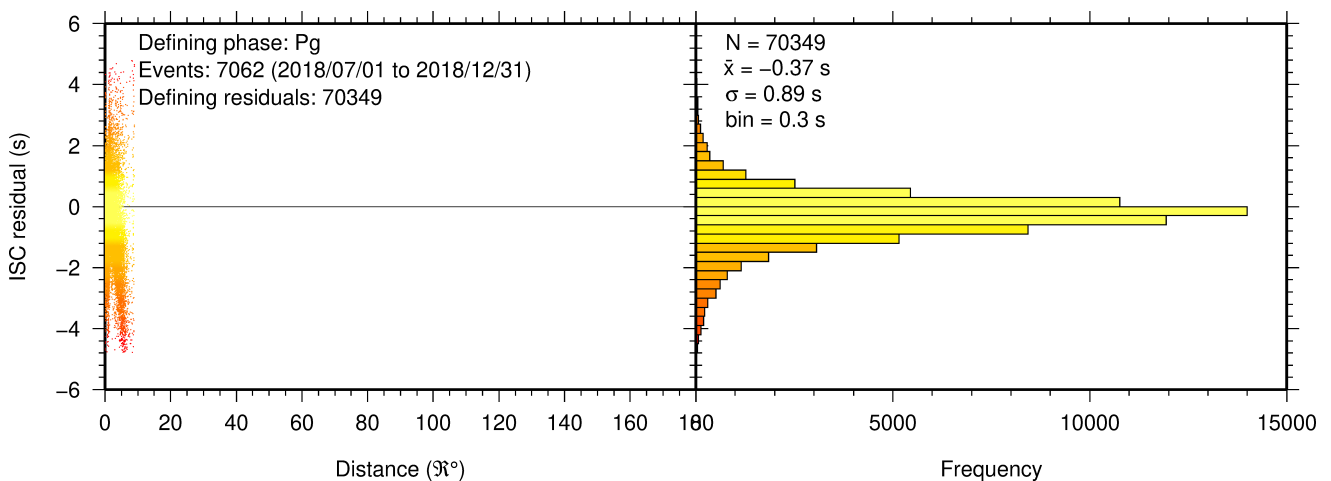
Figure 9.22: *Distribution of travel-time residuals for the defining Pg phases used in the computation of ISC located events in the Bulletin.*

9.3   Seismic Wave Amplitudes and Periods

The ISC Bulletin contains a variety of seismic wave amplitudes and periods measured by reporting agencies. For this Bulletin Summary, the total of collected amplitudes and periods is 3811980 (see Section 8.3). For the determination of the ISC magnitudes MS and mb, only a fraction of such data can be used. Indeed, the ISC network magnitudes are computed only for ISC located events. Here we recall the main features of the ISC procedure for MS and mb computation (see detailed description in Section 11.1.4 of the January to June 2018 Bulletin Summary). For each amplitude-period pair in a reading the ISC algorithm computes the magnitude (a reading can include several amplitude-period measurements) and the reading magnitude is assigned to the maximum A/T in the reading. If more than one reading magnitude is available for a station, the station magnitude is the median of the reading magnitudes. The network magnitude is computed then as the 20% alpha-trimmed median of the station magnitudes (at least three required). MS is computed for shallow earthquakes (depth $\leq$ 60 km) only and using amplitudes and periods on all three components (when available) if the period is within 10-60 s and the epicentral distance is between 20° and 160°. mb is computed also for deep earthquakes (depth down to

700 km) but only with amplitudes on the vertical component measured at periods $\leq$ 3 s in the distance range 21°-100°.

Table 9.2 is a summary of the amplitude and period data that contributed to the computation of station and ISC MS and mb network magnitudes for this Bulletin Summary.

Table 9.2: *Summary of the amplitude-period data used by the ISC Locator to compute MS and mb.*

	MS	mb
Number of amplitude-period data	184407	536952
Number of readings	162608	532841
Percentage of readings in the ISC located events with qualifying data for magnitude computation	16.0	42.4
Number of station magnitudes	157410	491837
Number of network magnitudes	3845	14049

A small percentage of the readings with qualifying data for MS and mb calculation have more than one amplitude-period pair. Notably, only 16% of the readings for the ISC located (shallow) events included qualifying data for MS computation, whereas for mb the percentage is much higher at 42%. This is due to the seismological practice of reporting agencies. Agencies contributing systematic reports of amplitude and period data are listed in Appendix Table 11.3. Obviously the ISC Bulletin would benefit if more agencies included surface wave amplitude-period data in their reports.

Figure 9.23 shows the distribution of the number of station magnitudes versus distance. For mb there is a significant increase in the distance range 70°-90°, whereas for MS most of the contributing stations are below 100°. The increase in number of station magnitude between 70°-90° for mb is partly due to the very dense distribution of seismic stations in North America and Europe with respect to earthquake occurring in various subduction zones around the Pacific Ocean.
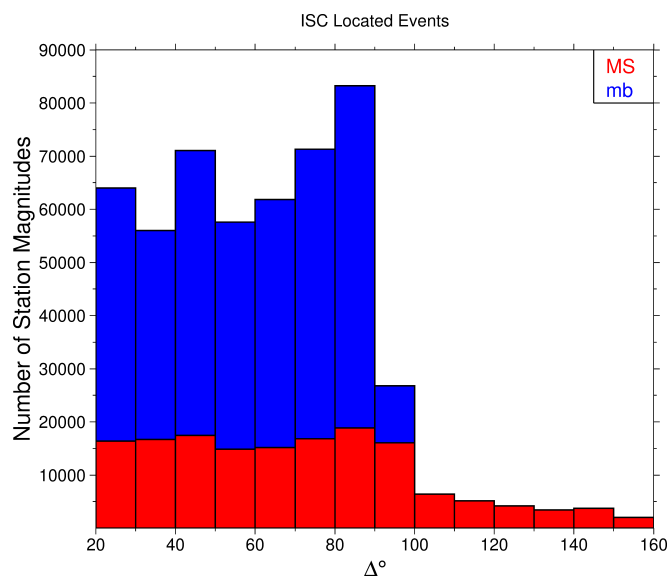
Figure 9.23: *Distribution of the number of station magnitudes computed by the ISC Locator for mb (blue) and MS (red) versus distance.*

Finally, Figure 9.24 shows the distribution of network MS and mb as well as the median number of stations for magnitude bins of 0.2. Clearly with increasing magnitude the number of events is smaller

but with a general tendency of having more stations contributing to the network magnitude.
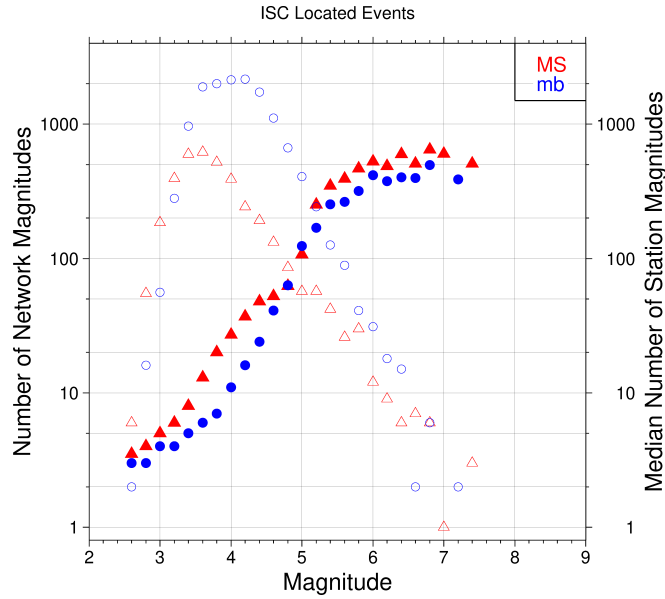
Figure 9.24: *Number of network magnitudes (open symbols) and median number of stations magnitudes (filled symbols). Blue circles refer to mb and red triangles to MS. The width of the magnitude interval δM is 0.2, and each symbol includes data with magnitude in M ± δM/2.*

9.4   Completeness of the ISC Bulletin

We define the magnitude of completeness (hereafter M_C) as the lowest magnitude threshold above which all events are believed to be recorded. The Bulletin with events bigger than the defined M_C is assumed to be complete.

Until Issue 53, Volume II (July - December 2016) of the Summary of the ISC an estimation of M_C was computed only with the maximum curvature technique (*Woessner and Wiemer*, 2005). After the completion of the Rebuild Project and relocation of ISC hypocenters from data years 1964 to 2010 (*Storchak et al.*, 2017), the estimate of M_C for the entire ISC Bulletin is re-computed using four catalogue based methodologies (*Adamaki*, 2017, and references therein): the previously used maximum curvature for comparison (maxC), Mc based on the b-value stability (MBS technique), the Goodness of Fit Test with a 90% level of fit (GFT90) and the modified Goodness of Fit Test (mGFT). Further details on each of these methodologies and their statistical behaviour can be found in *Leptokaropoulos et al.* (2018).

The magnitudes of completeness of the ISC Bulletin for this Summary period is shown in Figure 9.25. How M_C varies for the ISC Bulletin over the years is shown in Figure 9.26. The step change in 1996 corresponds with the inclusion of the Prototype IDC (EIDC) Bulletin, followed by the Reviewed Event Bulletin (REB) of the IDC.
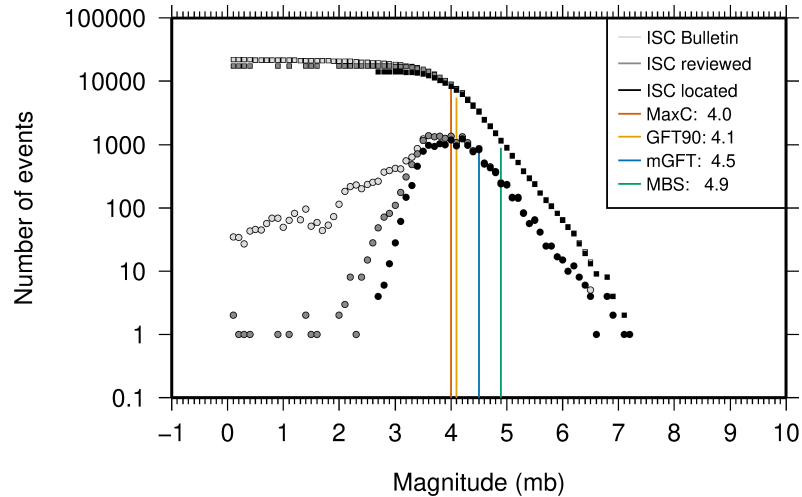
Figure 9.25: *Frequency and cumulative frequency magnitude distribution for all events in the ISC Bulletin, ISC reviewed events and events located by the ISC. The magnitude of completeness (M_C) is shown for the ISC Bulletin. Note: only events with values of mb are represented in the figure.*
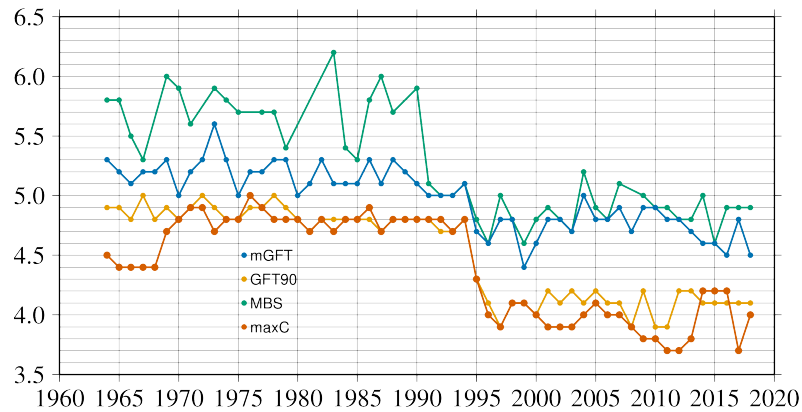
Figure 9.26: *Variation of magnitude of completeness (M_C) for each year in the ISC Bulletin. Note: M_C is calculated only using those events with values of mb.*

9.5 Magnitude Comparisons

The ISC Bulletin publishes network magnitudes reported by multiple agencies to the ISC. For events that have been located by the ISC, where enough amplitude data has been collected, the MS and mb magnitudes are calculated by the ISC (MS is computed only for depths ≤ 60 km). In this section, ISC magnitudes and some other reported magnitudes in the ISC Bulletin are compared.

The comparison between MS and mb computed by the ISC locator for events in this summary period is shown in Figure 9.27, where the large number of data pairs allows a colour coding of the data density. The scatter in the data reflects the fundamental differences between these magnitude scales.

Similar plots are shown in Figure 9.28 and 9.29, respectively, for comparisons of ISC mb and ISC MS with M_W from the GCMT catalogue. Since M_W is not often available below magnitude 5, these distributions are mostly for larger, global events. Not surprisingly, the scatter between mb and M_W is larger than the scatter between MS and M_W. Also, the saturation effect of mb is clearly visible for earthquakes with $M_W > 6.5$. In contrast, MS scales well with $M_W > 6$, whereas for smaller magnitudes MS appears to be systematically smaller than M_W.

In Figure 9.30 ISC values of mb are compared with all reported values of mb, values of mb reported by NEIC and values of mb reported by IDC. Similarly in Figure 9.31, ISC values of MS are compared with all reported values of MS, values of MS reported by NEIC and values of MS reported by IDC. There is a large scatter between the ISC magnitudes and the mb and MS reported by all other agencies.

The scatter decreases both for mb and MS when ISC magnitudes are compared just with NEIC and IDC magnitudes. This is not surprising as the latter two agencies provide most of the amplitudes and periods used by the ISC locator to compute MS and mb. However, ISC mb appears to be smaller than NEIC mb for $mb < 4$ and larger than IDC mb for $mb > 4$. Since NEIC does not include IDC amplitudes, it seems these features originate from observations at the high-gain, low-noise sites reported by the IDC. For the MS comparisons between ISC and NEIC a similar but smaller effect is observed for $MS < 4.5$, whereas a good scaling is generally observed for the MS comparisons between ISC and IDC.
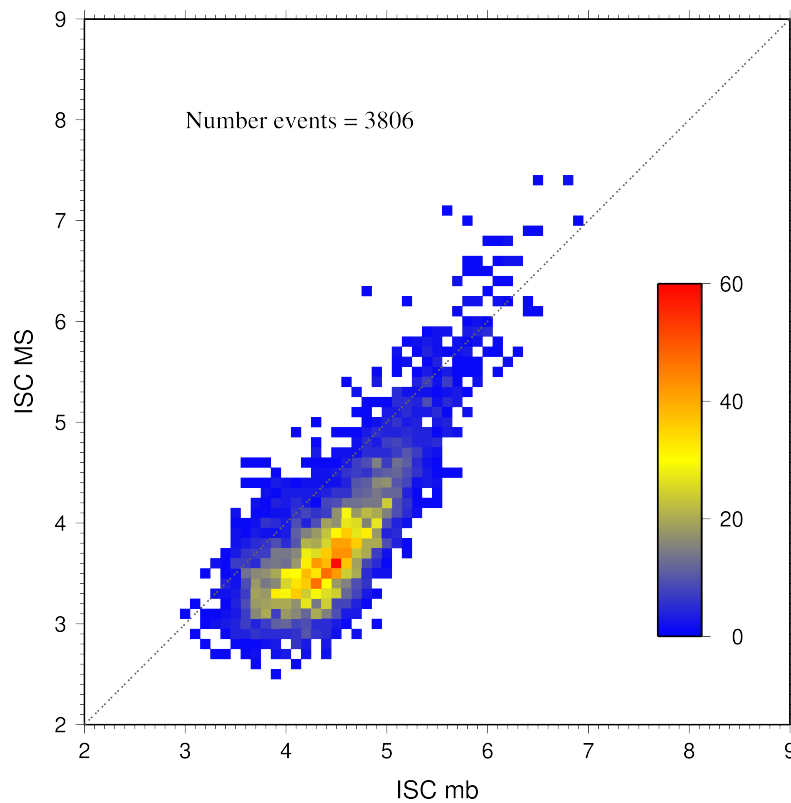
Figure 9.27: *Comparison of ISC values of MS with mb for common event pairs.*
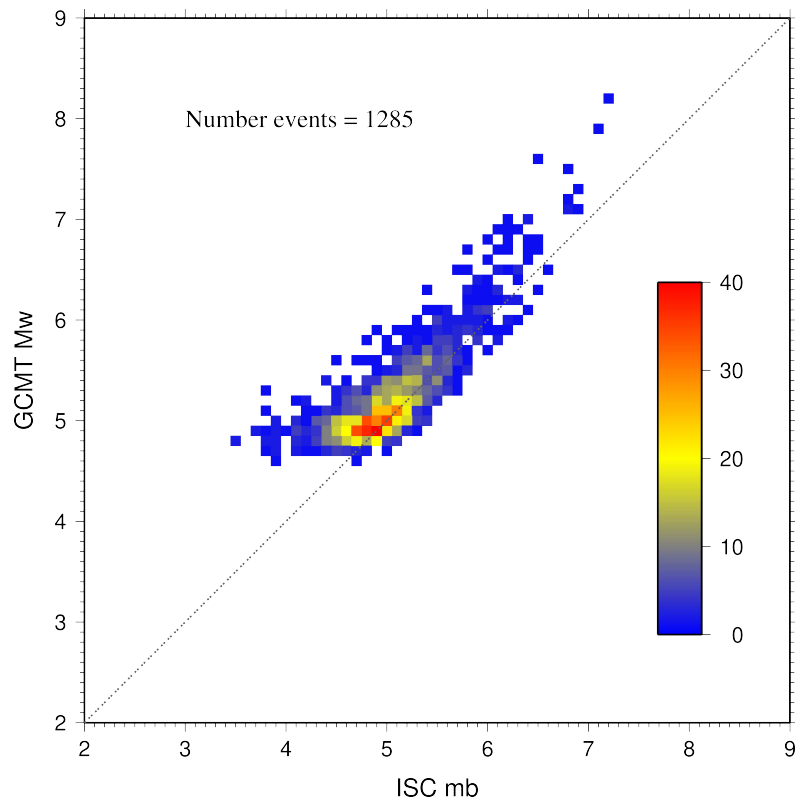
Figure 9.28: *Comparison of ISC values of mb with GCMT M_W for common event pairs.*
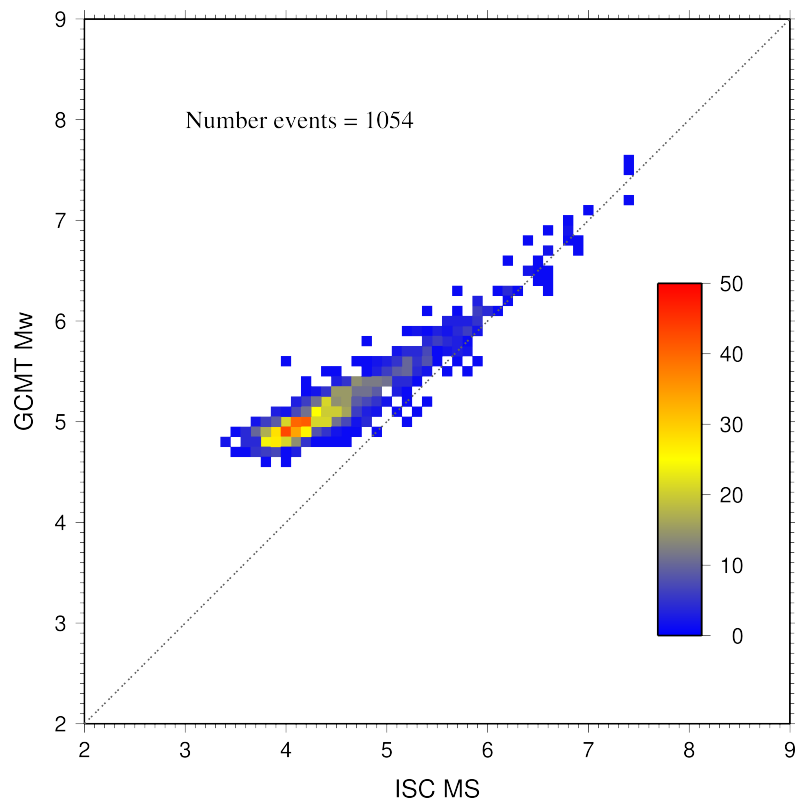
Figure 9.29: *Comparison of ISC values of MS with GCMT M_W for common event pairs.*
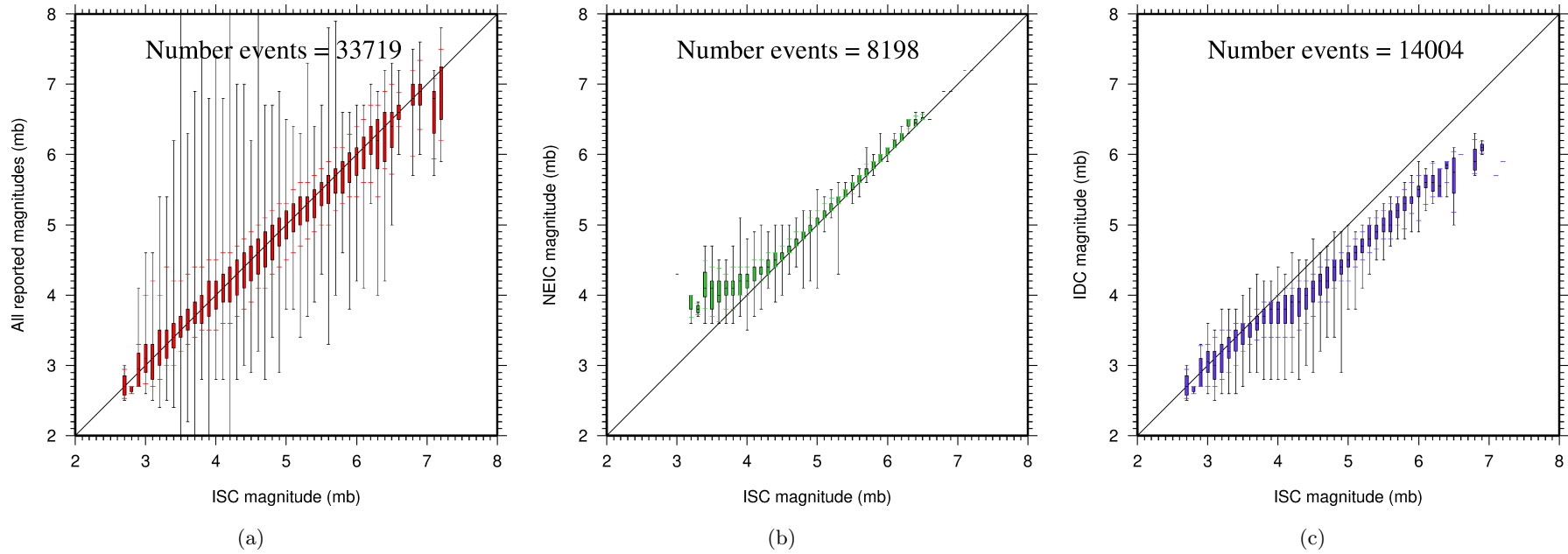
Figure 9.30: *Comparison of ISC magnitude data (mb) with additional agency magnitudes (mb). The statistical summary is shown in box-and-whisker plots where the 10th and 90th percentiles are shown in addition to the max and min values. (a): All magnitudes reported; (b): NEIC magnitudes; (c): IDC magnitudes.*
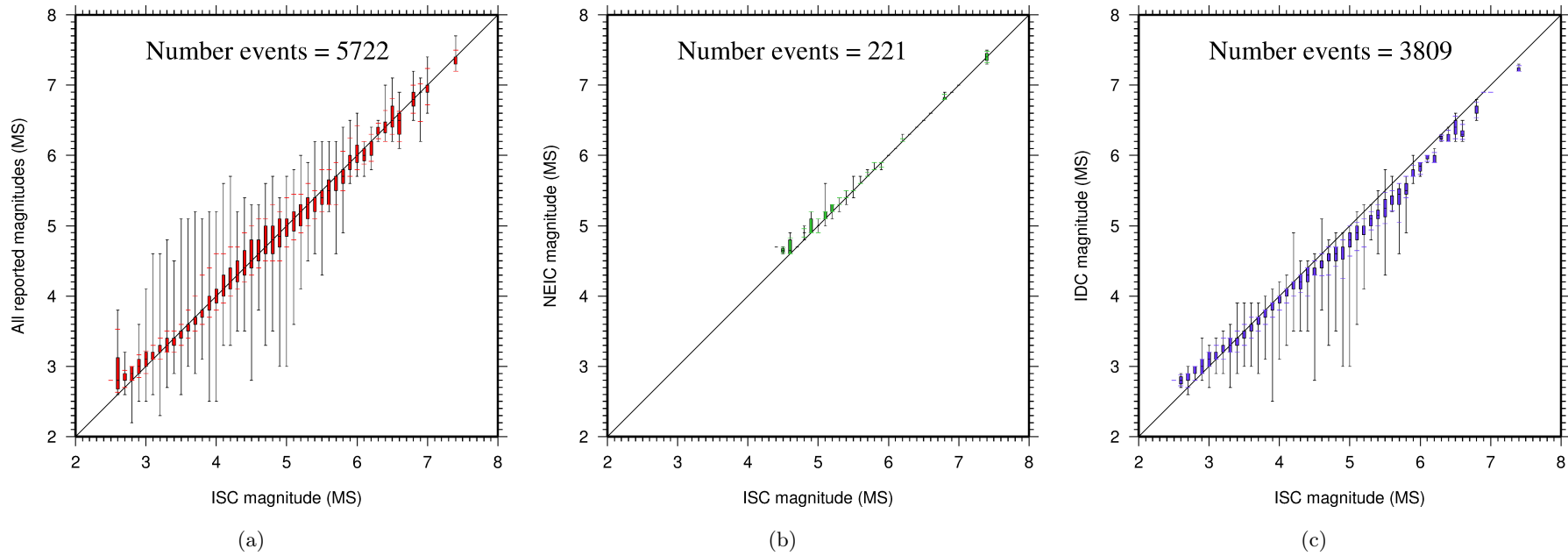
Figure 9.31: *Comparison of ISC magnitude data (MS) with additional agency magnitudes (MS). The statistical summary is shown in the box-and-whisker plots where the 10th and 90th percentiles are shown in addition to the max and min values. (a): All magnitudes reported; (b): NEIC magnitudes; (c): IDC magnitudes.*

10

The Leading Data Contributors

For the current six-month period, 151 agencies reported related bulletin data. Although we are grateful for every report, we nevertheless would like to acknowledge those agencies that made the most useful or distinct contributions to the contents of the ISC Bulletin. Here we note those agencies that:

- provided a comparatively large volume of parametric data (see Section 10.1),

- reported data that helped quite considerably to improve the quality of the ISC locations or magnitude determinations (see Section 10.2),

- helped the ISC by consistently reporting data in one of the standard recognised formats and in-line with the ISC data collection schedule (see Section 10.3).

We do not aim to discourage those numerous small networks who provide comparatively smaller yet still most essential volumes of regional data regularly, consistently and accurately. Without these reports the ISC Bulletin would not be as comprehensive and complete as it is today.

10.1   The Largest Data Contributors

We acknowledge the contribution of IDC, NEIC, MOS, BJI, UCC, NOU, AWI and a few others (Figure 10.1) that reported the majority of moderate to large events recorded at teleseismic distances. The contributions of NEIC, IDC, MEX, DJA and several others are also acknowledged with respect to smaller seismic events. The contributions of JMA, TAP, RSNC, AFAD, ISK and a number of others are also acknowledged with respect to small seismic events. Note that the NEIC bulletin accumulates a contribution of all regional networks in the USA. Several agencies monitoring highly seismic regions routinely report large volumes of small to moderate magnitude events, such as those in Japan, Chinese Taipei, Turkey, Italy, Greece, New Zealand, Mexico and Columbia. Contributions of small magnitude events by agencies in regions of low seismicity, such as Finland are also gratefully received.

We also would like to acknowledge contributions of those agencies that report a large portion of arrival time and amplitude data (Figure 10.2). For small magnitude events, these are local agencies in charge of monitoring local and regional seismicity. For moderate to large events, contributions of IDC, USArray, NEIC, MOS are especially acknowledged. Notably, three agencies (IDC, NEIC and MOS) together reported over 70% of all amplitude measurements made for teleseismically recorded events. We hope that other agencies would also be able to update their monitoring routines in the future to include the amplitude reports for teleseismic events compliant with the IASPEI standards.
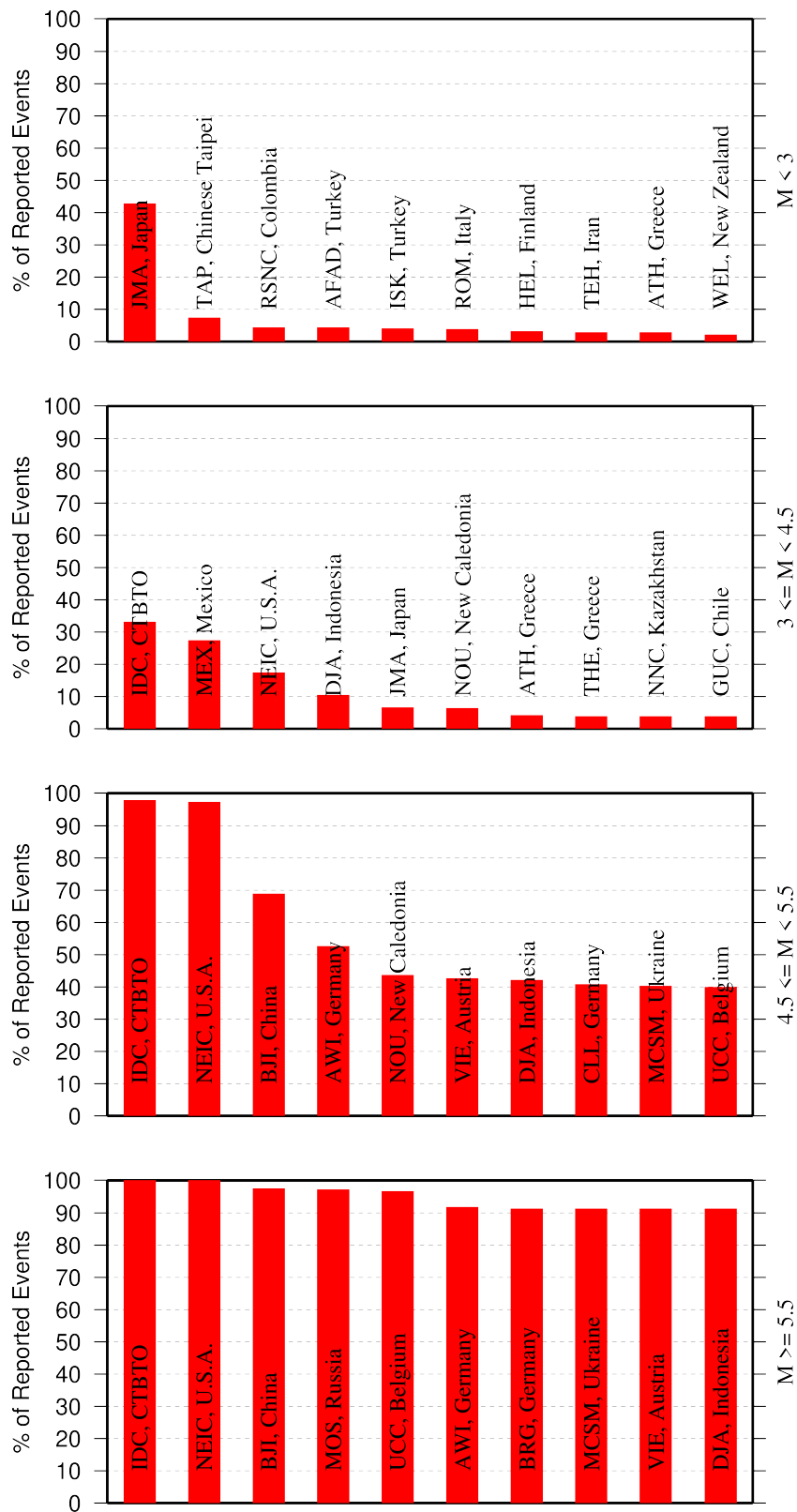
Figure 10.1: *Frequency of events in the ISC Bulletin for which an agency reported at least one item of data: a moment tensor, a hypocentre, a station arrival time or an amplitude. The top ten agencies are shown for four magnitude intervals.*
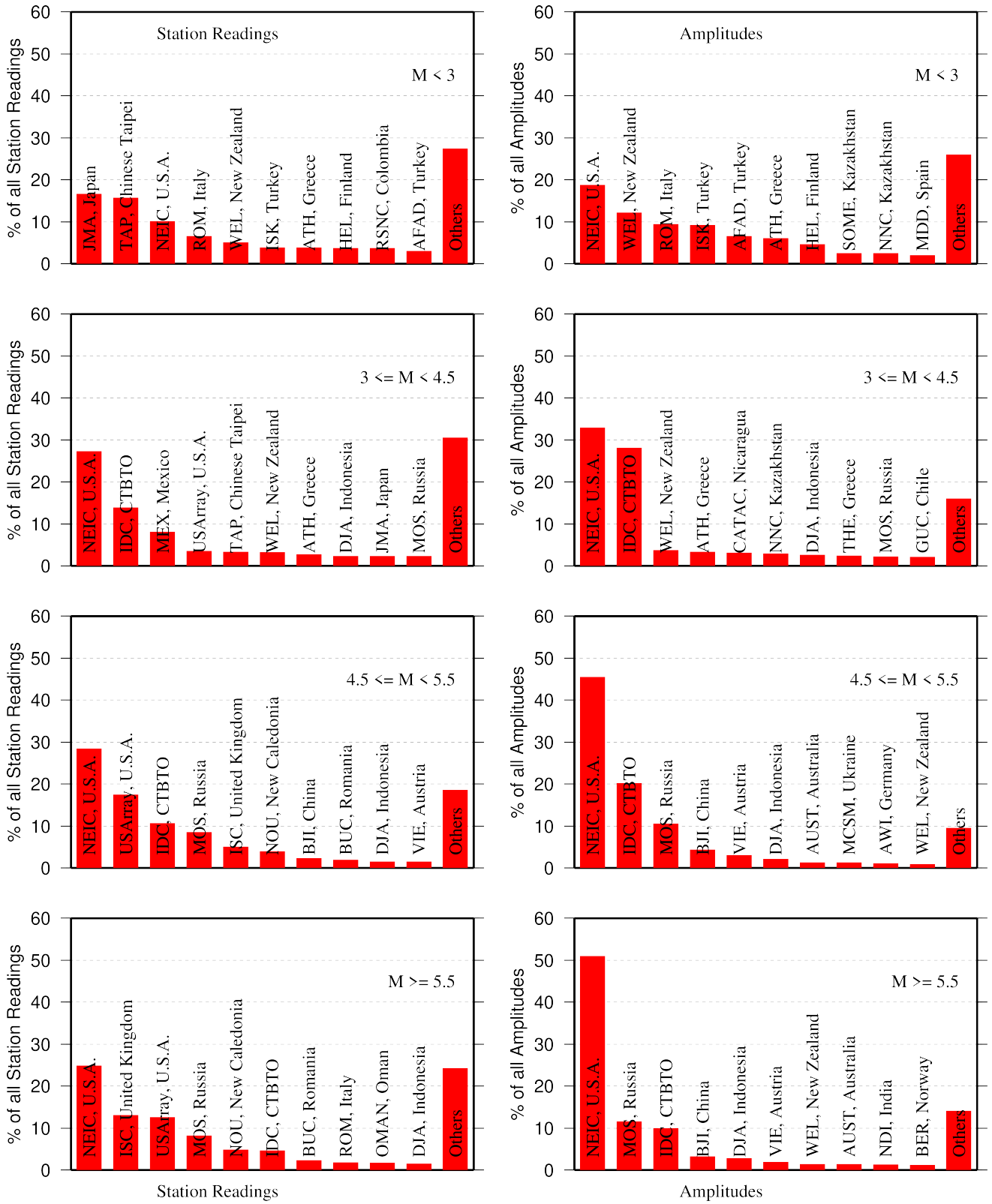
Figure 10.2: *Contributions of station arrival time readings (left) and amplitudes (right) of agencies to the ISC Bulletin. Top ten agencies are shown for four magnitude interwals.*

10.2   Contributors Reporting the Most Valuable Parameters

One of the main ISC duties is to re-calculate hypocentre estimates for those seismic events where a collective wealth of all station reports received from all agencies is likely to improve either the event location or depth compared to the hypocentre solution from each single agency. For areas with a sparse local seismic network or an unfavourable station configuration, readings made by other networks at teleseismic distances are very important. All events near mid-oceanic ridges as well as those in the majority of subduction zones around the world fall into this category. Hence we greatly appreciate the effort made by many agencies that report data for remote earthquakes (Figure 10.3). For some agencies, such as the IDC and the NEIC, it is part of their mission. For instance, the IDC reports almost every seismic event that is large enough to be recorded at teleseismic distance (20 degrees and beyond). This is largely because the International Monitoring System of primary arrays and broadband instruments is distributed at quiet sites around the world in order to be able to detect possible violations of the Comprehensive Nuclear-Test-Ban Treaty. The NEIC reported over 45% of those events as their mission requires them to report events above magnitude 4.5 outside the United States of America. For other agencies reporting distant events it is an extra effort that they undertake to notify their governments and relief agencies as well as to help the ISC and academic research in general. Hence these agencies usually report on the larger magnitude events. BJI, AWI, NAO, MOS, VIE, NOU, CLL and BRA each reported individual station arrivals for several percent of all relevant events. We encourage other agencies to report distant events to us.

In addition to the first arriving phase we encourage reporters to contribute observations of secondary seismic phases that help constrain the event location and depth: S, Sn, Sg and pP, sP, PcP (Figure 10.4). We expect though that these observations are actually made from waveforms, rather than just predicted by standard velocity models and modern software programs. It is especially important that these arrivals are manually reviewed by an operator (as we know takes place at the IDC and NEIC), as opposed to some lesser attempts to provide automatic phase readings that are later rejected by the ISC due to a generally poor quality of unreviewed picking.

Another important long-term task that the ISC performs is to compute the most definitive values of
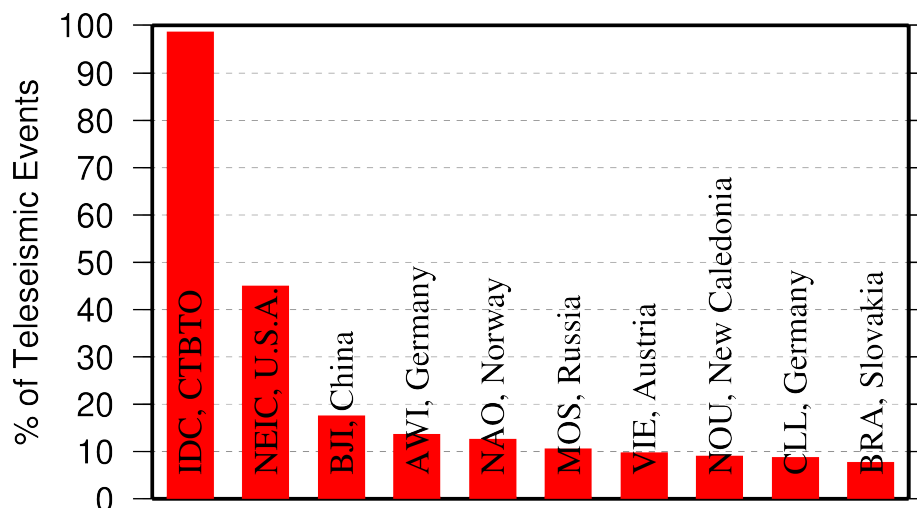
Figure 10.3: *Top ten agencies that reported teleseismic phase arrivals for a large portion of ISC events.*
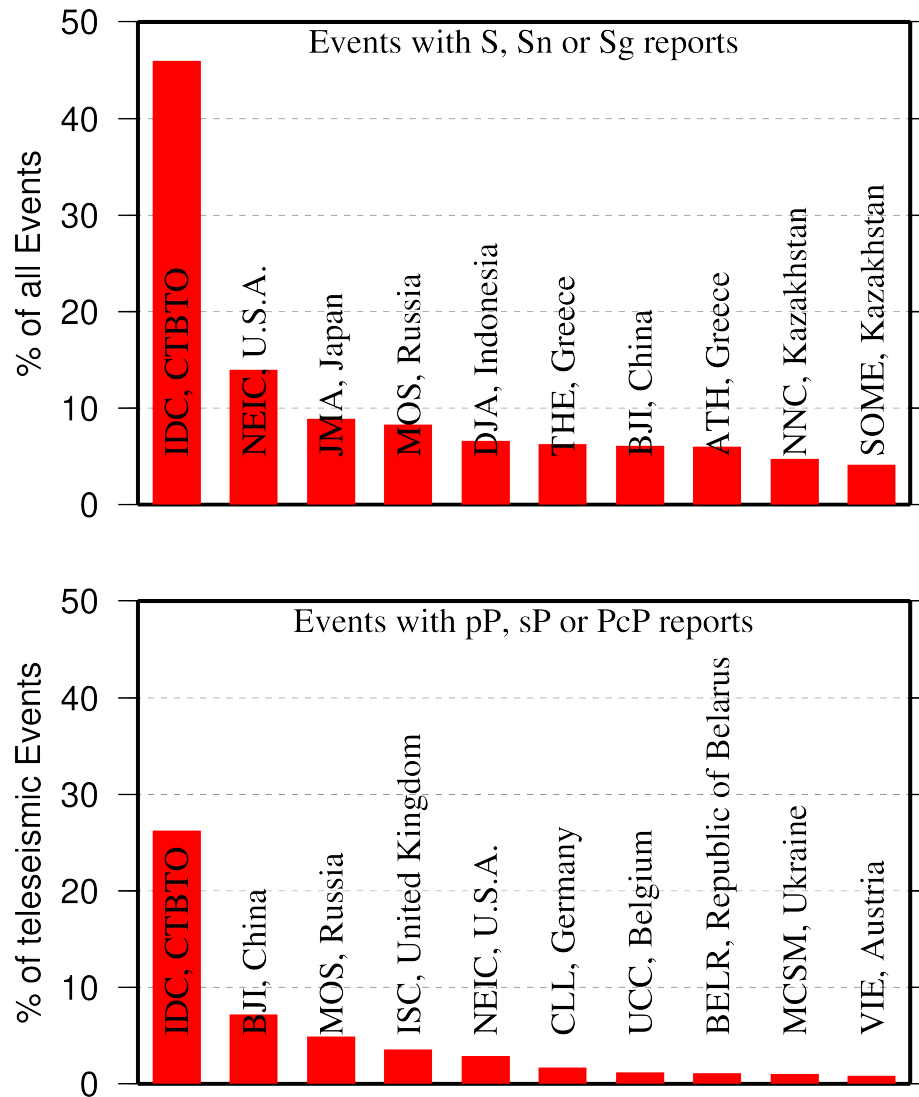
Figure 10.4: *Top ten agencies that reported secondary phases important for an accurate epicentre location (top) and focal depth determination (bottom).*

MS and mb network magnitudes that are considered reliable due to removal of outliers and consequent averaging (using alpha-trimmed median) across the largest network of stations, generally not feasible for a single agency. Despite concern over the bias at the lower end of mb introduced by the body wave amplitude data from the IDC, other agencies are also known to bias the results. This topic is further discussed in Section 9.5.

Notably, the IDC reports almost 100% of all events for which MS and mb are estimated. This is due to the standard routine that requires determination of body and surface wave magnitudes useful for discrimination purposes. NEIC, BJI, AWI, MOS, PRU, CLL and a few other agencies (Figure 10.5) are also responsible for the majority of the amplitude and period reports that contribute towards the ISC magnitudes.

The ISC only recently started to determine source mechanisms in addition to those reported by other agencies. For moment tensor magnitudes we rely on reports from other agencies (Figure 10.6).

Among other event parameters the ISC Bulletin also contains information on event type. We cannot
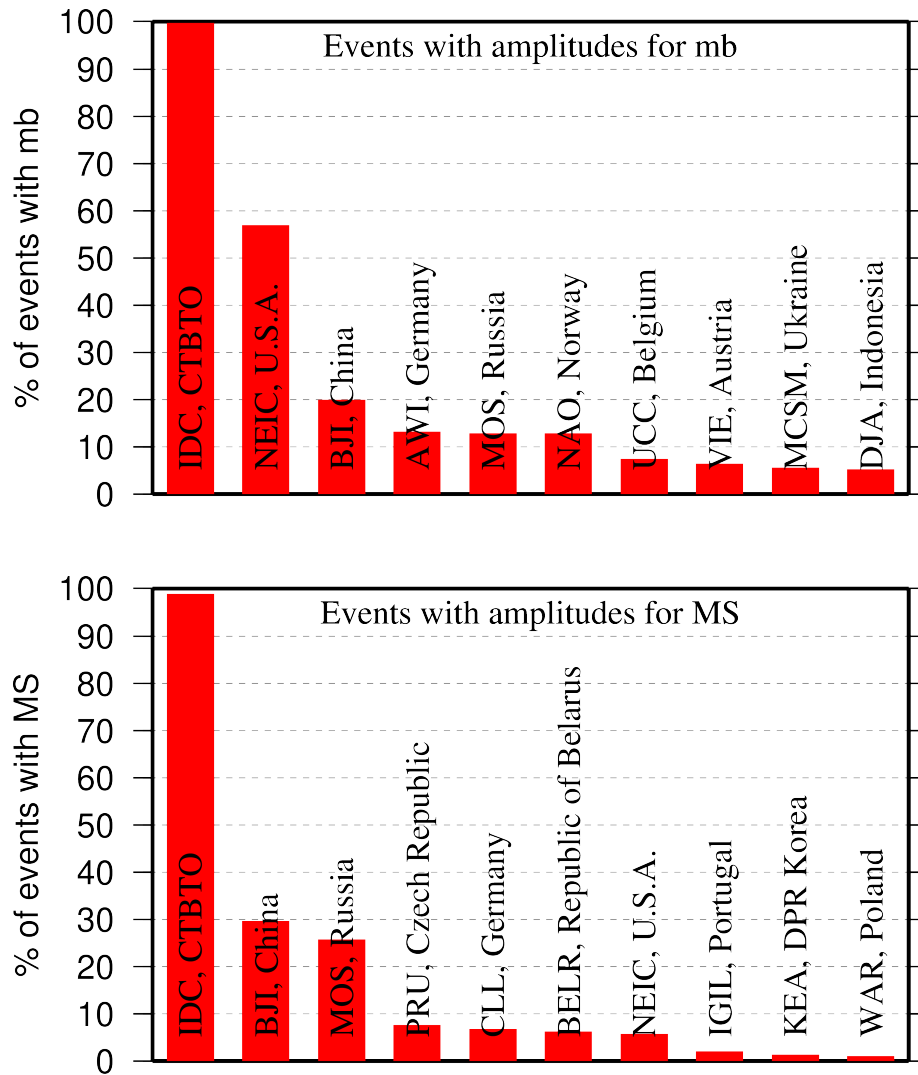
Figure 10.5: *Agencies that report defining body (top) and surface (bottom) wave amplitudes and periods for the largest fraction of those ISC Bulletin events with MS/mb determinations.*

independently verify the type of each event in the Bulletin and thus rely on other agencies to report the event type to us. Practices of reporting non-tectonic events vary greatly from country to country. Many agencies do not include anthropogenic events in their reports. Suppression of such events from reports to the ISC may lead to a situation where a neighbouring agency reports the anthropogenic event as an earthquake for which expected data are missing. This in turn is detrimental to ISC Bulletin users studying natural seismic hazard. Hence we encourage all agencies to join the agencies listed on Figure 10.7 and several others in reporting both natural and anthropogenic events to the ISC.

The ISC Bulletin also contains felt and damaging information when local agencies have reported it to us. Agencies listed on Figure 10.8 provide such information for the majority of all felt or damaging events in the ISC Bulletin.
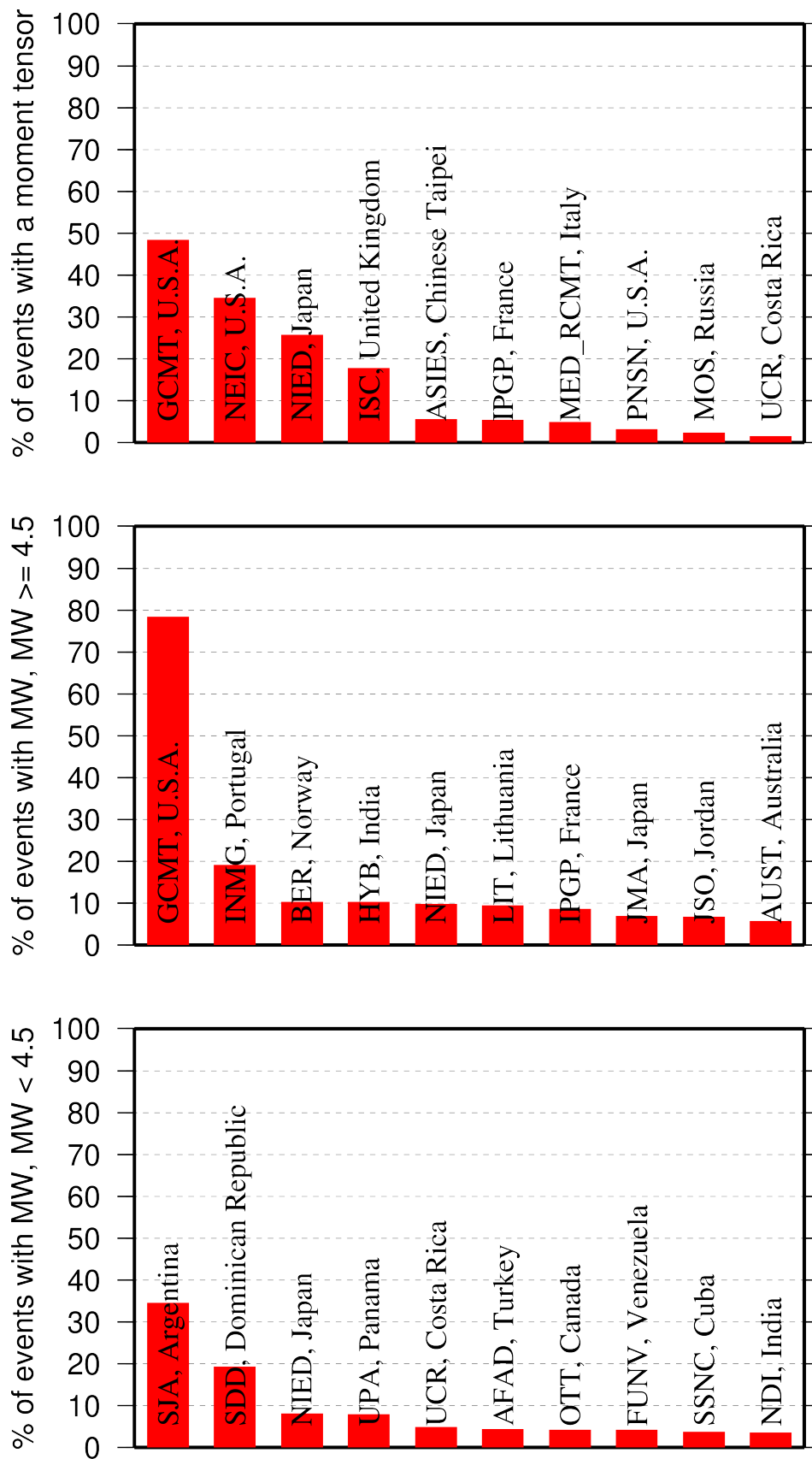
Figure 10.6: *Top ten agencies that most frequently report determinations of seismic moment tensor (top) and moment magnitude (middle/bottom for M greater/smaller than 4.5).*
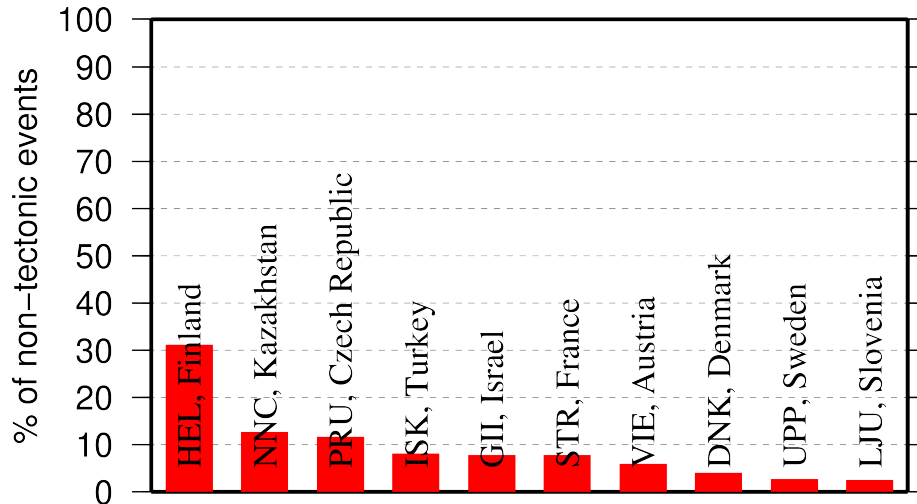
Figure 10.7: *Top ten agencies that most frequently report non-tectonic seismic events to the ISC.*
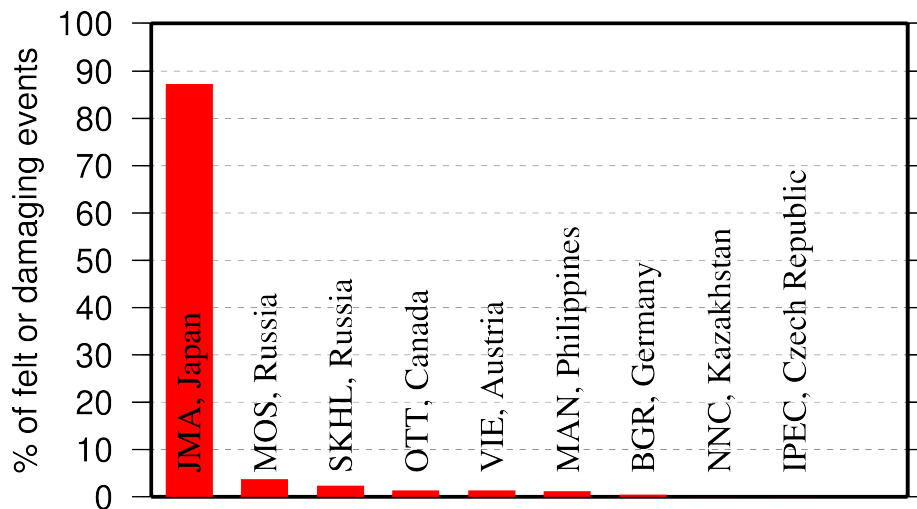
Figure 10.8: *Top ten agencies that most frequently report macroseismic information to the ISC.*

10.3 The Most Consistent and Punctual Contributors

During this six-month period, 38 agencies reported their bulletin data in one of the standard seismic formats (ISF, IMS, GSE, Nordic or QuakeML) and within the current 12-month deadline. Here we must reiterate that the ISC accepts reviewed bulletin data after a final analysis as soon as they are ready. These data, even if they arrive before the deadline, are immediately parsed into the ISC database, grouped with other data and become available to the ISC users on-line as part of the preliminary ISC Bulletin. There is no reason to wait until the deadline to send the data to the ISC. Table 10.1 lists all agencies that have been helpful to the ISC in this respect during the six-month period.

Table 10.1: *Agencies that contributed reviewed bulletin data to the ISC in one of the standard international formats before the submission deadline.*

Agency Code	Country	Average Delay from real time (days)
ZUR	Switzerland	16
WEL	New Zealand	19
LIC	Ivory Coast	26
IDC	Austria	27
ATH	Greece	29
IGIL	Portugal	32
KNET	Kyrgyzstan	33
LDG	France	38
NAO	Norway	42
BUC	Romania	43
ECX	Mexico	45
INAM	Angola	53
PPT	French Polynesia	94
ISK	Turkey	94
VIE	Austria	109
BGSI	Botswana	127
NEIC	U.S.A.	131
KEA	Democratic People's Republic of Korea	143
INMG	Portugal	152
SVSA	Portugal	154
AFAD	Turkey	155
PRE	South Africa	156
BGS	United Kingdom	160
MOLD	Moldova	162
BER	Norway	162
BJI	China	177
JSN	Jamaica	190
DSN	United Arab Emirates	198
THE	Greece	202
IPEC	Czech Republic	225
BEO	Serbia	254
BYKL	Russia	269
SOME	Kazakhstan	290
ISN	Iraq	290
UCC	Belgium	323
MRB	Spain	325
MOS	Russia	343
FUNV	Venezuela	355

11

Appendix

11.1 Tables

Table 11.1: *Listing of all 389 agencies that have directly reported to the ISC. The 151 agencies highlighted in bold have reported data to the ISC Bulletin for the period of this Bulletin Summary.*

Agency Code	Agency Name
AAA	Alma-ata, Kazakhstan
AAE	University of Addis Ababa, Ethiopia
AAM	University of Michigan, USA
ADE	Primary Industries and Resources SA, Australia
ADH	Observatorio Afonso Chaves, Portugal
AEIC	Alaska Earthquake Information Center, USA
AFAD	**Disaster and Emergency Management Presidency**, **Turkey**
AFAR	The Afar Depression: Interpretation of the 1960-2000 Earthquakes, Israel
AFUA	University of Alabama, USA
ALG	Algiers University, Algeria
ANDRE	USSR
ANF	USArray Array Network Facility, USA
ANT	Antofagasta, Chile
ARE	Instituto Geofisico del Peru, Peru
ARO	Observatoire Géophysique d'Arta, Djibouti
ASIES	**Institute of Earth Sciences, Academia Sinica**, **Chinese Taipei**
ASL	Albuquerque Seismological Laboratory, USA
ASM	University of Asmara, Eritrea
ASRS	**Altai-Sayan Seismological Centre, GS SB RAS**, **Russia**
ATA	The Earthquake Research Center Ataturk University, Turkey
ATH	**National Observatory of Athens**, **Greece**
AUST	**Geoscience Australia**, **Australia**
AVETI	USSR
AWI	**Alfred Wegener Institute for Polar and Marine Research**, **Germany**
AZER	**Republican Seismic Survey Center of Azerbaijan National Academy of Sciences**, **Azerbaijan**
BCIS	Bureau Central International de Sismologie, France
BDF	Observatório Sismológico da Universidade de Brasília, Brazil
BELR	**Centre of Geophysical Monitoring of the National Academy of Sciences of Belarus**, **Republic of Belarus**
BEO	**Seismological Survey of Serbia**, **Serbia**
BER	**University of Bergen**, **Norway**
BERK	Berkheimer H, Germany
BGR	**Bundesanstalt für Geowissenschaften und Rohstoffe**, **Germany**
BGS	**British Geological Survey**, **United Kingdom**
BGSI	**Botswana Geoscience Institute**, **Botswana**

Table 11.1: Continued.

Agency Code	Agency Name
BHUJ2	Study of Aftershocks of the Bhuj Earthquake by Japanese Research Team, Japan
BIAK	Biak earthquake aftershocks (17-Feb-1996), USA
BJI	**China Earthquake Networks Center**, **China**
BKK	**Thai Meteorological Department**, **Thailand**
BNS	Erdbebenstation, Geologisches Institut der Universität, Köl, Germany
BOG	Universidad Javeriana, Colombia
BRA	**Geophysical Institute, Slovak Academy of Sciences**, **Slovakia**
BRG	**Seismological Observatory Berggießhübel, TU Bergakademie Freiberg**, **Germany**
BRK	Berkeley Seismological Laboratory, USA
BRS	Brisbane Seismograph Station, Australia
BUC	**National Institute for Earth Physics**, **Romania**
BUD	Geodetic and Geophysical Research Institute, Hungary
BUEE	Earth & Environment, USA
BUG	Institute of Geology, Mineralogy & Geophysics, Germany
BUL	**Goetz Observatory**, **Zimbabwe**
BUT	Montana Bureau of Mines and Geology, USA
BYKL	**Baykal Regional Seismological Centre, GS SB RAS**, **Russia**
CADCG	Central America Data Centre, Costa Rica
CAN	Australian National University, Australia
CANSK	Canadian and Scandinavian Networks, Sweden
CAR	Instituto Sismologico de Caracas, Venezuela
CASC	Central American Seismic Center, Costa Rica
CATAC	**Central American Tsunami Advisory Center**, **Nicaragua**
CENT	Centennial Earthquake Catalog, USA
CERI	Center for Earthquake Research and Information, USA
CFUSG	**Inst. of Seismology and Geodynamics, V.I. Vernadsky Crimean Federal University**, **Republic of Crimea**
CLL	**Geophysikalisches Observatorium Collm**, **Germany**
CMWS	Laboratory of Seismic Monitoring of Caucasus Mineral Water Region, GSRAS, Russia
CNG	Seismographic Station Changalane, Mozambique
CNRM	**Centre National de Recherche**, **Morocco**
COSMOS	Consortium of Organizations for Strong Motion Observations, USA
CRAAG	**Centre de Recherche en Astronomie, Astrophysique et Géophysique**, **Algeria**
CSC	University of South Carolina, USA
CSEM	Centre Sismologique Euro-Méditerranéen (CSEM/EMSC), France
CUPWA	**Curtin University**, **Australia**
DASA	Defense Atomic Support Agency, USA
DBN	Koninklijk Nederlands Meteorologisch Instituut, Netherlands
DDA	General Directorate of Disaster Affairs, Turkey
DHMR	Yemen National Seismological Center, Yemen
DIAS	**Dublin Institute for Advanced Studies**, **Ireland**
DJA	**Badan Meteorologi, Klimatologi dan Geofisika**, **Indonesia**
DMN	**National Seismological Centre, Nepal**, **Nepal**
DNAG	USA
DNK	**Geological Survey of Denmark and Greenland**, **Denmark**

Table 11.1: *Continued.*

Agency Code	Agency Name
DRS	Dagestan Branch, Geophysical Survey, Russian Academy of Sciences, Russia
DSN	**Dubai Seismic Network**, **United Arab Emirates**
DUSS	Damascus University, Syria, Syria
EAF	**East African Network**, **Unknown**
EAGLE	Ethiopia-Afar Geoscientific Lithospheric Experiment, Unknown
EBR	Observatori de l'Ebre, Spain
EBSE	Ethiopian Broadband Seismic Experiment, Unknown
ECGS	European Center for Geodynamics and Seismology, Luxembourg
ECX	**Centro de Investigación Científica y de Educación Superior de Ensenada**, **Mexico**
EFATE	OBS Experiment near Efate, Vanuatu, USA
EHB	Engdahl, van der Hilst and Buland, USA
EIDC	Experimental (GSETT3) International Data Center, USA
EKA	Eskdalemuir Array Station, United Kingdom
ENT	Geological Survey and Mines Department, Uganda
EPSI	Reference events computed by the ISC for EPSI project, United Kingdom
ERDA	Energy Research and Development Administration, USA
EST	Geological Survey of Estonia, Estonia
EUROP	, Unknown
EVBIB	Data from publications listed in the ISC Event Bibliography, Unknown
FBR	Fabra Observatory, Spain
FCIAR	**Federal Center for Integrated Arctic Research**, **Russia**
FDF	Fort de France, Martinique
FIA0	Finessa Array, Finland
FOR	Unknown Historical Agency, Unknown - historical agency
FUBES	Earth Science Dept., Geophysics Section, Germany
FUNV	**Fundación Venezolana de Investigaciones Sismológicas**, **Venezuela**
FUR	Geophysikalisches Observatorium der Universität München, Germany
GBZT	Marmara Research Center, Turkey
GCG	**INSIVUMEH**, **Guatemala**
GCMT	**The Global CMT Project**, **USA**
GDNRW	Geologischer Dienst Nordrhein-Westfalen, Germany
GEN	**Dipartimento per lo Studio del Territorio e delle sue Risorse (RSNI)**, **Italy**
GEOAZ	UMR Géoazur, France
GEOMR	GEOMAR, Germany
GFZ	Helmholtz Centre Potsdam GFZ German Research Centre For Geosciences, Germany
GII	**The Geophysical Institute of Israel**, **Israel**
GOM	Observatoire Volcanologique de Goma, Democratic Republic of the Congo
GRAL	**National Council for Scientific Research**, **Lebanon**
GSDM	**Geological Survey Department Malawi**, **Malawi**
GSET2	Group of Scientific Experts Second Technical Test 1991, April 22 - June 2, Unknown
GTFE	German Task Force for Earthquakes, Germany
GUC	**Centro Sismológico Nacional, Universidad de Chile**, **Chile**

Table 11.1: *Continued.*

Agency Code	Agency Name
HAN	Hannover, Germany
HDC	Observatorio Vulcanológico y Sismológico de Costa Rica, Costa Rica
HEL	**Institute of Seismology, University of Helsinki**, **Finland**
HFS	Hagfors Observatory, Sweden
HFS1	Hagfors Observatory, Sweden
HFS2	Hagfors Observatory, Sweden
HIMNT	Himalayan Nepal Tibet Experiment, USA
HKC	**Hong Kong Observatory**, **Hong Kong**
HLUG	Hessisches Landesamt für Umwelt und Geologie, Germany
HLW	**National Research Institute of Astronomy and Geophysics**, **Egypt**
HNR	Ministry of Mines, Energy and Rural Electrification, Solomon Islands
HON	Pacific Tsunami Warning Center - NOAA, USA
HRVD	Harvard University, USA
HRVD_LR	Department of Geological Sciences, Harvard University, USA
HVO	Hawaiian Volcano Observatory, USA
HYB	**National Geophysical Research Institute**, **India**
HYD	National Geophysical Research Institute, India
IAG	Instituto Andaluz de Geofisica, Spain
IASBS	Institute for Advanced Studies in Basic Sciences, Iran
IASPEI	IASPEI Working Group on Reference Events, USA
ICE	Instituto Costarricense de Electricidad, Costa Rica
IDC	**International Data Centre, CTBTO**, **Austria**
IDG	Institute of Dynamics of Geosphere, Russian Academy of Sciences, Russia
IEC	Institute of the Earth Crust, SB RAS, Russia
IEPN	Institute of Environmental Problems of the North, Russian Academy of Sciences, Russia
IFREE	Institute For Research on Earth Evolution, Japan
IGGSL	Seismology Lab, Institute of Geology & Geophysics, Chinese Academy of Sciences, China
IGIL	**Instituto Dom Luiz, University of Lisbon**, **Portugal**
IGQ	**Servicio Nacional de Sismología y Vulcanología**, **Ecuador**
IGS	Institute of Geological Sciences, United Kingdom
INAM	**Instituto Nacional de Meteorologia e Geofisica - INAMET**, **Angola**
INDEPTH3	International Deep Profiling of Tibet and the Himalayas, USA
INET	Instituto Nicaraguense de Estudios Territoriales - INETER, Nicaragua
INMG	**Instituto Português do Mar e da Atmosfera, I.P.**, **Portugal**
INMGC	Instituto Nacional de Meteorologia e Geofísica, Cape Verde
IPEC	**The Institute of Physics of the Earth (IPEC)**, **Czech Republic**
IPER	Institute of Physics of the Earth, Academy of Sciences, Moscow, Russia
IPGP	**Institut de Physique du Globe de Paris**, **France**
IPRG	Institute for Petroleum Research and Geophysics, Israel
IRIS	**IRIS Data Management Center**, **USA**
IRSM	Institute of Rock Structure and Mechanics, Czech Republic
ISC	**International Seismological Centre**, **United Kingdom**
ISC-PPSM	International Seismological Centre Probabalistic Point Source Model, United Kingdom

Table 11.1: *Continued.*

Agency Code	Agency Name
ISK	**Kandilli Observatory and Research Institute**, **Turkey**
ISN	**Iraqi Meteorological and Seismology Organisation**, **Iraq**
ISS	International Seismological Summary, United Kingdom
IST	Institute of Physics of the Earth, Technical University of Istanbul, Turkey
ISU	**Institute of Seismology, Academy of Sciences, Republic of Uzbekistan**, **Uzbekistan**
ITU	Faculty of Mines, Department of Geophysical Engineering, Turkey
JEN	Geodynamisches Observatorium Moxa, Germany
JMA	**Japan Meteorological Agency**, **Japan**
JOH	Bernard Price Institute of Geophysics, South Africa
JSN	**Jamaica Seismic Network**, **Jamaica**
JSO	**Jordan Seismological Observatory**, **Jordan**
KBC	Institut de Recherches Géologiques et Minières, Cameroon
KEA	**Korea Earthquake Administration**, **Democratic People's Republic of Korea**
KEW	Kew Observatory, United Kingdom
KHC	Institute of Geophysics, Czech Academy of Sciences, Czech Republic
KISR	Kuwait Institute for Scientific Research, Kuwait
KLM	Malaysian Meteorological Service, Malaysia
KMA	**Korea Meteorological Administration**, **Republic of Korea**
KNET	**Kyrgyz Seismic Network**, **Kyrgyzstan**
KOLA	**Kola Regional Seismic Centre, GS RAS**, **Russia**
KRAR	Krasnoyarsk Scientific Research Inst. of Geology and Mineral Resources, Russia, Russia
KRL	Geodätisches Institut der Universität Karlsruhe, Germany
KRNET	**Institute of Seismology, Academy of Sciences of Kyrgyz Republic**, **Kyrgyzstan**
KRSC	**Kamchatka branch of the Geophysical Survey of the Russian Academy of Sciences**, **Russia**
KRSZO	**Geodetic and Geophysical Reasearch Institute, Hungarian Academy of Sciences**, **Hungary**
KSA	Observatoire de Ksara, Lebanon
KUK	Geological Survey Department of Ghana, Ghana
LAO	Large Aperture Seismic Array, USA
LDG	**Laboratoire de Détection et de Géophysique/CEA**, **France**
LDN	University of Western Ontario, Canada
LDO	Lamont-Doherty Earth Observatory, USA
LED	Landeserdbebendienst Baden-Württemberg, Germany
LEDBW	Landeserdbebendienst Baden-Württemberg, Germany
LER	Besucherbergwerk Binweide Station, Germany
LIB	Tripoli, Libya
LIC	**Station Géophysique de Lamto**, **Ivory Coast**
LIM	Lima, Peru
LIS	Instituto de Meteorologia, Portugal
LIT	**Geological Survey of Lithuania**, **Lithuania**
LJU	**Slovenian Environment Agency**, **Slovenia**
LPA	**Universidad Nacional de La Plata**, **Argentina**
LPZ	Observatorio San Calixto, Bolivia
LRSM	Long Range Seismic Measurements Project, Unknown

Table 11.1: *Continued.*

Agency Code	Agency Name
LSZ	**Geological Survey Department of Zambia, Zambia**
LVSN	**Latvian Seismic Network, Latvia**
MAN	**Philippine Institute of Volcanology and Seismology, Philippines**
MAT	The Matsushiro Seismological Observatory, Japan
MATSS	USSR
MCO	**Macao Meteorological and Geophysical Bureau, Macao, China**
MCSM	**Main Centre for Special Monitoring, Ukraine**
MDD	**Instituto Geográfico Nacional, Spain**
MED_RCMT	**MedNet Regional Centroid - Moment Tensors, Italy**
MERI	Maharashta Engineering Research Institute, India
MES	Messina Seismological Observatory, Italy
MEX	**Instituto de Geofísica de la UNAM, Mexico**
MIRAS	**Mining Institute of the Ural Branch of the Russian Academy of Sciences, Russia**
MNH	Institut für Angewandte Geophysik der Universitat Munchen, Germany
MOLD	**Institute of Geophysics and Geology, Moldova**
MOS	**Geophysical Survey of Russian Academy of Sciences, Russia**
MOZ	Direccao Nacional de Geologia, Mozambique
MOZAR	, Mozambique
MRB	**Institut Cartogràfic i Geològic de Catalunya, Spain**
MSI	Messina Seismological Observatory, Italy
MSSP	Micro Seismic Studies Programme, PINSTECH, Pakistan
MSUGS	Michigan State University, Department of Geological Sciences, USA
MUN	Mundaring Observatory, Australia
NAI	University of Nairobi, Kenya
NAM	**The Geological Survey of Namibia, Namibia**
NAO	**Stiftelsen NORSAR, Norway**
NCEDC	Northern California Earthquake Data Center, USA
NDI	**National Centre for Seismology of the Ministry of Earth Sciences of India, India**
NEIC	**National Earthquake Information Center, USA**
NEIS	National Earthquake Information Service, USA
NERS	**North Eastern Regional Seismological Centre, GS RAS, Russia**
NIC	**Cyprus Geological Survey Department, Cyprus**
NIED	**National Research Institute for Earth Science and Disaster Resilience, Japan**
NKSZ	USSR
NNC	**National Nuclear Center, Kazakhstan**
NORS	North Ossetia (Alania) Branch, Geophysical Survey, Russian Academy of Sciences, Russia
NOU	**IRD Centre de Nouméa, New Caledonia**
NSSC	National Syrian Seismological Center, Syria
NSSP	**National Survey of Seismic Protection, Armenia**
OBM	Research Centre of Astronomy and Geophysics, Mongolia
OGAUC	Centro de Investigação da Terra e do Espaço da Universidade de Coimbra, Portugal
OGSO	Ohio Geological Survey, USA
OMAN	**Sultan Qaboos University, Oman**
ORF	Orfeus Data Center, Netherlands

Table 11.1: *Continued.*

Agency Code	Agency Name
OSPL	**Observatorio Sismologico Politecnico Loyola**, **Dominican Republic**
OSUB	Osservatorio Sismologico Universita di Bari, Italy
OSUNB	**Observatory Seismological of the University of Brasilia**, **Brazil**
OTT	**Canadian Hazards Information Service, Natural Resources Canada**, **Canada**
PAL	Palisades, USA
PAS	California Institute of Technology, USA
PDA	Universidade dos Açores, Portugal
PDG	**Seismological Institute of Montenegro**, **Montenegro**
PEK	Peking, China
PGC	Pacific Geoscience Centre, Canada
PJWWP	**Private Observatory of Pawel Jacek Wiejacz, D.Sc.**, **Poland**
PLV	**Institute of Geophysics, Viet Nam Academy of Science and Technology**, **Viet Nam**
PMEL	Pacific seismicity from hydrophones, USA
PMR	Alaska Tsunami Warning Center,, USA
PNNL	Pacific Northwest National Laboratory, USA
PNSN	**Pacific Northwest Seismic Network**, **USA**
PPT	**Laboratoire de Géophysique/CEA**, **French Polynesia**
PRE	**Council for Geoscience**, **South Africa**
PRU	**Institute of Geophysics, Czech Academy of Sciences**, **Czech Republic**
PTO	Instituto Geofísico da Universidade do Porto, Portugal
PTWC	Pacific Tsunami Warning Center, USA
QCP	**Manila Observatory**, **Philippines**
QUE	Pakistan Meteorological Department, Pakistan
QUI	Escuela Politécnica Nacional, Ecuador
RAB	Rabaul Volcanological Observatory, Papua New Guinea
RBA	Université Mohammed V, Morocco
REN	MacKay School of Mines, USA
REY	**Icelandic Meteorological Office**, **Iceland**
RHSSO	**Republic Hydrometeorological Service, Seismological Observatory, Banja Luka**, **Bosnia and Herzegovina**
RISSC	**Laboratory of Research on Experimental and Computational Seimology**, **Italy**
RMIT	Royal Melbourne Institute of Technology, Australia
ROC	Odenbach Seismic Observatory, USA
ROM	**Istituto Nazionale di Geofisica e Vulcanologia**, **Italy**
RRLJ	Regional Research Laboratory Jorhat, India
RSMAC	Red Sísmica Mexicana de Apertura Continental, Mexico
RSNC	**Red Sismológica Nacional de Colombia**, **Colombia**
RSPR	**Red Sísmica de Puerto Rico**, **USA**
RYD	King Saud University, Saudi Arabia
SAPSE	Southern Alps Passive Seismic Experiment, New Zealand
SAR	Sarajevo Seismological Station, Bosnia and Herzegovina
SBDV	USSR
SCB	**Observatorio San Calixto**, **Bolivia**
SCEDC	Southern California Earthquake Data Center, USA

Table 11.1: *Continued.*

Agency Code	Agency Name
SCSIO	Key Laboratory of Ocean and Marginal Sea Geology, South China Sea, China
SDD	**Universidad Autonoma de Santo Domingo**, **Dominican Republic**
SEA	Geophysics Program AK-50, USA
SET	Setif Observatory, Algeria
SFS	**Real Instituto y Observatorio de la Armada**, **Spain**
SGS	**Saudi Geological Survey**, **Saudi Arabia**
SHL	Central Seismological Observatory, India
SIGU	**Subbotin Institute of Geophysics, National Academy of Sciences**, **Ukraine**
SIK	Seismic Institute of Kosovo, Unknown
SIO	Scripps Institution of Oceanography, USA
SJA	**Instituto Nacional de Prevención Sísmica**, **Argentina**
SJS	Instituto Costarricense de Electricidad, Costa Rica
SKHL	**Sakhalin Experimental and Methodological Seismological Expedition, GS RAS**, **Russia**
SKL	Sakhalin Complex Scientific Research Institute, Russia
SKO	**Seismological Observatory Skopje**, **North Macedonia**
SLC	Salt Lake City, USA
SLM	Saint Louis University, USA
SNET	**Servicio Nacional de Estudios Territoriales**, **El Salvador**
SNM	New Mexico Institute of Mining and Technology, USA
SNSN	Saudi National Seismic Network, Saudi Arabia
SOF	**National Institute of Geophysics, Geology and Geography**, **Bulgaria**
SOMC	**Seismological Observatory of Mount Cameroon**, **Cameroon**
SOME	**Seismological Experimental Methodological Expedition**, **Kazakhstan**
SPA	USGS - South Pole, Antarctica
SPGM	Service de Physique du Globe, Morocco
SPITAK	Armenia
SRI	Stanford Research Institute, USA
SSN	Sudan Seismic Network, Sudan
SSNC	**Servicio Sismológico Nacional Cubano**, **Cuba**
SSS	Centro de Estudios y Investigaciones Geotecnicas del San Salvador, El Salvador
STK	Stockholm Seismological Station, Sweden
STR	**EOST / RéNaSS**, **France**
STU	Stuttgart Seismological Station, Germany
SVSA	**Sistema de Vigilância Sismológica dos Açores**, **Portugal**
SYO	**National Institute of Polar Research**, **Japan**
SZGRF	Seismologisches Zentralobservatorium Gräfenberg, Germany
TAC	Estación Central de Tacubaya, Mexico
TAN	Antananarivo, Madagascar
TANZANIA	Tanzania Broadband Seismic Experiment, USA
TAP	**Central Weather Bureau (CWB)**, **Chinese Taipei**
TAU	University of Tasmania, Australia
TEH	**Tehran University**, **Iran**

Table 11.1: *Continued.*

Agency Code	Agency Name
TEIC	Center for Earthquake Research and Information, USA
THE	**Department of Geophysics, Aristotle University of Thessaloniki, Greece**
THR	**International Institute of Earthquake Engineering and Seismology (IIEES), Iran**
TIF	**Institute of Earth Sciences/ National Seismic Monitoring Center, Georgia**
TIR	**The Institute of Seismology, Academy of Sciences of Albania, Albania**
TRI	**Istituto Nazionale di Oceanografia e di Geofisica Sperimentale (OGS), Italy**
TRN	**The Seismic Research Centre, Trinidad and Tobago**
TTG	Titograd Seismological Station, Montenegro
TUL	Oklahoma Geological Survey, USA
TUN	**Institut National de la Météorologie, Tunisia**
TVA	Tennessee Valley Authority, USA
TXNET	Texas Seismological Network, University of Texas at Austin, USA
TZN	University of Dar Es Salaam, Tanzania
UAF	Department of Geosciences, USA
UATDG	The University of Arizona, Department of Geosciences, USA
UAV	Red Sismológica de Los Andes Venezolanos, Venezuela
UCB	University of Colorado, Boulder, USA
UCC	**Royal Observatory of Belgium, Belgium**
UCDES	Department of Earth Sciences, United Kingdom
UCR	**Sección de Sismología, Vulcanología y Exploración Geofísica, Costa Rica**
UCSC	Earth & Planetary Sciences, USA
UESG	School of Geosciences, United Kingdom
UGN	Institute of Geonics AS CR, Czech Republic
ULE	University of Leeds, United Kingdom
UNAH	Universidad Nacional Autonoma de Honduras, Honduras
UPA	**Universidad de Panama, Panama**
UPIES	Institute of Earth- and Environmental Science, Germany
UPP	**University of Uppsala, Sweden**
UPSL	**University of Patras, Department of Geology, Greece**
UREES	Department of Earth and Environmental Science, USA
USAEC	United States Atomic Energy Commission, USA
USCGS	United States Coast and Geodetic Survey, USA
USGS	United States Geological Survey, USA
UTEP	Department of Geological Sciences, USA
UUSS	The University of Utah Seismograph Stations, USA
UVC	Universidad del Valle, Colombia
UWMDG	University of Wisconsin-Madison, Department of Geoscience, USA
VAO	**Instituto Astronomico e Geofísico, Brazil**
VIE	**Zentralanstalt für Meteorologie und Geodynamik (ZAMG), Austria**
VKMS	Lab. of Seismic Monitoring, Voronezh region, GSRAS & Voronezh State University, Russia
VLA	Vladivostok Seismological Station, Russia

Table 11.1: *Continued.*

Agency Code	Agency Name
VSI	University of Athens, Greece
VUW	Victoria University of Wellington, New Zealand
WAR	**Institute of Geophysics, Polish Academy of Sciences, Poland**
WASN	USA
WBNET	**Institute of Geophysics, Czech Academy of Sciences, Czech Republic**
WEL	**Institute of Geological and Nuclear Sciences, New Zealand**
WES	Weston Observatory, USA
WUSTL	Washington University Earth and Planentary Sciences, USA
YARS	**Yakutiya Regional Seismological Center, GS SB RAS, Russia**
ZAG	**Seismological Survey of the Republic of Croatia, Croatia**
ZEMSU	USSR
ZUR	**Swiss Seismological Service (SED), Switzerland**
ZUR_RMT	Zurich Moment Tensors, Switzerland

Table 11.2: *Phases reported to the ISC. These include phases that could not be matched to an appropriate* ak135 *phases. Those agencies that reported at least 10% of a particular phase are also shown.*

Reported Phase	Total	Agencies reporting
P	4207714	TAP (11%)
S	1913564	TAP (20%), JMA (19%)
AML	746388	ROM (74%), AFAD (12%), ATH (12%)
IAML	614267	NEIC (74%)
NULL	600630	NEIC (32%), IDC (31%), AEIC (21%)
IAmb	516687	NEIC (97%)
Pn	381162	NEIC (50%), ISK (13%)
Pg	325278	ISK (20%), TEH (14%), STR (13%)
Sg	207328	STR (18%), ISK (16%)
LR	155682	IDC (65%), BJI (25%)
pmax	144740	MOS (68%), BJI (28%)
IAMs_20	122769	NEIC (99%)
Sn	81093	IDC (16%), NEIC (11%)
SG	72170	HEL (61%), PRU (18%), IPEC (11%)
PG	66537	HEL (63%), PRU (13%), IPEC (12%)
PKP	47148	IDC (38%), VIE (20%)
Lg	37145	NNC (71%), IDC (17%)
MSG	35196	HEL (100%)
PN	34987	MOS (42%), HEL (31%)
A	32863	INMG (36%), JMA (27%), SKHL (20%), SVSA (17%)
T	28858	IDC (99%)
SN	25621	HEL (77%), OTT (13%)
PKPbc	22074	IDC (56%), NEIC (16%), BGR (14%)
IAmb_Lg	20753	NEIC (100%)
pP	19874	BJI (33%), IDC (14%), ISC1 (14%), VIE (11%)
PKIKP	18776	MOS (99%)
MLR	18691	MOS (100%)
PKPdf	17372	NEIC (52%), INMG (12%)
Vmb_Lg	16383	MDD (100%)
PP	15339	BJI (21%), IDC (19%), BELR (15%)
PcP	15268	IDC (61%)
SB	13923	HEL (100%)
SS	11989	MOS (30%), BJI (20%), BELR (19%)
PB	11146	HEL (100%)
PKPab	8357	IDC (41%), INMG (20%), NEIC (18%)
sP	7931	BJI (64%), ISC1 (13%), INMG (11%)
smax	7677	MOS (82%), BJI (16%)
PKiKP	7416	VIE (27%), IDC (26%), IRIS (15%), AWI (12%)
AMS	6534	PRU (71%), CLL (14%), SKHL (12%)
x	6216	BRG (32%), NDI (26%), CLL (24%), PRU (11%)
Sb	5182	IRIS (99%)
Amp	5176	BRG (100%)
Trac	5040	OTT (100%)
LRM	4861	BELR (96%)
SPECP	4679	AFAD (100%)
AMB	4547	SKHL (86%), BJI (13%)
ScP	4490	IDC (67%), ISC1 (12%)
Pdiff	4433	IRIS (48%), AWI (19%), IDC (16%)

Table 11.2: *(continued)*

Reported Phase	Total	Agencies reporting
PPP	4413	MOS (52%), BELR (43%)
AMP	4231	TIR (74%), UPA (24%)
PKP2	3665	MOS (98%)
LQ	3561	BELR (53%), INMG (25%), PPT (21%)
SSS	3509	BELR (57%), MOS (34%)
PKKPbc	2841	IDC (88%)
*PP	2745	MOS (100%)
LG	2449	BRA (86%), OTT (13%)
sS	2394	BJI (67%), BELR (15%), INMG (11%)
pPKP	2370	VIE (47%), IDC (19%)
PKhKP	2276	IDC (100%)
IVmB_BB	2165	BER (47%), CATAC (43%)
Pb	2089	IRIS (94%)
I	2079	IDC (100%)
SKS	1795	BJI (34%), BELR (29%), PRU (12%), VIE (11%)
AMs_VX	1777	NEIC (100%)
IVMs_BB	1433	BER (88%)
SKPbc	1358	IDC (90%)
L	1343	BGR (57%), WAR (24%), MOLD (15%)
Vmb_V	1334	MDD (100%)
SKSac	1278	BER (38%), AWI (34%)
Smax	1258	BYKL (100%)
PKKP	1168	VIE (49%), IDC (35%)
PS	1164	MOS (40%), BELR (24%), CLL (18%)
ScS	1163	BJI (54%), IDC (16%)
Pdif	1119	NEIC (32%), BER (18%), BJI (11%)
PKPPKP	1076	IDC (93%)
X	1019	JMA (95%)
Pmax	1003	BYKL (89%)
PKHKP	927	MOS (100%)
END	831	ROM (100%)
SKP	747	IDC (46%), VIE (20%), INMG (12%), BELR (11%)
pPKPbc	676	IDC (57%), BGR (34%)
*SP	600	MOS (100%)
SKKS	559	BELR (51%), BJI (32%)
SP	518	BER (35%), MOS (25%)
PKPDF	516	PRU (99%)
E	494	ZAG (99%)
*SS	460	MOS (100%)
Sgmax	450	NERS (100%)
PDIFF	445	PRU (40%), BRA (40%), IPEC (20%)
sPKP	441	BJI (60%), BELR (16%), VIE (15%)
Sm	432	CFUSG (80%), SIGU (20%)
pPKiKP	407	VIE (68%), AWI (13%)
PKP2bc	357	IDC (100%)
PKKPab	354	IDC (88%)
max	353	BYKL (100%)
PKPAB	348	PRU (100%)
SKKPbc	294	IDC (92%)

Table 11.2: *(continued)*

Reported Phase	Total	Agencies reporting
IVmBBB	268	BER (100%)
Pm	267	CFUSG (66%), SIGU (34%)
pPKPdf	265	CLL (25%), BGR (15%), BER (13%)
PKS	251	BJI (43%), BELR (36%)
PcS	246	BJI (81%)
PPS	245	CLL (74%), MOS (18%)
SKPdf	224	BER (54%), CLL (31%), AWI (15%)
pPKPab	212	IDC (26%), AWI (24%), INMG (21%), CLL (20%)
AmB	212	KEA (100%)
P3KPbc	191	IDC (100%)
SSSS	188	CLL (100%)
PKKPdf	184	AWI (75%), BGR (14%)
PKPpre	180	NEIC (76%), PRU (14%)
p	170	ROM (100%)
SKKP	156	VIE (54%), IDC (33%)
PKP1	147	LIC (53%), PPT (35%), LDG (12%)
Pgmax	144	NERS (100%)
P'P'	128	VIE (92%)
pPdiff	126	VIE (57%), SYO (19%), AWI (17%)
P4KPbc	116	IDC (100%)
sPP	106	CLL (99%)
Rg	104	NNC (52%), IDC (27%), NDI (13%)
SKPab	95	IDC (91%)
SKKSac	90	CLL (64%), LJU (12%), WAR (12%)
P'P'df	83	AWI (94%)
PKP2ab	81	IDC (100%)
PKPdif	80	DIAS (75%), CLL (14%)
PmP	78	ZUR (64%), BGR (36%)
Sdif	74	CLL (62%), BELR (32%)
MSN	68	HEL (84%), BER (16%)
H	64	IDC (100%)
Snm	63	CFUSG (100%)
r	63	BRG (100%)
Px	63	CLL (100%)
PCP	61	PRU (67%), MOS (16%), LPA (11%)
sSKS	56	BELR (84%), MRB (16%)
PPPP	55	CLL (100%)
SmS	52	BGR (58%), ZUR (38%)
PKSdf	52	CLL (58%), BER (42%)
P3KP	47	IDC (96%)
SKPa	46	NAO (100%)
SKSdf	45	BER (38%), HYB (22%), AWI (22%), CLL (18%)
PKPmax	44	CLL (100%)
R2	41	CLL (100%)
LQM	41	MOLD (100%)
m	39	SIGU (100%)
pPP	38	CLL (66%), LPA (18%), LJU (16%)
PSKS	35	CLL (100%)
PgPg	33	BYKL (100%)

Table 11.2: *(continued)*

Reported Phase	Total	Agencies reporting
(PKPbc)	32	CLL (100%)
(PP)	32	CLL (100%)
ASPG	32	OSPL (97%)
ASSG	32	OSPL (97%)
sSS	31	CLL (100%)
ATPG	31	OSPL (97%)
ATSG	31	OSPL (97%)
SgSg	30	BYKL (100%)
Pnm	29	CFUSG (100%)
(PKPab)	28	CLL (100%)
(sP)	27	CLL (100%)
pPdif	26	CLL (42%), BELR (35%), HYB (19%)
Pif	26	BRG (100%)
sPPP	25	CLL (100%)
(PKP)	25	CLL (100%)
PKPf	25	BRG (100%)
Plp	24	CLL (100%)
(SS)	24	CLL (100%)
sPKPdf	24	CLL (54%), AWI (25%), SYO (12%)
pPcP	23	IDC (91%)
PKPPKPdf	23	CLL (100%)
Sgm	22	CFUSG (100%)
Sdiff	21	IDC (67%), LJU (33%)
sPKPab	21	INMG (81%), CLL (14%)
PnA	20	THR (100%)
(PKiKP)	19	CLL (100%)
IVmBB	18	BER (83%), HYB (17%)
(pP)	18	CLL (100%)
SKKPdf	18	CLL (44%), AWI (44%)
SA	18	CATAC (94%)
PKPlp	17	CLL (100%)
sPKiKP	16	BELR (56%), HYB (25%)
(SSS)	16	CLL (100%)
sPdif	15	CLL (40%), BELR (33%), HYB (27%)
SKiKP	15	IDC (60%), HYB (20%), LJU (13%)
tx	14	FCIAR (100%)
SKSp	14	BRA (86%), WAR (14%)
SKSP	14	CLL (86%), MOLD (14%)
sPKPbc	14	INMG (71%), LJU (14%)
Sif	13	BRG (100%)
SPP	13	CLL (54%), BELR (23%), MOS (23%)
P*	13	BGR (62%), BJI (31%)
PPPrev	12	CLL (100%)
Pgm	12	CFUSG (100%)
(sPP)	12	CLL (100%)
AP	12	MOS (100%)
Sx	12	CLL (100%)
rx	12	SKHL (100%)
sSdif	12	CLL (67%), BELR (33%)

Table 11.2: *(continued)*

Reported Phase	Total	Agencies reporting
PPlp	11	CLL (100%)
IVMsBB	11	BER (100%)
(Pg)	11	CLL (100%)
M	11	MOLD (82%), LJU (18%)
Pp	10	NDI (90%)
dur	10	MOLD (100%)
(SSSS)	10	CLL (100%)
pPKiPK	10	AWI (100%)
SKSSKSac	9	CLL (100%)
sSSS	9	CLL (100%)
PKPbcmax	9	CLL (100%)
sPS	9	CLL (100%)
SDIFF	9	BRA (56%), LPA (44%)
SKKSdf	9	CLL (67%), HYB (33%)
SKIKS	9	LPA (100%)
SKPPKPdf	8	CLL (100%)
(PKPdf)	8	CLL (100%)
PKSbc	8	CLL (100%)
P4	8	UCR (100%)
LH	8	CLL (100%)
pwP	8	ISC1 (75%), NEIC (25%)
R	8	NDI (100%)
sPPS	8	CLL (100%)
PE	7	BRA (100%)
pPPS	7	CLL (100%)
P4KP	7	IDC (86%), NAO (14%)
(PPP)	6	CLL (100%)
PKKS	6	BELR (33%), PRU (33%), IDC (17%), BRG (17%)
PSPS	6	CLL (100%)
sPKKPdf	6	CLL (100%)
RG	5	HEL (80%), BRA (20%)
(SKSac)	5	CLL (100%)
Lq	5	MOLD (100%)
pS	5	CLL (40%), WAR (20%), BRG (20%), HYB (20%)
sSKKSac	5	CLL (100%)
-MP	5	INMG (100%)
(PPS)	5	CLL (100%)
SbSb	5	UCC (100%)
SCS	4	LPA (100%)
rg	4	BRG (100%)
pPKKPbc	4	CLL (100%)
(Sdif)	4	CLL (100%)
PKPPKPbc	4	CLL (100%)
S*	4	BJI (100%)
PKIKS	4	LPA (100%)
pPn	4	SYO (75%), HYB (25%)
(Pdif)	4	CLL (100%)
(SKPdf)	4	CLL (100%)
pSKKSac	4	CLL (100%)

Table 11.2: *(continued)*

Reported Phase	Total	Agencies reporting
pScP	4	IDC (100%)
pPif	4	BRG (100%)
sSKSac	4	HYB (75%), CLL (25%)
PKPpB	4	WAR (100%)
sPdiff	4	SYO (100%)
LqM	4	MOLD (100%)
(PS)	4	CLL (100%)
SKIKP	4	LPA (100%)
sSP	4	CLL (100%)
P5KP	4	NAO (50%), IDC (25%), CLL (25%)
PKPc	4	WAR (100%)
(pPKPbc)	4	CLL (100%)
Sk	3	CLL (100%)
Pdifmax	3	CLL (100%)
PSP	3	LPA (100%)
PPmax	3	CLL (100%)
(Sg)	3	CLL (100%)
(PPPrev)	3	CLL (100%)
(pPKPab)	3	CLL (100%)
Pn_3	3	ATH (100%)
D	3	CATAC (100%)
LV	3	CLL (100%)
PSSrev	3	CLL (100%)
SKKPab	3	IDC (100%)
sPKPPKPd	3	CLL (100%)
Slp	3	CLL (100%)
PKiK	3	NAO (67%), BER (33%)
(PSKS)	3	CLL (100%)
(PcP)	3	CLL (100%)
P(2)	3	CLL (100%)
(Sn)	3	CLL (100%)
pPN	3	IPEC (100%)
SKPb	3	BER (33%), BRG (33%), NAO (33%)
(Pn	3	SKO (100%)
SSmax	3	CLL (100%)
PSS	3	CLL (100%)
(PPPP)	3	CLL (100%)
(SP)	3	CLL (100%)
SKPd	3	NAO (100%)
(pPKPdf)	3	CLL (100%)
sPSKS	2	CLL (100%)
PKKSdf	2	CLL (100%)
pSKKSacr	2	CLL (100%)
pPPPP	2	CLL (100%)
Pg_2	2	ATH (100%)
(PKSdf)	2	CLL (100%)
pPKKPdf	2	CLL (100%)
R3	2	CLL (100%)
PKPM	2	MOLD (100%)

Table 11.2: *(continued)*

Reported Phase	Total	Agencies reporting
SKKSa	2	BRG (100%)
pSKPbc	2	CLL (100%)
PKPdf4	2	BER (100%)
SN5	2	ISN (100%)
pSKPdf	2	CLL (100%)
pSP	2	CLL (100%)
PPKPDF	2	WAR (100%)
P7KP	2	NAO (100%)
(pPKiKP)	2	CLL (100%)
(SPP)	2	CLL (100%)
sSKPdf	2	CLL (100%)
pSKSac	2	CLL (50%), HYB (50%)
s	2	SGS (50%), KRSC (50%)
sSKSdf	2	CLL (50%), BELR (50%)
PKPbc(2)	2	CLL (100%)
Unk	2	FCIAR (100%)
(PKKPdf)	2	CLL (100%)
(PKPdif)	2	CLL (100%)
PKPdi	1	MOLD (100%)
KPdf	1	INMG (100%)
PKPdfmax	1	CLL (100%)
(SKKSdf)	1	CLL (100%)
AMSG	1	SJA (100%)
(PKKSdf)	1	CLL (100%)
SPKP	1	MOLD (100%)
pPmax	1	CLL (100%)
Sr	1	MEX (100%)
PKPPKPma	1	CLL (100%)
IAMs_BB	1	NDI (100%)
(pPKSab)	1	CLL (100%)
sp	1	SYO (100%)
PPPPrev	1	CLL (100%)
pPS	1	CLL (100%)
pPKP2	1	BJI (100%)
AMSN	1	SSNC (100%)
sSKSP	1	CLL (100%)
SKPbclp	1	CLL (100%)
q	1	KRSC (100%)
MPN	1	HEL (100%)
Pd1	1	ATH (100%)
SPZ	1	MOS (100%)
PKPPKP'	1	BRG (100%)
APKP	1	MOS (100%)
SPS	1	CLL (100%)
(SKPab)	1	CLL (100%)
SKPbcmax	1	CLL (100%)
PsP	1	MOLD (100%)
sPSPS	1	CLL (100%)
PKKPdfma	1	CLL (100%)

Table 11.2: *(continued)*

Reported Phase	Total	Agencies reporting
PKPabmax	1	CLL (100%)
(sSdif)	1	CLL (100%)
pPcPPKPr	1	CLL (100%)
Sd1	1	ATH (100%)
sSSSS	1	CLL (100%)
S5	1	INMG (100%)
sPSS	1	CLL (100%)
(SKKPbc)	1	CLL (100%)
SKPPKPab	1	CLL (100%)
(pSKSac)	1	CLL (100%)
sPSSrev	1	CLL (100%)
(sSP)	1	CLL (100%)
PSPSrev	1	CLL (100%)
sKKS	1	MRB (100%)
sg	1	ISN (100%)
Li	1	MOLD (100%)
pSKSdf	1	HYB (100%)
PKKPbcma	1	CLL (100%)
Pd2	1	ATH (100%)
Sd2	1	ATH (100%)
PKKSbc	1	HYB (100%)
pPSKS	1	CLL (100%)
sPmax	1	CLL (100%)
sSKKSdf	1	CLL (100%)
SKPPKP	1	BRG (100%)
Pnmax	1	CLL (100%)
pPKSdf	1	CLL (100%)
PKKPb	1	BRG (100%)
PN8	1	GUC (100%)
(Pn)	1	CLL (100%)
del	1	KNET (100%)
pSKKPbc	1	CLL (100%)
PSPN	1	MOS (100%)
PSKSrev	1	CLL (100%)
sPKKPbc	1	CLL (100%)
Sglp	1	CLL (100%)
PKPfd	1	INMG (100%)
SSSmax	1	CLL (100%)
pPiff	1	BRG (100%)
Pn(2)	1	CLL (100%)
SSS(2)	1	LPA (100%)
PgA	1	THR (100%)
PPP(2)	1	LPA (100%)
PcPPKPre	1	CLL (100%)
Pdif(2)	1	CLL (100%)
sPif	1	BRG (100%)
SKPPKPbc	1	CLL (100%)
(Sb)	1	CLL (100%)
sSKKSacr	1	CLL (100%)

Table 11.2: *(continued)*

Reported Phase	Total	Agencies reporting
PnPn	1	SYO (100%)
SnSn	1	UCC (100%)
P9	1	SVSA (100%)
SKSf	1	BRG (100%)
SKPP	1	CLL (100%)
pPKKSdf	1	CLL (100%)
(sPPP)	1	CLL (100%)
(pPdif)	1	CLL (100%)
(SKKSac)	1	CLL (100%)
sPKKPab	1	CLL (100%)
SKKSacr	1	CLL (100%)
PKPPKPab	1	CLL (100%)
SKKSf	1	BRG (100%)
pPKPdif	1	NEIC (100%)
_0	1	ATH (100%)

Table 11.3: *Reporters of amplitude data*

Agency	Number of reported amplitudes	Number of amplitudes in ISC located events	Number used for ISC mb	Number used for ISC MS
NEIC	1104021	349659	224590	56919
IDC	582616	553344	148451	75307
ROM	554174	12454	0	0
WEL	214940	32313	20	0
MOS	127149	123088	61204	12693
ATH	113066	25197	0	0
BJI	93793	87773	26514	30169
AFAD	93072	7758	0	0
NNC	87371	31109	47	0
ISK	80779	11833	0	0
DJA	73457	36749	7655	0
SOME	65243	22363	3510	0
AUST	55665	11417	8045	0
VIE	54841	36484	11904	0
HEL	35110	1491	0	0
CATAC	31799	18426	75	0
THE	30533	10991	0	0
GUC	27045	6433	8	0
SJA	19593	7441	0	0
AWI	19075	13073	4814	0
RSNC	18727	12394	10	0
JMA	17968	17884	0	0
MDD	17717	3284	0	0
LDG	16895	2837	0	0
MCSM	16254	16026	6950	0
SDD	14685	4170	0	0
INMG	14545	8167	2020	0
PPT	13369	12766	920	0
BER	12173	5851	1599	166
SKHL	11302	7303	1	0
PRE	11254	3023	1979	15
NAM	10648	1	0	0
PRU	9818	5494	0	3145
BELR	9513	3223	420	661
DNK	7707	4161	3283	51
SSNC	7693	1878	20	3
BGR	7182	6565	3961	0
NDI	7131	6381	2104	410
LJU	6761	356	0	3
ZUR	6480	191	0	0
GII	6389	1466	0	0
PDG	6095	4188	0	0
SVSA	5998	676	470	0
MRB	5866	191	0	0
WBNET	5839	22	0	0
OSPL	5231	1724	0	0

Table 11.3: *Continued.*

Agency	Number of reported amplitudes	Number of amplitudes in ISC located events	Number used for ISC mb	Number used for ISC MS
BRG	5176	2320	0	0
OTT	5029	203	0	0
ECX	4840	465	0	0
NIC	4556	2318	0	0
NOU	4148	3921	2637	0
CLL	3981	2585	429	406
BGS	3826	2529	1542	534
TIR	3136	1814	0	0
UCC	2937	2815	2422	0
SNET	2615	762	0	0
YARS	2590	150	1	0
BYKL	2548	1007	0	0
NAO	2516	2485	1804	0
ISN	2475	2090	0	0
KNET	2414	1074	0	0
BUC	2375	89	0	0
IPEC	1860	347	0	0
MIRAS	1750	338	0	0
MAN	1748	986	0	0
LVSN	1590	90	0	0
IGIL	1159	674	162	191
ASRS	1151	592	0	0
KRSZO	1056	165	0	0
UPA	1027	119	0	1
SKO	1015	312	0	0
SCB	948	233	0	0
BKK	874	345	19	0
BGSI	717	312	0	0
CFUSG	649	567	0	0
KEA	633	415	0	105
NERS	632	395	0	0
MOLD	562	369	87	0
FCIAR	471	124	7	0
LIC	395	346	167	0
THR	347	260	0	0
WAR	326	317	0	228
SIGU	294	180	0	0
HYB	257	252	2	0
PLV	148	34	0	0
EAF	135	72	0	29
INAM	56	56	45	0
DMN	54	54	0	0
ISC	12	11	0	0
PJWWP	3	3	0	0
LIT	3	0	0	0

12

Glossary of ISC Terminology

- Agency/ISC data contributor

  An academic or government institute, seismological organisation or company, geological/meteorological survey, station operator or author that reports or contributed data in the past to the ISC or one of its predecessors. Agencies may contribute data to the ISC directly, or indirectly through other ISC data contributors.

- Agency code

  A unique, maximum eight-character code for a data reporting agency (e.g. NEIC, GFZ, BUD) or author (e.g. ISC, ISC-EHB, IASPEI). Often the agency code is the commonly used acronym of the reporting institute.

- Arrival

  A phase pick at a station is characterised by a phase name and an arrival time.

- Associated phase

  Associated phase arrival or amplitude measurements represent a collection of observations belonging to (i.e. generated by) an event. The complete set of observations are associated to the prime hypocentre.

- Azimuthal gap/Secondary azimuthal gap

  The azimuthal gap for an event is defined as the largest angle between two stations with defining phases when the stations are ordered by their event-to-station azimuths. The secondary azimuthal gap is the largest azimuthal gap a single station closes.

- BAAS

  Seismological bulletins published by the British Association for the Advancement of Science (1913-1917) under the leadership of H.H. Turner. These bulletins are the predecessors of the ISS Bulletins and include reports from stations distributed worldwide.

- Bulletin

  An ordered list of event hypocentres, uncertainties, focal mechanisms, network magnitudes, as well as phase arrival and amplitude observations associated to each event. An event bulletin may list all the reported hypocentres for an event. The convention in the ISC Bulletin is that the preferred (prime) hypocentre appears last in the list of reported hypocentres for an event.

- Catalogue

  An ordered list of event hypocentres, uncertainties and magnitudes. An event catalogue typically lists only the preferred (prime) hypocentres and network magnitudes.

- CoSOI/IASPEI

  Commission on Seismological Observation and Interpretation, a commission of IASPEI that prepares and discusses international standards and procedures in seismological observation and interpretation.

- Defining/Non-defining phase

  A defining phase is used in the location of the event (time-defining) or in the calculation of the network magnitude (magnitude-defining). Non-defining phases are not used in the calculations because they suffer from large residuals or could not be identified.

- Direct/Indirect report

  A data report sent (e-mailed) directly to the ISC, or indirectly through another ISC data contributor.

- Duplicates

  Nearly identical phase arrival time data reported by one or more agencies for the same station. Duplicates may be created by agencies reporting observations from other agencies, or several agencies independently analysing the waveforms from the same station.

- Event

  A natural (e.g. earthquake, landslide, asteroid impact) or anthropogenic (e.g. explosion) phenomenon that generates seismic waves and its source can be identified by an event location algorithm.

- Grouping

  The ISC algorithm that organises reported hypocentres into groups of events. Phases associated to any of the reported hypocentres will also be associated to the preferred (prime) hypocentre. The grouping algorithm also attempts to associate phases that were reported without an accompanying hypocentre to events.

- Ground Truth

  An event with a hypocentre known to certain accuracy at a high confidence level. For instance, GT0 stands for events with exactly known location, depth and origin time (typically explosions); GT5 stands for events with their epicentre known to 5 km accuracy at the 95% confidence level, while their depth and origin time may be known with less accuracy.

- Ground Truth database

  On behalf of IASPEI, the ISC hosts and maintains the IASPEI Reference Event List, a bulletin of ground truth events.

- IASPEI

  International Association of Seismology and Physics of the Earth Interior, www.iaspei.org.

- International Registry of Seismograph Stations (IR)

  Registry of seismographic stations, jointly run by the ISC and the World Data Center for Seismology, Denver (NEIC). The registry provides and maintains unique five-letter codes for stations participating in the international parametric and waveform data exchange.

- ISC Bulletin

  The comprehensive bulletin of the seismicity of the Earth stored in the ISC database and accessible through the ISC website. The bulletin contains both natural and anthropogenic events. Currently the ISC Bulletin spans more than 50 years (1960-to date) and it is constantly extended by adding both recent and past data. Eventually the ISC Bulletin will contain all instrumentally recorded events since 1900.

- ISC Governing Council

  According to the ISC Working Statutes the Governing Council is the governing body of the ISC, comprising one representative for each ISC Member.

- ISC-located events

  A subset of the events selected for ISC review are located by the ISC. The rules for selecting an event for location are described in Section 11.1.3 of the January to June 2018 Bulletin Summary; ISC-located events are denoted by the author ISC.

- ISC Member

  An academic or government institute, seismological organisation or company, geological/meteorological survey, station operator, national/international scientific organisation that contribute to the ISC budget by paying membership fees. ISC members have voting rights in the ISC Governing Council.

- ISC-reviewed events

  A subset of the events reported to the ISC are selected for ISC analyst review. These events may or may not be located by the ISC. The rules for selecting an event for review are described in Section 11.1.3 of the January to June 2018 Bulletin Summary. Non-reviewed events are explicitly marked in the ISC Bulletin by the comment following the prime hypocentre "Event not reviewed by the ISC".

- ISF

  International Seismic Format (www.isc.ac.uk/standards/isf). A standard bulletin format approved by IASPEI. The ISC Bulletin is presented in this format at the ISC website.

- ISS

  International Seismological Summary (1918-1963). These bulletins are the predecessors of the ISC Bulletin and represent the major source of instrumental seismological data before the digital era. The ISS contains regionally and teleseismically recorded events from several hundreds of globally distributed stations.

- Network magnitude

  The event magnitude reported by an agency or computed by the ISC locator. An agency can report several network magnitudes for the same event and also several values for the same magnitude type. The network magnitude obtained with the ISC locator is defined as the median of station magnitudes of the same magnitude type.

- Phase

  A maximum eight-character code for a seismic, infrasonic, or hydroacoustic phase. During the ISC processing, reported phases are mapped to standard IASPEI phase names. Amplitude measurements are identified by specific phase names to facilitate the computation of body-wave and surface-wave magnitudes.

- Prime hypocentre

  The preferred hypocentre solution for an event from a list of hypocentres reported by various agencies or calculated by the ISC.

- Reading

  Parametric data that are associated to a single event and reported by a single agency from a single station. A reading typically includes one or more phase names, arrival time and/or amplitude/period measurements.

- Report/Data report

  All data that are reported to the ISC are parsed and stored in the ISC database. These may include event bulletins, focal mechanisms, moment tensor solutions, macroseismic descriptions and other event comments, as well as phase arrival data that are not associated to events. Every single report sent to the ISC can be traced back in the ISC database via its unique report identifier.

- Shide Circulars

  Collections of station reports for large earthquakes occurring in the period 1899-1912. These reports were compiled through the efforts of J. Milne. The reports are mainly for stations of the British Empire equipped with Milne seismographs. After Milne's death, the Shide Circulars were replaced by the Seismological Bulletins of the BAAS.

- Station code

  A unique, maximum six-character code for a station. The ISC Bulletin contains data exclusively from stations registered in the International Registry of Seismograph Stations.

13

Acknowledgements

References

Adamaki, A. (2017), Seismicity analysis using dense network data : Catalogue statistics and possible foreshocks investigated using empirical and synthetic data, Ph.D. thesis, Uppsala University, `urn: nbn:se:uu:diva-328057`.

Balfour, N., R. Baldwin, and A. Bird (2008), Magnitude calculations in Antelope 4.10, *Analysis Group Note of Geological Survey of Canada*, pp. 1–13.

Bisztricsany, E. A. (1958), A new method for the determination of the magnitude of earthquakes, *Geofiz. Kozl*, pp. 69–76.

Bondár, I., and D. Storchak (2011), Improved location procedures at the International Seismological Centre, *Geophysical Journal International*, *186*, 1220–1244.

Bormann, P., and J. W. Dewey (2012), The new iaspei standards for determining magnitudes from digital data and their relation to classical magnitudes, is 3.3, *New Manual of Seismological Observatory Practice 2 (NMSOP-2), P. Bormann (Ed.)*, pp. 1–44, doi:10.2312/GFZ.NMSOP-2_IS_3.3,10.2312/ GFZ.NMSOP-2, `http://nmsop.gfz-postsdam.de`.

Bormann, P., and J. Saul (2008), The new IASPEI standard broadband magnitude mB, *Seism. Res. Lett*, *79*(5), 698–705.

Bormann, P., R. Liu, X. Ren, R. Gutdeutsch, D. Kaiser, and S. Castellaro (2007), Chinese national network magnitudes, their relation to NEIC magnitudes and recommendations for new IASPEI magnitude standards, *Bulletin of the Seismological Society of America*, *97*(1B), 114–127, doi:10.1785/012006007835.

Bormann, P., R. Liu, Z. Xu, R. Ren, and S. Wendt (2009), First application of the new IASPEI teleseismic magnitude standards to data of the China National Seismographic Network, *Bulletin of the Seismological Society of America*, *99*, 1868–1891, doi:10.1785/0120080010.

Choy, G. L., and J. L. Boatwright (1995), Global patterns of readiated seismic energy and apparent stress, *J. Geophys. Res.*, *100*(B9), 18,205–18,228.

Dziewonski, A. M., T.-A. Chou, and J. H. Woodhouse (1981), Determination of earthquake source parameters from waveform data for studies of global and regional seismicity, *J. Geophys. Res.*, *86*, 2825–2852.

Engdahl, E. R., and A. Villaseñor (2002), Global seismicity: 1900-1999, *International Handbook of Earthquake Engineering and Seismology, International Geophysics series*, *81A*, 665–690.

Engdahl, E. R., R. van der Hilst, and R. Buland (1998), Global teleseismic earthquake relocation with improved travel times and procedures for depth determination, *Bulletin of the Seismological Society of America*, *88*, 722–743.

Gutenberg, B. (1945a), Amplitudes of P, PP and S and magnitude of shallow earthquakes, *Bulletin of the Seismological Society of America*, *35*, 57–69.

Gutenberg, B. (1945b), Magnitude determination of deep-focus earthquakes, *Bulletin of the Seismological Society of America*, *35*, 117–130.

Gutenberg, B. (1945c), Amplitudes of surface waves and magnitudes of shallow earthquakes, *Bulletin of the Seismological Society of America*, *35*, 3–12.

Hutton, L. K., and D. M. Boore (1987), The ML scale in southern California, *Bulletin of the Seismological Society of America*, *77*, 2074–2094.

IASPEI (2005), Summary of magnitude working group recommendations on standard procedures for determining earthquake magnitudes from digital data, `http://www.iaspei.org/commissions/CSOI.html#wgmm,http://www.iaspei.org/commissions/CSOI/summary_of_WG_recommendations_2005.pdf`.

IASPEI (2013), Summary of magnitude working group recommendations on standard procedures for determining earthquake magnitudes from digital data, `http://www.iaspei.org/commissions/CSOI/Summary_of_WG_recommendations_20130327.pdf`.

IDC (1999), IDC processing of seismic, hydroacoustic and infrasonic data, *IDC Documentation*.

Kanamori, H. (1977), The energy release in great earthquakes, *J. Geophys. Res.*, *82*, 2981–2987.

Lee, W. H. K., R. Bennet, and K. Meagher (1972), A method of estimating magnitude of local earthquakes from signal duration, *U.S. Geol. Surv.*, Open-File Rep.

Leptokaropoulos, K. M., A. K. Adamaki, R. G. Roberts, C. G. Gkarlaouni, and P. M. Paradisopoulou (2018), Impact of magnitude uncertainties on seismic catalogue properties, *Geophysical Journal International*, *213*(2), 940–951, `https://doi.org/10.1093/gji/ggy023`.

Nuttli, O. W. (1973), Seismic wave attenuation and magnitude relations for eastern North America, *J. Geophys. Res.*, *78*, 876–885.

Richter, C. F. (1935), An instrumental earthquake magnitude scale, *Bulletin of the Seismological Society of America*, *25*, 1–32.

Ringdal, F. (1976), Maximum-likelihood estimation of seismic magnitude, *Bulletin of the Seismological Society of America*, *66*(3), 789–802.

Storchak, D., J. Harris, L. Brown, K. Lieser, B. Shumba, R. Verney, D. Di Giacomo, and E. I. M. Korger (2017), Rebuild of the bulletin of the international seismological centre (isc), part 1: 1964–1979, *Seismological Research Letters*, *4*(32), doi:10.1186/s40,562–017–0098–z.

Tsuboi, C. (1954), Determination of the Gutenberg-Richter's magnitude of earthquakes occurring in and near Japan, *Zisin (J. Seism. Soc. Japan)*, *Ser. II*(7), 185–193.

Tsuboi, S., K. Abe, K. Takano, and Y. Yamanaka (1995), Rapid determination of Mw from broadband P waveforms, *Bulletin of the Seismological Society of America*, *85*(2), 606–613.

Vaněk, J., A. Zapotek, V. Karnik, N. V. Kondorskaya, Y. V. Riznichenko, E. F. Savarensky, S. L. Solov'yov, and N. V. Shebalin (1962), Standardization of magnitude scales, *Izvestiya Akad. SSSR.*, *Ser. Geofiz.*(2), 153–158, pages 108–111 in the English translation.

Woessner, J., and S. Wiemer (2005), Assessing the quality of earthquake catalogues: estimating the magnitude of completeness and its uncertainty, *Bulletin of the Seismological Society of America*, *95*(2), doi:10/1785/012040,007.

Named after Swiss peaks, *arolla* and *nair* are the pinnacle of GeoSIG instrumentation and offer *peak* performance.

"Will ya give me now?"

BID

"Going once, going twice.... sold!"

GeoSIG
swiss made to measure

Swiss manufacturer GeoSIG will auction several prototype broadband seismometers which were used in the initial development phase of *arolla*. They will be in full working order with a specification suitable for use in scientific research.

If you are interested in the auction and would like to be notified about the auction date, please send your email address to kcrutchlow@geosig.com

We will provide you with additional details about the auction as soon as a date has been decided.

The proceeds of the auction will be given to a non-profit organisation involved in the field of seismology.

TDE-324CI/FI Digitizer

Key Features：

o True 26-bit, exceptionally low noise, up to 1000sps,

   high dynamic range > 145dB@100sps

o High precision time Service：better than 0.05ppm

o Records in MiniSEED, standard storages 32GB, max 256GB

   supports Liss, Seedlink, JOPENS data streaming protocols

o Compatible with any seismometers & accelerometers

o Humanized Interface, include pushbuttons and large LCD,

   setup & display real-time wave and running status

o Built-in seismic station performance and data quality analysis,

   include PSD/PDF, sine/pulse calibration, sensor response, waveform,

   run rate, environmental status monitoring etc.

o Installation checking & setup available for both android and IOS devices

o Remote control multiple seismometers calibration, mass center, mass lock/unlock

TDE-324CI Digitizer

TDE-324FI Digitizer
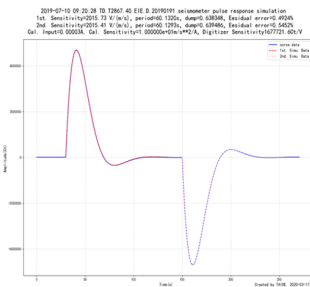
Built in auto pulse cal. signal analysis   Built-in 1 day's seismic wave display   Built-in 1 day's PDF analysis   Built-in seismometer response analysis
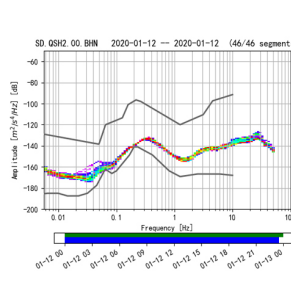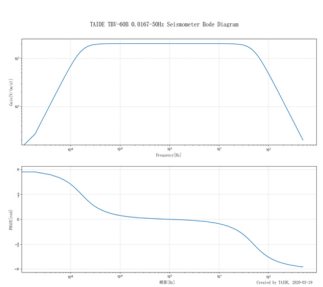
Technical Specifications：

Channels	TDE-324CI: 3 channels TDE-324FI: 6 channels	Main channel resolution	True 26 bits, ≥145dB@100sps Support 24 bits output
Input noise	＜1.0μVrms(input ±20Vpp)	Interface	Standard 10/100M RJ45/LAN
Time Service	Support Beidou,GPS Satellites Support NTP Time Service Time error: better than 0.01ms Timing accuracy:better than 0.05ppm	Signal input	Differential Input, ±20Vpp Full Scale, Program Gain 1/2/4
Sample rate	1sps、10sps、20sps、50sps、100sps、200sps、500sps、1000sps	Environment	Temperature：-40℃～70℃, Humidity：0～100%(RH),IP67